LOAN DOCUMENT

PHOTOGRAPH THIS SHEET

LEVEL

INVENTORY

0

DTIC ACCESSION NUMBER

WL-TR-97-4040

DOCUMENT IDENTIFICATION

Apr 97

DISTRIBUTION STATEMENT A

Approved for public release;
Distribution Unlimited

DISTRIBUTION STATEMENT

H A N D L E W I T H C A R E

ACCESSION FOR

NTIS	GRA&I	☑
DTIC	TRAC	☐
UNANNOUNCED		☐
JUSTIFICATION		

BY

DISTRIBUTION/

AVAILABILITY CODES

DISTRIBUTION	AVAILABILITY AND/OR SPECIAL	
A-1		

DISTRIBUTION STAMP

DATE ACCESSIONED

DATE RETURNED

19970703 058

DATE RECEIVED IN DTIC

REGISTERED OR CERTIFIED NUMBER

PHOTOGRAPH THIS SHEET AND RETURN TO DTIC-FDAC

DTIC FORM JUN 90 70A

DOCUMENT PROCESSING SHEET

PREVIOUS EDITIONS MAY BE USED UNTIL STOCK IS EXHAUSTED.

LOAN DOCUMENT

WL-TR-97-4040

PROCEEDINGS OF THE ANNUAL MECHANICS OF COMPOSITES REVIEW (3RD)

Sponsored by:

Air Force Materials Laboratory
Nonmetallic Materials Division

and

Air Force Flight Dynamics Laboratory
Structures Division

and

Air Force Office of Scientific Research
Directorate of Aerospace Sciences

APRIL 1997

FINAL REPORT FOR PERIOD 25-27 OCTOBER 1977

Approved for public release; distribution unlimited

MATERIALS DIRECTORATE
WRIGHT LABORATORY
AIR FORCE MATERIEL COMMAND
WRIGHT-PATTERSON AFB OH 45433-7734

REPORT DOCUMENTATION PAGE

Form Approved
OMB No. 0704-0188

1. AGENCY USE ONLY *(Leave blank)*	2. REPORT DATE	3. REPORT TYPE AND DATES COVERED
	April 1997	Final Report 25-27 October 1977

4. TITLE AND SUBTITLE

PROCEEDINGS OF THE ANNUAL MECHANICS OF COMPOSITES REVIEW 3RD)

5. FUNDING NUMBERS

6. AUTHOR(S)

7. PERFORMING ORGANIZATION NAME(S) AND ADDRESS(ES)

Air Force Materials Laboratory
Nonmetallic Materials Division
Wright-Patterson AFB OH 45433

8. PERFORMING ORGANIZATION REPORT NUMBER

9. SPONSORING/MONITORING AGENCY NAME(S) AND ADDRESS(ES)

Materials Directorate
Wright Laboratory
Air Force Materiel Command
Wright-Patterson AFB Ohio 45433-7734
POC:Tammy Oaks, WL/MLBM, 937-255-3068

10. SPONSORING/MONITORING AGENCY REPORT NUMBER

WL-TR-97-4040

11. SUPPLEMENTARY NOTES

12a. DISTRIBUTION AVAILABILITY STATEMENT

APPROVED FOR PUBLIC RELEASE; DISTRIBUTION IS UNLIMITED

12b. DISTRIBUTION CODE

13. ABSTRACT *(Maximum 200 words)*

This report contains the basic unedited vu-graphs of the presentations at the "Mechanics" of Composites Review" sponsored jointly by the Non-metallic Materials Division of the Air Force Materials Laboratory, the Structures Division of the Air Force Flight Dynamics Laboratory and the Directorate of Aerospace Sciences of the Air Force Office of Scientific Research. The presentations cover current in-house and contract programs under the sponsorship of these three organizations.

14. SUBJECT TERMS

epoxy-matrix composites; composite materials; resin matrix composites; composite bonded joints; fatigue of graphite/epoxy composites; fracture and fatigue of bi-materials

15. NUMBER OF PAGES

231

16. PRICE CODE

17. SECURITY CLASSIFICATION OF REPORT	18. SECURITY CLASSIFICATION OF THIS PAGE	19. SECURITY CLASSIFICATION OF ABSTRACT	20. LIMITATION OF ABSTRACT
UNCLASSIFIED	UNCLASSIFIED	UNCLASSIFIED	SAR

TABLE OF CONTENTS

TABLE OF CONTENTS (Continued)

FOREWORD

This report contains the basic unedited Vu-graphs of the presentations at the "Mechanics of Composites Review" sponsored jointly by the Nonmetallic Materials Division of the Air Force Materials Laboratory, the Structures Division of the Air Force Flight Dynamics Laboratory and the Directorate of Aerospace Sciences of the Air Force Office of Scientific Research. The presentations cover current in-house and contract programs under the sponsorship of these three organizations.

Since this is a review of on-going programs, much of the information in this report has not been published as yet and is subject to changes. But timely dissemination of the rapidly expanding technology of advanced composites is deemed highly desirable. Works in the area of mechanics of composites have long been typified by disciplined approaches. It is hoped that such a high standard of rigor is reflected in the majority, if not all, of the presentations in this report.

Feedback and open critique of the presentations are welcome. Special thanks are due to James M. Whitney of the Nonmetallic Materials Division for his effort in organizing this review. Again, suggestions and recommendations from all participants will be most important in the planning of future reviews.

J. M. KELBLE, Chief
Nonmetallic Materials Division
Air Force Materials Laboratory

AGENDA

MECHANICS OF COMPOSITES REVIEW

OCTOBER 25 - 27, 1977

TUESDAY, OCTOBER 25

7:45 AM	REGISTRATION
8:15	OPENING REMARKS: J. M. Kelble, Chief, Nonmetallic Materials Division, Air Force Materials Laboratory
8:30	MOISTURE EFFECTS IN EPOXY MATRIX COMPOSITES: George S. Springer, University of Michigan
9:15	HYGROTHERMAL COUPLING EFFECTS ON COMPOSITE MATERIALS: G. C. M. Sih, Lehigh University
10:00	COFFEE BREAK
10:30	TIME DEPENDENT ENVIRONMENTAL BEHAVIOR OF EPOXY MATRIX COMPOSITES: K. G. Kibler, General Dynamics, Fort Worth
11:00	EFFECT OF MOISTURE ON THE COMPRESSION STRENGTH OF LAMINATED EPOXY MATRIX COMPOSITES: K. N. Lauraitis, Lockheed California, Rye Canyon Research Laboratory
11:30	STRESS FIELDS IN COMPOSITE LAMINATES: N. J. Pagano, AFML, Inhouse
12:00	LUNCH
1:00 PM	COMPOSITE STRUCTURE OPTIMAL DESIGN BY ENERGY METHODS: R. W. McLay, University of Vermont
1:45	LINEAR & NONLINEAR EFFECTS IN THE VIBRATION OF ELASTIC STRUCTURES/BEHAVIOR OF ADVANCED ISO-GRID STRUCTURES: L. W. Rehfield, Georgia Institute of Technology
2:30	RESIDUAL STRENGTH DEGRADATION AND EFFECT OF HIGH LOADS FOR FATIGUE BEHAVIOR OF COMPOSITE LAMINATES: C. T. Sun, Purdue University
3:00	COFFEE BREAK

3:30	ADVANCED RESIDUAL STRENGTH DEGRADATION MODELING FOR ADVANCED COMPOSITES: D. Pettit, Lockheed California, Rye Canyon Research Laboratory
4:00	MECHANICS OF COMPOSITES WITH DIFFERENT MODULUS IN TENSION AND COMPRESSION: R. M. Jones, Southern Methodist University
4:45	MECHANICS OF COMPOSITE MATERIALS: G. Hegemier, University of California, San Diego
5:30	COCKTAIL PARTY: Bergamo Center

WEDNESDAY, OCTOBER 26

8:00 AM	CONTINUUM THEORY OF FRACTURE: M. E. Gurtin, Carnegie-Mellon University
8:45	FRACTURE OF ADHESIVE JOINTS AND ADVANCED COMPOSITES: W. G. Knauss, California Institute of Technology
9:30	DIFFUSION IN POLYMERIC MATRIX COMPOSITES: C. D. Shirrell, AFFDL, Inhouse
10:00	COFFEE BREAK
10:30	FRACTURE AND FATIGUE OF BI-MATERIALS: J. Mar, Massachusetts Institute of Technology
11:15	EFFECT OF COMPRESSIVE LOADING ON FATIGUE BEHAVIOR OF COMPOSITES: J. T. Ryder, Lockheed California, Rye Canyon Research Laboratory
12:00	LUNCH
1:00 PM	STRUCTURAL INTEGRITY RESEARCH/COMPOSITES: G. P. Sendeckyj, AFFDL, Inhouse
1:45	COMPOSITES SERVICEABILITY PROGRAM: D. Y. Konishi, Rockwell International
2:30	STATISTICAL FAILURE ANALYSIS OF COMPOSITE MATERIALS: P. C. Chou, Drexel University

3:00	COFFEE BREAK
3:30	CHARACTERIZATION OF COMPOSITE PROPERTIES USING TUBULAR SPECIMENS: H. T. Hahn, AFML, Inhouse
4:00	ENVIRONMENTAL EFFECTS, DAMPING AND COUPLING PROPERTIES OF COMPOSITE LAMINATES: S. Kulkarni, Materials Science Corporation
4:45	ENVIRONMENTAL EFFECTS ON THE THERMO-MECHANICAL BEHAVIOR OF COMPOSITES: T. S. Cook, Southwest Research Institute
5:30	ADJOURN

THURSDAY, OCTOBER 27

8:00 AM	DEFECT/PROPERTY RELATIONSHIPS IN COMPOSITE LAMINATES: K. L. Reifsnider, Virginia Polytechnic Institute and State University
8:45	ENVIRONMENTAL SENSITIVITY: J. B. Whiteside, Grumman Aerospace Corporation
9:30	ANALYSIS OF TEMPERATURE AND MOISTURE CONCENTRATION PROFILES IN A COMPOSITE LAMINATE: F. Crossman, Lockheed Missles and Space, Palo Alto Research Laboratory
10:00	COFFEE BREAK
10:30	SPECTRUM LOAD/ENVIRONMENTAL INTERACTION IN ADVANCED FIBER REINFORCED COMPOSITES: E. M. Wu, Lawrence Livermore Laboratory
11:00	WEAR OF MATERIALS UNDER REPEATED NORMAL AND SLIDING IMPACT: S. L. Rice, University of Connecticut
11:30	STUDY OF RESIDUAL STRESSES IN COMPOSITES AND MIXED FINITE ELEMENT FORMULATION FOR NONLINEAR MECHANICS: T. McDonough, ARAP, Inc.
12:00	LUNCH

1:00 PM	TIME-DEPENDENT FRACTURE OF PARTICULATE COMPOSITE MATERIALS: R. A. Schappery; Texas A&M University
1:45	EVALUATION OF THE EMBEDDED SPAR COMPOSITE DESIGN CONCEPT: R. B. Pipes, University of Delaware
2:15	MECHANICAL RESPONSE OF STRUCTURAL ELEMENTS TO DYNAMIC LOADS: G. Herrmann, Stanford University
3:00	ULTRASONIC PROCEDURES FOR THE DETERMINATION OF BOND STRENGTH: J. Rose, Drexel University
3:45	INTERDISCIPLINARY MECHANICS AND COMPOSITE MATERIALS PROGRAM: J. Diefendorf, Rensselaer Polytechnic Institute
4:15	ANALYSIS AND DESIGN OF COMPOSITE BONDED JOINTS UNDER A DYNAMIC TYPE LOAD: J. Vinson, University of Delaware
5:00	ADJOURN

MOISTURE EFFECTS ON EPOXY-MATRIX COMPOSITES

George S. Springer
Department of Mechanical Engineering
The University of Michigan

I. LOSS OF PERFORMANCE
TENSILE STRENGTH
COMPRESSIVE STRENGTH
etc.

ENVIRONMENTAL
EXPOSURE
TEMPERATURE
MOISTURE

(2)

II. MOISTURE CONTENT
TEMPERATURE

(1)

ENVIRONMENTAL
EXPOSURE
TEMPERATURE
MOISTURE

"MOISTURE PROBLEM"

I GIVEN

Ambient Moisture Content → Find → Material
Ambient Temperature

a) Moisture Content
   Weight Gain
   Moisture Distribution
b) Temperature Distribution

II SINGLE LAYER - Steady State Solution

III EXPERIMENTAL PROCEDURES

IV MULTILAYER - Unsteady (numerical) Solution

MOISTURE ABSORPTION IN ACTUAL ENVIRONMENTS

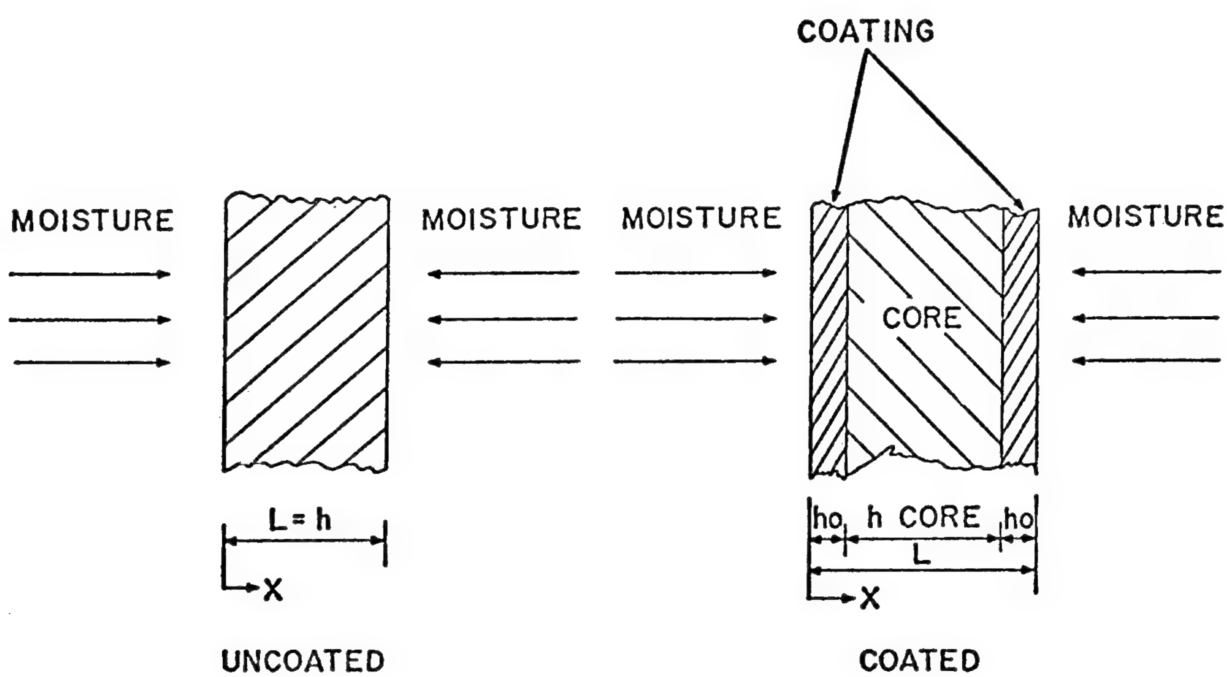

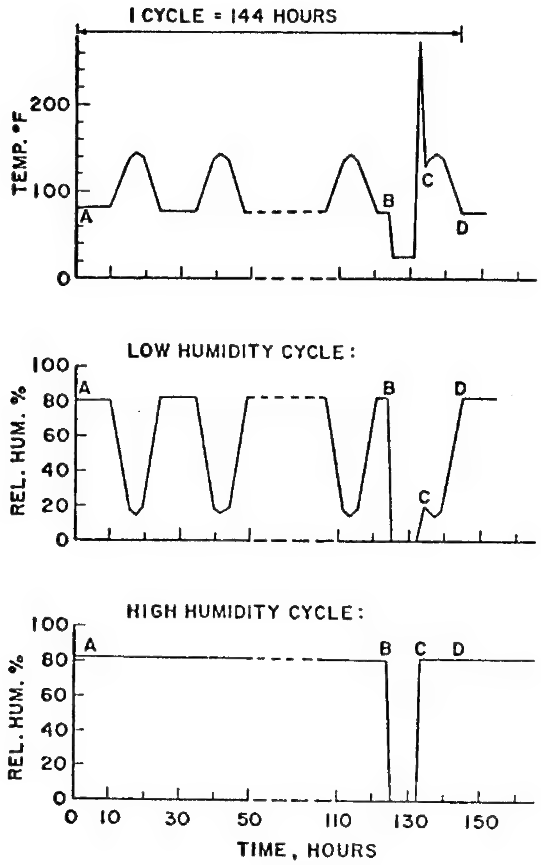

I CYCLE = 144 HOURS
TEMP. °F
LOW HUMIDITY CYCLE:
REL. HUM. %
HIGH HUMIDITY CYCLE:
REL. HUM. %
TIME, HOURS

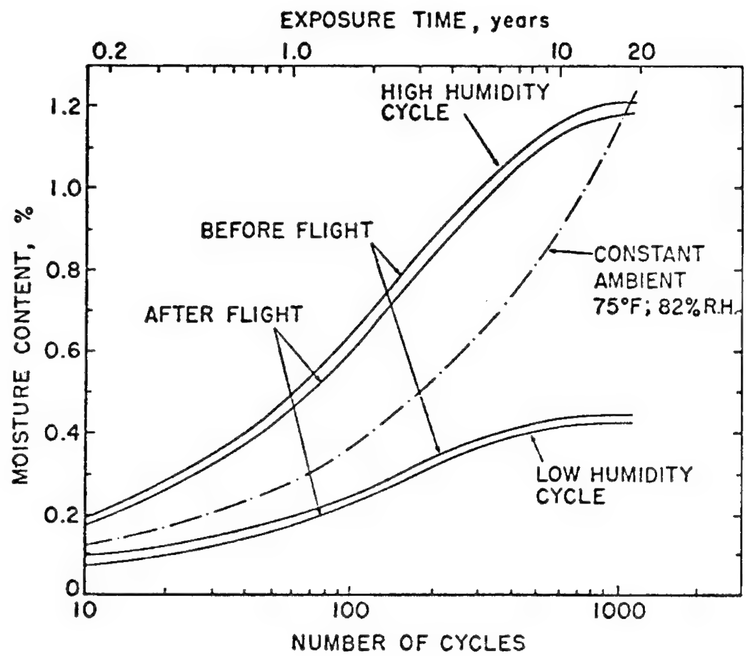

EXPOSURE TIME, years
HIGH HUMIDITY CYCLE
BEFORE FLIGHT
AFTER FLIGHT
CONSTANT AMBIENT 75°F; 82% R.H.
LOW HUMIDITY CYCLE
MOISTURE CONTENT, %
NUMBER OF CYCLES

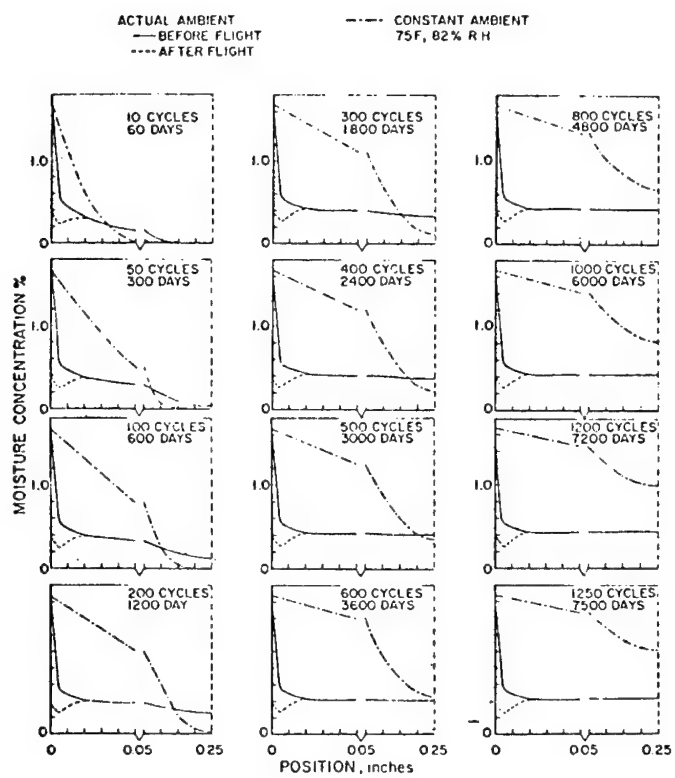

ACTUAL AMBIENT
BEFORE FLIGHT
AFTER FLIGHT
CONSTANT AMBIENT
75F, 82% R H
MOISTURE CONCENTRATION %
POSITION, inches

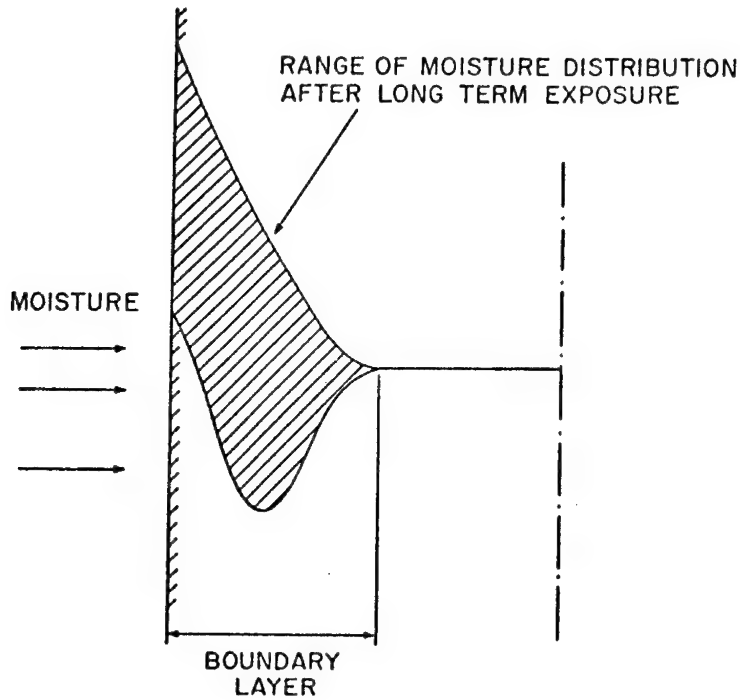

RANGE OF MOISTURE DISTRIBUTION
AFTER LONG TERM EXPOSURE
MOISTURE
BOUNDARY
LAYER

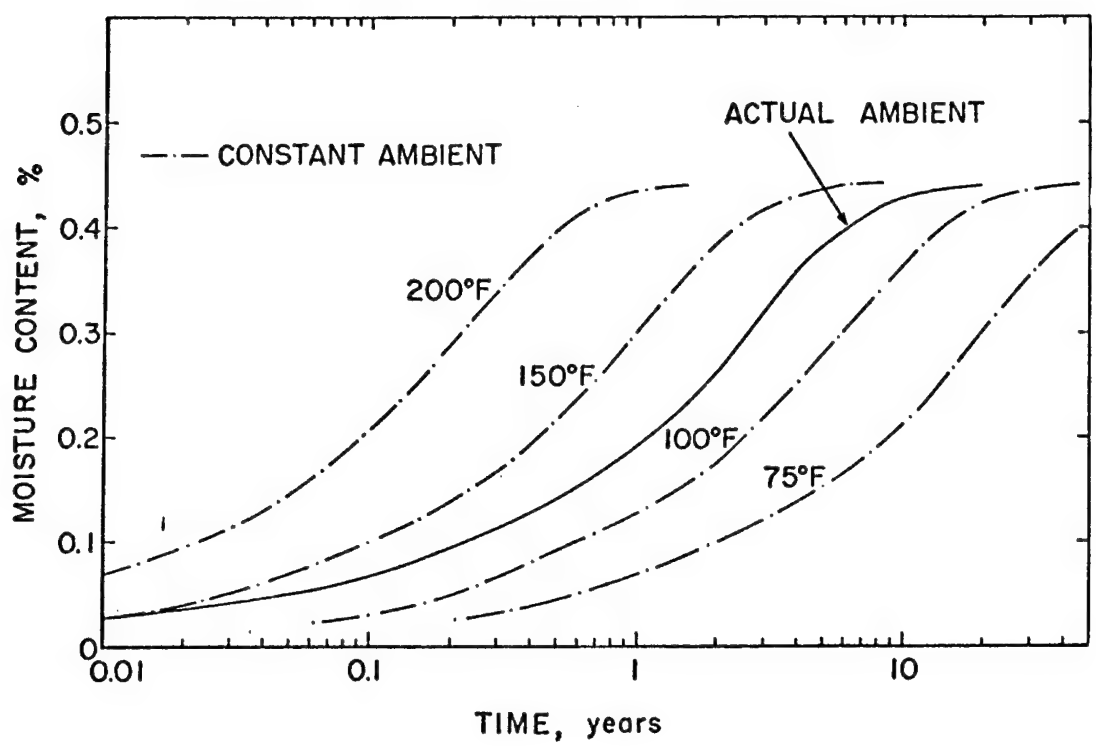

CONSTANT AMBIENT
ACTUAL AMBIENT
200°F
150°F
100°F
75°F
MOISTURE CONTENT, %
0.5
0.4
0.3
0.2
0.1
0
0.01
0.1
1
10
TIME, years

ACTUAL ENVIRONMENT - CONCLUSIONS

1) Moist. Content Reaches S. S. after Long Time

2) Moist. Distrib. never Reaches S. S. - B. L. Effect

3) Accelerated Test : a) Cannot Replace Actual Environment by S. S.

   b) Requires Numerical Solution

ELASTIC MODULI (E_b)

ENVIRONMENTAL DEPENDENCE

1) Moisture
2) Temperature
3) Combined Moisture and Temperature

MATERIAL DEPENDENCE

1) Composition
2) Fiber Orientation

NEEDED : COMPREHENSIVE SET OF DATA

1) For "Absolute" Values

2) For Showing Trends

3) For Extracting Information from Existing Data

4) For Guidance in Future Tests

DATA

THORNEL 300 / FIBERITE 1034

MOISTURE CONTENT	TEMPERATURE °F 77	120	160	200	250	300
Dry						
33% Saturated						
50% Saturated						
67% Saturated						
100% Saturated						

FIBER ORIENTATION $\left\{ \begin{array}{l} 0 \\ 90 \\ \pi/4 \end{array} \right.$

Table I. Summary of Experimental Data on the Effects of Moisture and Temperature on the Elastic Modulus of Composite Materials

Composite	Reference	Laminate Lay-Up Orientation					
		0°		$\pi/4$		90°	
		Moist	Temp	Moist	Temp	Moist	Temp
	BUCKLING TEST						
Thornel 300/Fiberite 1034	Shen & Springer 1977	N	N	N	N	S	S
	TENSILE TEST						
Hercules AS-5/3501	Browning, et al 1976 [5]	L	N	L	N	S	S
	Verette 1975 [6]	N	N	N	-	S	S
	Kerr et al 1975 [7]	-	N	-	N	-	-
Thornel 300/Narmco 5208	Hofer et al 1975 [8]	N	N	N	N	N	N
	Husman 1976 [9]	-	-	-	-	S	S
Modmor II/Narmco 5206	Hofer et al 1974 [10]	N	N	N	N	S	S
Courtaulds HMS/Hercules 3002M	Hofer et al 1974 [10]	N	N	N	N	N	S
HT-S/ERLA-4617	Browning 1972 [11]	-	-	N	S	-	-
HT-S/Fiberite X-911	Browning 1972 [11]	-	-	N	N	-	-
HT-S/UCC X-2546	Browning 1972 [11]	-	-	N	L	-	-
PRD-49/ERLB-4617	Hanson 1972 [12]	-	S	-	-	-	-
HT-S/(8183/137-NDA-BF_3: MEA)	Hertz 1973 [13]	-	-	-	-	N	S
HT-S/Hysol ADX-516	Browning 1972 [11]	-	-	N	S	-	-
HT-S/710 Polyimide	Kerr et al 1975 [7]	-	N	-	N	-	-
HT-S/P13N Polyimide	Browning 1972 [11]	-	-	-	L	-	-
Boron/AVCO 5505	Hofer et al 1974 [10]	N	N	N	N	S	S
Boron/Narmco 5505	Browning 1972 [11]	-	-	N	N	-	-
	COMPRESSIVE TEST						
Hercules AS-5/3501	Verette 1975 [6]	N	N	-	-	L	S
Thornel 300/Narmco 5208	Hofer et al 1975 [8]	L	N	N	N	L	N
Modmor II/Narmco 5206	Hofer et al 1974 [10]	N	N	N	N	S	S
Courtaulds HMS/Hercules 3002M	Hofer et al 1974 [10]	N	N	N	N	S	S
Boron/AVCO 5505	Hofer et al 1974 [10]	N	N	N	N	S	S

a) N = Negligible effect

b) L = Little effect (<30%)

c) S = Strong effect (>30%)

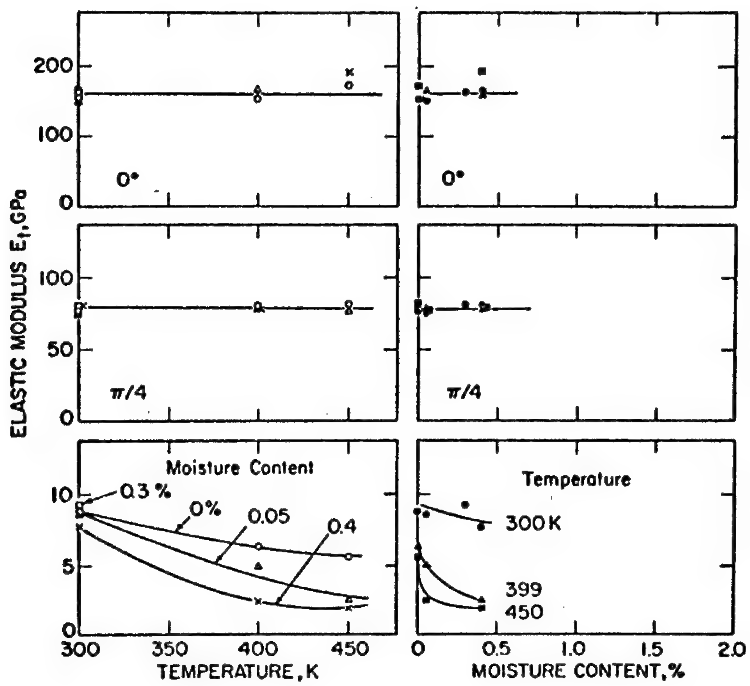

GENERAL CONCLUSIONS - ELASTIC MODULI

A. Temperature

1) 0^0 and $\pi/4$ ⟶ Negligible Effects

2) 90^0 ⟶ Significant Effects
   - a) Moisture Dependent
   - b) 60-90% Reduction in Moduli

B. Moisture

1) 0^0 and $\pi/4$ ⟶ Small Effects
   - a) Negligible Below 1%
   - b) Small Reduction in Moduli Above 1%

2) 90^0 ⟶ Significant Effects
   - a) Temperature Dependent
   - b) 60-90% Reduction in Moduli

SUMMARY - ELASTIC MODULI

1) Extensive Set of Data for Thornel 300 / Fiberite 1034
2) Summary of Existing Data
3) Interpretation of Existing Data
4) General Trends Due to Moisture and Temperature
5) Guidelines for Future Tests

THERMAL SPIKING

1) Moisture Absorption
2) Ultimate Tensile Strength
3) Elastic Moduli

THERMAL SPIKES

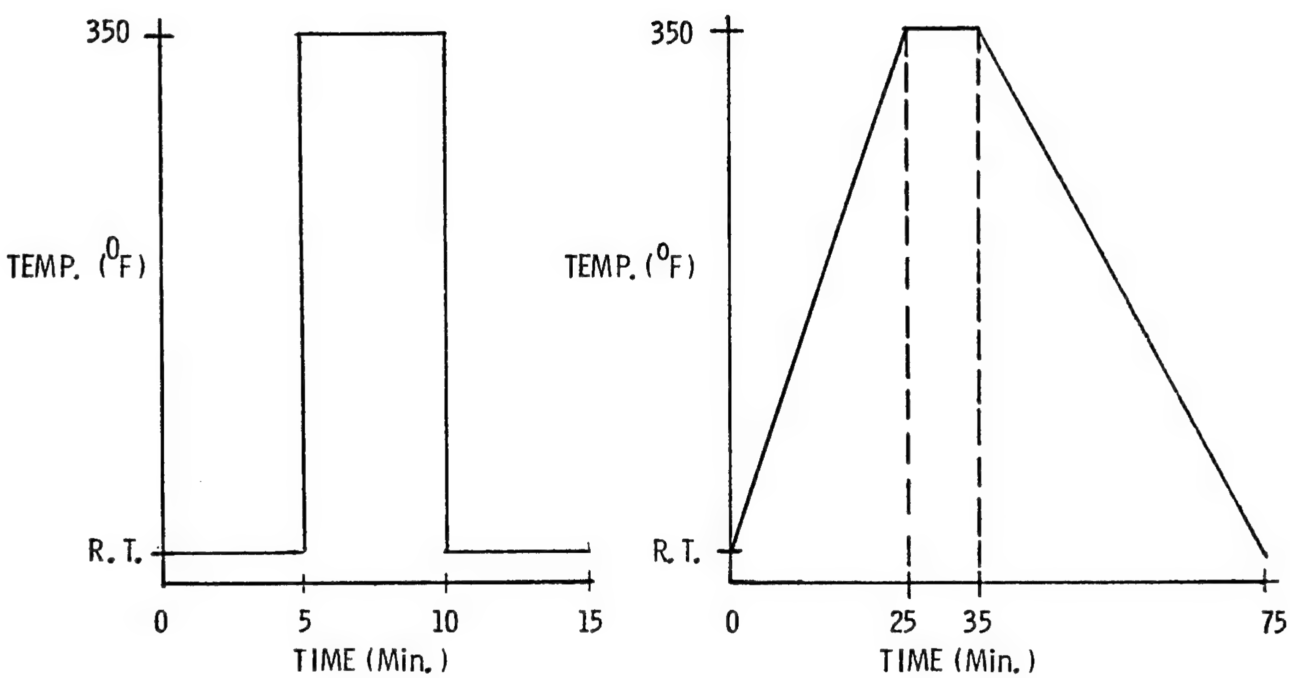

INTERACTION OF TEMPERATURE AND MOISTURE IN DIFFUSION

Investigators: G. C. Sih, R. J. Hartranft and T. S. Chen
Lehigh University, Bethlehem, Pa. 18015

Progress: Covering the period May to Aug. 1977

Contract No. F49620-77-C-0054
Air Force Office of Scientific Research
Bolling Air Force Base, D.C. 20332

Summary: Several analytical results reveal the details of the diffusion process for the case of a thick slab of material subjected to sudden environmental changes. The fundamental conclusion is that the interpretation of experimental results based on the classical, uncoupled theory of diffusion can significantly underestimate the coefficient of diffusion. Additional experiments are proposed to evaluate the temperature and moisture coupling effect.

TEMPERATURE AND MOISTURE COUPLING EQUATIONS

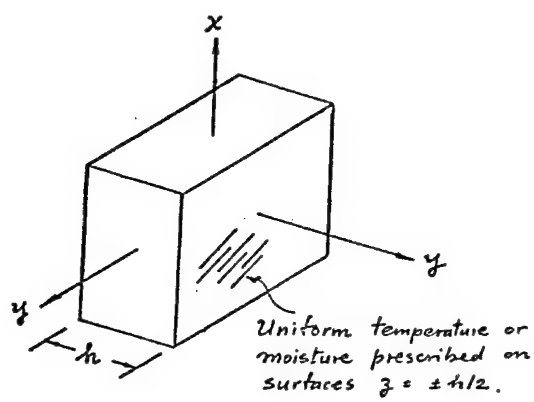

Coupling Equations

$$D \nabla^2 C - \frac{\partial}{\partial t}(C - \lambda T) = 0$$

$$\mathcal{D} \nabla^2 T - \frac{\partial}{\partial t}(T - \nu C) = 0$$

where

D = moisture diffusivity

$\mathcal{D}$ = temperature diffusivity

λ, ν = coupling constants

SUDDEN MOISTURE CHANGE

Initial Conditions

$$T(z,0) = T_i \quad ; \quad C(z,0) = C_i$$

Boundary Conditions

$$T(\pm\tfrac{h}{2},t) = T_i \quad ; \quad C(\pm\tfrac{h}{2},t) = C_f \quad \text{for } t>0$$

Coupled Solution

$$T - T_i = -(C_f - C_i)\, u \nu Q \left[\psi\left(\tfrac{2z}{h}, \tfrac{4D_1 t}{h^2}\right) - \psi\left(\tfrac{2z}{h}, \tfrac{4D_2 t}{h^2}\right)\right],$$

$$C - C_i = (C_f - C_i)\left[(1-P)\,\psi\left(\tfrac{2z}{h}, \tfrac{4D_1 t}{h^2}\right) + P\,\psi\left(\tfrac{2z}{h}, \tfrac{4D_2 t}{h^2}\right)\right].$$

Total Moisture $\left(\bar{\psi}(t) = \frac{1}{h}\int_{-h/2}^{h/2} \psi(z,t)\,dz\right)$

$$\frac{M_T - M_{Ti}}{M_{Tf} - M_{Ti}} = (1+N_1)\,\bar{\psi}\left(\tfrac{4D_1 t}{h^2}\right) - N_1\,\bar{\psi}\left(\tfrac{4D_2 t}{h^2}\right)$$

where

$$N_1 = u\lambda\nu Q - P$$

and

$$u = \frac{D \text{ (moisture diffusion)}}{\mathcal{D} \text{ (thermal diffusion)}}$$

CONTRACTION OF PARAMETERS AND FUNCTIONS

$$\psi(\xi,\theta) = \sum_{n=1}^{\infty} (-1)^{n+1}\left[\operatorname{erfc}\left(\frac{2n-1-\xi}{2\sqrt{\theta}}\right) + \operatorname{erfc}\left(\frac{2n-1+\xi}{2\sqrt{\theta}}\right)\right]$$

where

$$\operatorname{erfc}(z) = 1 - \frac{2}{\sqrt{\pi}}\int_0^z e^{-s^2}\,ds$$

The parameters P and Q stand for

$$P = \frac{\frac{D}{D_1} - 1}{\frac{D}{D_1} - \frac{D}{D_2}} \quad ; \quad Q = \frac{1}{\frac{D}{D_1} - \frac{D}{D_2}}$$

in which

$$D_1/D = 2\Big/\left[1+u+\sqrt{(1-u)^2+4u\lambda\nu}\right]$$

$$D_2/D = 2\Big/\left[1+u-\sqrt{(1-u)^2+4u\lambda\nu}\right]$$

and as $\lambda\nu \to 0$:

$$D_1 \to D \quad ; \quad D_2 \to \mathcal{D}$$

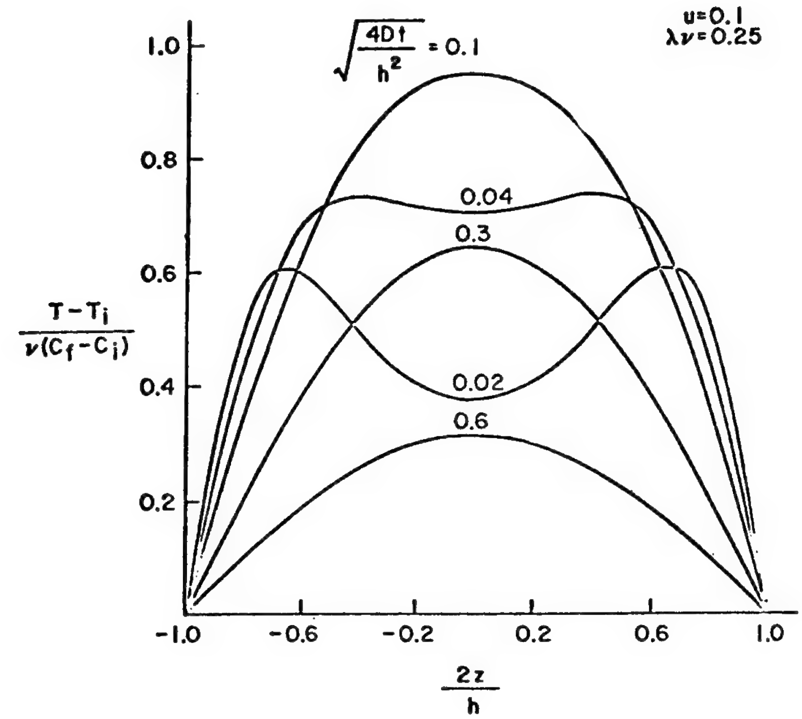

Variation of temperature through the slab for $\lambda\nu$ = 0.25 and u = 0.1 when the surface temperature is held constant

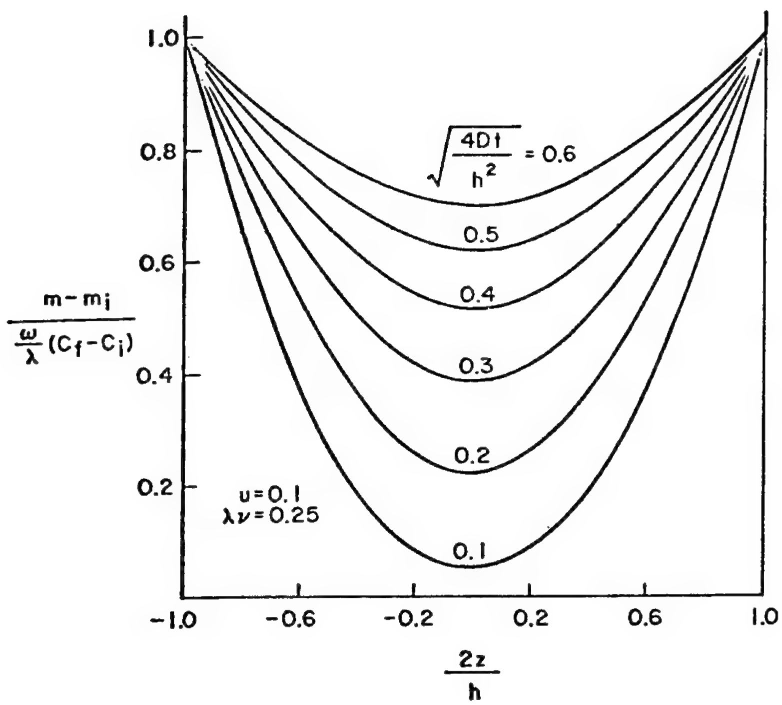

Distribution of the total moisture per unit volume of the solid for $\lambda\nu$ = 0.25 and u = 0.1

Diffusion Coefficient
(Varying C ; Constant T)

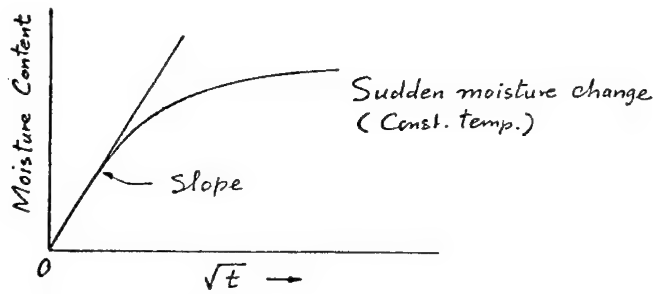

Experimental Measurement

Slope: $\left.\frac{dM_T}{d\sqrt{t}}\right|_{t=0} = (M_{Tf} - M_{Ti}) \frac{2}{h} \frac{2}{\sqrt{\pi}} \sqrt{D_e^c}$

Theoretical Prediction

$$\left.\frac{dM_T}{d\sqrt{t}}\right|_{t=0} = (M_{Tf} - M_{Ti}) \frac{2}{h} \frac{2}{\sqrt{\pi}} \left[(1+N_1)\sqrt{D_1} - N_1 \sqrt{D_2} \right]$$

Hence,

$$\sqrt{D_e^c} = (1+N_1)\sqrt{D_1} - N_1 \sqrt{D_2}$$

where

$D_e^c = D$ for $\lambda\nu = 0$ (no coupling or the classical solution)

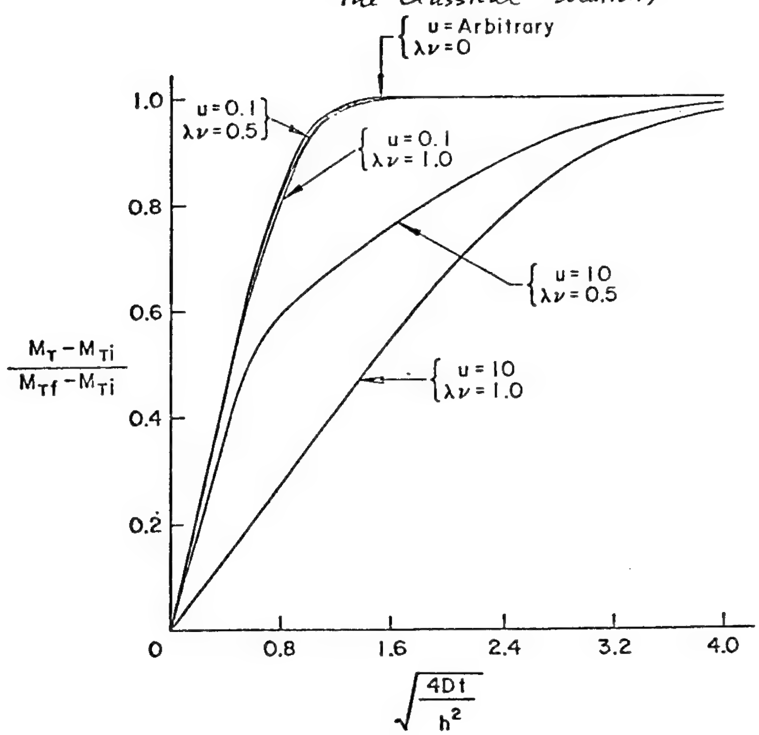

Total moisture absorbed by the solid and contained in the void spaces as a function of time. Surface temperature is held constant

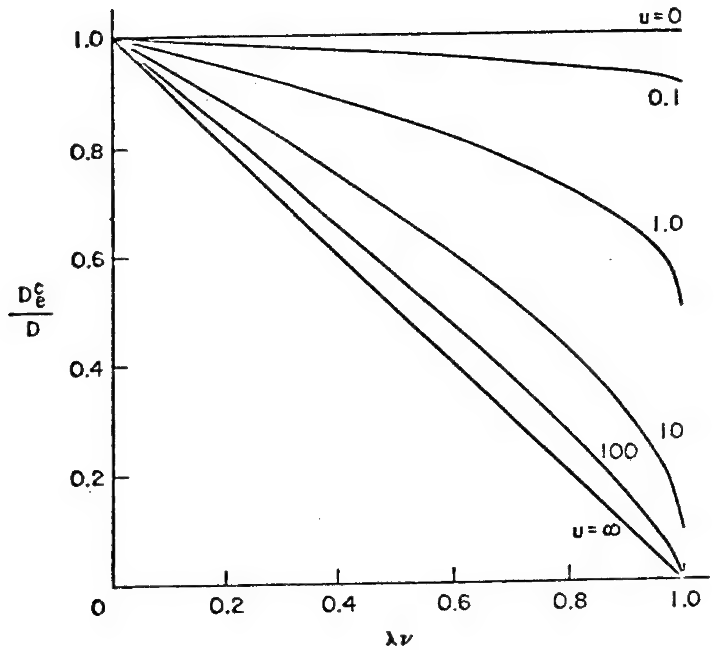

Experimental estimate, D_e, of the diffusion coefficient, D, for various combinations of $u = D/\mathcal{D}$ and $\lambda\nu$. The surfaces of the slab are held at constant temperature while the moisture concentration is suddenly increased

SUDDEN TEMPERATURE CHANGE

Initial Conditions

$$T(z,0) = T_i \quad ; \quad C(z,0) = C_i$$

Boundary Conditions

$$T(\pm\tfrac{h}{2}, t) = T_f \quad ; \quad C(\pm\tfrac{h}{2}, t) = C_i \quad \text{for } t > 0$$

Coupled Solution

$$T - T_i = (T_f - T_i)\left[P\,\psi\left(\frac{2z}{h}, \frac{4D_1 t}{h^2}\right) + (1-P)\,\psi\left(\frac{2z}{h}, \frac{4D_2 t}{h^2}\right)\right]$$

$$C - C_i = -(T_f - T_i)\lambda Q\left[\psi\left(\frac{2z}{h}, \frac{4D_1 t}{h}\right) - \psi\left(\frac{2z}{h}, \frac{4D_2 t}{h^2}\right)\right]$$

Total Moisture

$$\frac{M_T - M_{Ti}}{M_{Tf} - M_{Ti}} = N_2\,\bar{\psi}\left(\frac{4D_1 t}{h^2}\right) + (1-N_2)\,\bar{\psi}\left(\frac{4D_2 t}{h^2}\right)$$

where

$$N_2 = P + Q$$

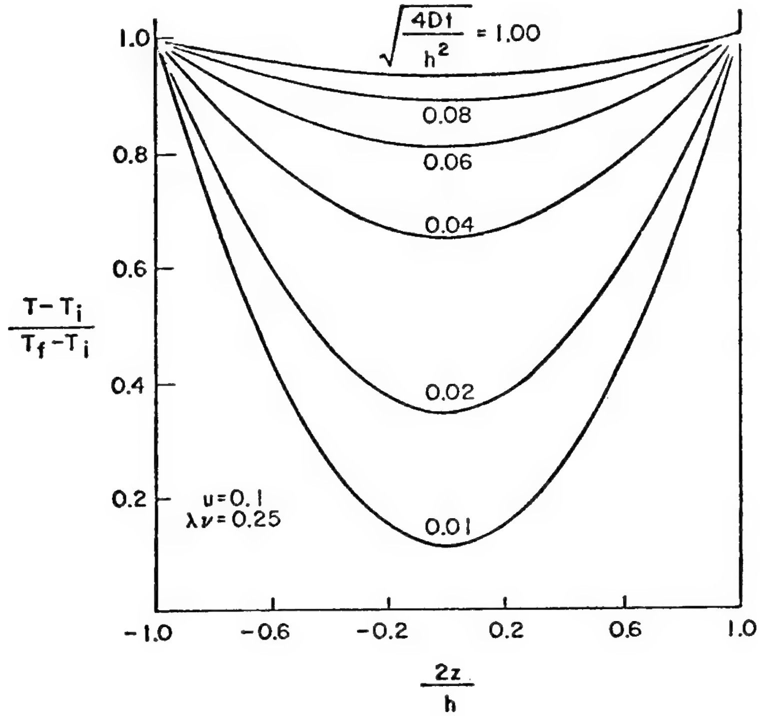

Variation of temperature through the slab for $\lambda\nu = 0.25$ and $u = 0.1$ when the moisture concentration at the surface is held constant

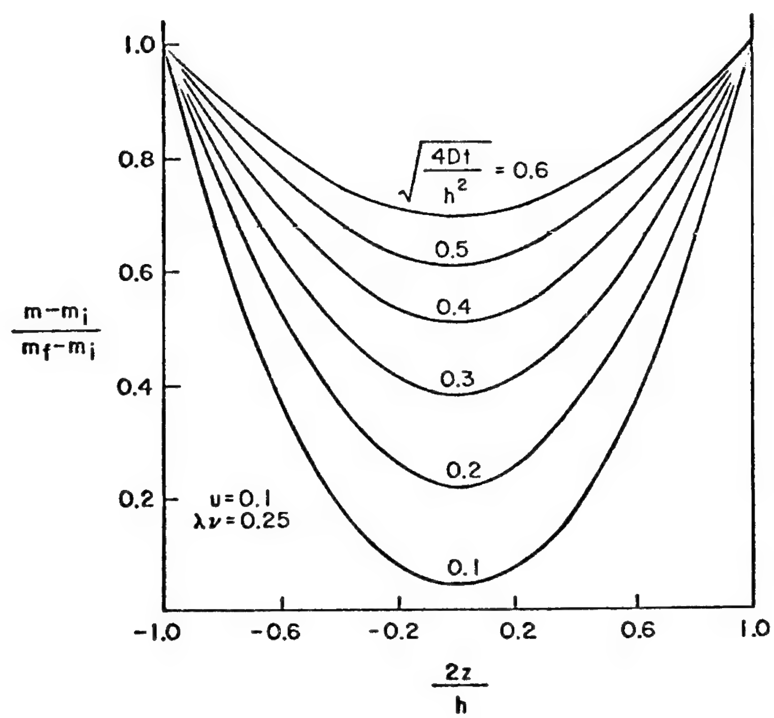

Distribution of mass of moisture per unit mass of solid for $u = 0.10$ and $\lambda\nu = 0.25$

DIFFUSION COEFFICIENT
(Varying T; Constant C)

Experimental Measurement

Slope: $$\left.\frac{dM_T}{d\sqrt{t}}\right|_{t=0} = (M_{Tf} - M_{Ti})\frac{2}{h}\frac{2}{\sqrt{\pi}}\sqrt{D_e^T}$$

Theoretical Prediction

$$\left.\frac{dM_T}{d\sqrt{t}}\right|_{t=0} = (M_{Tf} - M_{Ti})\frac{2}{h}\frac{2}{\sqrt{\pi}}\left[N_2\sqrt{D_1} + (1-N_2)\sqrt{D_2}\right]$$

Hence,

$$\sqrt{D_e^T} = N_2\sqrt{D_1} + (1-N_2)\sqrt{D_2}$$

In the limit as $\lambda\nu \to 0$

$$D_e^T \to \frac{D}{(1+\sqrt{u})^2}$$

Note that coupling effect always prevails, i.e.,
$D_e^T \neq D$.

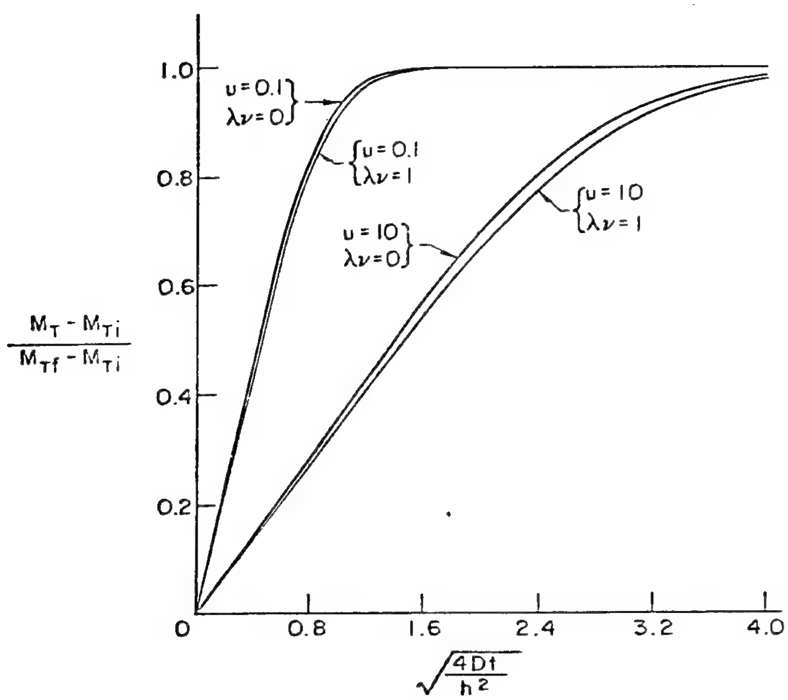

Total moisture absorbed by the solid and contained in the void spaces as a function of time. Surface moisture concentration is held constant

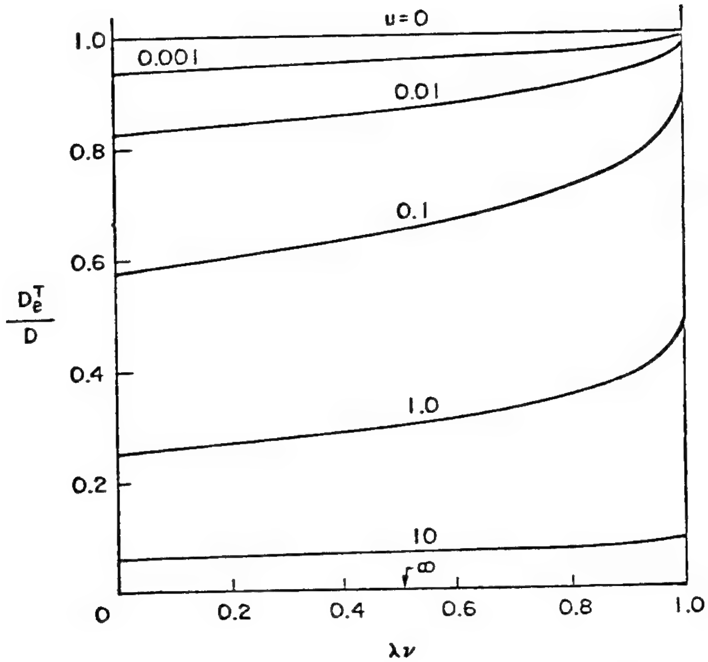

Experimental estimate D_e, of the diffusion coefficient, D, for various combinations of $u = D/\mathcal{D}$ and $\lambda\nu$. The surfaces of the slab are held at constant moisture concentration while the temperature is suddenly increased

ADDITIONAL EXPERIMENTAL CONSIDERATIONS

Three Unknown Constants

$$\sqrt{\frac{D_e^c}{D_e^T}} = 1 + \sqrt{\frac{D}{D_1}\frac{D}{D_2}} = 1 + \sqrt{(1-\lambda\nu)u}$$

Additional Considerations (H = heat content)

$$\left.\frac{dH_T}{d\sqrt{t}}\right|_{t=0} = (H_{Tf} - H_{Ti})\frac{2}{h}\frac{2}{\sqrt{\pi}}\sqrt{\mathcal{D}_e}$$

to be determined for the following conditions:

(1) Varying C; Constant T

$$\sqrt{\mathcal{D}_e^c} = N_2\sqrt{D_1} + (1-N_2)\sqrt{D_2}$$

(2) Varying T; Constant C

$$\sqrt{\mathcal{D}_e^T} = N_3\sqrt{D_1} + (1-N_3)\sqrt{D_2}$$

in which

$$N_3 = P + \lambda\nu Q$$

TIME-DEPENDENT ENVIRONMENTAL BEHAVIOR

OF

GRAPHITE/EPOXY COMPOSITES

(F33615-77-C-5109)

K. G. KIBLER

GENERAL DYNAMICS
P.O. BOX 748
FORT WORTH, TX 76101

OBJECTIVE

DETERMINE ANALYTICALLY AND EXPERIMENTALLY THE COUPLED AND UNCOUPLED EFFECTS OF TEMPERATURE AND MOISTURE ON THE TIME-DEPENDENT MECHANICAL BEHAVIOR OF GRAPHITE/EPOXY COMPOSITES.

F33615-77-C-5109 TIME-DEPENDENT ENVIRONMENTAL BEHAVIOR OF GRAPHITE/EPOXY COMPOSITES

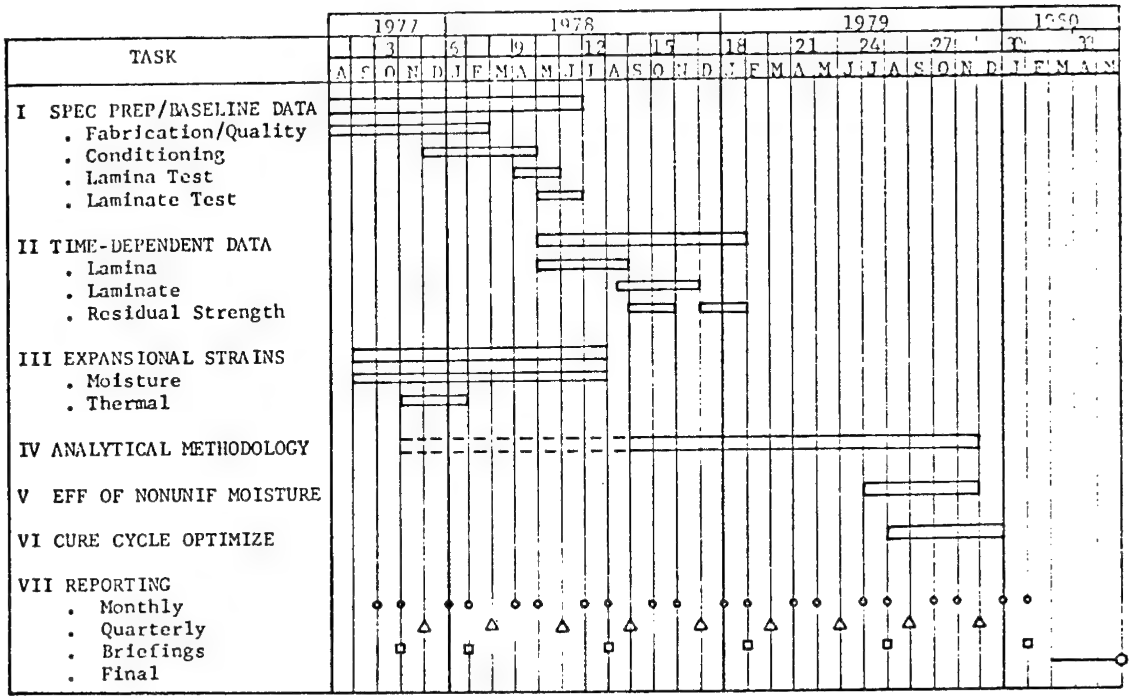

PROGRAM SCHEDULE

" APPROACH "

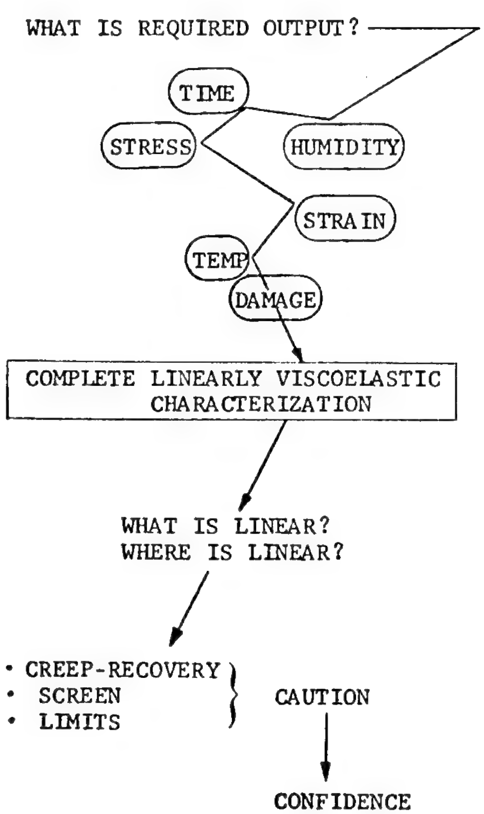

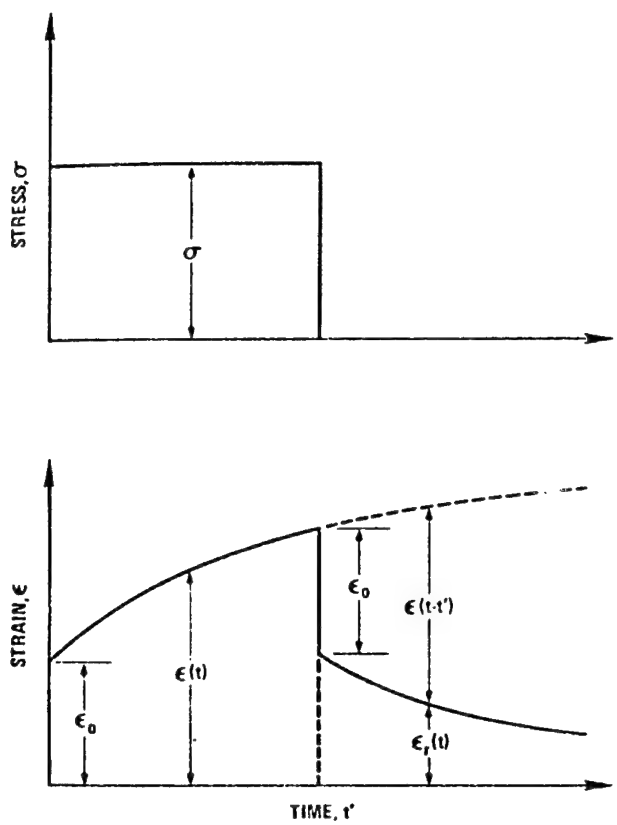

SCOPE

I SPECIMEN PREPARATION AND BASELINE DATA

- UNIDIRECTIONAL AND LAMINATED TENSILE COUPONS OF TWO MATERIAL SYSTEMS

$(0)_6$ $(90)_{15}$ $(\pm 45)_{2S}$	UNIDIRECTIONAL PROPERTIES
$(0/\pm 45)_S$ $(90/\pm 45)_S$ $(0/90/\pm 45)_S$	LAMINATE PROPERTIES
$(+45)_{6S}$ $(90/\pm 45)_{4S}$	EFFECTS OF NON-UNIF MOIST. DIST.

- BASELINE STRESS-STRAIN
  - RT AND ELEVATED TEMP
  - DRY AND TWO UNIF. MOISTURE CONTENTS

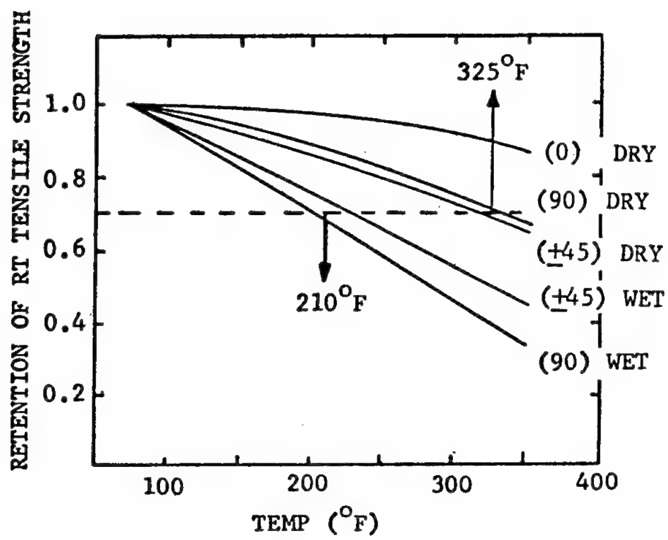

II TIME-DEPENDENT DATA

- CREEP AND STRESS RELAXATION
- RT AND FOUR ELEVATED TEMPS
- DRY AND TWO UNIF MOISTURE CONTENT
- RT RESIDUAL STRENGTH
- INITIAL SCREENING ON (±45)
  - "DAMAGE" ASSESSMENT
  - RANGE OF LINEARITY
  - ISOTHERMAL AND TRANSIENT

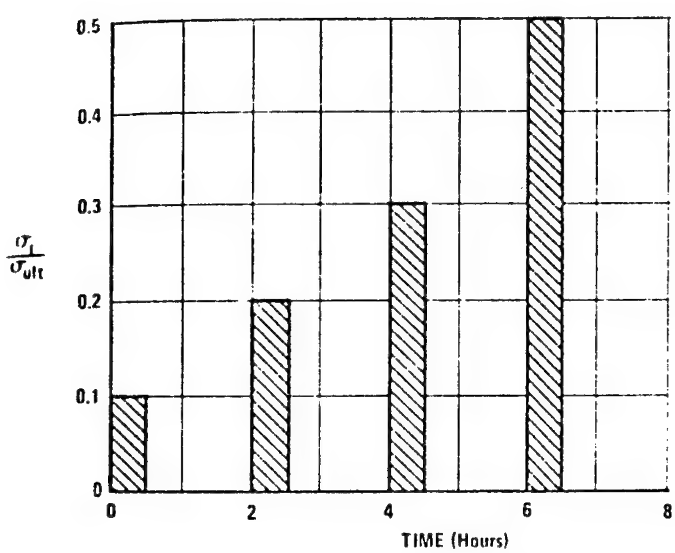

Typical Creep - Recovery Cycles

SCOPE (CONT.)

III EXPANSIONAL STRAINS

- LONGITUDINAL AND TRANSVERSE STRAINS DUE TO TEMP AND MOISTURE

IV ANALYTICAL METHODOLOGY

- DEVELOPMENT OF ANALYTICAL PROCEDURES TO PREDICT TIME-DEPENDENT MECHANICAL BEHAVIOR OF LAMINA AND LAMINATES, INCLUDING EFFECTS OF RESIDUAL STRESS, USING DATA FROM TASKS I - III

V EFFECT OF NON-UNIFORM MOISTURE DISTRIBUTION

- EXPERIMENTAL AND ANALYTICAL ASSESSMENT OF EFFECT ON STATIC AND TIME-DEPENDENT PROPERTIES

VI CURE CYCLE OPTIMIZATION

- DEVELOPMENT OF ANALYTICAL PROCEDURE TO REDUCE RESIDUAL STRESS DUE TO CURE

VII REPORTING

- - EXAMPLE - -

INITIAL SCREENING TESTS - $(\pm 45)_{2S}$

TEST NO.	ENV. CONDITIONS		TEST
1	75°F	DRY	• CREEP-RECOVERY • $\sigma_i / \sigma_o \sim$ 5%, 10%, 20%, 30%, 50% • MULTIPLE CYCLES PER LOAD
2	225°F	DRY	
3	375°F	DRY	
4	75°F	98% RH	
5	150°F	98% RH	
6	210°F	98% RH	
7	75°F	DRY	• STRESS RELAXATION • INITIAL STRESSES AS ABOVE • PRECONDITIONING AS NECESSARY
8	225°F	DRY	
9	375°F	DRY	
10	75°F	98% RH	
11	150°F	98% RH	
12	210°F	98% RH	
13	75°-375°-75°	DRY	• CONSTANT RATE THERMAL CYCLE • $\sigma_1 / \sigma_o \sim 10\%$ • COMPLIANCE VS. TEMP.
14	75°-210°-75°	75% RH	
15	75°-210°-75°	98% RH	

EFFECT OF ENVIRONMENT ON THE COMPRESSIVE STRENGTHS OF LAMINATED EPOXY MATRIX COMPOSITES

CONTRACT NO: F33615-77-C-5140

LOCKHEED-CALIFORNIA COMPANY

OBJECTIVES:

1) Determine the predominant failure modes which occur under structural application of compression loading of epoxy matrix composites in the presence of various environmental conditions and identify the associated test methods which produce these modes of failure.

2) Determine the effect of absorbed moisture and temperature on compression strengths of these composites.

SCOPE:

1) Conduct baseline tension tests for two material systems to characterize the longitudinal, transverse and shear stress-strain response of the test laminates.

2) Evaluate the compression/buckling behavior under full restraint and at 7 column lengths for 3 laminates, 2 materials in both longitudinal and transverse directions.

3) Conduct buckling tests at 4 temperatures on specimens containing uniform and non-uniform moisture distributions, microcracks, and varying moisture contents.

4) Develop analytical model to predict column buckling behavior as function of absorbed moisture and temperature.

COMPRESSION TEST SPECIMEN ADVANTAGES

- MORE UNIFORM STRESS DISTRIBUTION
  - RELATIVE DISPLACEMENT DUE TO SHEAR LAG MUST BE ACCOMODATED WITHIN TEST LENGTH
- LESS SENSITIVE TO SMALL TEST MISALIGNMENT AND ECCENTRICITY
  - SIX-INCH GAGE LENGTH IMPORTANT IN MINIMIZING STRESS VARIATIONS DUE TO FABRICATION AND TEST INSTALLATION, REDUCING SCATTER
- SIZE SUFFICIENT TO PROVIDE GOOD PROBABILITY OF INCLUDING MATERIAL AND LAYUP VARIATIONS
  - SIZE EFFECTS, TEST SCATTER AND NUMBER OF TESTS REDUCED
- GEOMETRY CAN BE USED FOR STATIC TENSION AND COMPRESSION AND FOR TENSION-TENSION OR TENSION-COMPRESSION FATIGUE TESTS
- DIMENSIONS ARE CONVENIENT FOR FABRICATION AND MACHINING
  - TOLERANCES ACHIEVABLE WITHOUT EXTRAORDINARY MEASURES

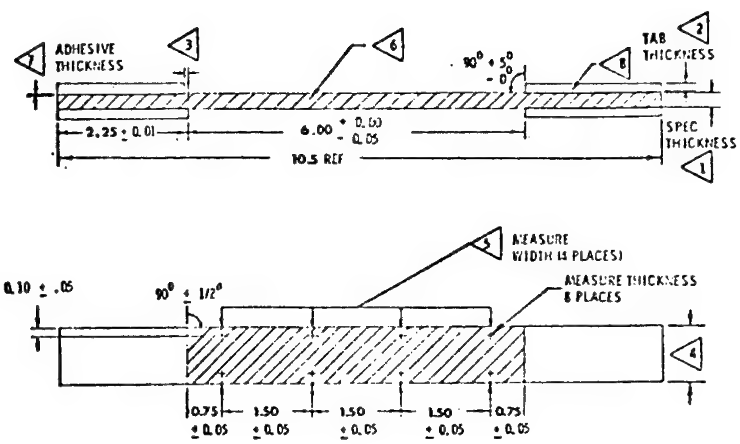

9 SPECIMENS TO BE FLAT OVER THE ENTIRE 10.5 INCH LENGTH WITHIN 0.01 INCHES.

8 TAB EDGES TO BE PARALLEL TO SIDES OF SPECIMEN WITHIN 0.02 INCHES. OVERHANG NOT TO EXCEED 0.15

7 THE TAB AND SPECIMEN BONDING SURFACES TO BE THOROUGHLY SOLVENT CLEANED USING METHYL-ETHYL KETONE PRIOR TO BONDING. A 250°F CURING ADHESIVE IS TO BE USED AND MUST COVER ENTIRE SURFACE UNIFORMLY. ADHESIVE THICKNESS IS TO BE 0.003 – 0.005 INCHES

6 WATER SPRAY MIST TO BE USED DURING SAWING OPERATIONS AND SOLUBLE OIL DURING GRINDING. MACHINED SURFACES TO BE RMS 50 OR BETTER. NO EDGE DAMAGE OR FIBER SEPARATION SHOULD BE VISIBLE UNDER 10X MAGNIFICATION.

5 MEASURE SPECIMEN WIDTH 4 PLACES. WIDTH MUST NOT VARY BY MORE THAN 0.004 INCHES.

4 SPECIMEN WIDTH TO BE 1.00 $^{+0.00}_{-0.02}$ INCHES.

3 MISMATCH OF TABS FROM SIDE TO SIDE NOT TO EXCEED 0.01 INCHES.

2 TABS TO BE CUT FROM AN 8 PLY LAMINATE FABRICATED FROM PREPREG of 1581 GLASS FABRIC IN A 250°F CURING EPOXY HAVING A CURED THICKNESS OF 0.065 – 0.070 INCHES.

1 SPECIMEN THICKNESS TO BE WITHIN ±0.003 INCHES OF THE AVERAGE OF 8 THICKNESS MEASUREMENTS.

Composite Compression Specimen Configuration

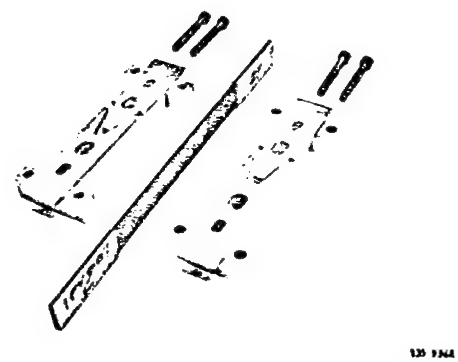

"Full-Fixity" Apparatus, Showing Auxiliary Platens

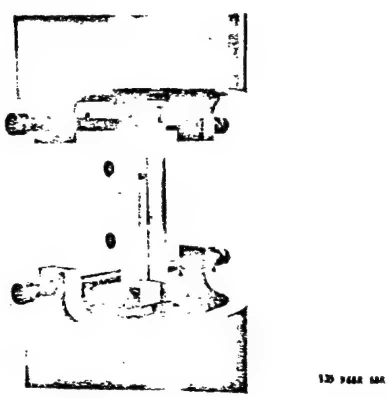

Specimen and Restraint Fixture Installed in Grips

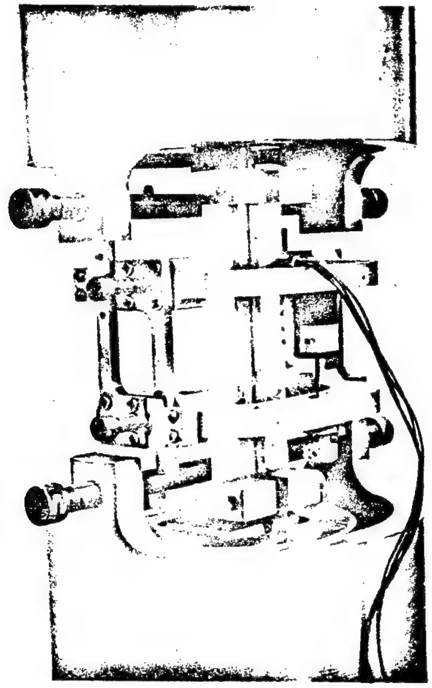

Installation of Lockheed Extensometer

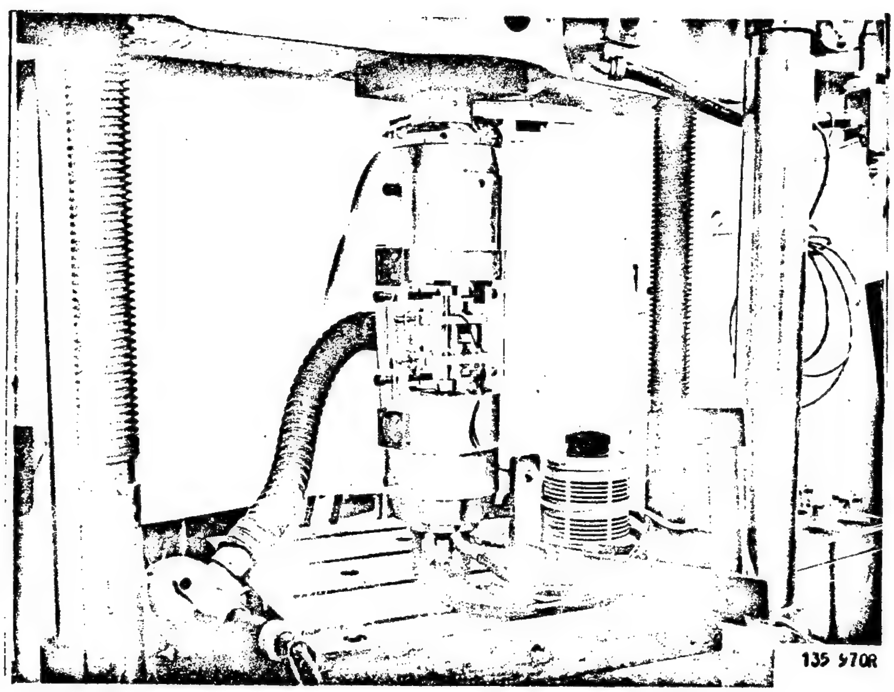

Overall View of Composite Compression Test Apparatus, with Acrylic Enclosure and Warm Air Supply

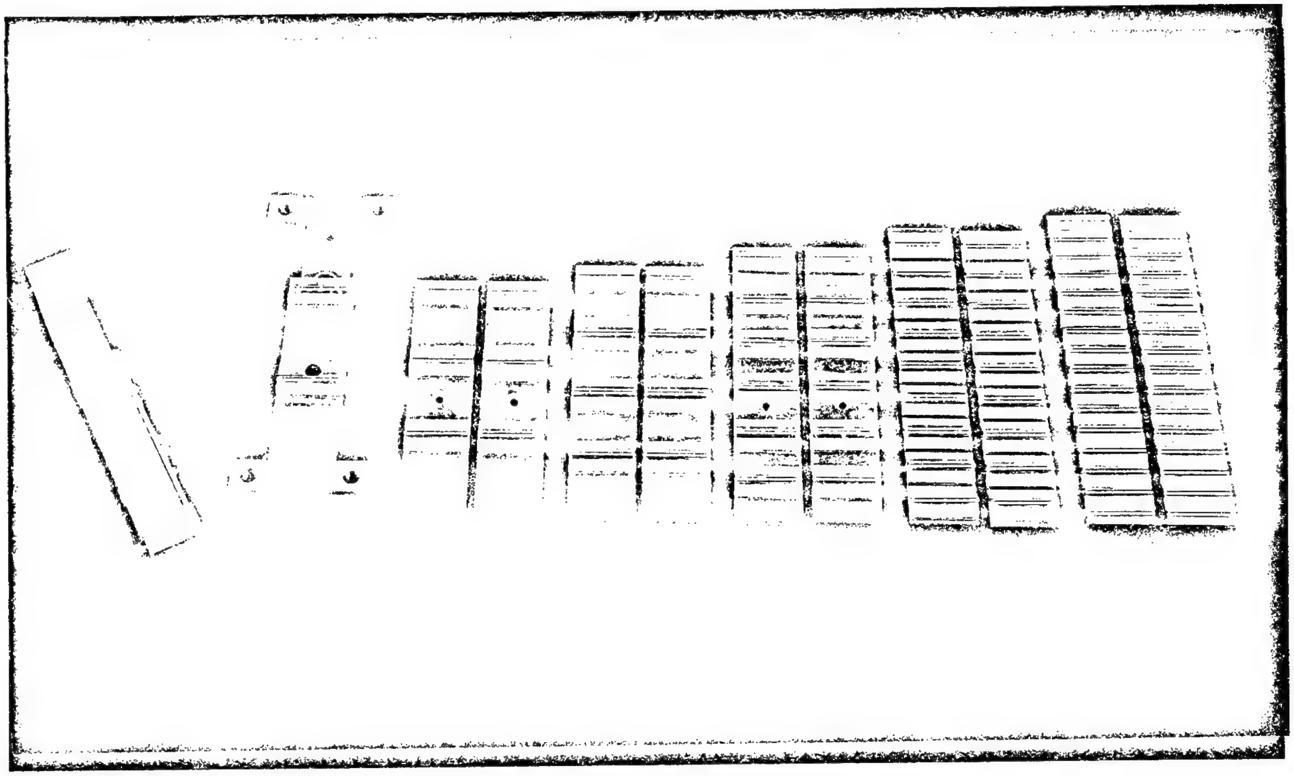

136218R

Column Test Platens of Various Pin-End Lengths

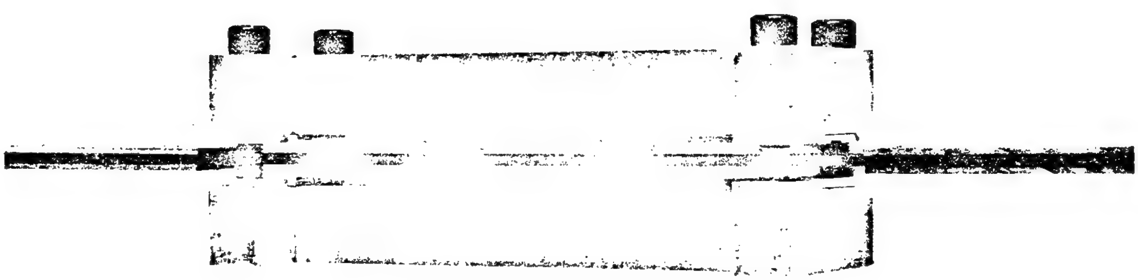

136217R

Composite Specimen Column Test Fixture

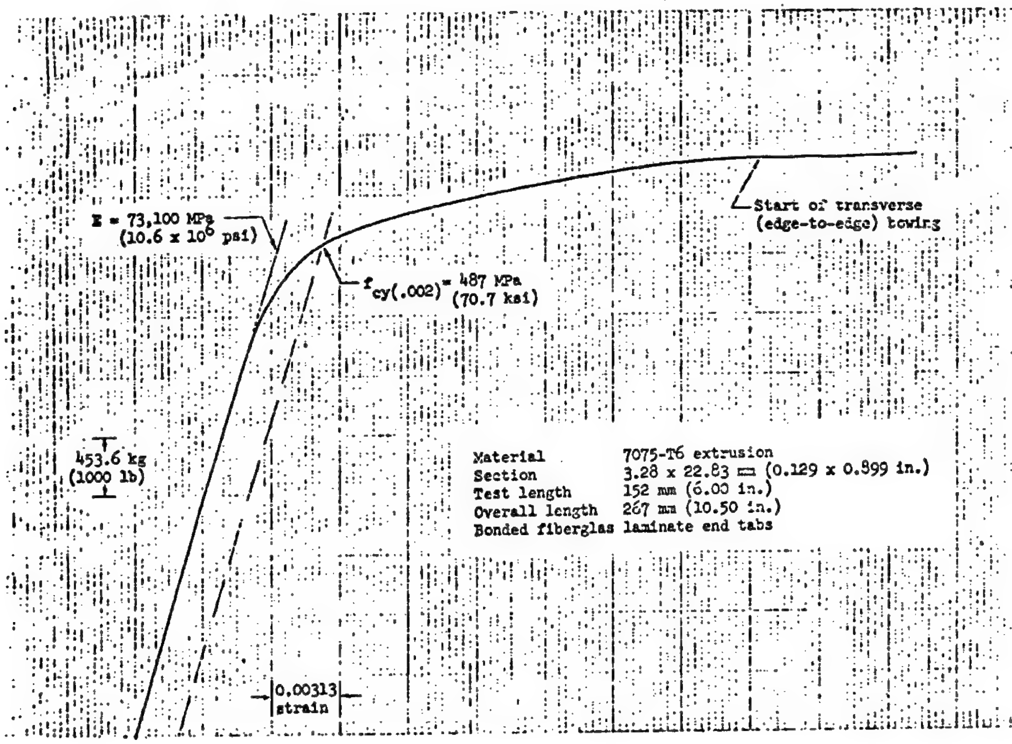

Automatically Recorded Extensometer Data Obtained During Compression Test of Al Alloy Coupon in Full Fixity Apparatus

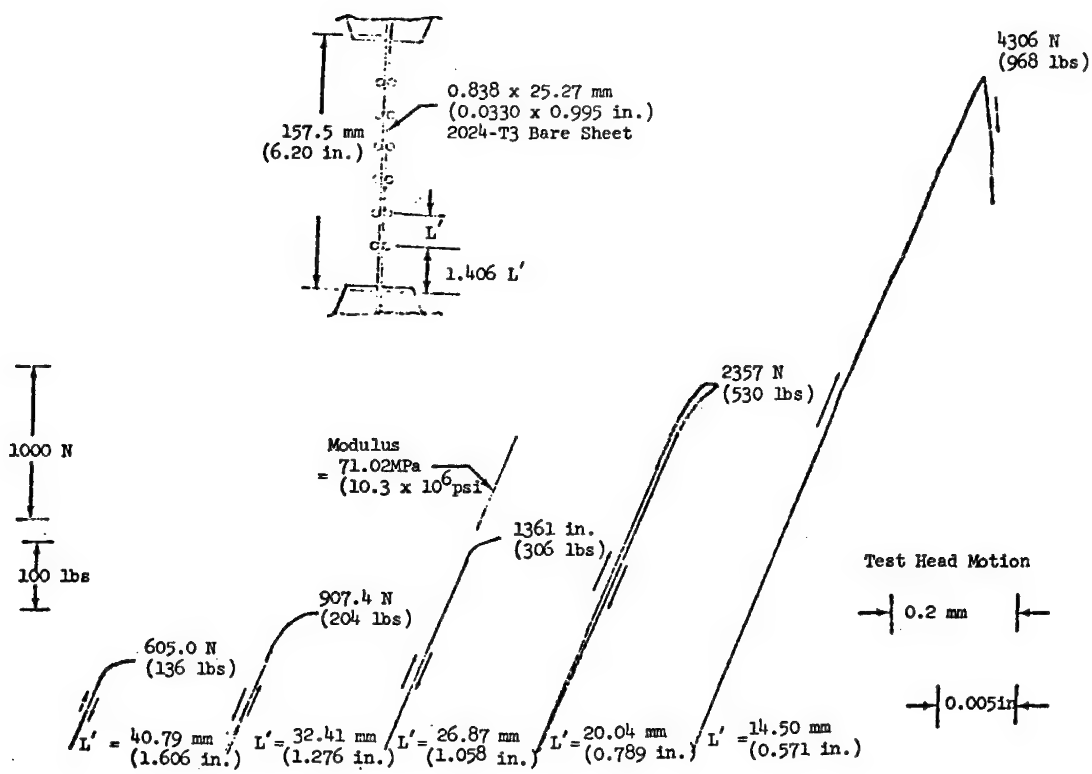

Load-Deflection Data Obtained in Tests of Aluminum Alloy Sheet Material in Column Test Apparatus

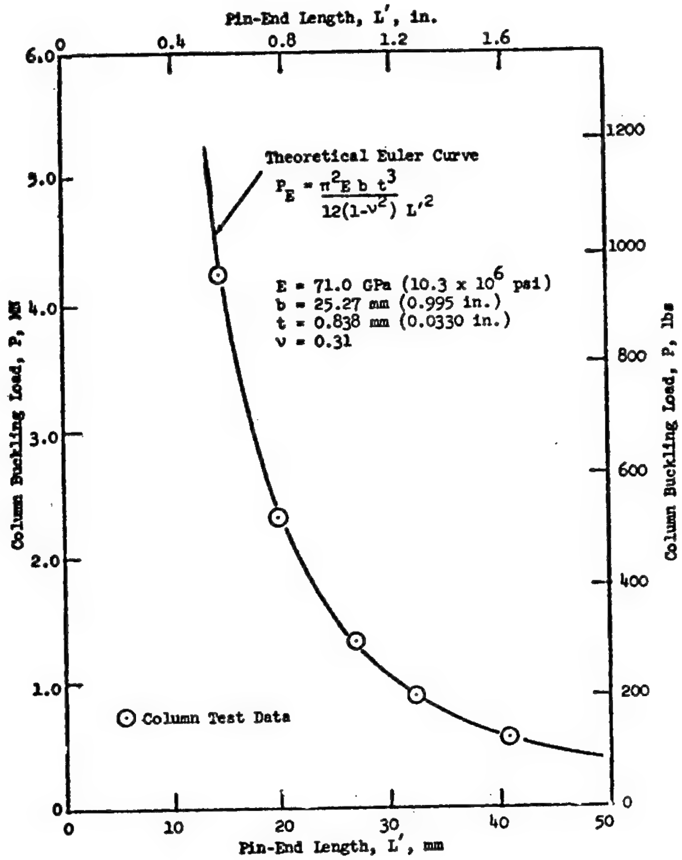

Test Data Obtained with Column Test Fixture on 2024-T3 Aluminum Alloy Specimen Compared with Euler Relation

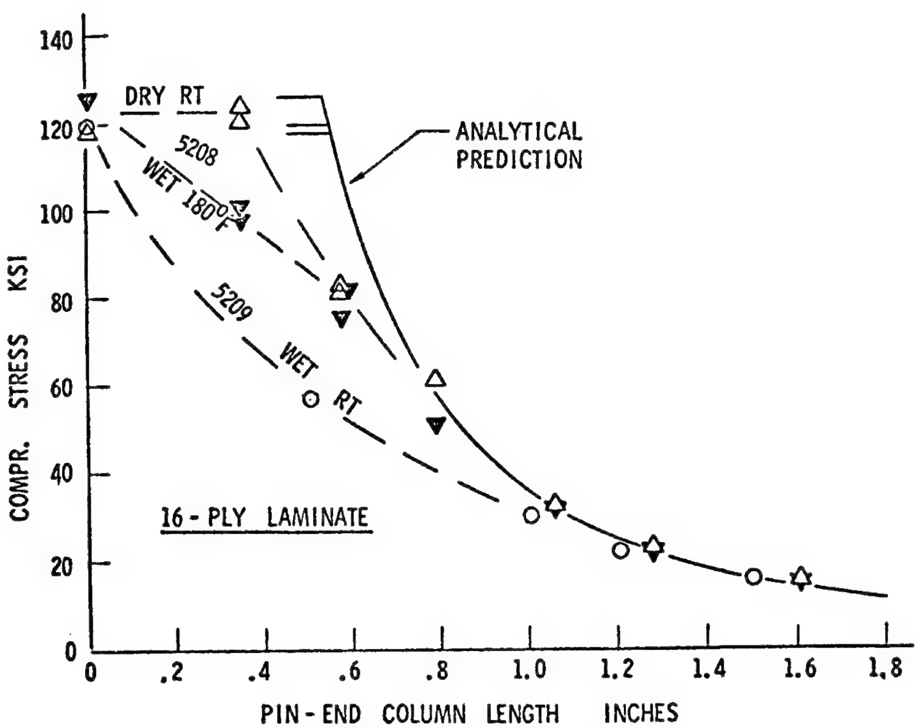

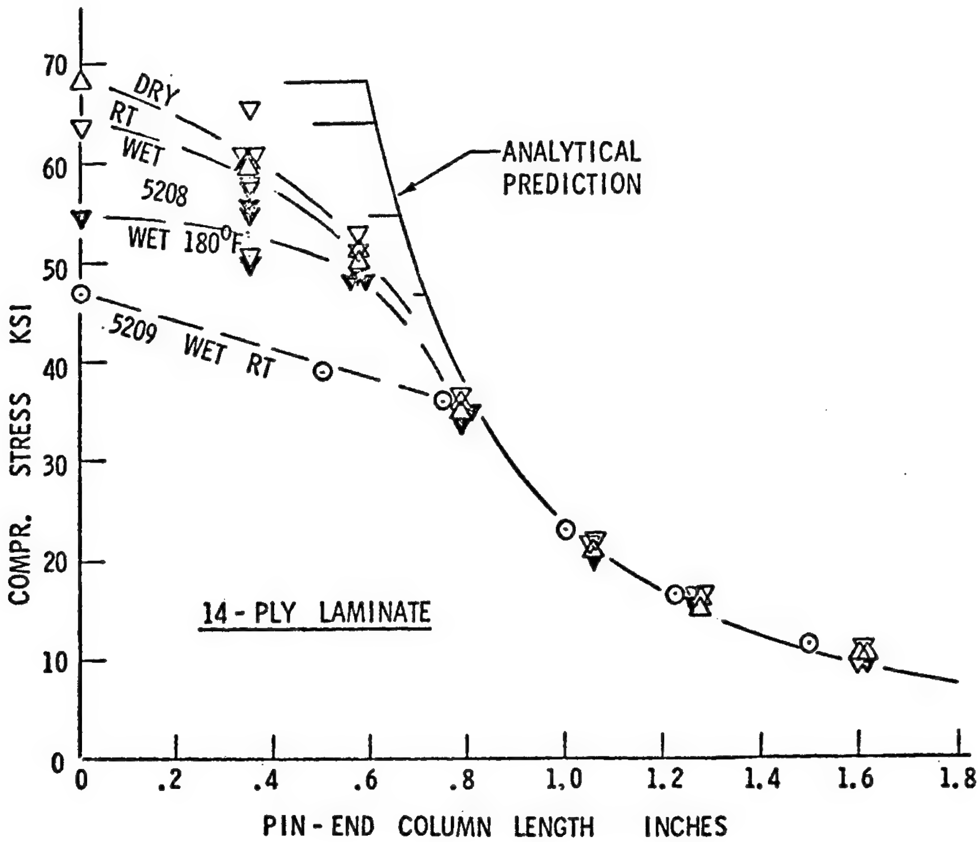

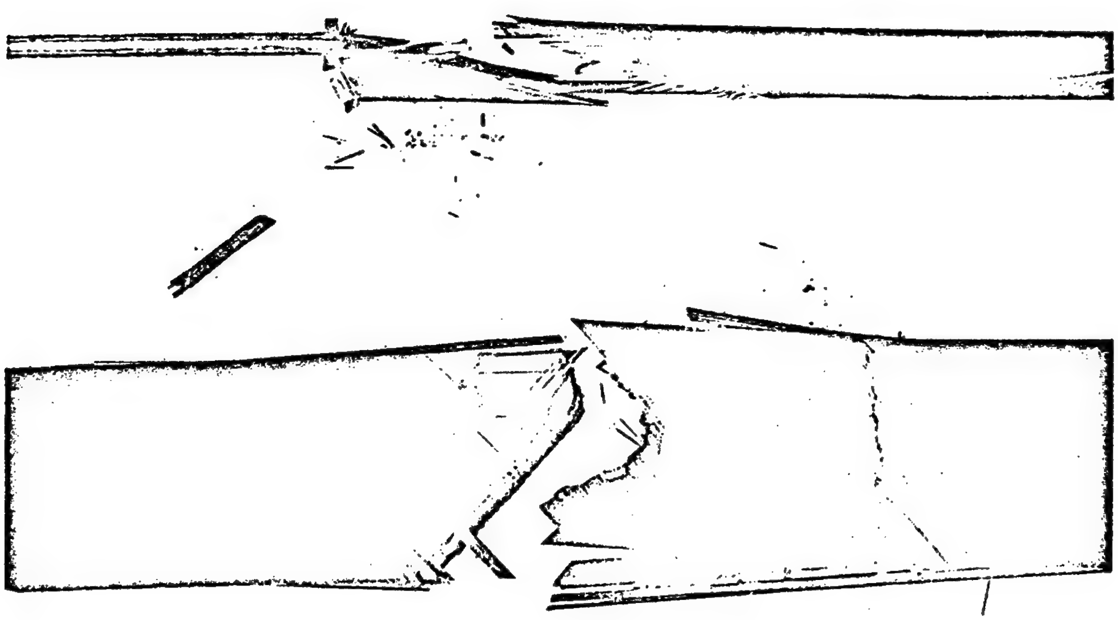

136242R

Typical Failures of T300/934 Laminate $(\pm45/0/\pm45/0_3)_s$ Dry, 70°F in Full-Fixity Apparatus

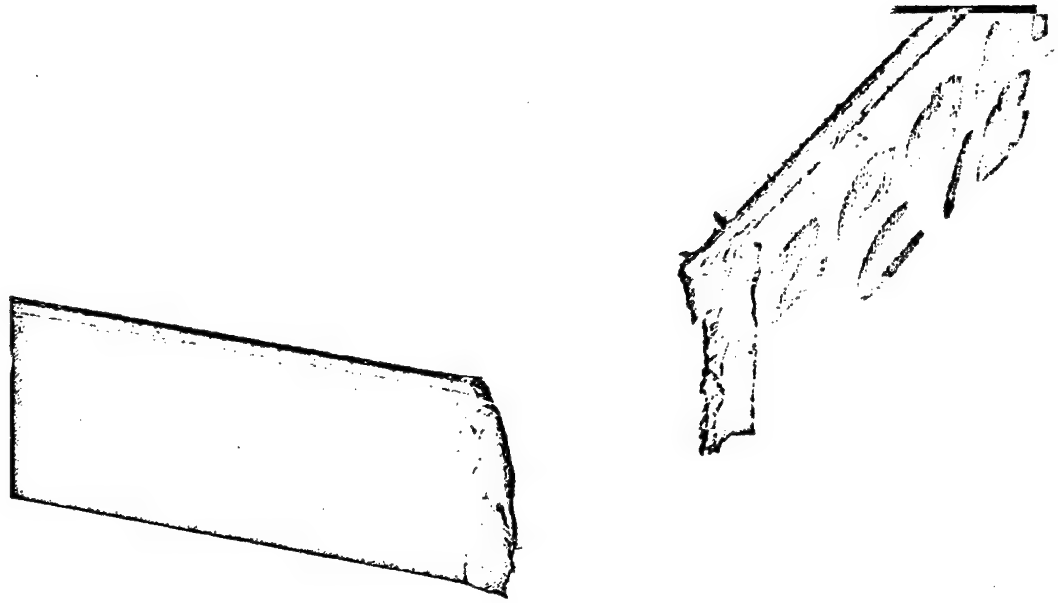

136239R

Failure Obtained in T300/5209 Laminate $(\pm45/0/\pm45/0_3)_s$ 1.0% H_2O, 70°F
Tested in Compression

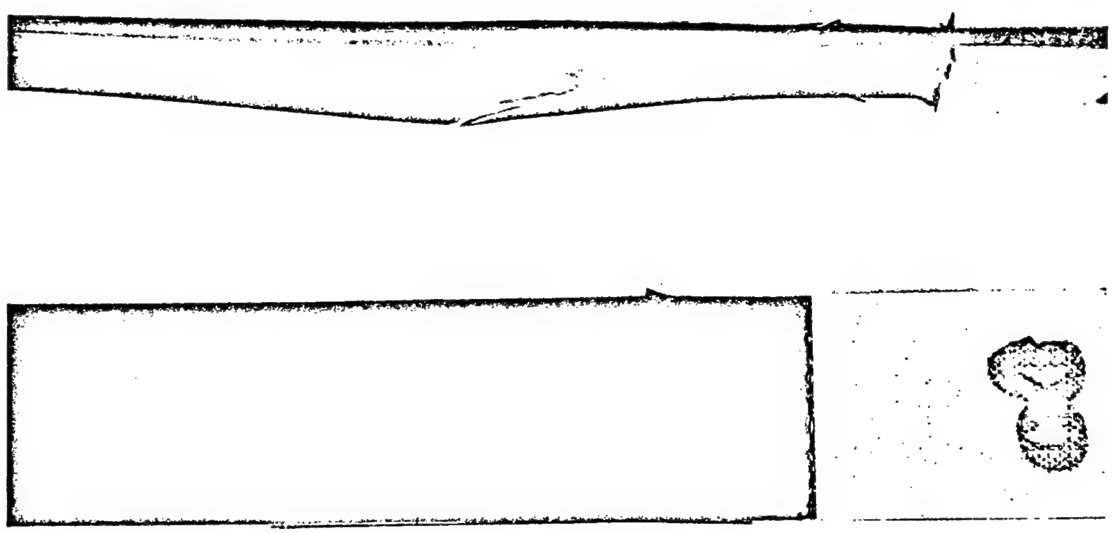

136236R

Typical Failures of T300/5208 Laminate $(\pm45/0/\pm45_2)_s$ 1.0% H_2O, 180°F in
Full-Fixity Apparatus

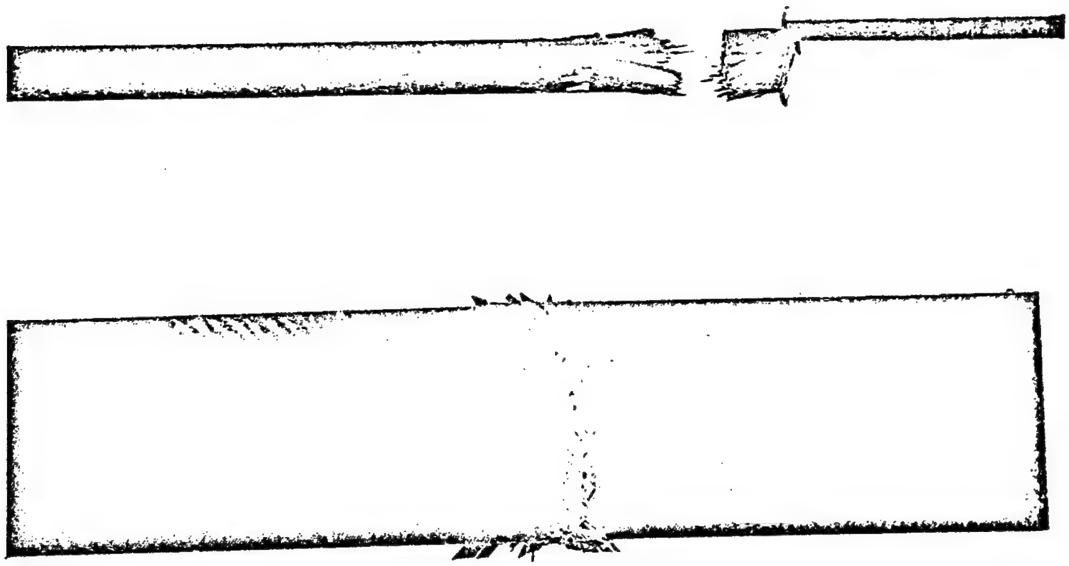

136244R

Typical Failures of T300/5208 Laminate $(\pm 45/0/\pm 45_3)_s$ Dry, 70°F Tested In Pin-End Column Apparatus, $L' = 0.571$

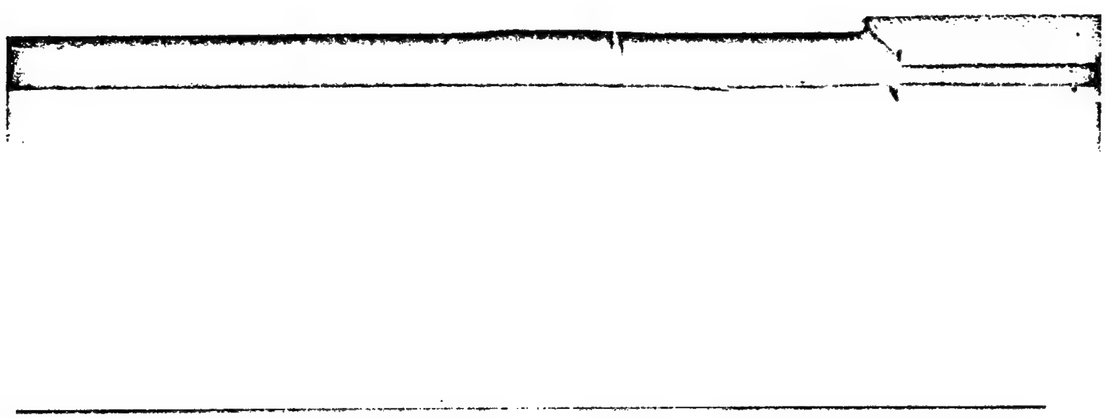

136241R

Typical Failure of T300/5208 Laminate $(\pm 45/0/\pm 45_3)$ Dry, 70°F Tested in Pin-End Column Apparatus, $L' = 0.789$

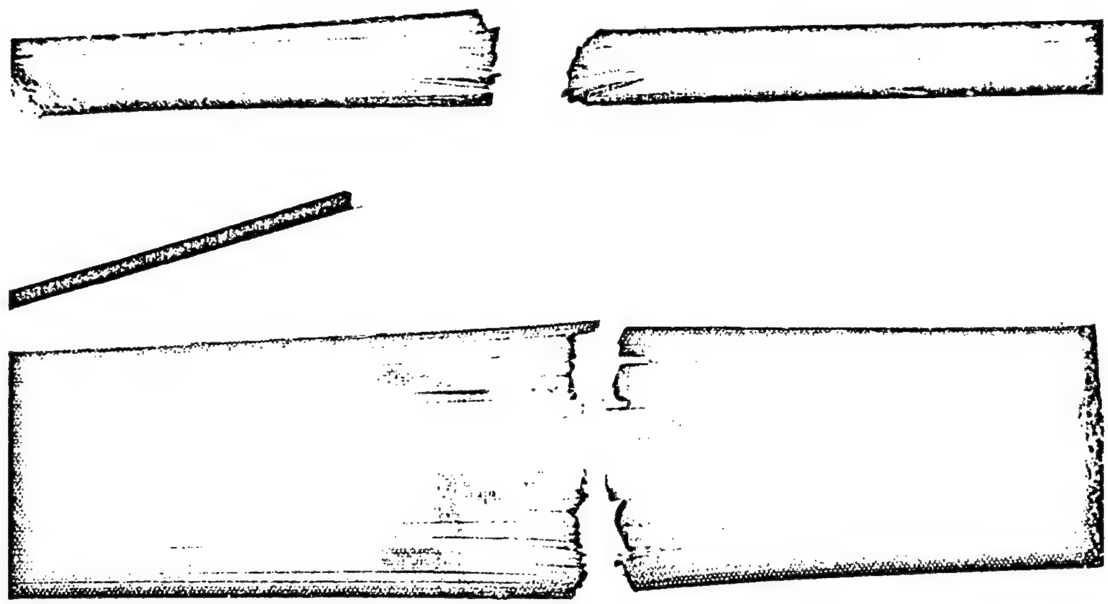

136237R

Typical Failures of T300/5209 16 Ply Unidirectional Laminate Dry, 70°F Tested in Full-Fixity Apparatus

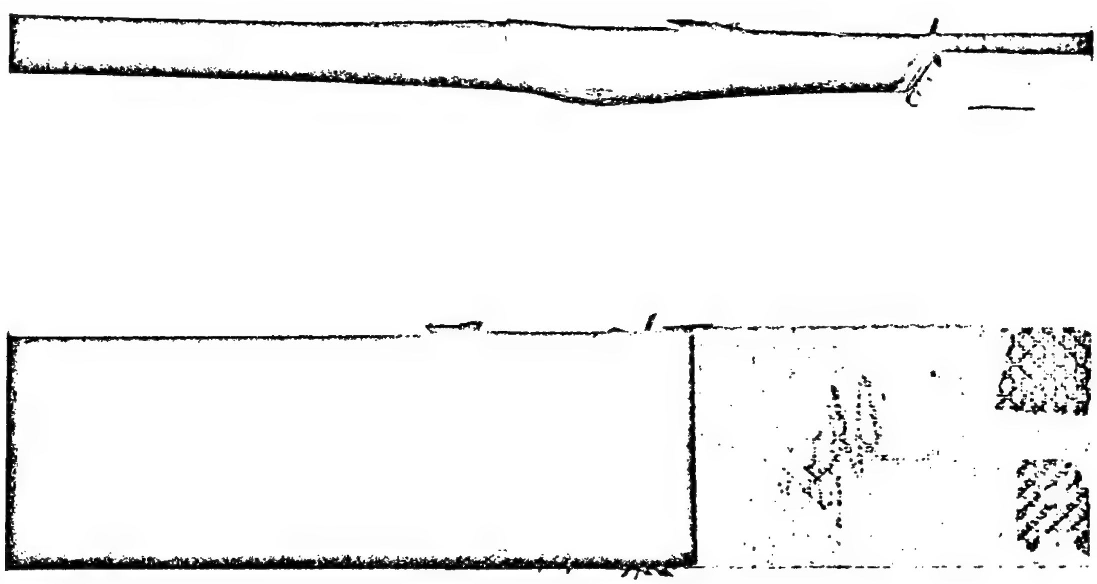

136245R

Typical Failures of T300/5208 Laminate $(\pm45/0/\pm45_3)_s$ Dry, 70°F Tested in Pin-End Column Apparatus, $L' = 0.347$

STRESS FIELDS IN COMPOSITE LAMINATES

N. J. PAGANO
NONMETALLIC MATERIALS DIVISION
AIR FORCE MATERIALS LABORATORY

<u>OBJECTIVE:</u> TO DEVELOP A TRACTABLE, REALISTIC THEORY TO PREDICT STRESS FIELDS IN COMPOSITE LAMINATES SATISFYING:

a) SIX NON-ZERO STRESS COMPONENTS

b) TRACTION AND DISPLACEMENT CONTINUITY AT INTERFACES

c) PRINCIPLE OF LAYER EQUILIBRIUM

<u>APPROACH:</u> EXTENSION OF REISSNER'S VARIATIONAL THEOREM FOR LAMINATES. USE OF ASSUMED EQUILIBRIUM STRESS FIELD.

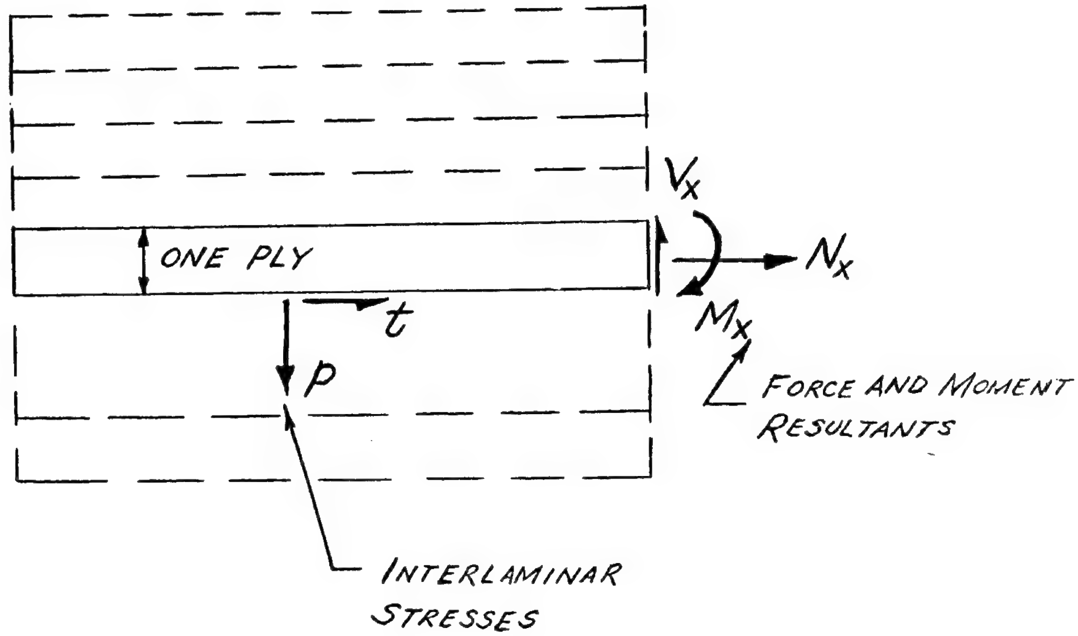

VARIATIONAL PRINCIPLE FOR LAMINATES

Let $\delta Q = 0$

where $Q = \int_V F dV - \int_{S'} P_i U_i dS$

S' = Traction boundary surface

$$F = \frac{\sigma_{ij}}{2}(U_{i,j} + U_{j,i}) - W$$

W = Complementary energy = $W(\sigma_{ij}, e_{ij})$

e_{ij} = expansional strain tensor

P_i = prescribed tractions

For a body with interfaces, we get

$$\delta Q = \sum_{K=1}^{N} \int_{V_K} \left[\left(\frac{U_{i,j}+U_{j,i}}{2} - W_{,\sigma_{ij}} \right) \delta\sigma_{ij} - \sigma_{ij,j}\delta U_i \right]^{(K)} dV_K + \int_{S'} (\tau_i - P_i)\, \delta U_i dS$$

$$+ \int_{S''} \tau_i\, \delta U_i dS + \sum_{K=1}^{N-1} \int_{I_K} \left(\tau_i^{(K)}\, \delta U_i^{(K)} + \tau_i^{(K+1)}\, \delta U_i^{(K+1)} \right) dI_K = 0$$

FORMULATION OF LAMINATE THEORY

Assumed stress (within each layer)

$$\sigma_x = \frac{1}{h}\left(N_x + \frac{6M_x\xi}{h}\right)$$

$$\sigma_y = \frac{1}{h}\left(N_y + \frac{6M_y\xi}{h}\right) \qquad \xi = \frac{2z}{h}$$

$$\tau_{xy} = \frac{1}{h}\left(N_{xy} + \frac{6M_{xy}\xi}{h}\right)$$

$$\tau_{xz} = \left(\frac{t_2-t_1}{2}\right)\xi + \left(\frac{t_1+t_2}{4}\right)(3\xi^2-1) + \frac{3V_x}{2h}(1-\xi^2)$$

$$\tau_{yz} = \left(\frac{s_2-s_1}{2}\right)\xi + \left(\frac{s_1+s_2}{4}\right)(3\xi^2-1) + \frac{3V_y}{2h}(1-\xi^2)$$

$$\sigma_z = \left(\frac{p_1+p_2}{4}\right)(3\xi^2-1) + \left(\frac{p_2-p_1}{4}\right)(5\xi^3-3\xi) + \frac{3N_z}{2h}(1-\xi^2) + \frac{15M_z}{h^2}(\xi-\xi^3)$$

Subst. into variational integral leads to <u>seven</u> equil. eqs., weighted displacement functions, and edge conditions in terms of force, moment-resultants and interfacial shear stresses. Furthermore, traction <u>and</u> disp. I.C.C. can be satisfied.

Constitutive Equations:

$$h\left(\frac{\bar{u},_x}{2} - e_x\right) = S_{11}N_x + S_{12}N_y + S_{13}N_z + S_{16}N_{xy}$$

$$h\left(\frac{\bar{v},_y}{2} - e_y\right) = S_{12}N_x + S_{22}N_y + S_{23}N_z + S_{26}N_{xy}$$

$$3w^* - he_z = S_{13}N_x + S_{23}N_y + \frac{6}{5}S_{33}N_z + S_{36}N_{xy} - \frac{S_{33}h}{10}(p_1+p_2)$$

$$h\left(\frac{\bar{u},_y + \bar{v},_x}{2} - e_{xy}\right) = S_{16}N_x + S_{26}N_y + S_{36}N_z + S_{66}N_{xy}$$

$$\frac{h^2}{4}u^*,_x = S_{11}M_x + S_{12}M_y + S_{13}M_z + S_{16}M_{xy}$$

$$\frac{h^2}{4}v^*,_y = S_{12}M_x + S_{22}M_y + S_{23}M_z + S_{26}M_{xy}$$

$$\frac{5h}{4}(3\hat{w} - \bar{w}) = S_{13}M_x + S_{23}M_y + \frac{10}{7}S_{33}M_z + S_{36}M_{xy} + \frac{S_{33}h^2}{28}(p_1 - p_2)$$

$$\frac{h^2}{4}(u^*,_y + v^*,_x) = S_{16}M_x + S_{26}M_y + S_{36}M_z + S_{66}M_{xy}$$

$$\frac{3}{4}\left(\bar{w},_y - \hat{w},_y + \frac{4v^*}{h}\right) = \frac{6}{5h}(S_{44}V_y + S_{45}V_x) - \frac{S_{44}}{10}(s_1+s_2) - \frac{S_{45}}{10}(t_1+t_2)$$

$$\frac{3}{4}\left(\bar{w},_x - \hat{w},_x + \frac{4u^*}{h}\right) = \frac{6}{5h}(S_{45}V_y + S_{55}V_x) - \frac{S_{45}}{10}(s_1+s_2) - \frac{S_{55}}{10}(t_1+t_2)$$

Interface Conditions:

a) Continuity ($k = 1, 2, \cdots N-1$)

$$t_2^{(k)} = t_1^{(k+1)}$$

$$s_2^{(k)} = s_1^{(k+1)}$$

$$p_2^{(k)} = p_1^{(k+1)}$$

$$\beta_4^{(k)} - S_{44}^{(k)} T_4^{(k)} - S_{45}^{(k)} T_5^{(k)} + \alpha_4^{(k+1)} - S_{44}^{(k+1)} Q_4^{(k+1)} - S_{45}^{(k+1)} Q_5^{(k+1)} = 0$$

$$\beta_5^{(k)} - S_{45}^{(k)} T_4^{(k)} - S_{55}^{(k)} T_5^{(k)} + \alpha_5^{(k+1)} - S_{45}^{(k+1)} Q_4^{(k+1)} - S_{55}^{(k+1)} Q_5^{(k+1)} = 0$$

$$\gamma_2^{(k)} - S_{33}^{(k)} R_2^{(k)} + \gamma_1^{(k+1)} - S_{33}^{(k+1)} R_1^{(k+1)} = 0$$

Equilibrium Equations:

$$N_{x,x} + N_{xy,y} + t_2 - t_1 = 0$$

$$N_{xy,x} + N_{y,y} + s_2 - s_1 = 0$$

$$V_{x,x} + V_{y,y} + \frac{20M_z}{h^2} + p_1 - p_2 - \frac{h}{6}(t_{1,x} + t_{2,x} + s_{1,y} + s_{2,y}) = 0$$

$$M_{x,x} + M_{xy,y} - V_x + \frac{h}{2}(t_1 + t_2) = 0$$

$$M_{xy,x} + M_{y,y} - V_y + \frac{h}{2}(s_1 + s_2) = 0$$

$$N_z - \frac{(p_1 + p_2)h}{2} + \frac{h^2}{12}(t_{1,x} - t_{2,x} + s_{1,y} - s_{2,y}) = 0$$

$$V_{x,x} + V_{y,y} + \frac{60M_z}{h^2} + 5(p_1 - p_2) - \frac{h}{2}(t_{1,x} + t_{2,x} + s_{1,y} + s_{2,y}) = 0$$

b) Prescribed Tractions and/or Displacements (k = 1, 2 ⋯ N-1)

$$\overset{(k)}{t}_2 = \overset{(k)}{\tilde{t}}_2 \quad \text{or} \quad \overset{(k)}{\beta}_5 - \overset{(k)}{S}_{45}\overset{(k)}{T}_4 - \overset{(k)}{S}_{55}\overset{(k)}{T}_5 = -\overset{(k)}{\tilde{u}}_2$$

$$\overset{(k)}{s}_2 = \overset{(k)}{\tilde{s}}_2 \quad \text{or} \quad \overset{(k)}{\beta}_4 - \overset{(k)}{S}_{44}\overset{(k)}{T}_4 - \overset{(k)}{S}_{45}\overset{(k)}{T}_5 = -\overset{(k)}{\tilde{v}}_2$$

$$\overset{(k)}{p}_2 = \overset{(k)}{\tilde{p}}_2 \quad \text{or} \quad \overset{(k)}{\gamma}_2 - \overset{(k)}{S}_{33}\overset{(k)}{R}_2 = -\overset{(k)}{\tilde{w}}_2$$

$$\overset{(k+1)}{t}_1 = \overset{(k+1)}{\tilde{t}}_1 \quad \text{or} \quad \overset{(k+1)}{\alpha}_5 - \overset{(k+1)}{S}_{45}\overset{(k+1)}{Q}_4 - \overset{(k+1)}{S}_{55}\overset{(k+1)}{Q}_5 = \overset{(k+1)}{\tilde{u}}_1$$

$$\overset{(k+1)}{s}_1 = \overset{(k+1)}{\tilde{s}}_1 \quad \text{or} \quad \overset{(k+1)}{\alpha}_4 - \overset{(k+1)}{S}_{44}\overset{(k+1)}{Q}_4 - \overset{(k+1)}{S}_{45}\overset{(k+1)}{Q}_5 = \overset{(k+1)}{\tilde{v}}_1$$

$$\overset{(k+1)}{p}_1 = \overset{(k+1)}{\tilde{p}}_1 \quad \text{or} \quad \overset{(k+1)}{\gamma}_1 - \overset{(k+1)}{S}_{33}\overset{(k+1)}{R}_1 = \overset{(k+1)}{\tilde{w}}_1$$

Boundary Conditions:

a) Edge Surface

For the edge surface, one term from each of the following products must be prescribed <u>for each layer</u> (superscripts k are omitted)

$$N_n\bar{u}_n,\ N_{ns}\bar{u}_s,\ M_n u_n^*,\ M_{ns}u_s^*,\ \left(\frac{3V_n}{h} - \frac{r_1 + r_2}{2}\right)\bar{w},$$

$$(r_2 - r_1)\,w^*,\ \left(r_1 + r_2 - \frac{2V_n}{h}\right)\hat{w}$$

b) Top Surface

The boundary conditions on the top surface are the same as the first three lines of (28) with k = N.

c) Bottom Surface

The boundary conditions on the bottom surface are the same as the last three lines of (28) with k = 0.

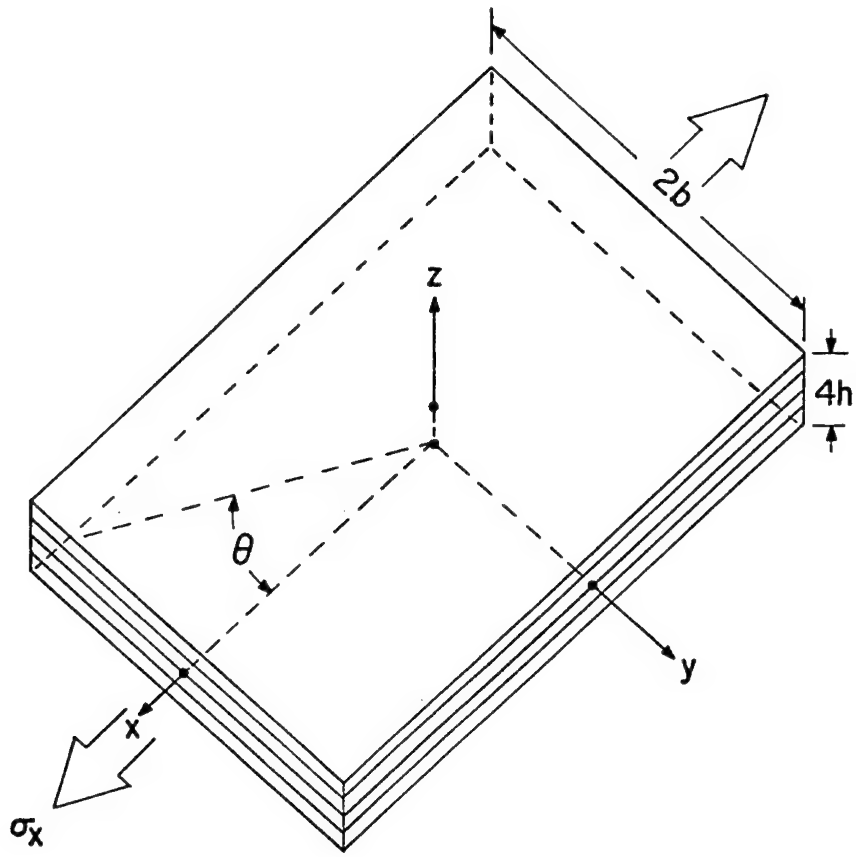

2b
z
4h
θ
y
x
σx

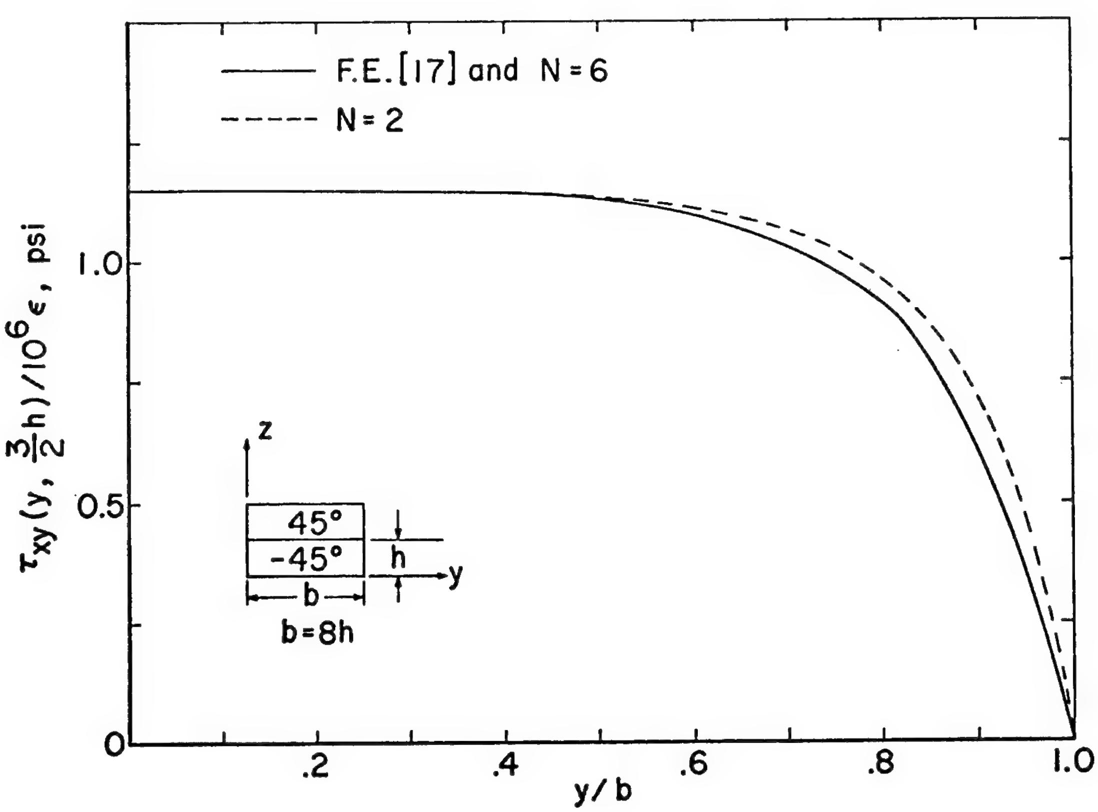

F.E. [17] and N = 6
N = 2
τxy(y, 3/2 h)/10⁶ε, psi
1.0
0.5
0
.2
.4
.6
.8
1.0
y/b
z
45°
-45°
h
y
b
b=8h

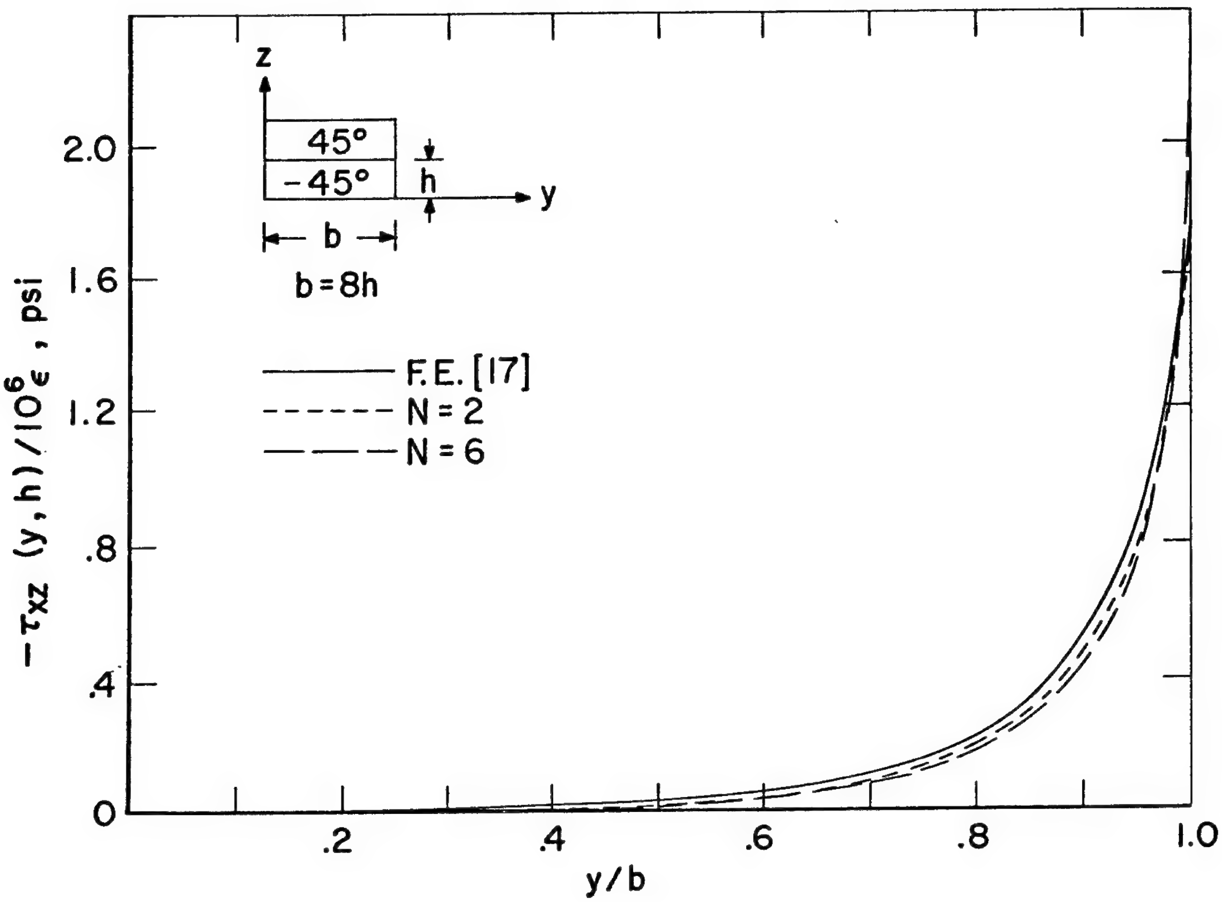

z
45°
-45°
h
y
b
b=8h
F.E. [17]
N = 2
N = 6
$-\tau_{xz}\ (y,h)/10^6\epsilon$, psi
2.0
1.6
1.2
.8
.4
0
.2
.4
.6
.8
1.0
y/b

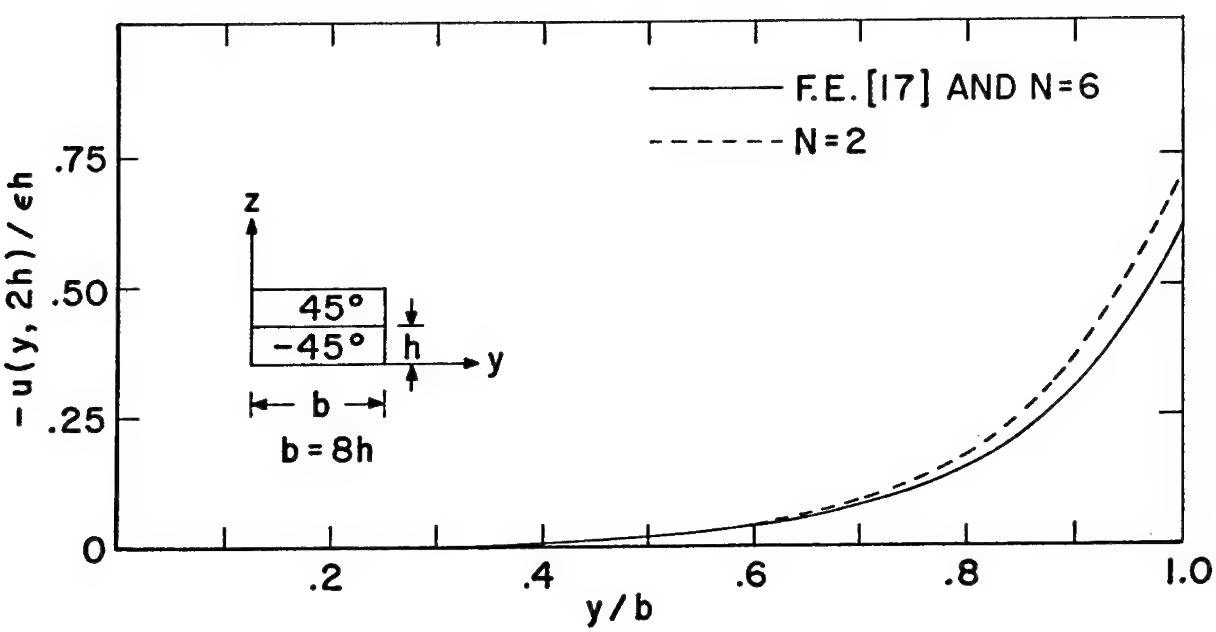

F.E. [17] AND N=6
N=2
z
45°
-45°
h
y
b
b = 8h
$-u(y, 2h)/\epsilon h$
.75
.50
.25
0
.2
.4
.6
.8
1.0
y/b

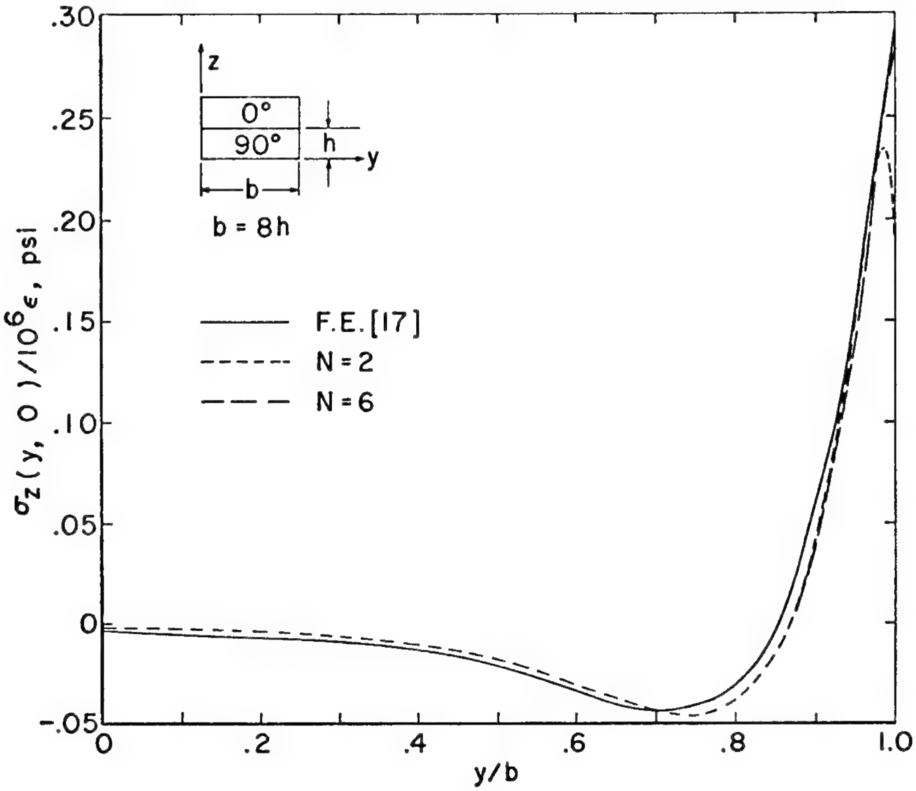
.30
.25
.20
.15
.10
.05
0
-.05
0
.2
.4
.6
.8
1.0
y/b
$\sigma_z(y, 0)/10^6\epsilon$, psi
z
0°
90°
h
y
b
b = 8h
F.E. [17]
N = 2
N = 6

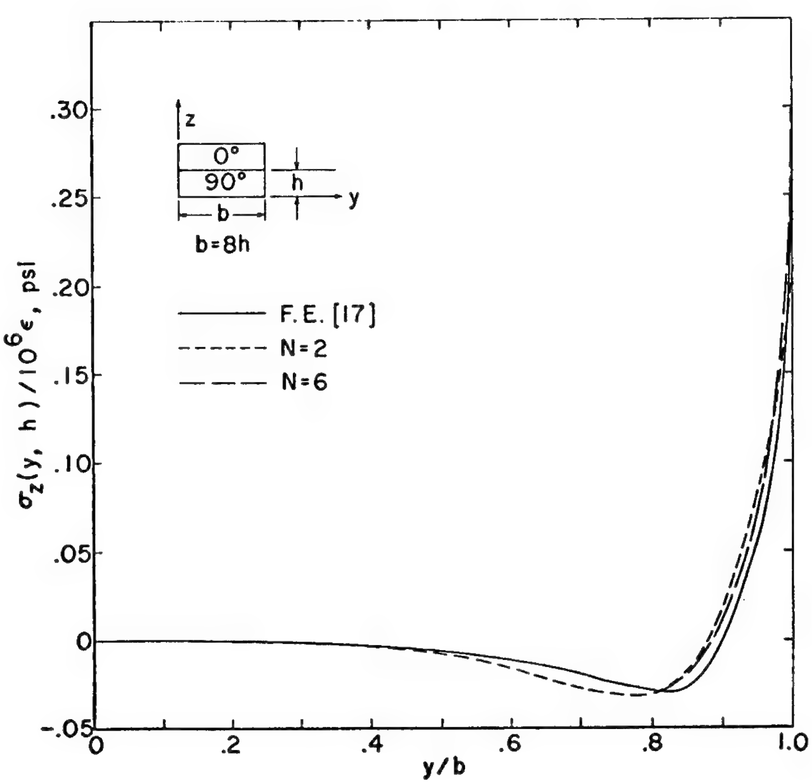
.30
.25
.20
.15
.10
.05
0
-.05
0
.2
.4
.6
.8
1.0
y/b
$\sigma_z(y, h)/10^6\epsilon$, psi
z
0°
90°
h
y
b
b=8h
F.E. [17]
N=2
N=6

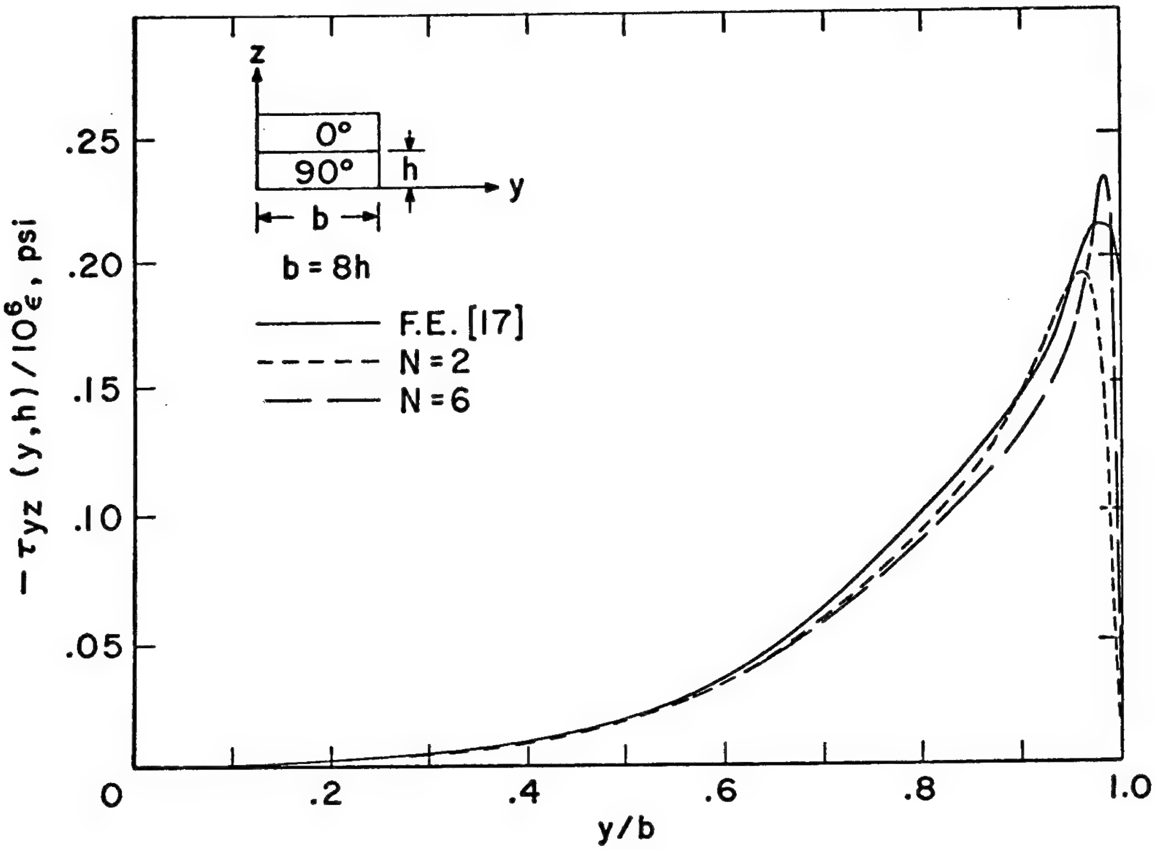

CONCLUSIONS

1. APPROXIMATE THEORY MAY BE ADEQUATE FOR LAMINATE ANALYSIS.
2. LIMITATIONS IMPOSED BY SOLUTION TECHNIQUE.
3. NATURE OF INDICATED SINGULARITIES NEED FURTHER STUDY.
4. METHOD TO INTERPRET (SINGULAR) STRESS FIELDS NEEDED.

COMPOSITE STRUCTURE OPTIMAL

DESIGN BY ENERGY METHODS

R.W. McLay
University of Vermont

M.C. Murphy
Norwich University

OBJECTIVES: To formulate and test appropriate optimization criteria for the design of fail-safe aerospace composite structures. Since design criteria are based on failure modes and since many composites of interest in aerospace applications fail by fracture, a specific research objective is the development of criteria predicting fracture onset, fracture pattern, and fracture arrest.

ACCOMPLISHMENTS: A theory of fracture has been developed for a quasi-static, quasi-reversible fracture process in a composite with n fracture energies describing the dissipative processes. A minimum principle has been developed from the Calculus of Variations for predicting the crack pattern in a composite. The development leads to a theory of crack movement and extends the conditions for crack initiation and crack arrest previously established for an isotropic material. Numerical methods including the use of the J-integral have been developed and are being evaluated. Test methods for measuring the fiber-matrix interface parameters continue under evaluation.

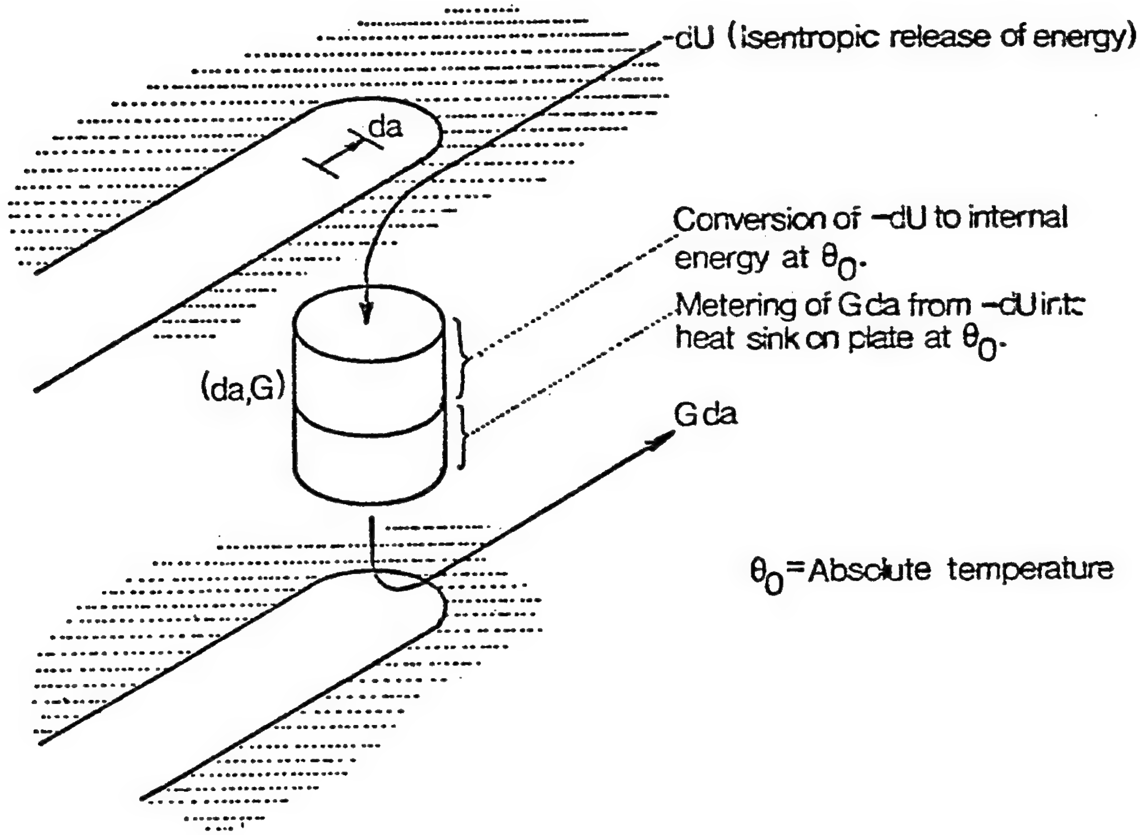

$$\frac{dS}{dt} = \frac{1}{\theta_0}\left[-\frac{\partial U}{\partial a}\frac{da}{dt} - \sum_i \frac{\partial U}{\partial al_i}\frac{dal_i}{dt} - G_{Mat}\frac{da}{dt} - \sum_i G_{Int}\frac{dal_i}{dt}\right] \geq 0.$$

$$I = -\frac{\partial U}{\partial a}\frac{da}{dt} - \sum_i \frac{\partial U}{\partial al_i}\frac{dal_i}{dt} - G_{Mat}\frac{da}{dt} - \sum_i G_{Int}\frac{dal_i}{dt}$$

$$\int_0^t I\, d\tau = -U(a,al_i) + U(0) - G_{Mat}\, a - \sum_i G_{Int}\, al_i > 0.$$

$$-U(\overline{a},\overline{al}_i) - G_{Mat}\,\overline{a} - \sum_i G_{Int}\,\overline{al}_i \geq$$
$$- U(\overline{a},al_i) - G_{Mat}\,\overline{a} - \sum_i G_{Int}\,al_i$$

Of all crack patterns in a linear planar composite, the one minimizing

$$U(\overline{a}, al_i) + \sum_i G_{Int}\, al_i$$

subject to the constraint

$$-\frac{\partial U}{\partial a} = G_{Mat}$$

maximizes the system entropy.

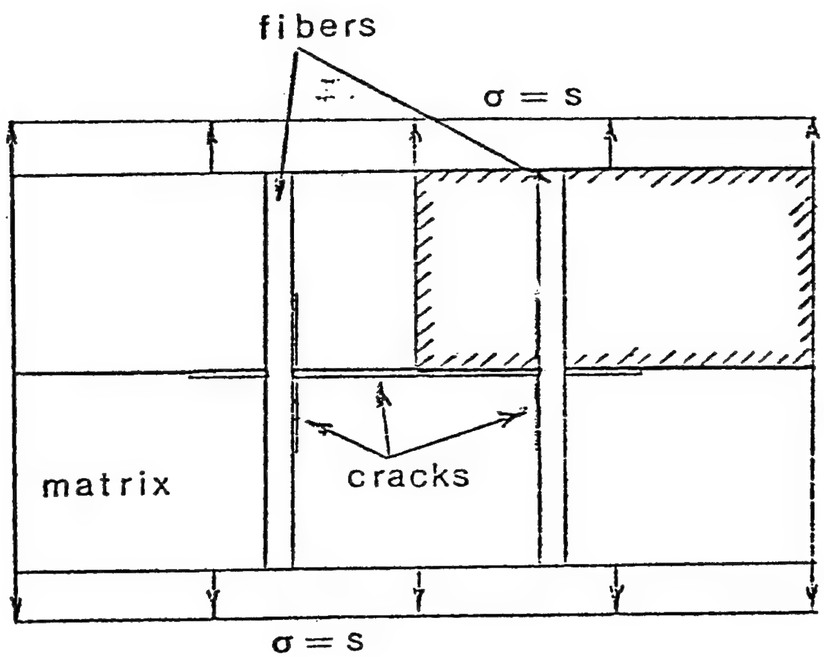

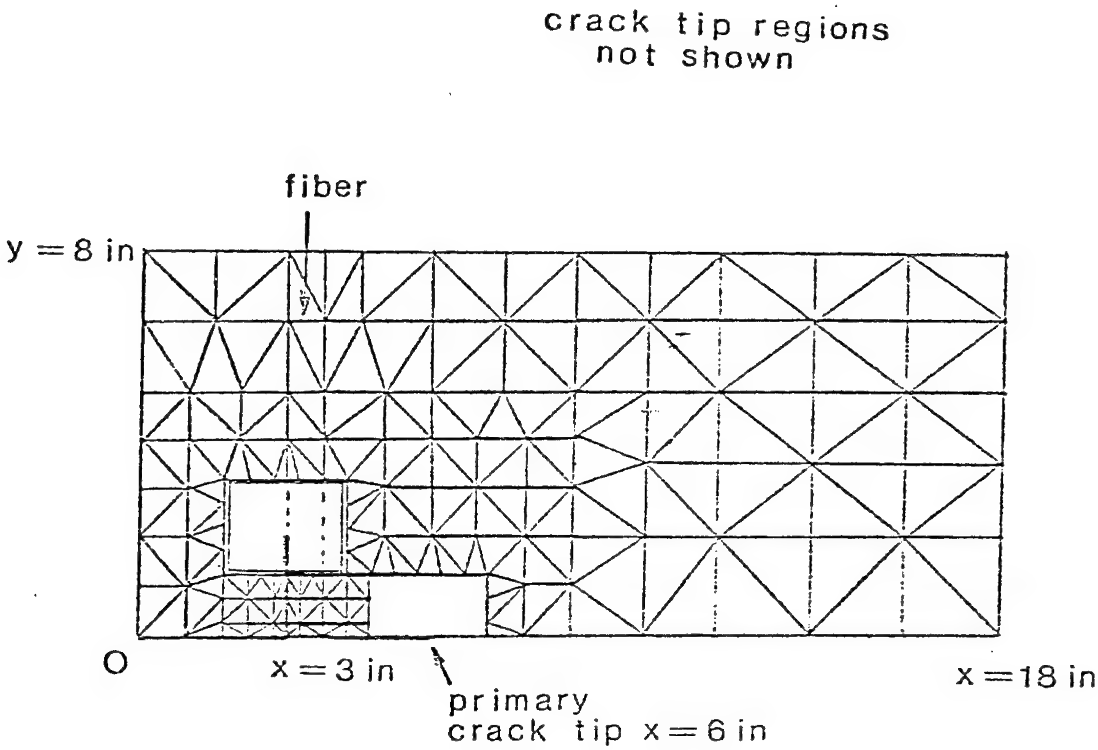
crack tip regions
not shown
fiber
y = 8 in
O
x = 3 in
primary
crack tip x = 6 in
x = 18 in

[28]

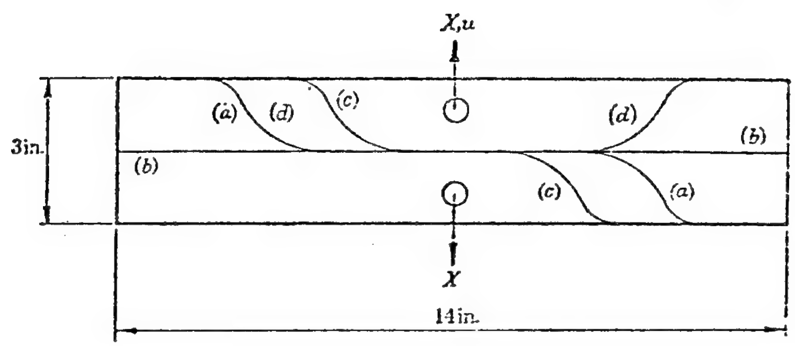
X,u
X
3in.
14in.
(a)
(b)
(c)
(d)

INFLUENCE OF MOISTURE ABSORPTION/ELEVATED TEMPERATURE ON THE DYNAMIC BEHAVIOR OF RESIN MATRIX COMPOSITES: PRELIMINARY RESULTS

G. Maymon, R. P. Briley, L. W. Rehfield

School of Aerospace Engineering
Georgia Institute of Technology
Atlanta, Georgia 30332

Presented at the ASTM Symposium on
Environmental Effects on Advanced Composite
Materials
Dayton, Ohio
September 29-30, 1977

This work was supported by the United States Air Force Office of Scientific Research under Grant AFOSR-73-2479.

OBJECTIVE

Determine the nature and extent of the influence of moisture/elevated temperature on the dynamic behavior of resin matrix composites.

SCOPE

Changes in fundamental natural frequency and damping due to moisture absorption and elevated temperature have been determined for cantilever graphite/epoxy beams. Specimens of three distinct layups have been tested at two limiting reference conditions--- dry at room temperature ($77^{o}F$, $25^{o}C$) and near complete moisture saturation at $200^{o}F$ ($93^{o}C$).

OVERVIEW OF EXPERIMENTAL PROGRAM

1. Specimens are oven dried, weighed and vibration tested at room temperature.

2. Conditioning in a constant temperature water bath at 200°F until moisture saturation is completed.

3. Specimens are weighed, vibration tested in the hot, wet condition, and re-weighed.

4. A re-drying cycle is completed.

5. Room temperature vibration tests are repeated.

SPECIMENS

- Manufactured from Narmco 5208/T300 unidirectional tape by McDonnell Douglas

- Symmetric layups, 12-plies thick, fiber volume fraction 61.5 percent

- Three distinct layups:

  A. All $[0]$ plies

  B. $[\pm 45]$ ply layup

  C. $[0_2, +45_2, 90_1, -45_1]_s$

- Beam specimens nominally 1" x 8"

TESTING TECHNIQUE

- Transient excitation is used for a short duration test.

- Response is sensed by a piezoelectric accelerometer mounted on the beam tip.

- Fundamental frequency is determined simply by counting the number of peak values contained in a suitably chosen time interval.

- Values of damping coefficient are obtained by the logarithmic decay method.

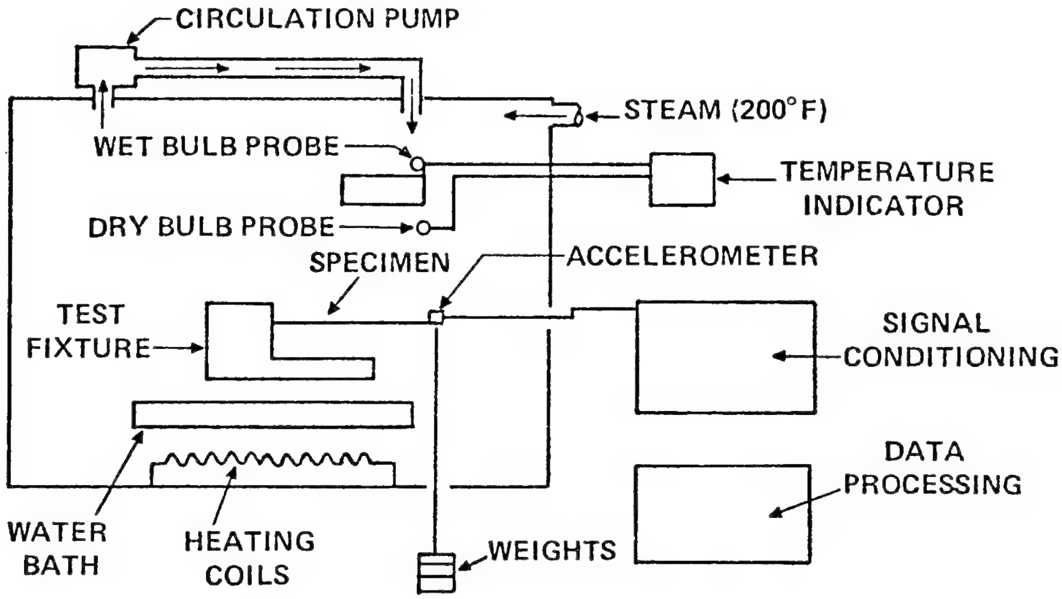

RESULTS

Fundamental frequency information is presented in terms of E_f, the effective dynamic modulus in simple flexure.

$$E_f = \frac{128\ L^4}{\pi^2 I} \left[m\left(\frac{3}{2} - \frac{4}{\pi}\right) + \frac{M_t}{L} \right] f_1^{\,2}$$

SUMMARY OF MAJOR FINDINGS

1. Stiffness of A and C specimens is largely unchanged by environmental effects. A substantial, reversible degradation of stiffness occurs for B specimens due to hot, wet conditioning.

2. Damping is altered for all specimens due to hot, wet conditioning. (A-increase; B, C-decrease)

3. Damping and data scatter appear to be sensitive to matrix microcracking.

CONCLUSION

Moisture absorption and elevated temperature can alter stiffness reversibly in matrix controlled modes of deformation and damping characteristics substantially in both fiber and matrix controlled modes. Flutter and vibration engineers are alerted that these factors cannot be ignored when dynamic requirements dictate aspects of vehicle structural design.

BEHAVIOR OF ADVANCED COMPOSITE ISOGRID STRUCTURES

United States Air Force Office of Scientific Research

Contract F49620-77-C-0077

Principal Investigator:

L. W. Rehfield

MCDONNELL DOUGLAS CORPORATION

OBJECTIVE

Explore the potential of a new, advanced structural concept that has emerged from a manufacturing technology program at McDonnell Douglas Corporation.

The concept combines synergistically the efficiency of a stiffened structure with the superior specific stiffness and strength of an advanced composite materials system in a manner consistent with automated manufacturing technology.

ISOGRID IS AN EFFICIENT, LOW-COST STIFFENING APPROACH

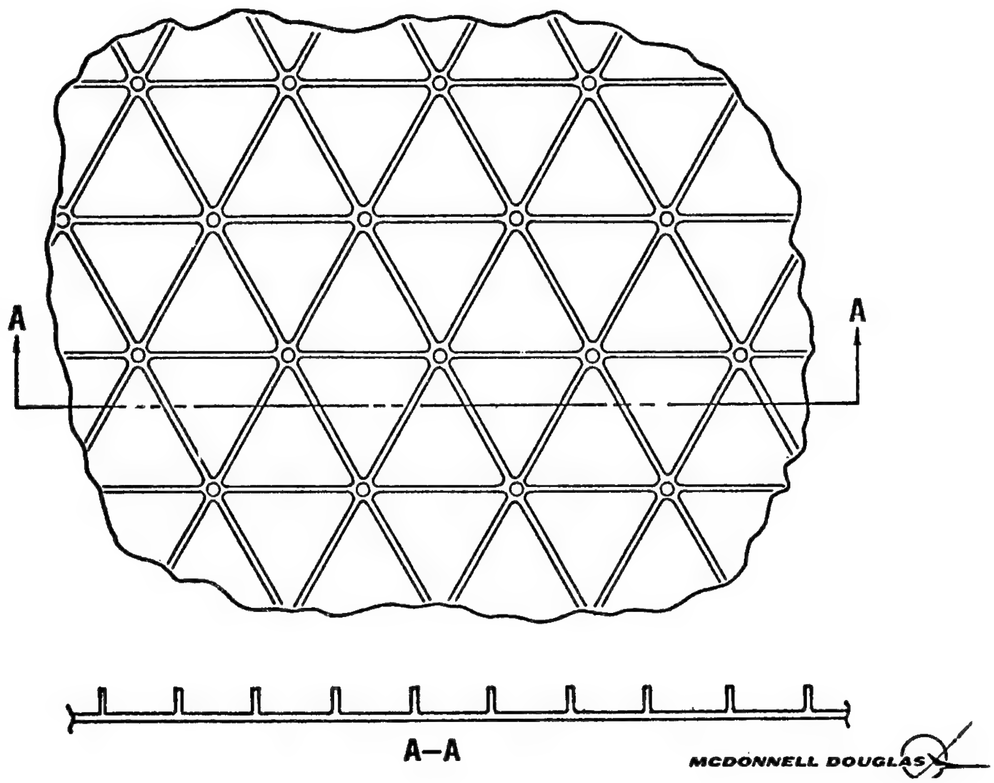

WIDE COLUMN DESIGN

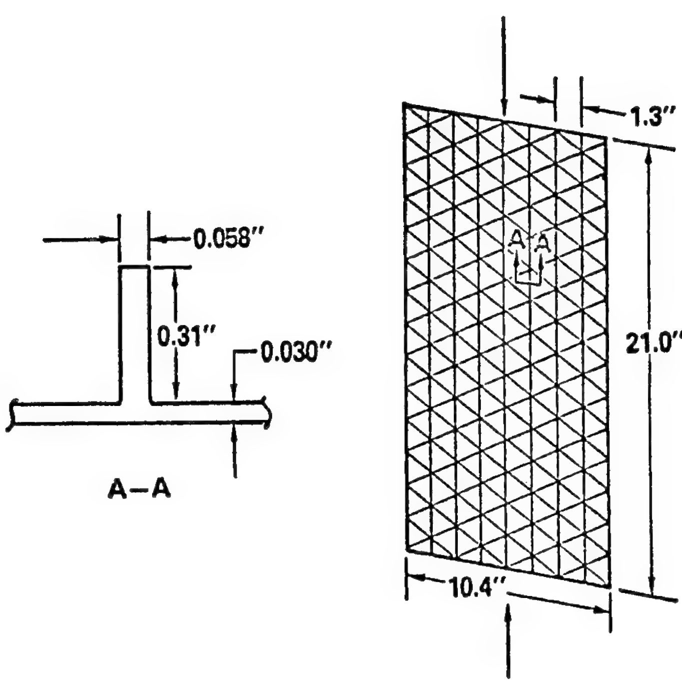

CYLINDER DESIGN

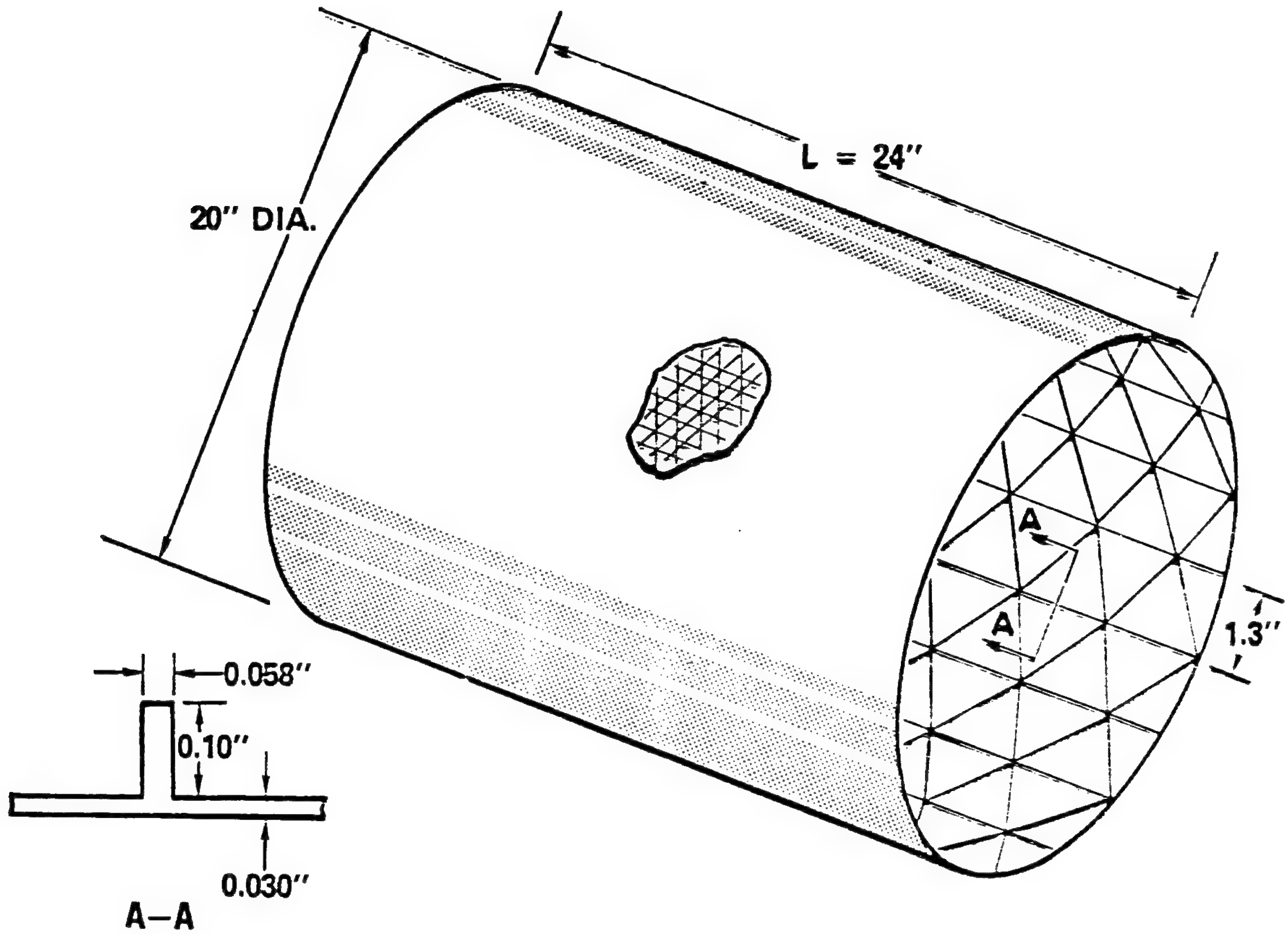

RESIDUAL STRENGTH DEGRADATION AND EFFECT OF HIGH LOADS ON FATIGUE BEHAVIOR OF COMPOSITE LAMINATES

PRINCIPAL INVESTIGATORS

C. T. SUN
PURDUE UNIVERSITY

J. N. YANG
GEORGE WASHINGTON UNIVERSITY

PROJECT PERIOD: 6/7/77 - 6/1/78

OBJECTIVES:

1. PERFORM TESTS ON GRAPHITE/EPOXY UNNOTCHED LAMINATES UNDER CONSTANT AMPLITUDE FATIGUE LOADING WITH LARGE SAMPLE SIZE.
2. CORRELATE THE LARGE DATA BASE GENERATED WITH THE THEORETICAL RESIDUAL STRENGTH DEGRADATION MODEL.
3. ANALYZE THE EXISTING TENSION-COMPRESSION FATIGUE DATA WITH A RESIDUAL STRENGTH DEGRADATION MODEL.

FATIGUE AND RESIDUAL STRENGTH DEGRADATION FOR GRAPHITE/EPOXY COMPOSITES UNDER TENSION-COMPRESSION CYCLIC LOADING

(A) OBJECTIVE

(1) GENERALIZATION OF RESIDUAL STRENGTH DEGRADATION MODEL FOR GRAPHITE/EPOXY COMPOSITES UNDER TENSION-COMPRESSION FATIGUE

(2) VERIFICATION OF THE THEORETICAL MODEL BY THE EXPERIMENTAL RESULTS

(B) PRINCIPAL FINDING AND CONCLUSION

(1) THE THEORETICAL MODEL CORRELATES VERY WELL WITH THE EXPERIMENTAL RESULTS FOR GRAPHITE/EPOXY COMPOSITES UNDER BOTH TENSION-COMPRESSION AND TENSION-TENSION FATIGUE

(2) THE CORRELATION IS BASED ON THE STATISTICAL DISTRIBUTIONS OF BOTH THE FATIGUE LIFE AND THE RESIDUAL STRENGTH

(1) THEORETICAL DISTRIBUTION OF FATIGUE LIFE

$$F_N(n) = 0 \qquad ; \quad n<0$$

$$= 1 - \exp\left\{-\left[\frac{n+(\sigma_{max}^c/\beta^c K S^b)}{1/KS^b}\right]^{\alpha/c}\right\} ; \quad n \geq 0$$

(2) THEORETICAL DISTRIBUTION OF RESIDUAL STRENGTH FOR SURVIVING SPECIMENS

$$F_{R^*(n)}(x) = 1 - \exp\left\{\left[\frac{\sigma_{max}^c+\beta^c K S^b n}{\beta^c}\right]^{\alpha/c} - \left[\frac{x^c+\beta^c K S^b n}{\beta^c}\right]^{\alpha/c}\right\} ; \quad x \geq \sigma_{max}$$

IN WHICH

N = FATIGUE LIFE

n = NO. OF CYCLES

σ_{max} = MAXIMUM STRESS LEVEL

S = STRESS RANGE

$R^*(n)$ = RESIDUAL STRENGTH AFTER n CYCLES

α = SHAPE PARAMETER OF ULTIMATE STRENGTH

β = CHARACTERISTIC ULTIMATE STRENGTH (SCALE PARAMETER)

c = CONSTANT

b = CONSTANT

K = CONSTANT

THEORETICAL RESULT (Gr/E LAMINATES)

$\alpha = 24.954$, $\beta = 70.7$ ksi

(i) TENSION-COMPRESSION FATIGUE ($\sigma_{min} = -16$ ksi)

$c = 12.0$, $b = 12.267$, $K = 5.56\times10^{-27}$

(ii) TENSION-TENSION FATIGUE ($\sigma_{min} = 0$ ksi)

$c = 12.13$, $b = 17.34$, $K = 4.99\times10^{-35}$

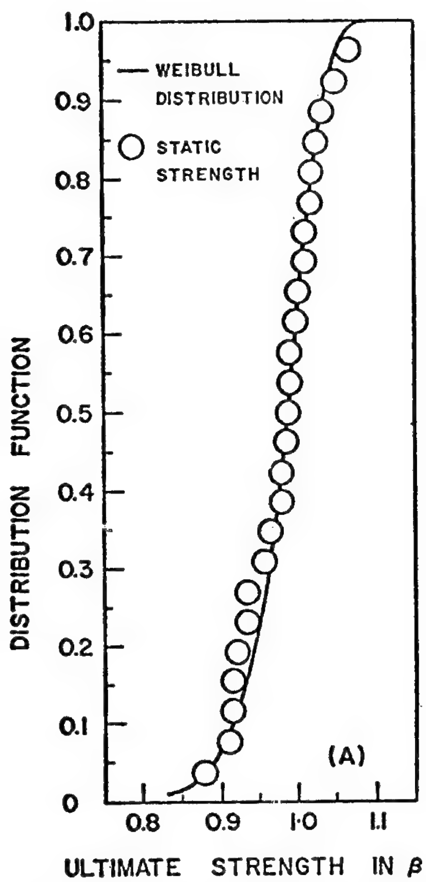

Fig. 1: Distribution Function of Ultimate Strength.

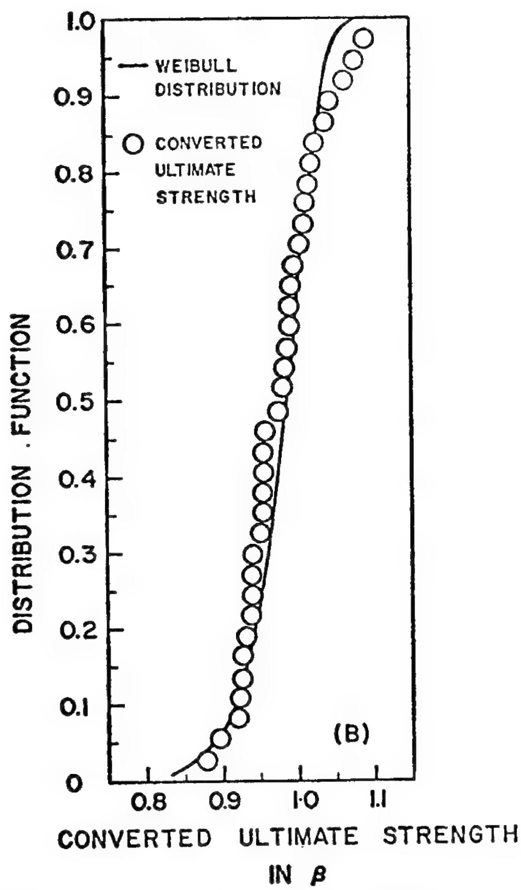

Fig. 2: Distribution Function of Converted Ultimate Strength From Tension-Compression Fatigue Data.

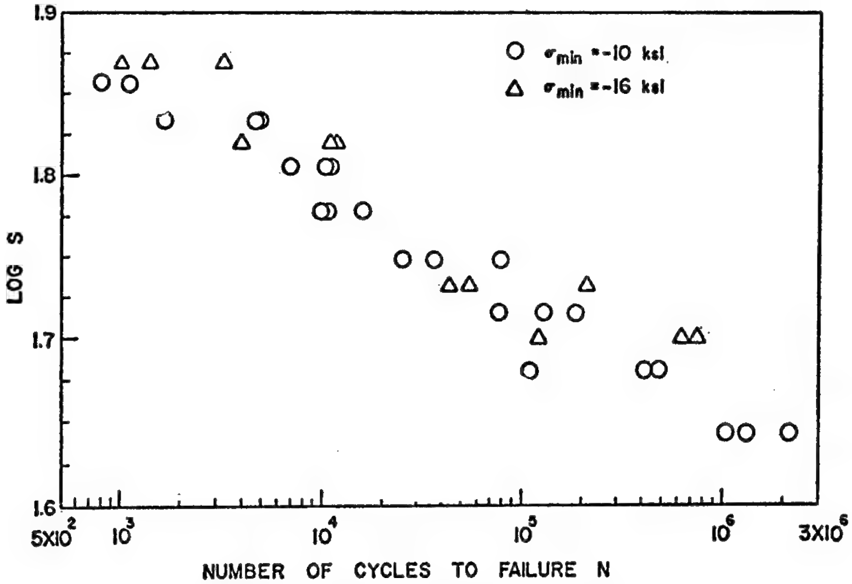

Fig. 3: Stress Range S vs. Number of Cycles to Failure N.

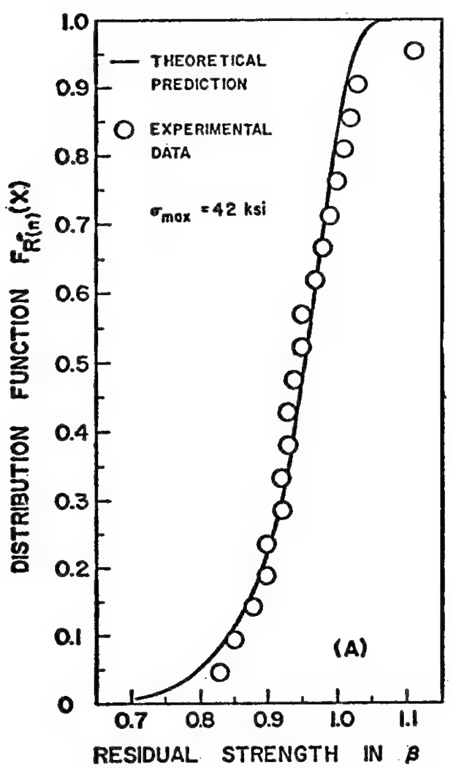

Fig. 4: Distribution Function of Residual Strength,
σ_{min} = -16 ksi , σ_{max}=42 ksi , n=14,400 cycles.

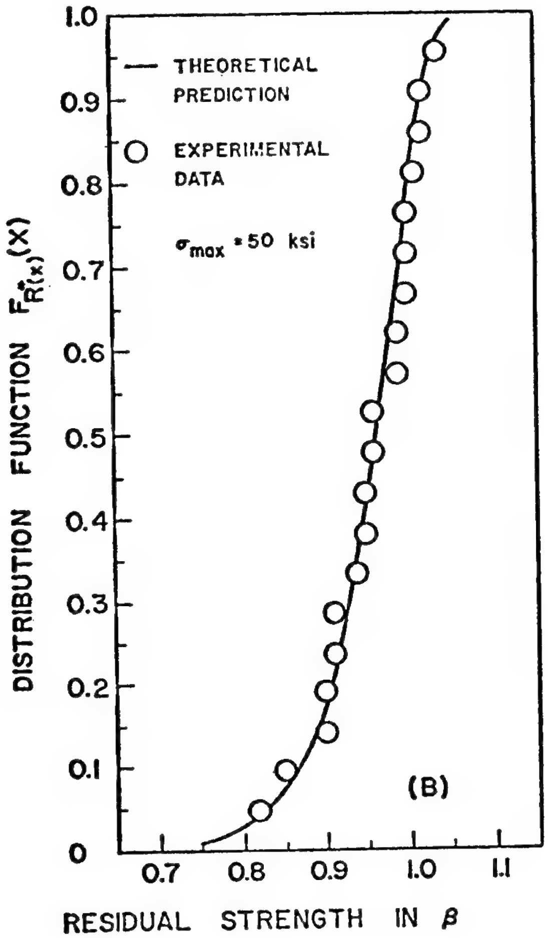

Fig. 5: Distribution Function of Residual Strength, σ_{min}= -16 ksi , σ_{max}=50 ksi , n=2,150 cycles.

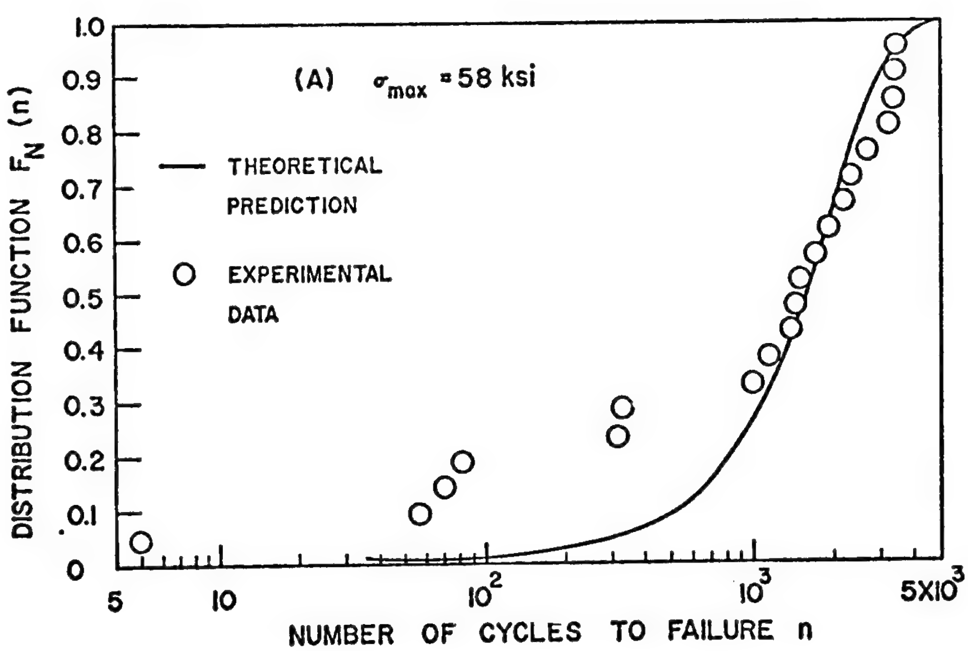

Fig. 6: Distribution Function of Fatigue Life, σ_{min}= -16 ksi , σ_{max}=58 ksi.

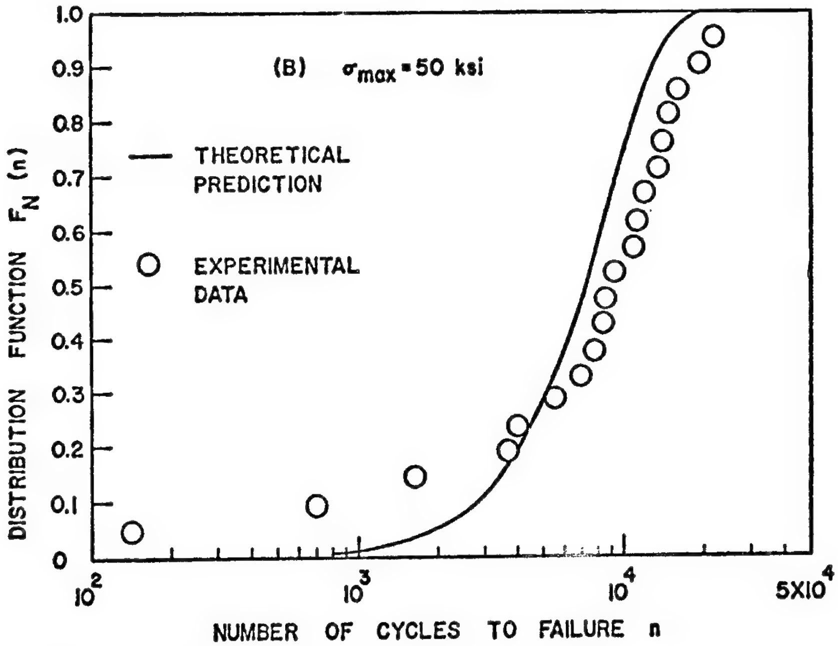

Fig. 7: Distribution Function of Fatigue Life,

σ_{min}= -16 ksi , σ_{max}=50 ksi.

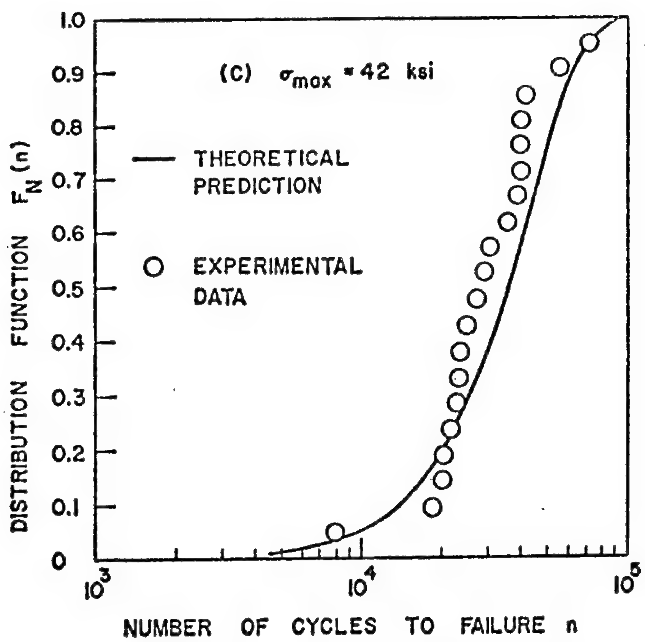

Fig. 8: Distribution Function of Fatigue Life,

σ_{min}= -16 ksi , σ_{max}=42 ksi.

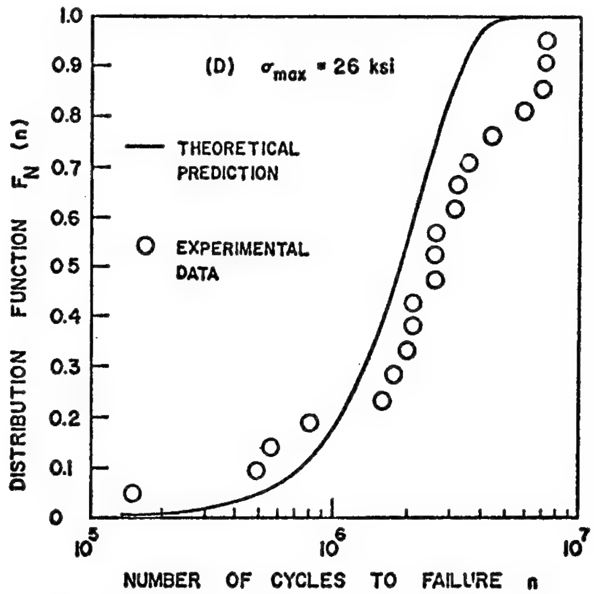

Fig. 9: Distribution Function of Fatigue Life, σ_{min}= +16 ksi , σ_{max}=26 ksi.

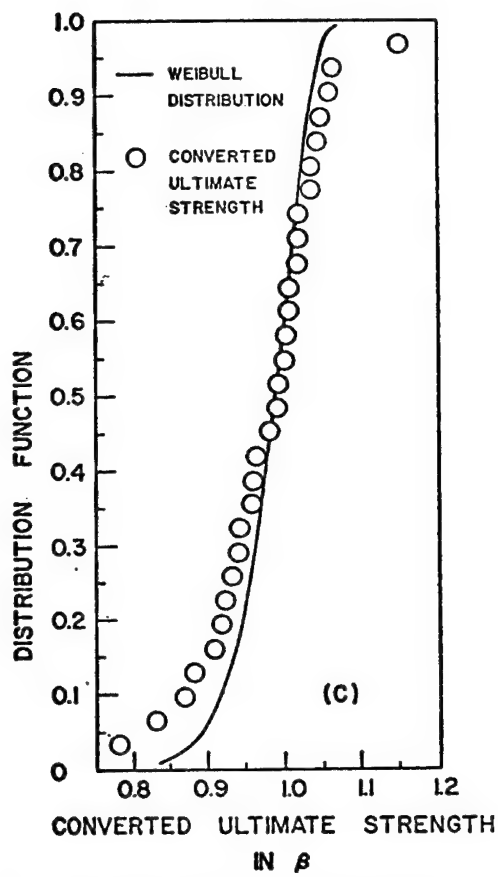

Fig. 10: Distribution Function of Converted Ultimate Strength From Tension-Tension Fatigue Data.

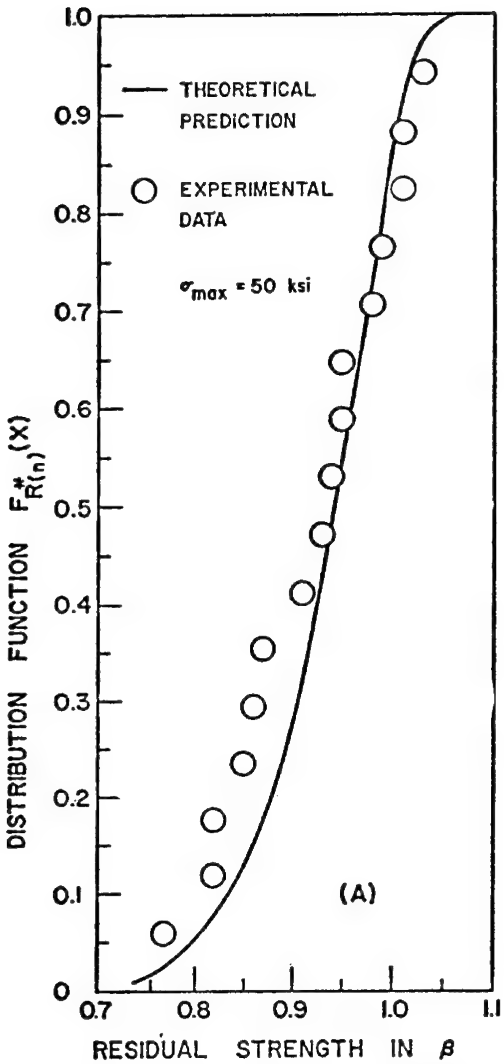

11: Distribution Function of Residual Strength, $\sigma_{min}=0$, $\sigma_{max}=50$ ksi.

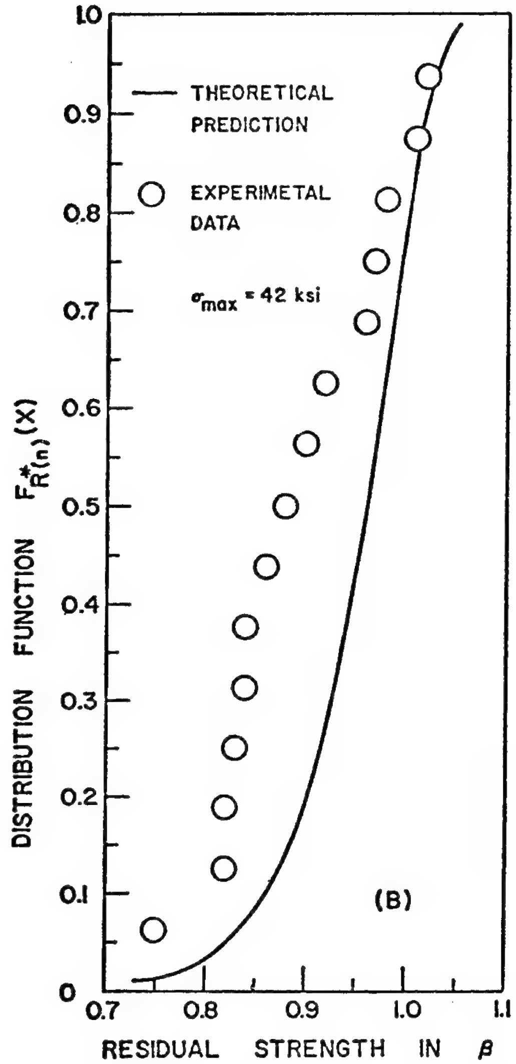

Fig. 12: Distribution Function of Residual Strength, $\sigma_{min}=0$, $\sigma_{max}=42$ ksi.

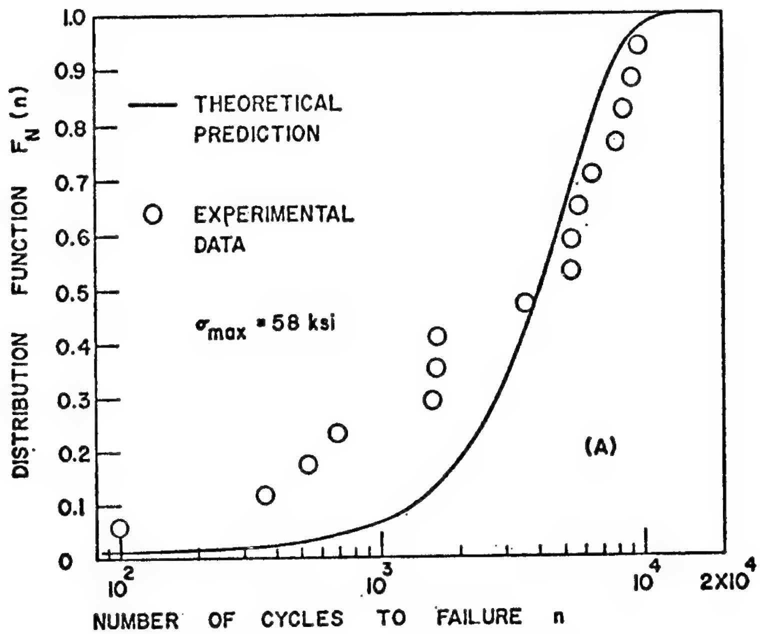

Fig. 13: Distribution Function of Fatigue Life, $\sigma_{min}=0$, $\sigma_{max}=58$ ksi.

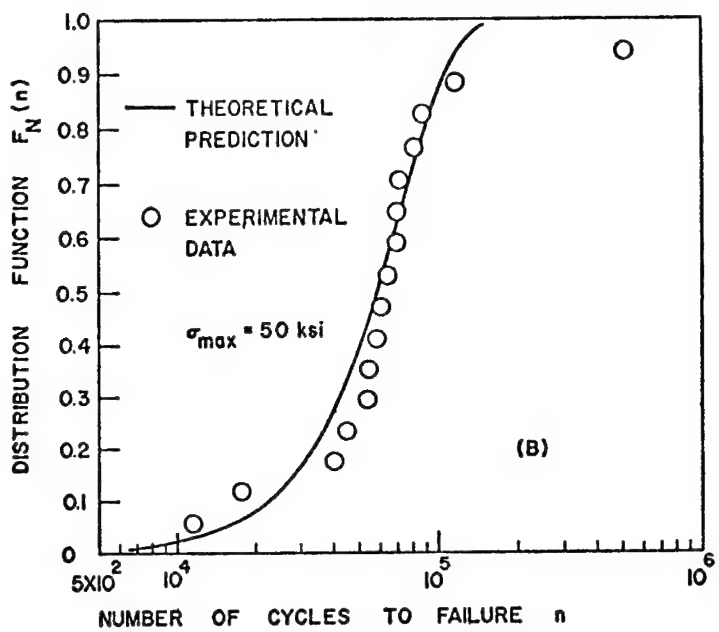

Fig. 14: Distribution Function of Fatigue Life, $\sigma_{min}=0$, $\sigma_{max}=50$ ksi.

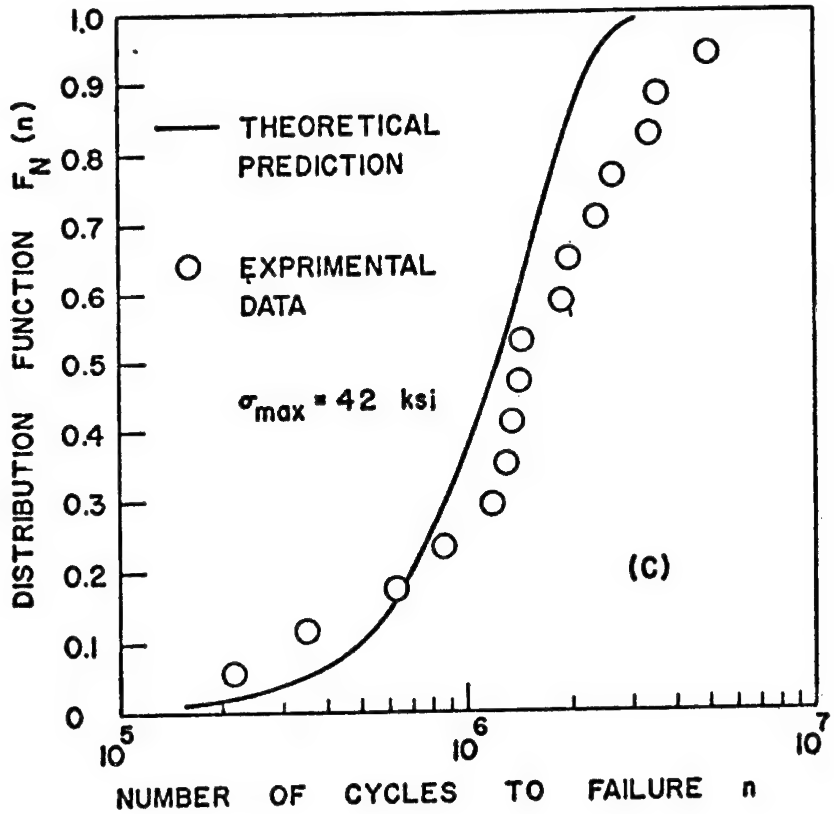

Fig. 15: Distribution Function of Fatigue Life, $\sigma_{min}=0$, $\sigma_{max}=42$ ksi.

ADVANCED RESIDUAL STRENGTH DEGRADATION

MODELING FOR ADVANCED COMPOSITES

LOCKHEED-CALIFORNIA COMPANY

OBJECTIVE: DEVELOP AN ANALYSIS METHODOLOGY FOR PREDICTING:

1. GROWTH OF DAMAGE UNDER FATIGUE LOADING
2. RESULTING RESIDUAL STRENGTH DUE TO PROPAGATION DAMAGE
3. CHARACTERISTICS OF DAMAGE GROWTH
4. THRESHOLD DAMAGE SIZE WHICH WILL NOT PROPAGATE

BASIC PROGRAM TASKS

TASK I: PRELIMINARY SCREENING

- o SELECT STRESS RISER AND NDI METHOD
- o DEVELOP PRELIMINARY DATA
  - TENSION, COMPRESSION
  - FATIGUE AND DAMAGE GROWTH

TASK II: DAMAGE GROWTH AND RESIDUAL STRENGTH DEGRADATION METHODOLOGY

- o DEVELOP STATISTICALLY BASED DATA SET
  - INITIAL TENSION AND COMPRESSION
  - FATIGUE LIFE DISTRIBUTION
  - RESIDUAL STRENGTH
  - DAMAGE GROWTH
- o DEVELOP ANALYSIS METHODOLOGY
- o DEVELOP REQUIRED MATERIAL PROPERTY INPUT DATA

TASK III: EFFECT OF FATIGUE LOADING/ENVIRONMENT PERTURBATIONS

- o EVALUATE MODEL FOR 3 NEW LOADING/ENVIRONMENT CONDITIONS

TASK I: PRELIMINARY SCREENING

MATERIAL

- o TWO LAMINATES OF T300/5208
- o 24 PLY 67% 0^0 LAMINATE $(0/+45/0_2/-45/0_2/+45/0_2/-45/0)_s$
- o 32 PLY 25% 0^0 LAMINATE $(0/+45/90/-45_2/90/+45/0)_{2s}$

DAMAGE TYPES

- o LOW VELOCITY IMPACT (SIMULATED TOOL DROP)
- o BADLY DRILLED HOLE (HIGH NORMAL FORCE, DULL TOOL)

SPECIMEN FABRICATION SEQUENCE

- QUALITY CONTROL PLAN ENFORCED
  - PREPREG QUALITY
  - LAMINATE FABRICATION SEQUENCE
  - SPECIMEN FABRICATION PROCEDURE AND TOLERANCES
- MATERIAL ACCEPTANCE
- LAMINATE FABRICATION
- STATISTICAL SPECIMEN RANDOMIZATION AND SPECIMEN LAYOUT
- PRELIMINARY PANEL DAMAGE EVALUATION TESTS
- IMPACT TEST PANEL AT SPECIFIED LOCATIONS
- MACHINE TEST SPECIMENS, DRILL "HOLES", AND TAB
- FINAL Q. C. MEASUREMENTS AND STORE

3-INCH WIDE SPECIMEN CONFIGURATION, DRAWING TL1038

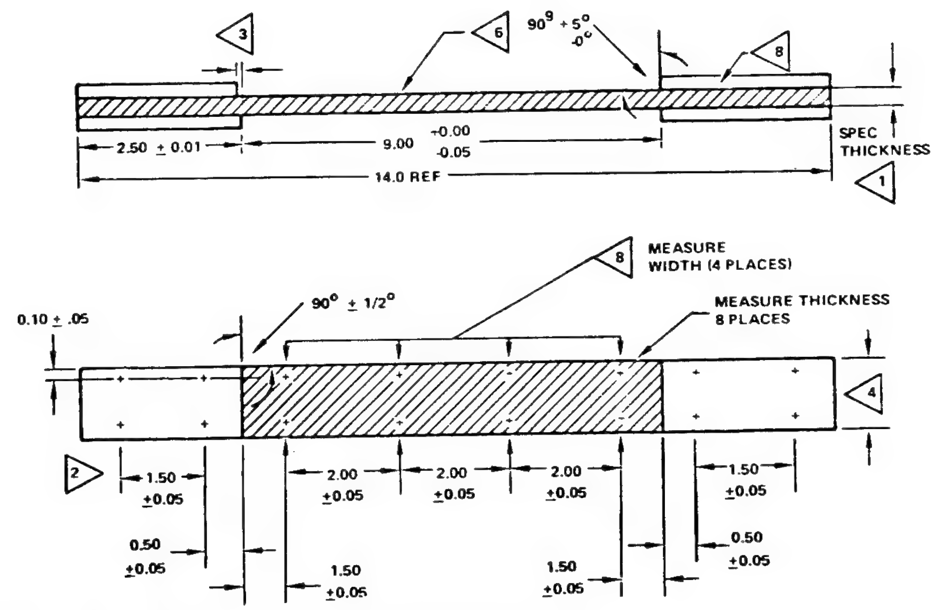

9 SPECIMENS TO BE FLAT OVER THE ENTIRE 14.0 INCH LENGTH WITHIN 0.01 INCHES.

8 TAB EDGES TO BE PARALLEL TO SIDES OF SPECIMEN WITHIN 0.02 INCHES. OVERHANG NOT TO EXCEED 0.15

7 THE TAB AND SPECIMEN BONDING SURFACES TO BE THOROUGHLY SOLVENT CLEANED USING METHYL-ETHYL-KETONE PRIOR TO BONDING. A 350°F CURING ADHESIVE IS TO BE USED AND MUST COVER ENTIRE SURFACE UNIFORMLY'

6 WATER SPRAY MIST TO BE USED DURING SAWING OPERATIONS AND SOLUBLE OIL DURING GRINDING. MACHINED SURFACES TO BE RMS 50 OR BETTER. NO EDGE DAMAGE OR FIBER SEPARATION SHOULD BE VISIBLE

5 MEASURE SPECIMEN WIDTH 4 PLACES. WIDTH MUST NOT VARY BY MORE THAN 0.004 INCHES.

4 SPECIMEN WIDTH TO BE 3.00 $^{+0.00}_{-0.02}$ INCHES.

3 MISMATCH OF TABS FROM SIDE TO SIDE NOT TO EXCEED 0.01 INCHES.

2 TABS TO BE CUT FROM AN 6 PLY LAMINATE FABRICATED FROM PREPREG OF 1581 GLASS FABRIC IN A 350°F CURING EPOXY. TAB PLUS ADHESIVE THICKNESS MUST NOT VARY SIDE TO SIDE OR END TO END BY MORE THAN 0.01 INCH AS MEASURED 8 PLACES.

1 SPECIMEN THICKNESS TO BE WITHIN ±0.003 INCHES OF THE AVERAGE OF 8 THICKNESS MEASUREMENTS.

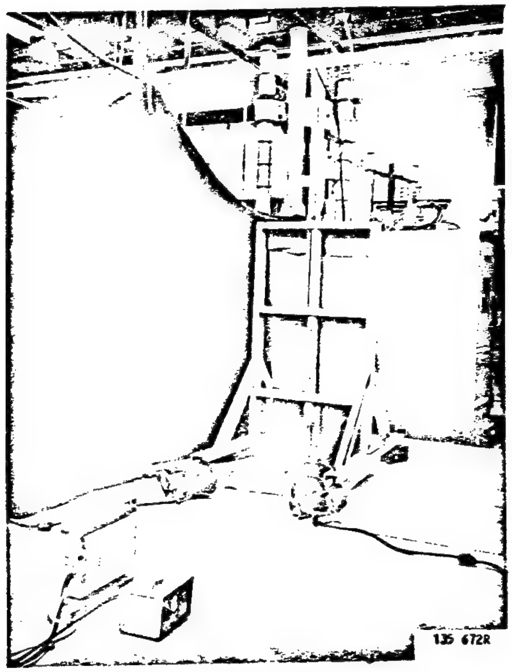

Typical Tool Drop Simulation Set Up.

TASK I: PRELIMINARY SCREENING

INITIAL STATIC TENSION AND COMPRESSION TESTS

- o BASE TENSION TESTS
  - 10 REPLICATES X 2 LAMINATES X 2 DAMAGE TYPES
  - DETERMINE INITIAL STATIC TENSION STRENGTH DISTRIBUTION
- o BASE COMPRESSION TESTS
  - FULLY RESTRAINED, 10 REPLICATES X 2 LAMINATES X 2 DAMAGE TYPES
  - COLUMN BUCKLING, 1 EACH X 4 COLUMN LENGTHS X 2 LAMINATES X 2 DAMAGE TYPES
  - DETERMINE INITIAL STATIC COMPRESSION STRENGTH DISTRIBUTION AND COLUMN BUCKLING BEHAVIOR
  - EVALUATE FATIGUE SPECIMEN SUPPORT
- o SECONDARY COMPRESSION TESTS
  - FULLY RESTRAINED, 6 REPLICATES X 2 LAMINATES X 2 DAMAGE TYPES (TBE X-RAY MONITOR)
  - EVALUATE EFFECT OF TBE ON STATIC COMPRESSION BEHAVIOR

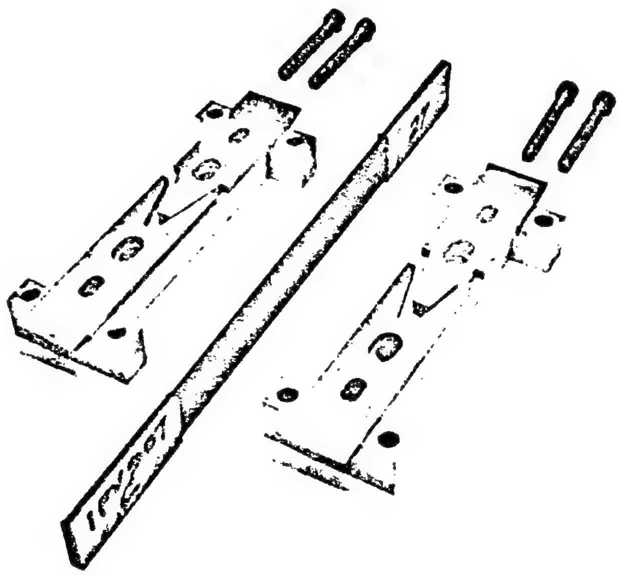

"Full-Fixity" Apparatus, Showing Auxiliary Platens

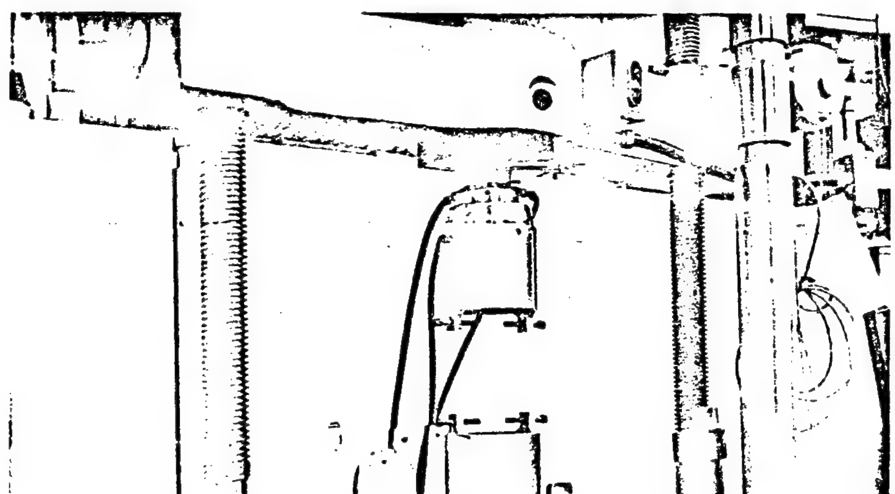

Installation of Modified Hydraulic Grips in 60,000 Universal Test Machine

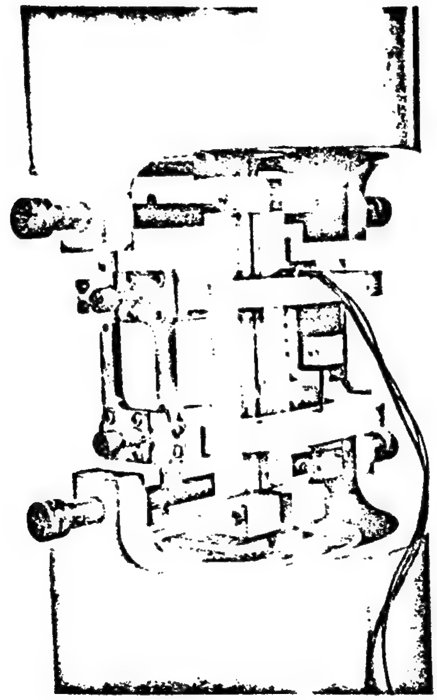

135 Y69R

Installation of Lockheed Extensometer

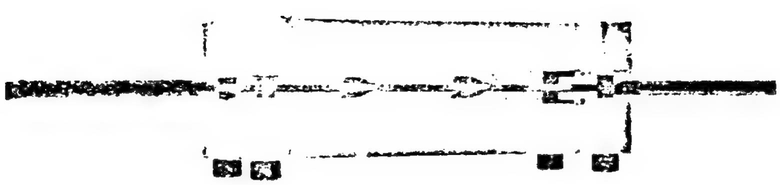

136 217K

Composite Specimen Column Test Fixture

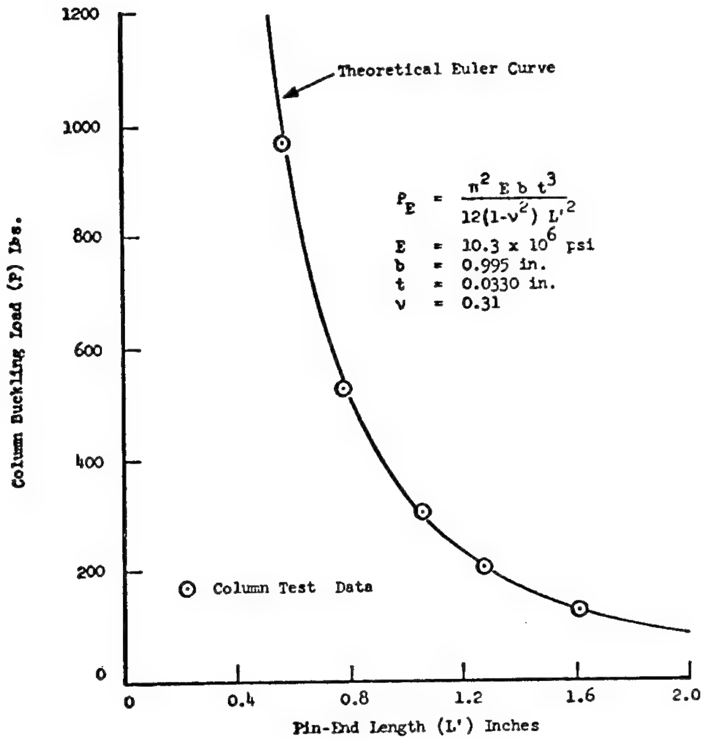

Test Data Obtained with Column Test Fixture on Aluminum Alloy Specimen Compared with Euler Relation

TASK I: PRELIMINARY SCREENING

FATIGUE AND DAMAGE PROPAGATION TESTS

- o BASE S-N FATIGUE DATA
  - 2 LAMINATES X 2 DAMAGE TYPES X 3 REPLICATES X 6 STRESS LEVELS
- o BASE DAMAGE PROPAGATION DATA
  - MONITOR ALL S-N FATIGUE TEST SPECIMENS
  - MONITOR DAMAGE WITH "HOLOSCAN" ULTRASONIC UNIT
  - RECORD DAMAGE SIZE, SHAPE, AND CHARACTERISTICS AS f (CYCLES, STRESS LEVEL)
  - DETERMINE BASIC DAMAGE GROWTH CHARACTERISTICS
- o SECONDARY DAMAGE GROWTH DATA
  - 2 LAMINATES X 2 DAMAGE TYPES X 2 REPLICAS X 3 STRESS LEVELS
  - MONITOR DAMAGE BY TBE ENHANCED X-RAY
  - EVALUATE EFFECT OF TBE ON LIFE AND DAMAGE GROWTH
  - IF NONE, PROVIDES ADDED DAMAGE CHARACTERIZATION DATA

Section 1-MM

Section 2-AA

Composite Section

Resulting Data

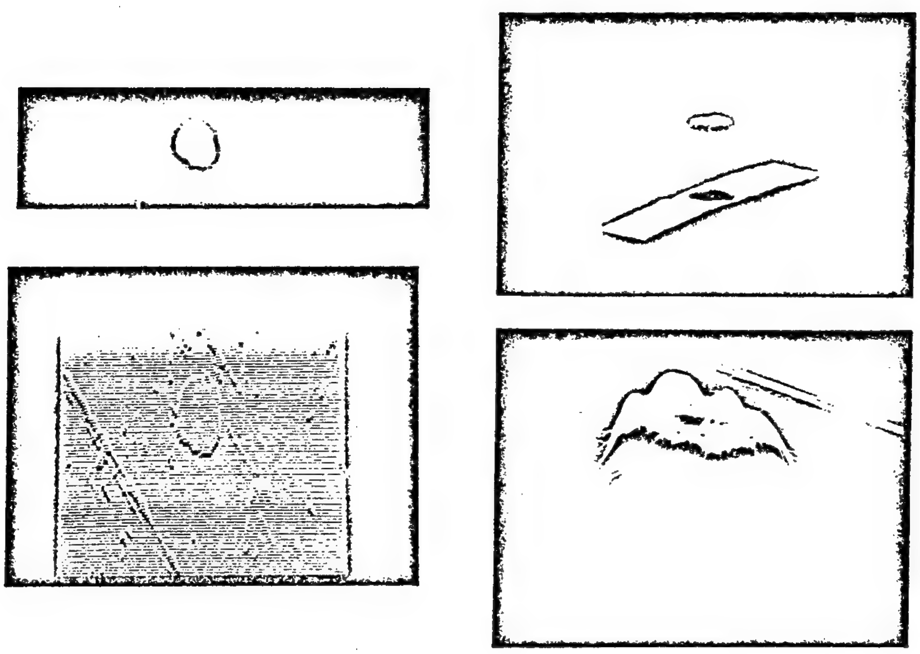

TASK II: DAMAGE GROWTH AND RESIDUAL STRENGTH DEGRADATION PREDICTION

- o <u>FATIGUE TESTS</u>
  - FATIGUE LIFE DISTRIBUTION AT SELECTED STRESS LEVEL
    - 2 LAMINATES X 1 DAMAGE X 20 REPLICATES
    - DETERMINE FATIGUE LIFE DISTRIBUTION
  - BASED ON LIFE DISTRIBUTION, SELECT 5 CYCLE INTERVALS, N_1, N_2, N_3, N_4, N_5
  - FATIGUE CYCLE 23 REPLICATE SPECIMENS TO EACH CYCLIC INTERVAL, N_i
    - 23 REPLICATES X 2 LAMINATES X 1 DAMAGE X 5 CYCLIC INTERVALS
  - MEASURE AND RECORD DAMAGE SIZE OF EACH SPECIMEN AFTER N_i CYCLES OF LOADING
- o <u>RESIDUAL STRENGTH TESTS</u>
  - TENSILE RESIDUAL STRENGTH TESTS
    - 10 REPLICATES X 2 LAMINATES X 5 CYCLIC INTERVALS
  - COMPRESSION RESIDUAL STRENGTH TESTS
    - 10 REPLICATES X 2 LAMINATES X 5 CYCLIC INTERVALS
  - DESTRUCTIVE METALLOGRAPHIC SECTIONING
    - 3 REPLICATES X 2 LAMINATES X 5 CYCLIC INTERVALS
  - DETERMINE RESIDUAL STRENGTHS AND STRENGTH DISTRIBUTION AS f (DAMAGE CYCLES)
- o DEVELOP FINAL MODEL FOR DAMAGE GROWTH AND RESIDUAL STRENGTH PREDICTION

TASK III: EFFECT OF FATIGUE LOADING/ENVIRONMENT PERTURBATIONS

- o INITIAL STATIC STRENGTH TESTS
  - TENSION TESTS, 2 LAMINATES X 1 DAMAGE X 5 REPLICATES
  - COMPRESSION TESTS, 2 LAMINATES X 1 DAMAGE X 5 REPLICATES
- o S-N FATIGUE DATA AND DAMAGE PROPAGATION TESTS
  - 3 NEW TEST CONDITIONS
    - TASK II R AND σ, 180°F WET
    - TASK II R, NEW σ
    - NEW R AND σ
  - MONITOR DAMAGE GROWTH AND RECORD LIFE
  - SELECT 3 N_i AND FATIGUE 6 REPLICATES X 2 LAMINATES X 1 DAMAGE X 3 N_i FOR RESIDUAL STRENGTH TESTING
- o RESIDUAL STRENGTH TESTS
  - TENSION RESIDUAL STRENGTH
    - 3 REPLICATES X 3 N_i X 3 TEST CONDITIONS X 2 LAMINATES X 1 DAMAGE
  - COMPRESSION RESIDUAL STRENGTH
    - 3 REPLICATES X 3 N_i X 3 TEST CONDITIONS X 2 LAMINATES X 1 DAMAGE
- o EVALUATE MODEL AND MODIFY AS REQUIRED

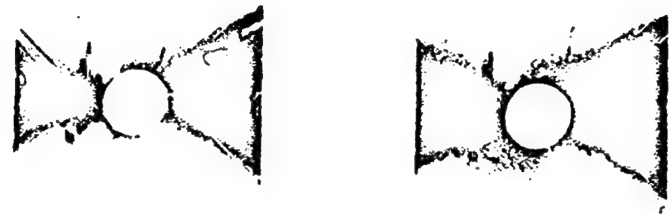

Exposure t_1 Exposure $t_2 > t_1$

Specimen A

Exposure t_1 Exposure $t_2 > t_1$

Specimen B

Typical TBE Enhanced X-Ray Results of Damaged Graphite/Epoxy Composite Material

TASK II: DAMAGE GROWTH AND RESIDUAL STRENGTH DEGRADATION PREDICTION

STATIC TESTS

- o INITIAL TENSION STRENGTH TESTS
  - 2 LAMINATES X 1 DAMAGE X 15 REPLICATES
  - DETERMINE INITIAL TENSION STRENGTH DISTRIBUTION
- o SECONDARY TENSION TESTS
  - 2 LAMINATES X 1 DAMAGE X 6 STRAIN LEVELS AND UNLOAD
  - DETAILED DAMAGE GROWTH DETERMINATION UNDER STATIC TENSION LOAD
- o INITIAL COMPRESSION STRENGTH TESTS
  - 2 LAMINATES X 1 DAMAGE X 15 REPLICATES
  - DETERMINE INITIAL COMPRESSION STRENGTH DISTRIBUTION
- o SECONDARY COMPRESSION TESTS
  - 2 LAMINATES X 1 DAMAGE X 6 STRAIN LEVELS AND UNLOAD
  - DETAILED DAMAGE GROWTH DETERMINATION UNDER STATIC COMPRESSION LOAD
- o COLUMN BUCKLING TESTS
  - 2 LAMINATES X 1 DAMAGE X 3 REPLICATES X 4 COLUMN LENGTHS
  - DETERMINE COMPRESSION COLUMN STABILITY
- o BASIC MATERIAL/LAMINATE PROPERTY TESTS - AS REQUIRED FOR INPUT TO MODEL.

MECHANICS OF COMPOSITE MATERIALS WITH DIFFERENT MODULI IN TENSION AND COMPRESSION

ROBERT M. JONES
SOUTHERN METHODIST UNIVERSITY
DALLAS, TEXAS

THEME OF PRESENTATION

- PAST ACCOMPLISHMENTS REVIEWED
- NEW COMPUTER PROGRAM CAPABILITIES DEVELOPED, BUT NOT EXPLOITED
- CHANGE IN THRUST OF TECHNOLOGY APPLICATION FROM REENTRY VEHICLE NOSETIPS TO ROCKET NOZZLE

OUTLINE

- INTRODUCTION
- NONLINEAR MULTIMODULUS MATERIAL MODEL
- JNMDATA COMPUTER PROGRAM
- NONSYMMETRIC COMPLIANCE MATRIX APPROACH
- MATERIAL MODELING ACCOMPLISHMENTS
- MATERIAL MODELING IN PROGRESS
- SUMMARY

INTRODUCTION

BILINEAR MODEL FOR MULTIMODULUS MATERIALS

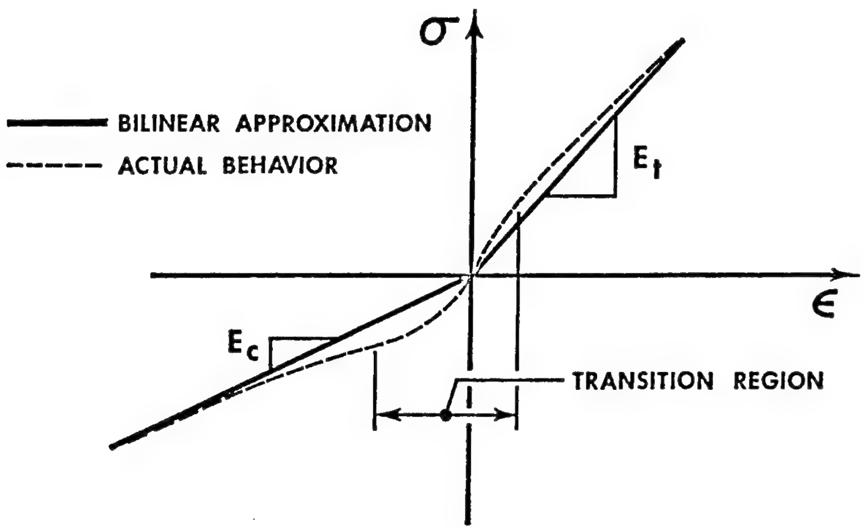

TABLE 1

TENSION AND COMPRESSION MODULI RELATIONSHIPS
FOR SEVERAL COMMON COMPOSITE MATERIALS

MATERIAL	FIBROUS OR GRANULAR	REPRESENTATIVE MODULI RELATIONSHIP
GLASS/EPOXY	FIBROUS	$E_t = 1.2E_c$
BORON/EPOXY	FIBROUS	$E_c = 1.2E_t$
GRAPHITE/EPOXY	FIBROUS	$E_t = 1.4E_c$
CARBON/CARBON	FIBROUS	$E_t = 2\text{-}5E_c$
ZTA GRAPHITE	GRANULAR	$E_c = 1.2E_t$
ATJ-S GRAPHITE	GRANULAR	$E_t = 1.2E_c$

TYPICAL STRESS-STRAIN BEHAVIOR OF FIBER-REINFORCED COMPOSITE MATERIALS

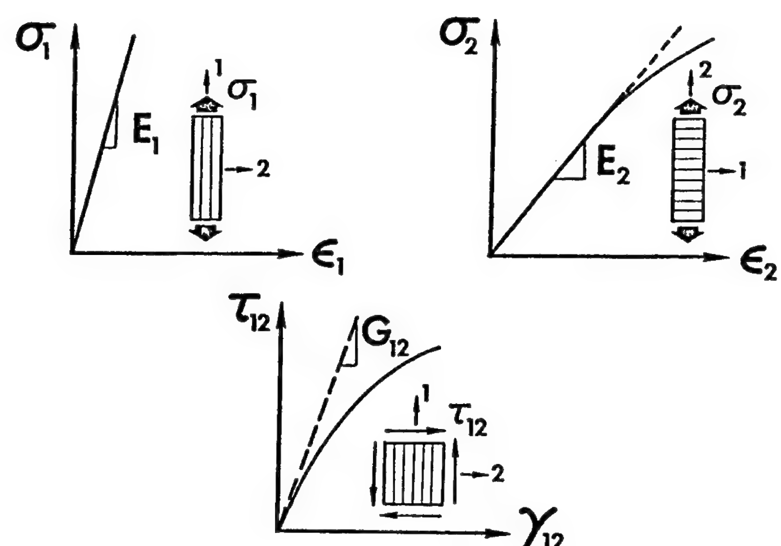

EFFECT OF MOISTURE AND TEMPERATURE ON STRESS-STRAIN CURVE NONLINEARITY

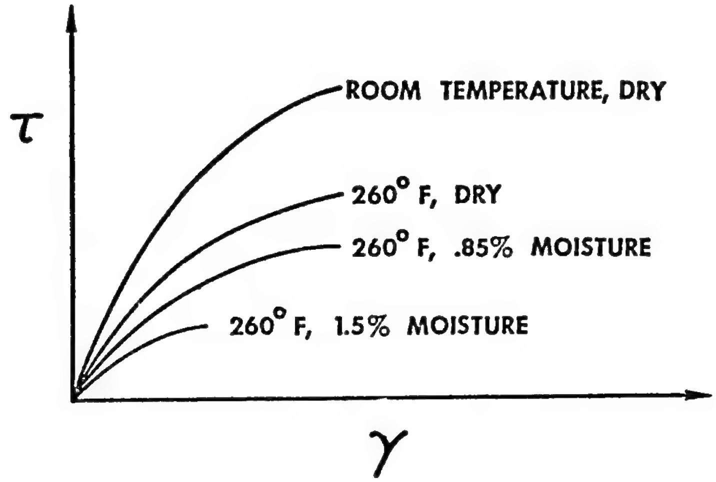

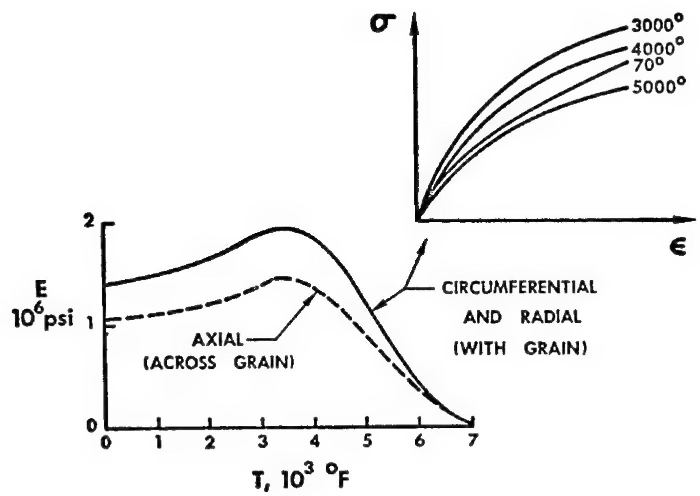

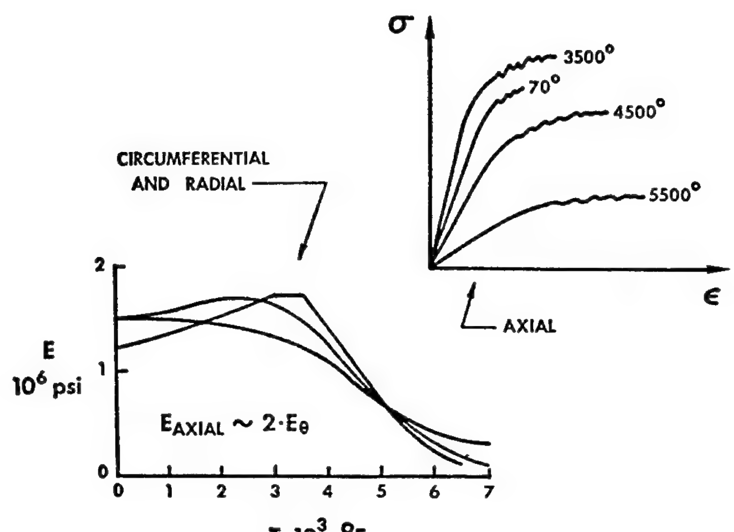

OBJECTIVES

MECHANICS OF COMPOSITE MATERIALS WITH DIFFERENT MODULI IN TENSION AND COMPRESSION

- DEVELOP MATERIAL MODEL FOR NONLINEAR MULTIMODULUS BEHAVIOR OF VARIOUS CLASSES OF COMPOSITE MATERIALS
- ANALYZE STRESS EQUILIBRIUM BEHAVIOR OF SOLID BODIES (E.G., THERMAL STRESSES → SIMULTANEOUS TENSILE AND COMPRESSIVE STRESSES)
  - LINEAR ELASTIC MULTIMODULUS
  - NONLINEAR ELASTIC
  - NONLINEAR ELASTIC MULTIMODULUS
- ANALYZE BENDING, BUCKLING, AND VIBRATION BEHAVIOR OF LAMINATED PLATES AND SHELLS
  - LINEAR ELASTIC (LAMINATION ASYMMETRIES)
  - LINEAR ELASTIC MULTIMODULUS
  - NONLINEAR ELASTIC
  - NONLINEAR ELASTIC MULTIMODULUS

NONLINEAR MULTIMODULUS MATERIAL MODEL

ORTHOTROPIC STRESS-STRAIN RELATIONS

AXISYMMETRIC BEHAVIOR

$$\begin{Bmatrix} \epsilon_r \\ \epsilon_z \\ \epsilon_\theta \\ \gamma_{rz} \end{Bmatrix} = \begin{bmatrix} \frac{1}{E_r} & -\frac{\nu_{rz}}{E_r} & -\frac{\nu_{r\theta}}{E_r} & 0 \\ -\frac{\nu_{rz}}{E_r} & \frac{1}{E_z} & -\frac{\nu_{z\theta}}{E_z} & 0 \\ -\frac{\nu_{r\theta}}{E_r} & -\frac{\nu_{z\theta}}{E_z} & \frac{1}{E_\theta} & 0 \\ 0 & 0 & 0 & \frac{1}{G_{rz}} \end{bmatrix} \begin{Bmatrix} \sigma_r \\ \sigma_z \\ \sigma_\theta \\ \tau_{rz} \end{Bmatrix}$$

MATERIAL PROPERTY-ENERGY RELATIONS

$$\text{MATERIAL PROPERTY}_i = A_i \left[1 - B_i \left(\frac{U}{U_{0_i}} \right)^{C_i} \right]$$

A_i = INITIAL ELASTIC VALUE

B_i = INITIAL CURVATURE OF σ-ϵ CURVE

C_i = RATE OF CHANGE OF CURVATURE

U = STRAIN ENERGY

U_{0_i} = UNIT STRAIN ENERGY

STRAIN ENERGY FUNCTION

$$U = \frac{1}{2}(\sigma_r \epsilon_r + \sigma_z \epsilon_z + \sigma_\theta \epsilon_\theta + \tau_{rz} \gamma_{rz})$$

UNIAXIAL INTERPRETATION OF THE STRAIN ENERGY

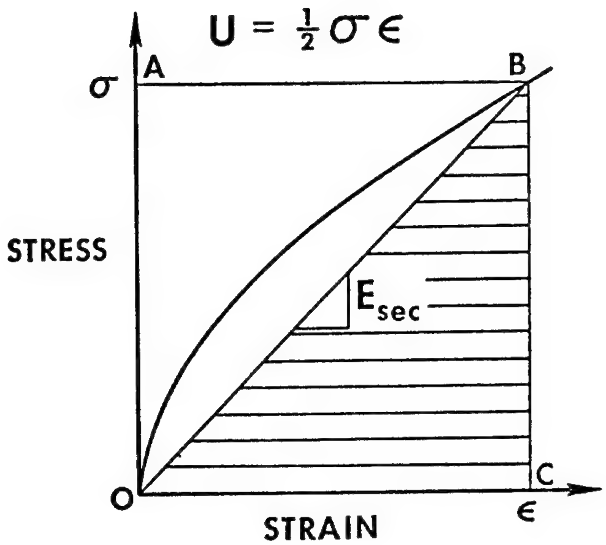

REPRESENTATION OF STRESS-STRAIN BEHAVIOR

DIRECT MODULI

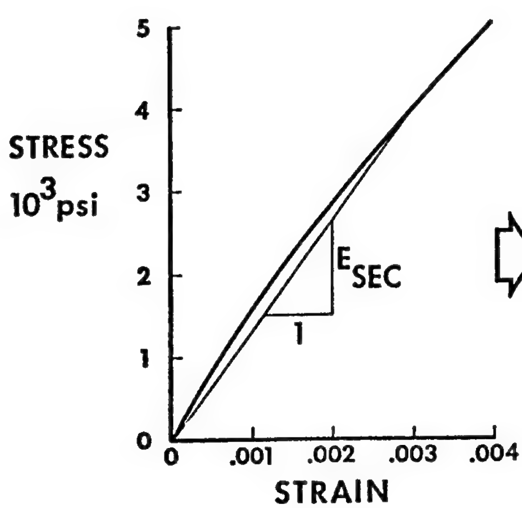

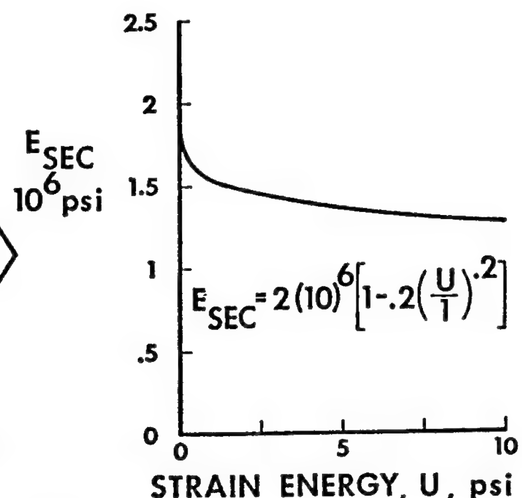

ITERATION PROCEDURE

PMD = PRINCIPAL MATERIAL DIRECTIONS

PSD = PRINCIPAL STRESS DIRECTIONS

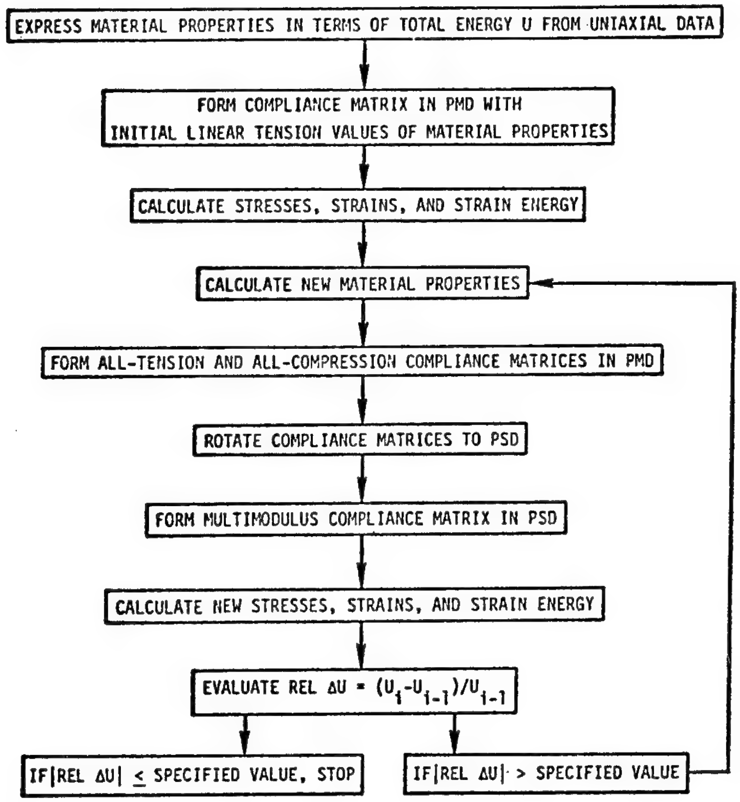

CONVERGENCE OF ITERATION PROCEDURE

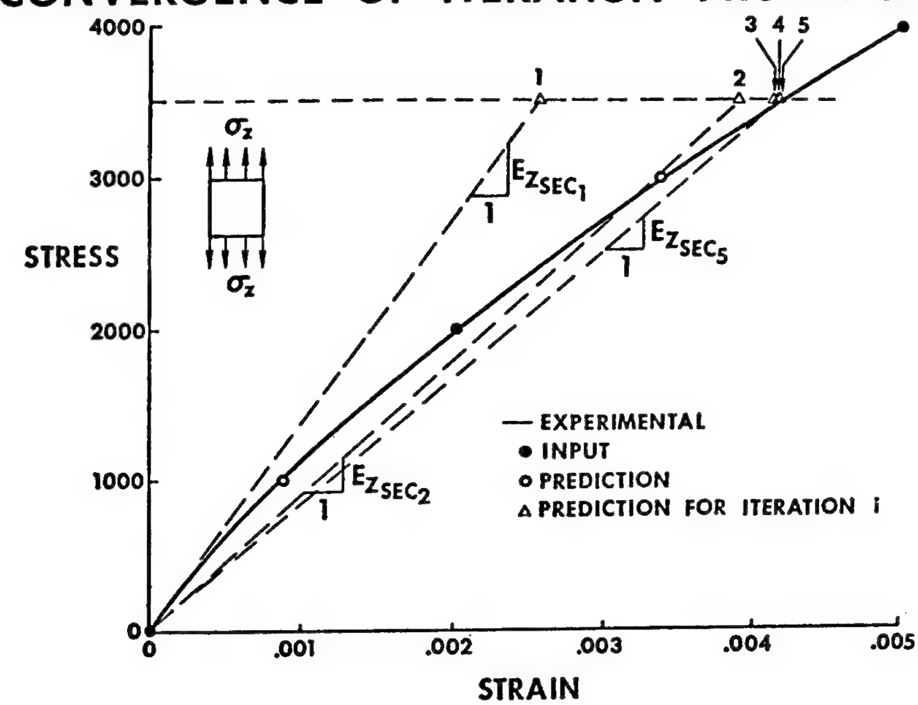

JNMDATA COMPUTER PROGRAM

OBJECTIVE

- CALCULATE JONES-NELSON MATERIAL MODEL PARAMETERS FROM INPUT STRESS-STRAIN CURVE DATA POINTS
- PLOT APPROXIMATE MECHANICAL PROPERTY VERSUS STRAIN ENERGY CURVE ALONG WITH ACTUAL DATA
- PLOT IMPLIED STRESS-STRAIN CURVE ALONG WITH ACTUAL DATA

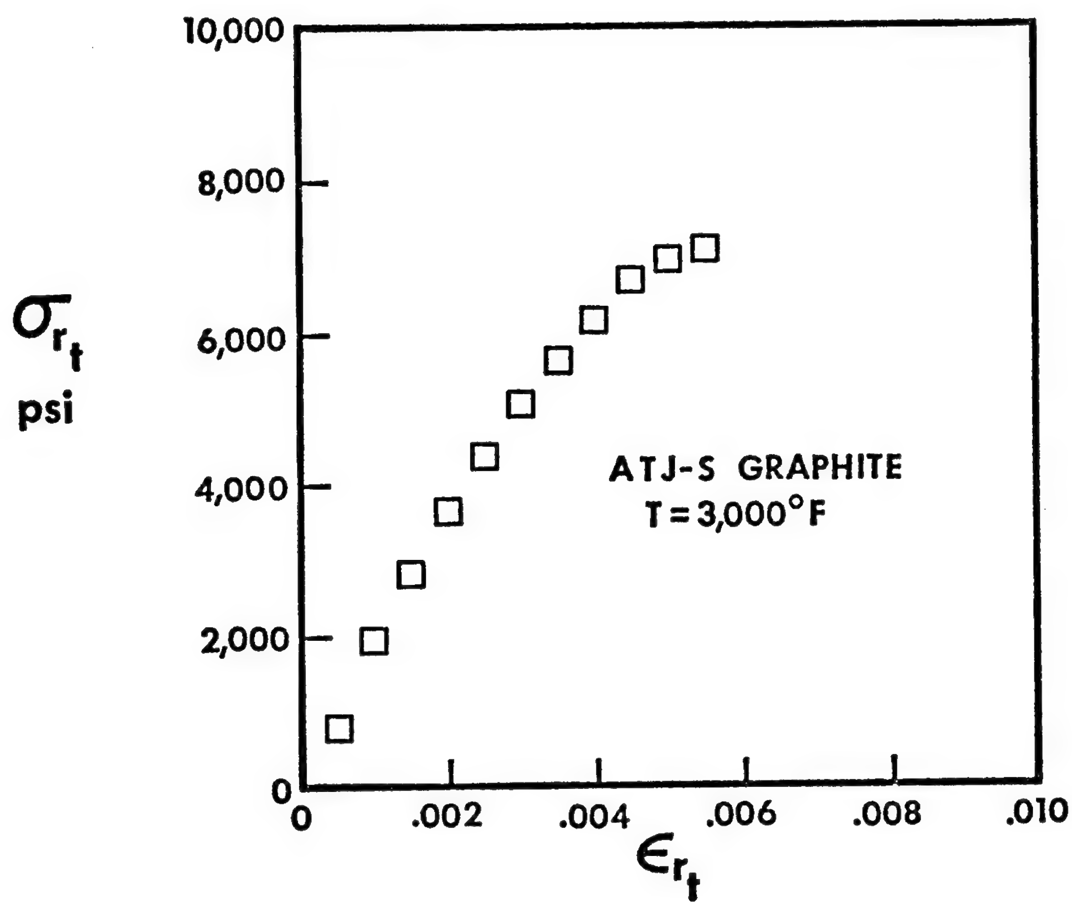

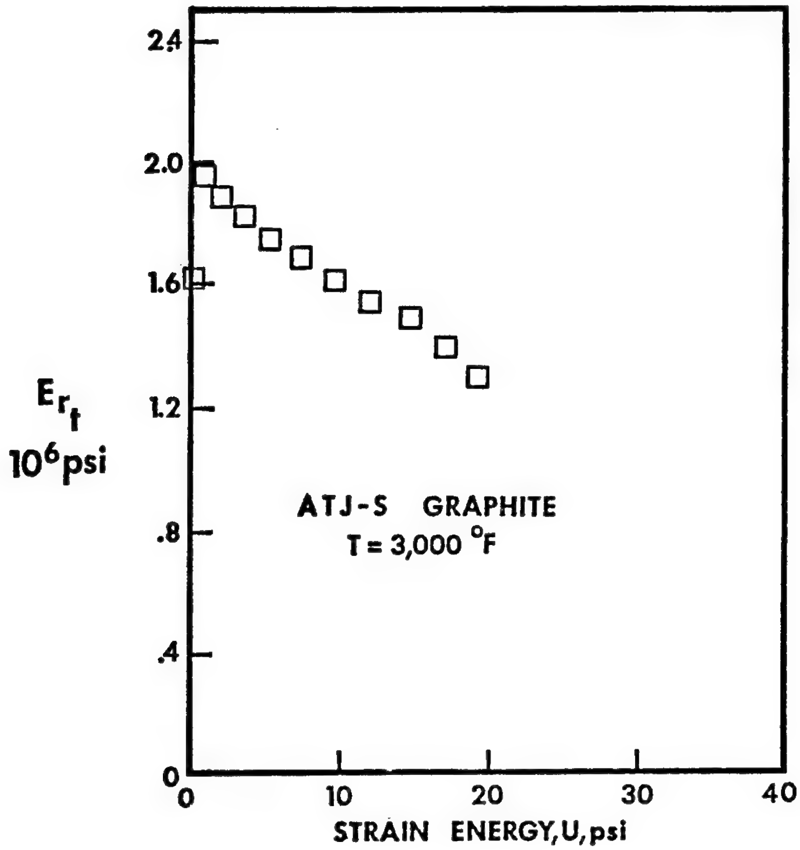
2.4
2.0
1.6
1.2
.8
.4
0
E_{r_t}
10^6psi
ATJ-S GRAPHITE
T = 3,000 °F
0
10
20
30
40
STRAIN ENERGY, U, psi

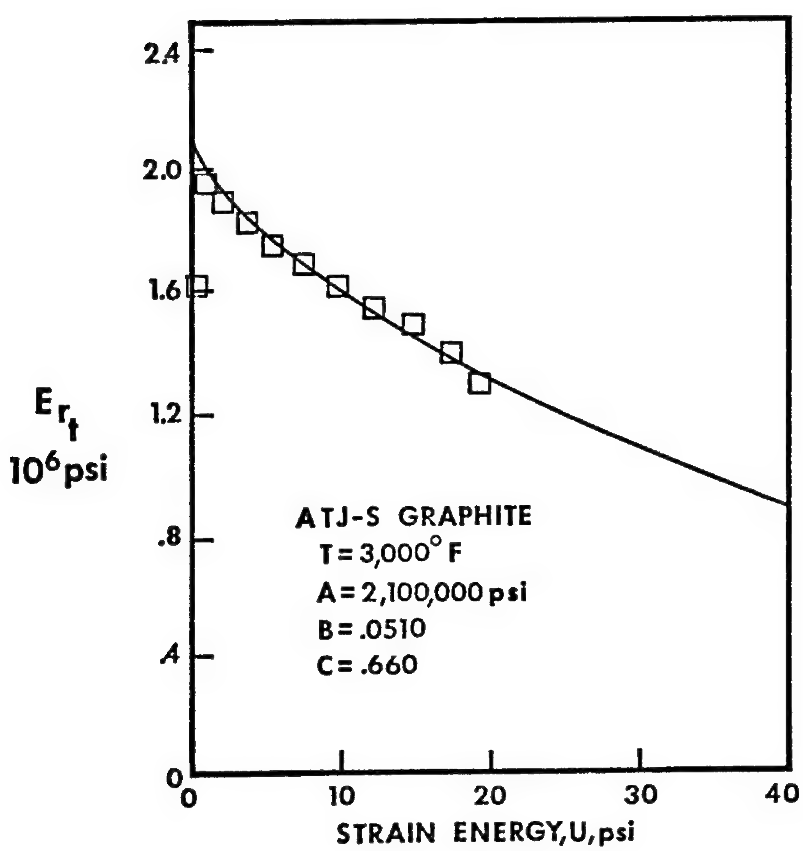
2.4
2.0
1.6
1.2
.8
.4
0
E_{r_t}
10^6psi
ATJ-S GRAPHITE
T = 3,000° F
A = 2,100,000 psi
B = .0510
C = .660
0
10
20
30
40
STRAIN ENERGY, U, psi

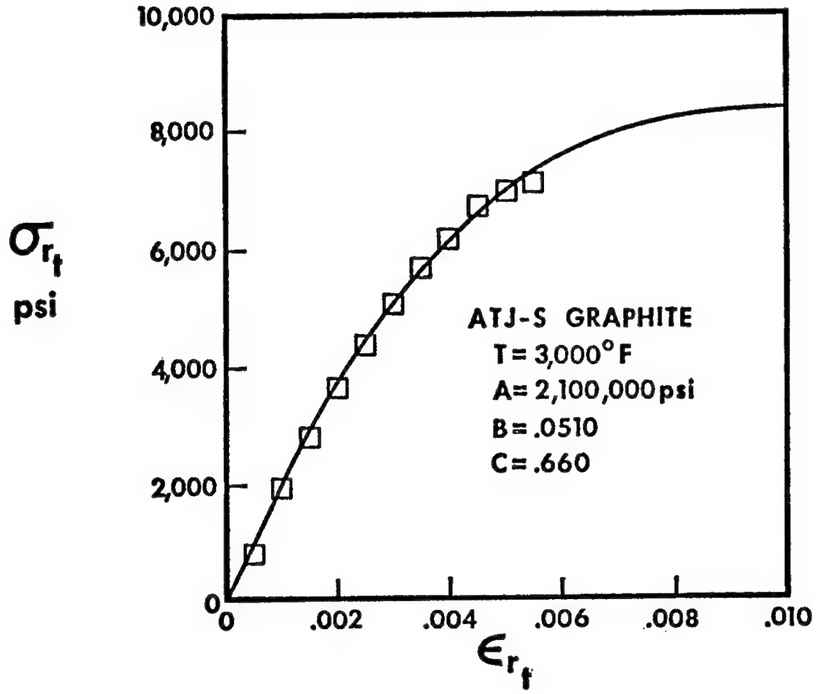

JNMDATA COMPUTER PROGRAM

READ INPUT STRESS-STRAIN CURVE DATA

↓

CALCULATE JNM MODEL PARAMETERS

↓

PUNCH SAAS IIIM MATERIAL PROPERTY CARDS

↓

PLOT MECHANICAL PROPERTY VERSUS STRAIN ENERGY CURVES AND CONVERTED INPUT DATA

↓

PLOT IMPLIED STRESS-STRAIN CURVES AND INPUT DATA

JNMDATA COMPUTER PROGRAM

- NONLINEAR REGRESSION ANALYSIS
- CYLINDRICALLY ORTHOTROPIC MATERIALS

SUMMARY

- THE JNDATA COMPUTER PROGRAM IS AN EXCEPTIONALLY USEFUL ADJUNCT TO THE JONES-NELSON NONLINEAR MATERIAL MODEL
  - AUTOMATED PROCEDURE
  - RAPID AND HIGHLY VISIBLE MATERIAL MODELING
- INPUT
  - ACTUAL STRESS-STRAIN CURVE DATA
  - DESIRED VALUES OF A, B, AND C
- OUTPUT
  - ACTUAL AND IMPLIED MECHANICAL PROPERTY VERSUS STRAIN ENERGY CURVES
  - ACTUAL AND IMPLIED STRESS-STRAIN CURVES

NONSYMMETRIC COMPLIANCE MATRIX APPROACH

NONSYMMETRIC COMPLIANCE MATRIX APPROACH

- SYMMETRIC VERSUS NONSYMMETRIC COMPLIANCE MATRIX?
- PREVIOUS APPROACHES
  - RESTRICTED COMPLIANCE MATRIX (ISABEKYAN AND KHACHATRYAN)
  - WEIGHTED COMPLIANCE MATRIX (JONES)
- RESULTS OF NONSYMMETRIC COMPLIANCE MATRIX APPROACH INSIGNIFICANT FOR ATJ-S GRAPHITE

MATERIAL MODELING ACCOMPLISHMENTS

MATERIAL MODELING ACCOMPLISHMENTS

MATERIAL	TYPE OF MATERIAL	NUMBER OF NONLINEARITIES		MATERIAL MODEL		
		TENSION	COMPRESSION	MULTIMODULUS ELASTIC	NONLINEAR	NONLINEAR MULTIMODULUS
ATJ-S GRAPHITE	TRANSVERSELY ISOTROPIC	5	5			✓
BORON/EPOXY	ORTHOTROPIC LAMINA	1	1	✓	✓	
GRAPHITE/EPOXY	ORTHOTROPIC LAMINA	1	1	✓	✓	
BORON/ALUMINUM	ORTHOTROPIC LAMINA	3	3		✓	
CARBON-CARBON	ORTHOTROPIC LAMINA AND ANISOTROPIC 3-D WEAVE	4-9	4-9	✓		

MATERIAL MODELING ACCOMPLISHMENTS

MATERIAL	COMPARISON WITH EXPERIMENT				
	UNIAXIAL		BIAXIAL		
	PMD*	OFF-AXIS	TUBE	DISK	LAMINATE
ATJ-S GRAPHITE	✓	✓	✓	✓	N/A
BORON/EPOXY	✓	✓			✓
GRAPHITE/EPOXY	✓	✓			
BORON/ALUMINUM	✓				✓
CARBON-CARBON					

*PMD = PRINCIPAL MATERIAL DIRECTIONS

MATERIAL MODELING IN PROGRESS

MATERIAL MODELING IN PROGRESS

- EXTENSION OF MODEL TO CARBON-CARBON
  - BEHAVIORAL CHARACTERISTICS OF CARBON-CARBON
  - BASIC CHARACTERISTICS OF MODEL
  - APPARENT FLEXURAL MODULUS AND STRENGTH OF MULTIMODULUS MATERIALS
  - COMPARISON OF PREDICTED AND MEASURED OFF-AXIS STRAINS FOR AVAILABLE TEST SPECIMENS
  - MODEL OF VARIATION IN MECHANICAL PROPERTIES DUE TO CHANGES IN RADIAL DIRECTION OF POLAR WEAVE CARBON-CARBON
  - MODEL OF NONLINEAR BEHAVIOR UNDER UNLOADING

SUMMARY

PRINCIPAL FINDINGS AND CONCLUSIONS

MECHANICS OF COMPOSITE MATERIALS WITH DIFFERENT MODULI IN TENSION AND COMPRESSION

- MATERIAL MODEL
  - STRESS-STRAIN RELATIONS FOR MATERIALS WITH DIFFERENT MODULI IN TENSION AND COMPRESSION, AIAA JOURNAL, JANUARY 1977.
  - A NEW MATERIAL MODEL FOR THE NONLINEAR BIAXIAL BEHAVIOR OF ATJ-S GRAPHITE JOURNAL OF COMPOSITE MATERIALS, JANUARY 1975.
  - FURTHER CHARACTERISTICS OF A NONLINEAR MATERIAL MODEL FOR ATJ-S GRAPHITE, JOURNAL OF COMPOSITE MATERIALS, JULY 1975.
  - MATERIAL MODELS FOR NONLINEAR DEFORMATION OF GRAPHITE, AIAA JOURNAL, JUNE 1976.
  - THEORETICAL-EXPERIMENTAL CORRELATION OF MATERIAL MODELS FOR NONLINEAR DEFORMATION OF GRAPHITE, AIAA JOURNAL, OCTOBER 1976.
  - A NONSYMMETRIC COMPLIANCE MATRIX APPROACH TO NONLINEAR MULTIMODULUS ORTHOTROPIC MATERIALS, AIAA JOURNAL, OCTOBER 1977.

- SOLID BODIES
  - ABOVE REFERENCES PLUS
  - NONLINEAR DEFORMATION OF A THERMALLY STRESSED GRAPHITE ANNULAR DISK AIAA JOURNAL, AUGUST 1977.
  - APPARENT FLEXURAL MODULUS AND STRENGTH OF MULTIMODULUS MATERIALS JOURNAL OF COMPOSITE MATERIALS, OCTOBER 1976.

PRINCIPAL FINDINGS AND CONCLUSIONS, CONTINUED

MECHANICS OF COMPOSITE MATERIALS WITH DIFFERENT MODULI IN TENSION AND COMPRESSION

- LAMINATED PLATES AND SHELLS
  - LAMINATION ASYMMETRIES
    - BUCKLING AND VIBRATION OF UNSYMMETRICALLY LAMINATED CROSS-PLY RECTANGULAR PLATES, AIAA JOURNAL, DECEMBER 1973.
    - BUCKLING AND VIBRATION OF ANTISYMMETRICALLY LAMINATED ANGLE-PLY RECTANGULAR PLATES, JOURNAL OF APPLIED MECHANICS, DECEMBER 1973.
    - BUCKLING AND VIBRATION OF CROSS-PLY LAMINATED CIRCULAR CYLINDRICAL SHELLS, AIAA JOURNAL, MAY 1975.
    - DEFLECTION OF UNSYMMETRICALLY LAMINATED CROSS-PLY RECTANGULAR PLATES, PROCEEDINGS OF 12th ANNUAL MEETING OF THE SOCIETY OF ENGINEERING SCIENCE, OCTOBER 1975.
  - LINEAR ELASTIC MULTIMODULUS
    - BUCKLING OF STIFFENED LAMINATED COMPOSITE CIRCULAR CYLINDRICAL SHELLS WITH DIFFERENT MODULI IN TENSION AND COMPRESSION, AFOSR-TR-75-0547, FEBRUARY 1975.
    - BUCKLING OF LAMINATED COMPOSITE CIRCULAR CYLINDRICAL SHELLS WITH DIFFERENT MODULI IN TENSION AND COMPRESSION, PROCEEDINGS OF 1975 INTERNATIONAL CONFERENCE ON COMPOSITE MATERIALS, APRIL 1975.
    - BENDING AND EXTENSION OF CROSS-PLY LAMINATES WITH DIFFERENT MODULI IN TENSION AND COMPRESSION, PROCEEDINGS OF 17th AIAA/ASME SDM CONFERENCE, MAY 1976.
  - NONLINEAR ELASTIC
    - ANALYSIS OF NONLINEAR STRESS-STRAIN BEHAVIOR OF FIBER-REINFORCED COMPOSITE MATERIALS, PROCEEDINGS OF 17th AIAA/ASME SDM CONFERENCE, MAY 1976, AIAA JOURNAL, DECEMBER 1977.

SUMMARY

- SIGNIFICANT MULTIMODULUS EFFECTS FOR GRANULAR COMPOSITE MATERIALS
- MIXED MULTIMODULUS EFFECTS FOR FIBER-REINFORCED COMPOSITE MATERIALS
  - LOW FOR BORON/EPOXY AND GRAPHITE/EPOXY AT ROOM TEMPERATURE AND LOW HUMIDITY
  - (EXPECTED) HIGHER FOR BORON/EPOXY AND GRAPHITE/EPOXY AT ELEVATED TEMPERATURE AND HUMIDITY
  - (EXPECTED) HIGH FOR CARBON-CARBON UNDER ALL CONDITIONS
- MULTIMODULUS AND NONLINEAR EFFECTS ARE SUSCEPTIBLE TO RATIONAL ANALYSIS
- FUTURE WORK WILL BE CONCENTRATED ON CARBON-CARBON WITH SPECIAL ATTENTION TO ROCKET NOZZLE APPLICATIONS

CONTINUUM THEORY OF FRACTURE

M. E. GURTIN

CARNEGIE-MELLON UNIVERSITY

1. Conservation Laws

(a) Bimaterial Body

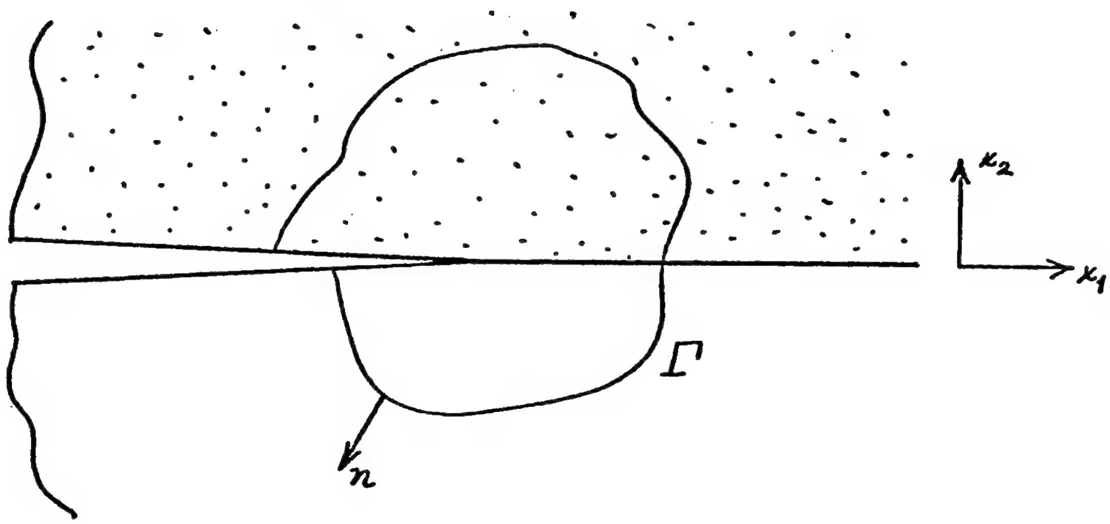

Result (with R. Smelser):

$$J = \int_{\Gamma} (W n_1 - \sigma n \cdot u_{,1})\, ds$$

independent of Γ

J... energy release rate

can be related to stress intensity factors

(b) *Dual-State Integral*

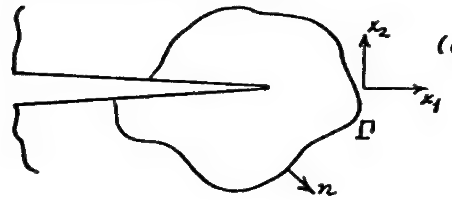

(u, ε, σ), $(\bar{u}, \bar{\varepsilon}, \bar{\sigma})$ solns.

$$\mathcal{J} = \int_\Gamma \{ \bar{\sigma}\cdot\varepsilon\, n_1 - \sigma n \cdot \bar{u}_{,1} - \bar{\sigma} n \cdot u_{,1} \}\, ds$$

independent of Γ (cf. Chen & Shield)

$\mathcal{J}$ can be related to s.i.f. — useful for mixed-mode loading — applicable to bimaterials

(c) *Elastodynamics*

$$I = \int_\Gamma \{ \tfrac{1}{2}[\sigma * \varepsilon + \rho u * \ddot{u}]\, n_1 - \sigma n * u_{,1} \}\, ds$$

independent of Γ

I can be related to s.i.f.

2. *Patched Variational Principles*

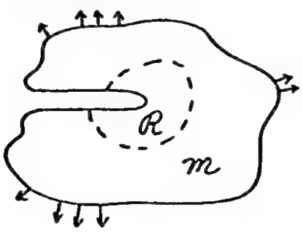

(with G. Fix)

Problem: determine numerically stresses around crack

Idea: use different var. princ. near crack ($\mathcal{R}$) and in far field ($\mathcal{M}$)

$$\delta \left\{ \int_{\mathcal{M}} W(\varepsilon)\, dV + \int_{\mathcal{R}} [\sigma\cdot\varepsilon - \hat{W}(\sigma)]\, dV - \int_{\mathcal{S}} s\cdot u\, dA \right\} = 0$$

$\mathcal{M}$: strain-disp.
stress-strain
disp. b.c.

$\mathcal{R}$: strain-disp.
disp. b.c.

Example:

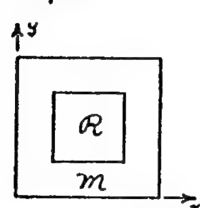

$\Delta\varphi = f$

$\varphi = \varphi_0$ on bdry

φ_0, f such that

$\varphi(x,y) = \sin(x+y)$

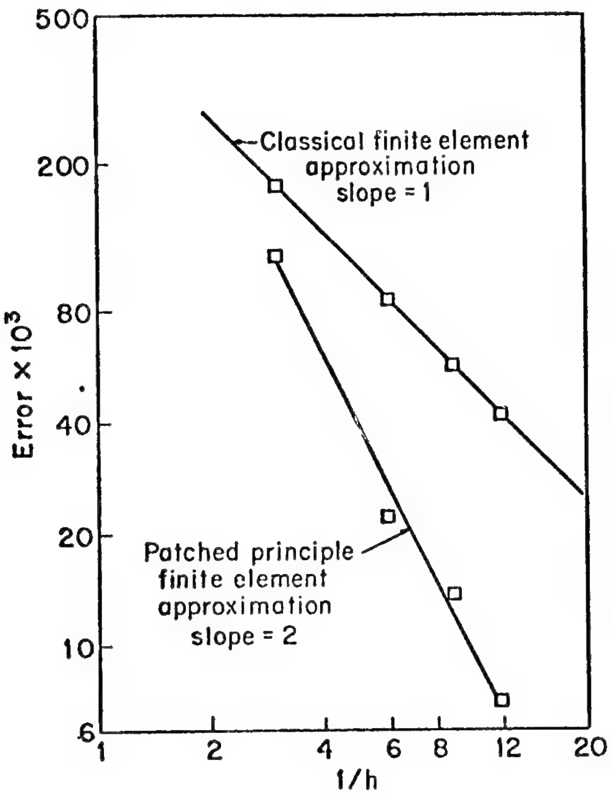

$L_2(\mathcal{R})$ *error in* $\nabla\varphi$

3. *Diffusion (Two Phase Flow)*

c... concentration in matrix
u... concentration in holes

Basic Equations (one space dim.)

$$c_t = \kappa c_{xx} + \alpha u - \beta c$$

$$u_t = -\alpha u + \beta c$$

Simple Problem (with C. Yatomi)

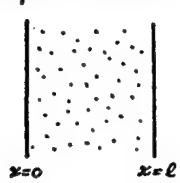

c, u prescribed initially (const.)

c, u prescribed at x = 0, ℓ for all time (const.)

Interested in:

$$G(t) = \frac{m(t) - m(0)}{m_s - m(0)}$$

m(t)... total weight at time t.
m_s... total weight when saturated

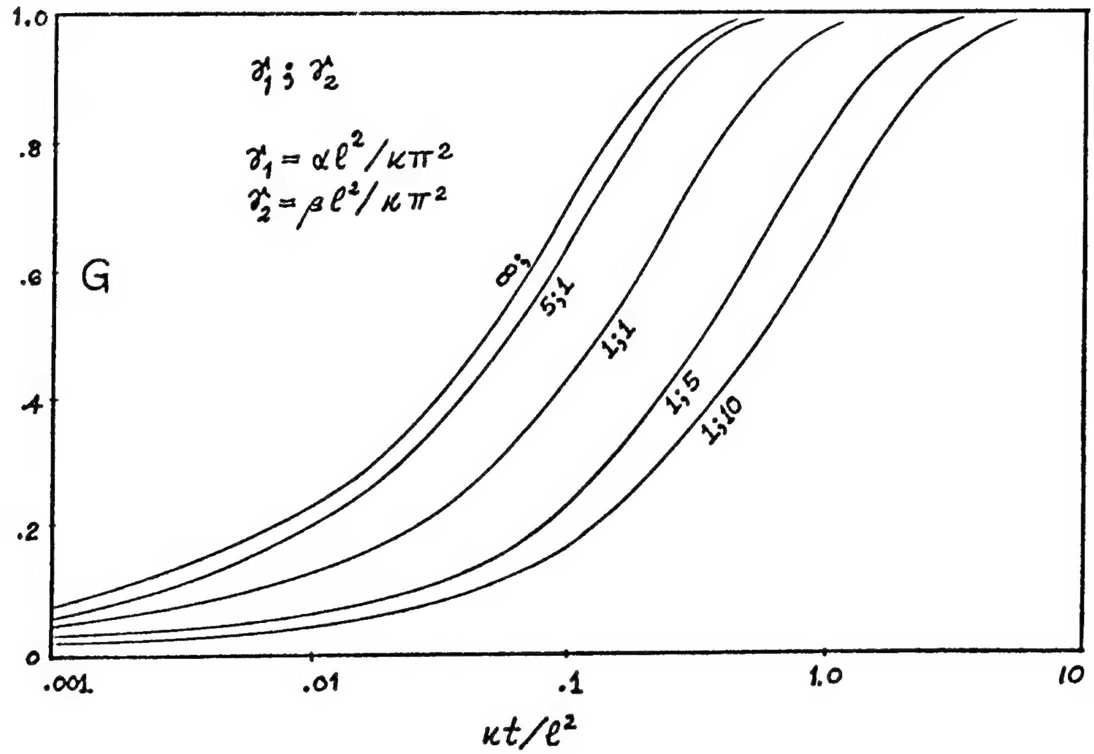
1.0
.8
.6
.4
.2
0
$\gamma_1 ; \gamma_2$
$\gamma_1 = \alpha \ell^2/\kappa\pi^2$
$\gamma_2 = \beta \ell^2/\kappa\pi^2$
G
∞;
5;1
1;1
1;5
1;10
.001
.01
.1
1.0
10
$\kappa t/\ell^2$

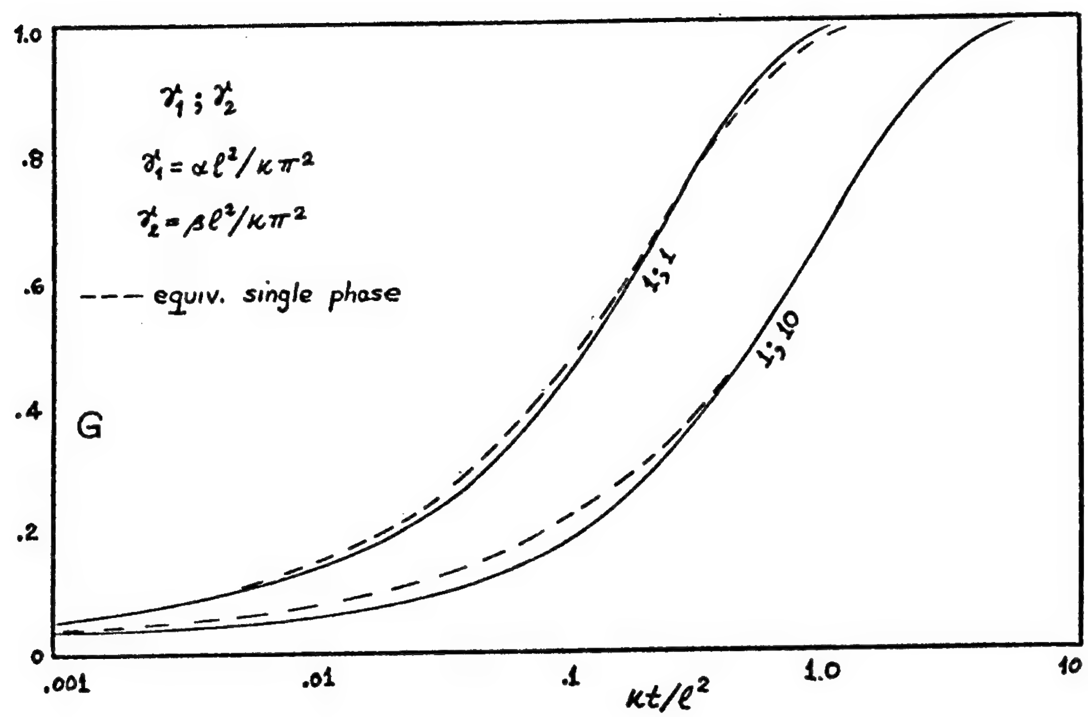
1.0
.8
.6
.4
.2
0
$\gamma_1 ; \gamma_2$
$\gamma_1 = \alpha \ell^2/\kappa\pi^2$
$\gamma_2 = \beta \ell^2/\kappa\pi^2$
--- equiv. single phase
G
1;1
1;10
.001
.01
.1
1.0
10
$\kappa t/\ell^2$

FRACTURE OF ADHESIVE JOINTS AND ADVANCED COMPOSITES
W. G. KNAUSS
CALIFORNIA INSTITUTE OF TECHNOLOGY

TIME DEPENDENT PROCESSES RELATED TO SERVICE LIFE PREDICTION OF BONDED JOINTS AND COMPOSITES

IMMEDIATE PURPOSE: STUDY THE MECHANICS OF THE TIME DEPENDENT DEBONDING PROCESS

A: LONG TIME, STEADY LOAD
B: CYCLIC LOADING

RELEVANCE: UNBONDING OF ADHESIVE JOINTS
UNBONDING OF FIBERS IN COMPOSITES
POSSIBLE: DELAMINATION

MODE I, II INTERACTION

DEGREE OF APPLICABILITY OF LINEARIZED THEORIES

A. ELASTIC
B. VISCOELASTIC
C. ARE NONLINEAR EFFECT IMPORTANT

CAN ADHESION BE CHARACTERIZED BY AN ADHESIVE FRACTURE ENERGY WHICH IS AN INTERFACE CHARACTERISTIC. PROBABLY.

EXAMPLE OF VISCOELASTIC EFFECT

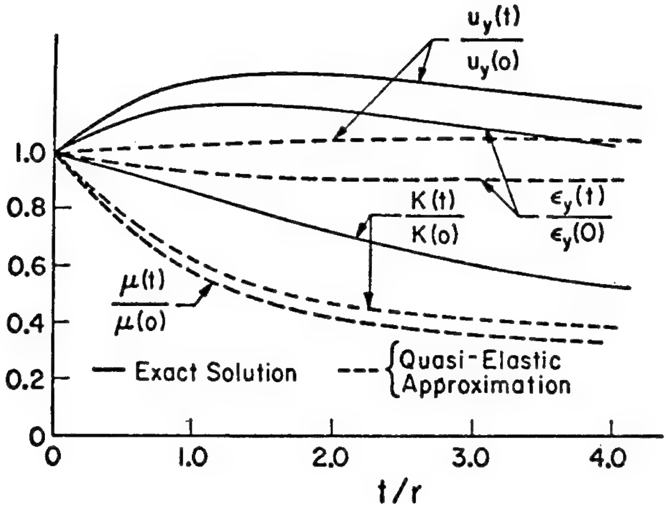

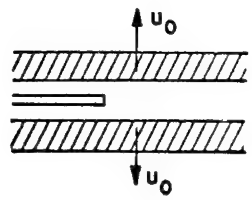

MEASURE DISPLACEMENTS OF CRACK OR DISBOND;
COMPARE WITH THEORY

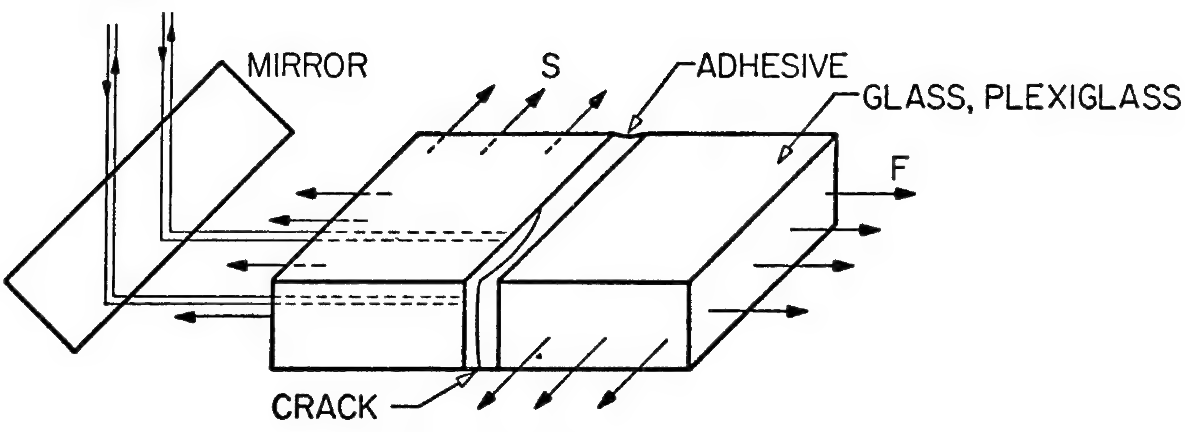

BUTT SPECIMEN

THERMAL DILATATION LOADING MACHINE

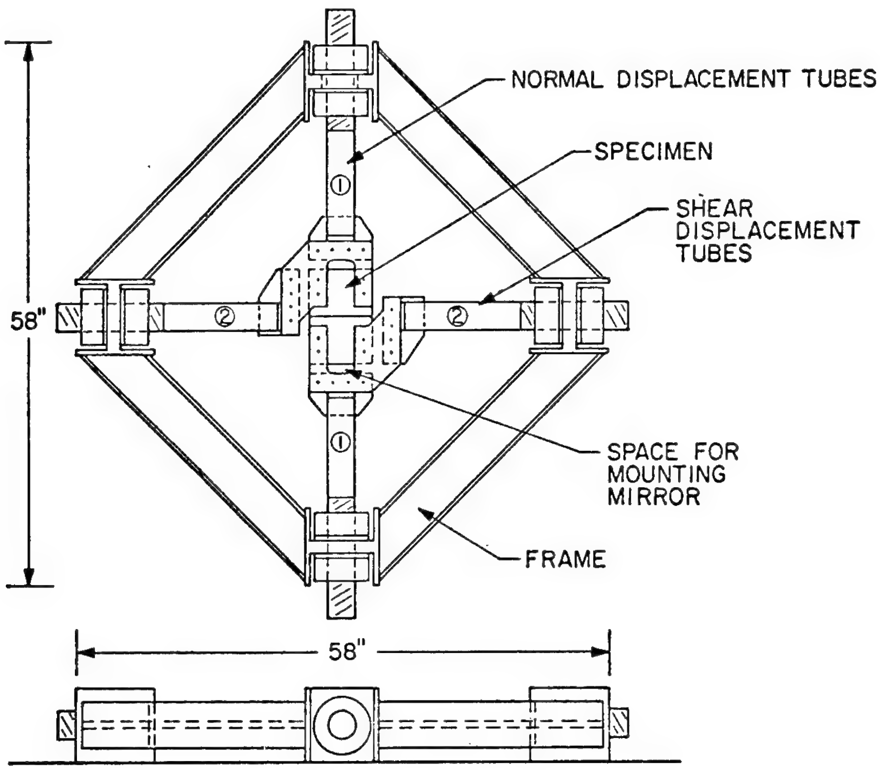

CRACK PROFILE IN A DEBOND BETWEEN PLEXIGLASS AND SOLITHANE

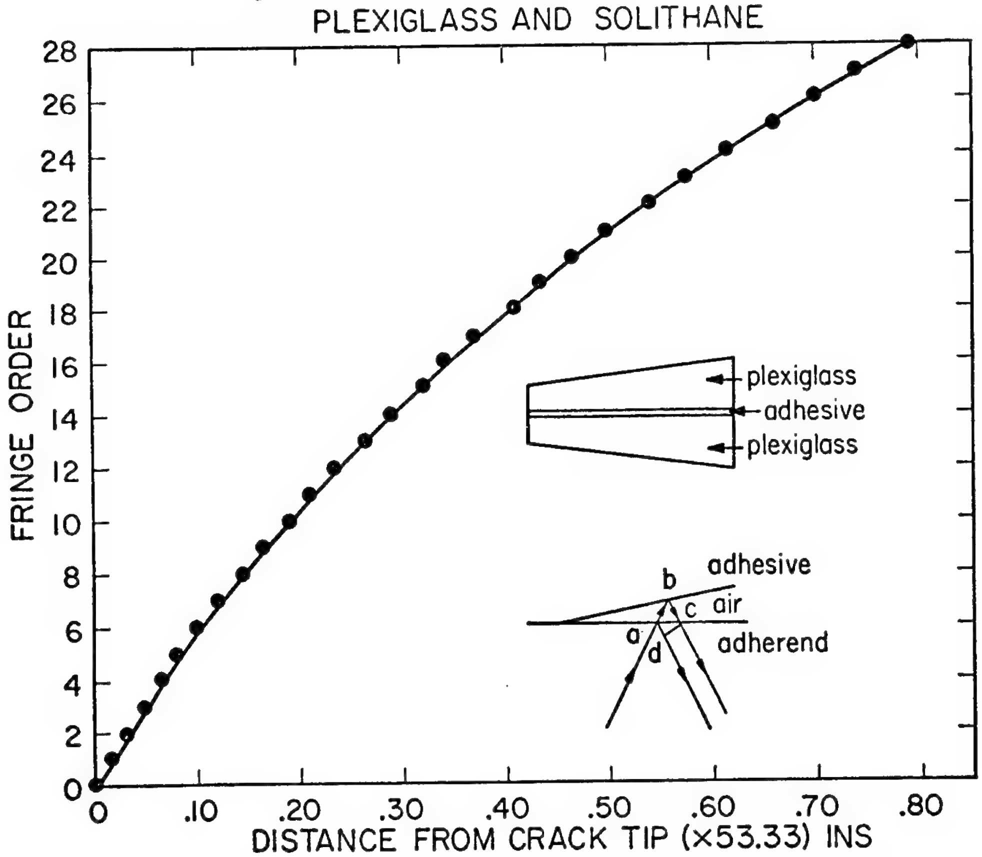

MOISTURE DIFFUSION IN ADVANCED COMPOSITE RESIN MATRIX LAMINATES

BY

C. D. SHIRRELL
STRUCTURAL MECHANICS DIVISION
AIR FORCE FLIGHT DYNAMICS LABORATORY
WRIGHT-PATTERSON AFB, OH

TYPES OF DIFFUSION

- CONCENTRATION DEPENDENT FICKIAN DIFFUSION
- CONCENTRATION INDEPENDENT FICKIAN DIFFUSION
- TIME DEPENDENT DIFFUSION ANOMALIES
- CASE II DIFFUSION TRANSPORT
- SOLVENT CRAZING/STRESS CRACKING

RELATIONSHIP BETWEEN DIFFUSION MECHANISMS

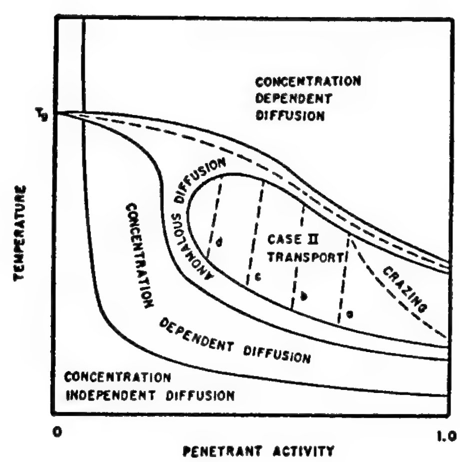

- HOPFENBERG AND FRISCH

EXPERIMENTAL DETERMINATION OF THE DIFFUSIVITY

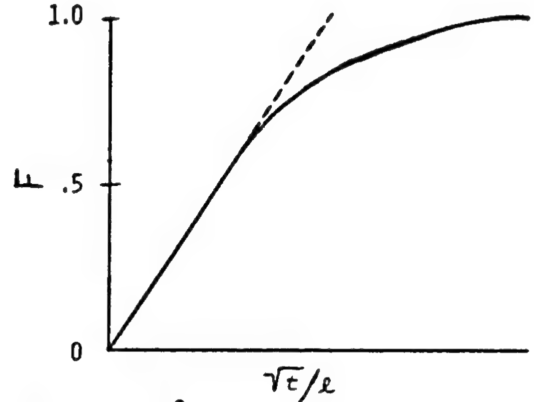

WHERE $F \equiv \frac{M_t - M_0}{M_\infty - M_0}$

- $D = \left(\frac{\pi}{16}\right)\left(\frac{F}{\sqrt{t}/\ell}\right)^2$ FOR $F \leq 0.6$
- REDUCED SORPTION CURVE

TEST MATERIALS

- T300/5208 GRAPHITE/EPOXY LAMINATES
- A MIDPLANE SYMMETRIC AND BALANCED CROSS-PLY (0°/90°) LAMINATE
- CURED IN AUTOCLAVE WITH STANDARD VACUUM BAG AND MANUFACTURERS CURE CYCLE
- LAMINATES WERE 7 PLY, 14 PLY, AND 21 PLY THICK
- 778 SPECIMENS WERE USED IN THIS STUDY - 19 WERE USED IN QUALITY CONTROL TESTS AND THE REMAINING 759 WERE MOISTURE CONDITIONED
- 84 OF THE SEVEN PLY SPECIMENS WERE POSTCURED AT 400°F FOR 4 HOURS

DENSITY AND RESIN CONTENT RESULTS

NUMBER OF PLIES	NUMBER OF SPECIMENS TESTED	DENSITY (GMS/CM^3)	RESIN CONTENT (WT. %)	VOID CONTENT (VOL. FRACTION, %)
7	39	1.59(1)	26.1(6)	0.1
14	9	1.59(1)	26.4(3)	-.1
21	9	1.59(1)	26.7(5)	-.8

EXPERIMENTS PERFORMED IN THIS STUDY

- PERIODICALLY MONITOR THE WEIGHT GAIN OF SPECIMENS AS THEY GO FROM 0% MOISTURE CONTENT TO EQUILIBRIUM MOISTURE CONTENT AT ONE OF 33 DIFFERENT HYDROTHERMAL CONDITIONS FORMED FROM:
  - 4 TEMPERATURES: 70°F, 110°F, 145°F, AND 180°F
  - 13 DIFFERENT RELATIVE HUMIDITIES

- UPON REACHING THE EQUILIBRIUM MOISTURE CONTENT AT A GIVEN HUMIDITY SWITCH THE SPECIMEN TO ANOTHER RELATIVE HUMIDITY AND PERIODICALLY MONITOR WEIGHT GAIN/LOSS AS THEY GO TO THE NEW EQUILIBRIUM MOISTURE CONTENT.

TYPICAL SORPTION EXPERIMENT

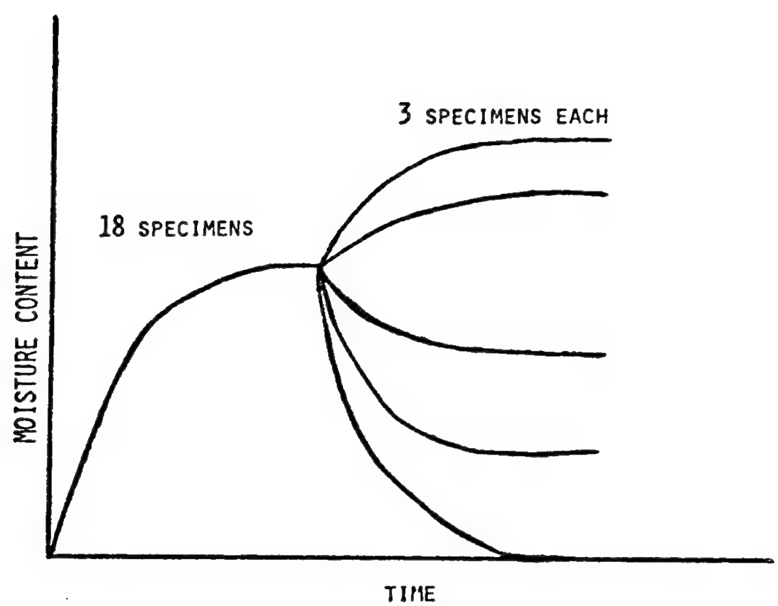

- INTEGRAL ABSORPTION CURVE, INTEGRAL DESORPTION CURVE, AND INTERVAL SORPTION CURVE.

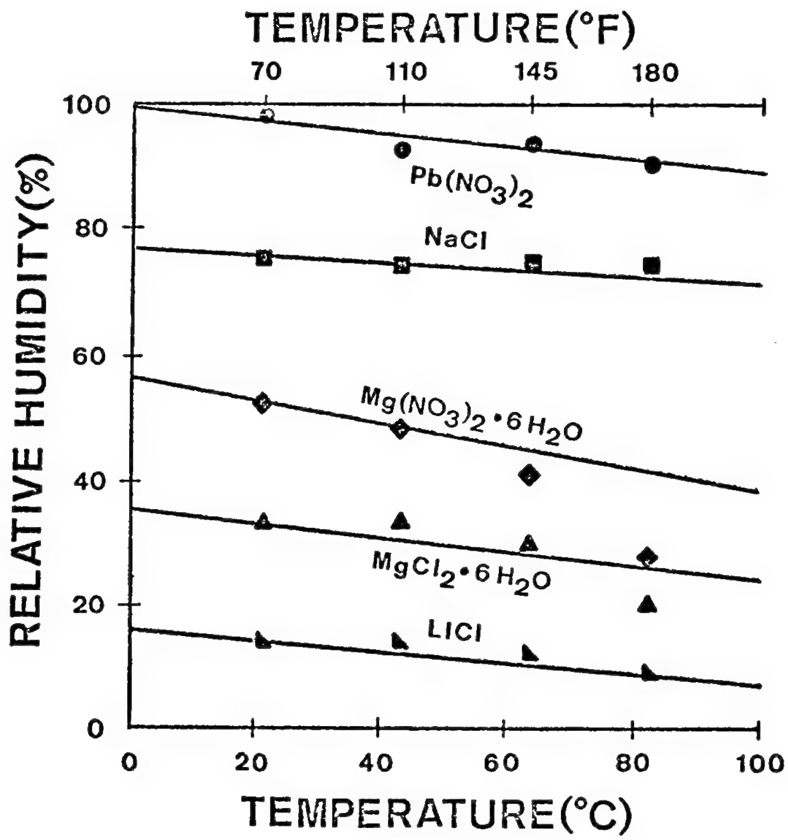

DEFINITIONS OF MOISTURE CONTENT

$$M_t = \frac{(W_t - W_i)\rho_r}{f_r W_i} \qquad m_t = \frac{W_t - W_i}{W_i} \times 100$$

M_t - MOISTURE CONTENT, GMS OF WATER PER CM^3 OF RESIN

m_t - MOISTURE CONTENT, WT % OF THE LAMINATE

f_r - WEIGH FRACTION RESIN IN THE COMPOSITE LAMINATE

ρ_r - DENSITY OF THE RESIN, 1.265 GMS/CM^3

W_i - INITIAL DRY WEIGHT OF THE SPECIMEN, GMS

W_t - WEIGHT OF THE SPECIMEN AT TIME t, GMS

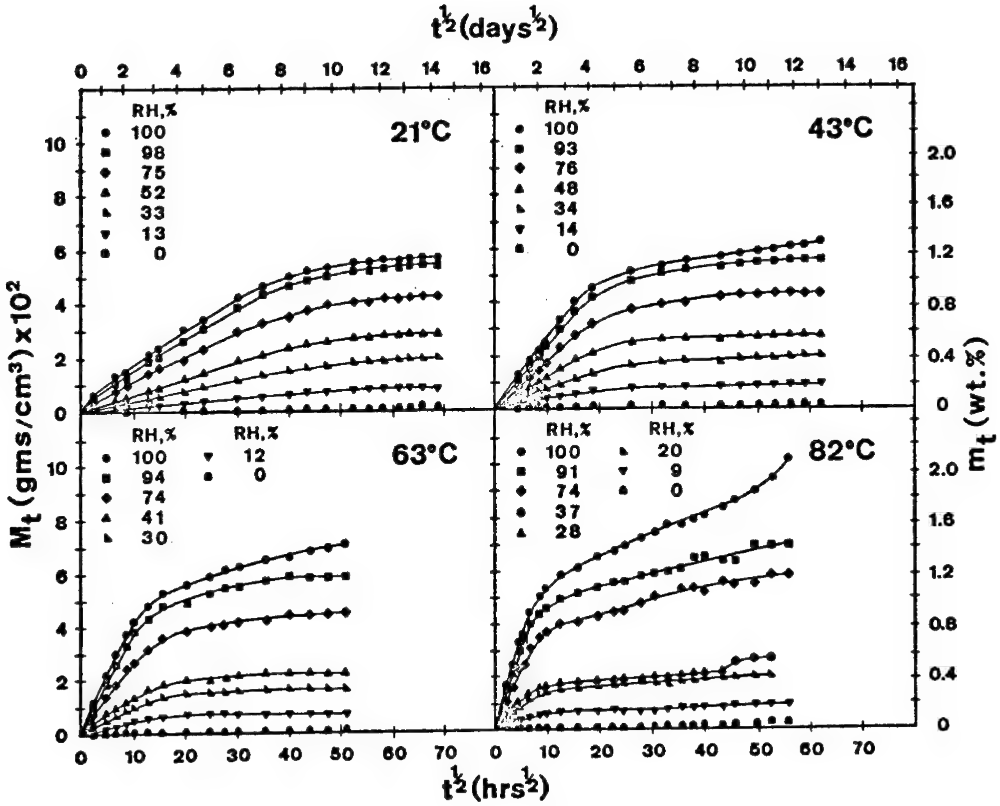
t½(days½)
21°C
43°C
63°C
82°C
RH,%
M_t (gms/cm³) x10²
m_t (wt.%)
t½(hrs½)

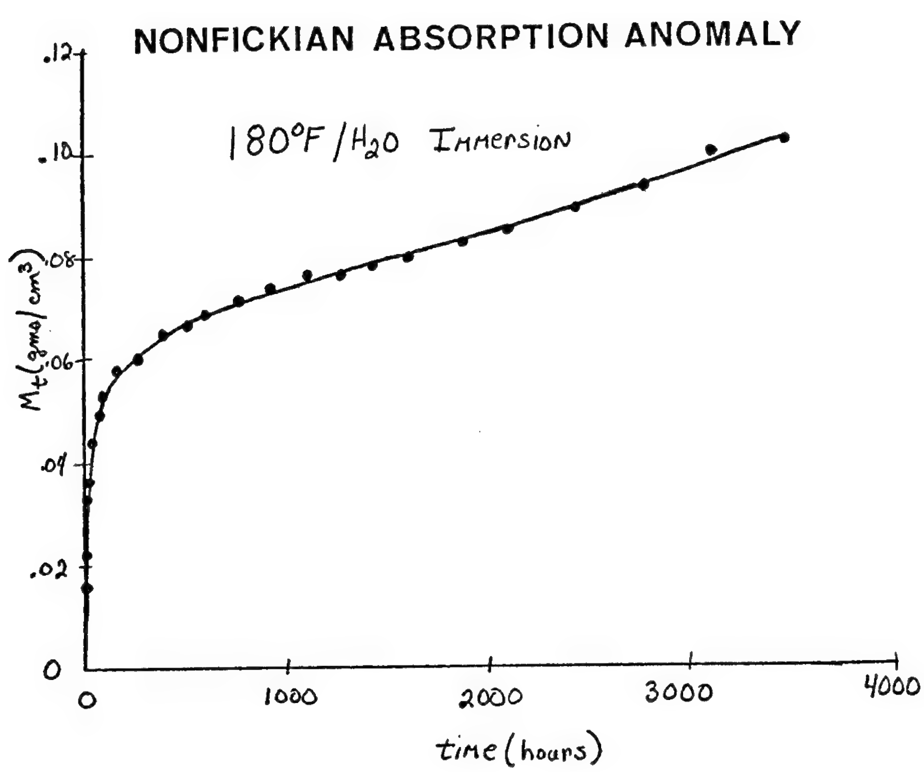
NONFICKIAN ABSORPTION ANOMALY
180°F / H₂O Immersion
M_t (gms/cm³)
time (hours)

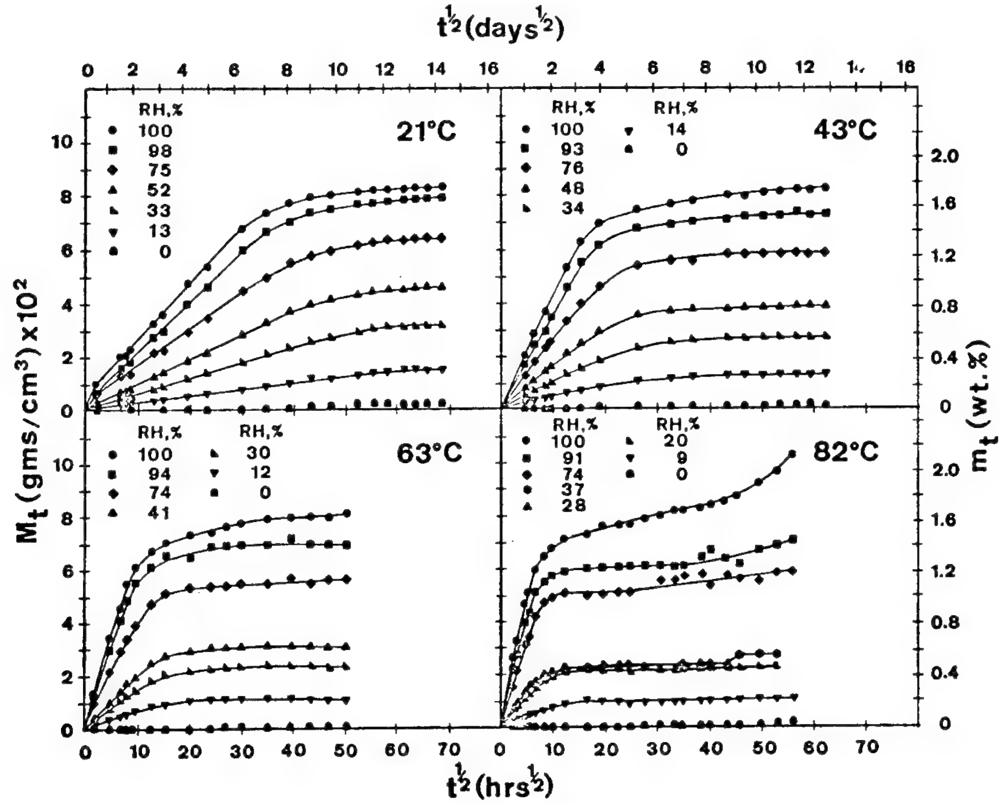

t½(days½)
21°C
43°C
63°C
82°C
RH,%
M_t (gms/cm³) x10²
m_t (wt.%)
t½(hrs½)

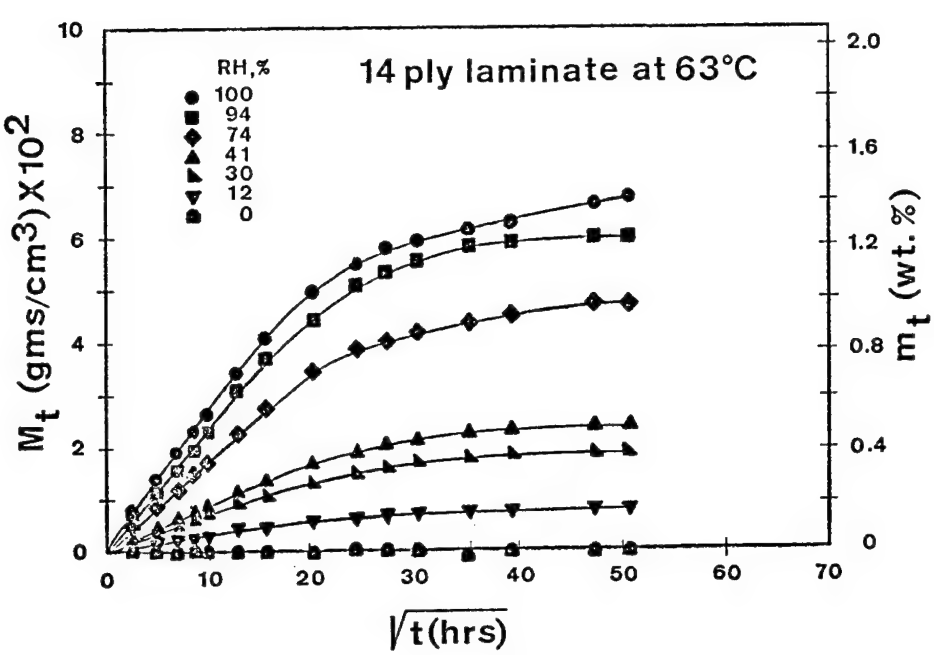

14 ply laminate at 63°C
RH,%
100
94
74
41
30
12
0
M_t (gms/cm³) X10²
m_t (wt.%)
√t(hrs)

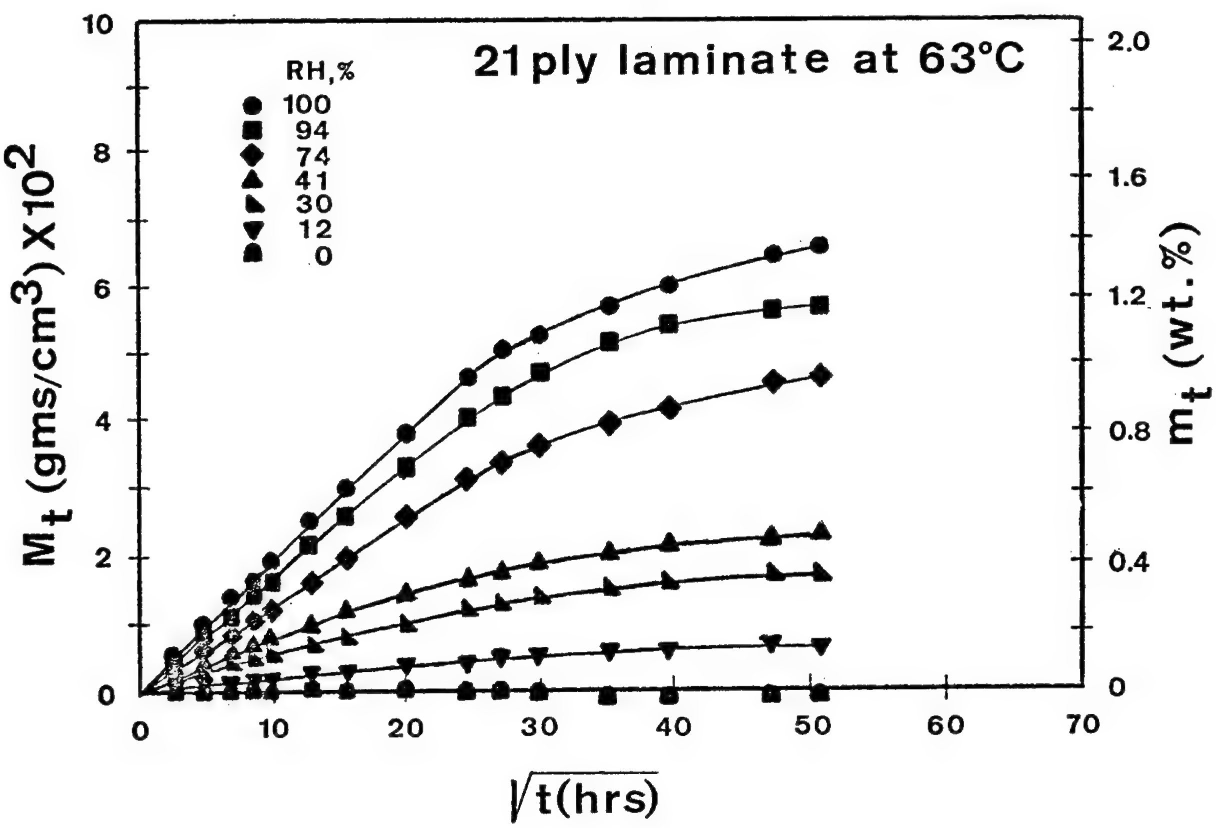
21ply laminate at 63°C
RH,%
100
94
74
41
30
12
0
M_t (gms/cm^3) X10^2
m_t (wt.%)
$\sqrt{t}$(hrs)

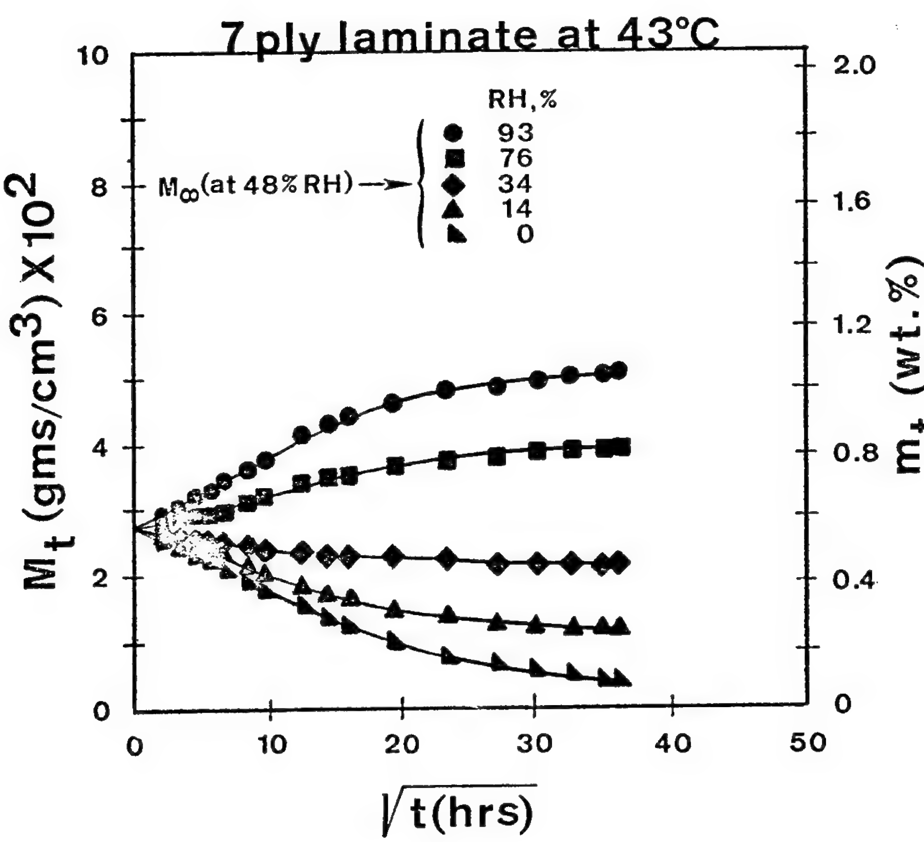
7ply laminate at 43°C
RH,%
93
76
34
14
0
M_∞(at 48% RH)
M_t (gms/cm^3) X10^2
m_t (wt.%)
$\sqrt{t}$(hrs)

EQUILIBRIUM SOLUBILITY OF MOISTURE IN T300/5208 LAMINATES

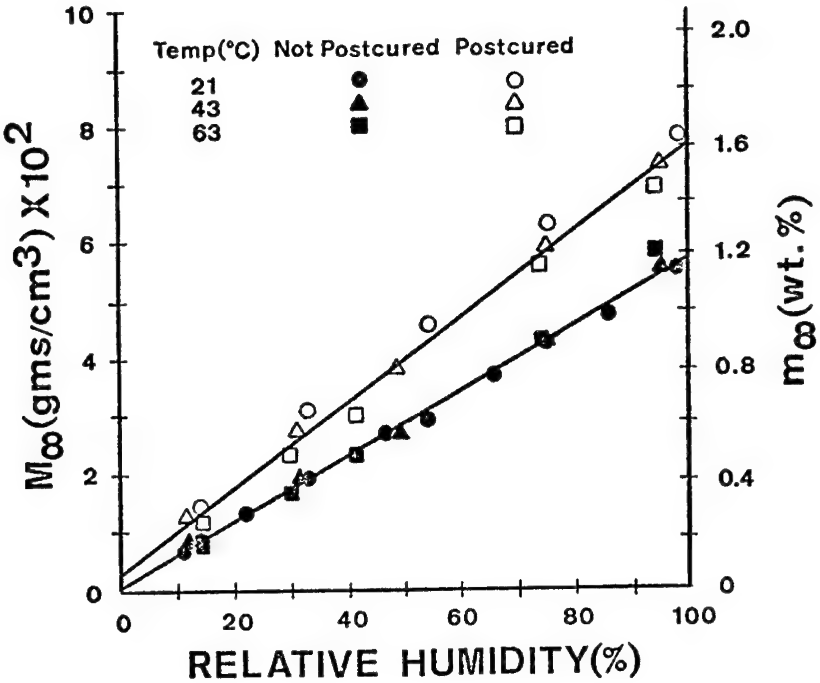

EQUILIBRIUM MOISTURE CONTENT

$M_\infty = a(RH)^b$ $\qquad\qquad$ $m_\infty = a'(RH)^{b'}$

a, b, a', AND b' - EMPIRICAL PARAMETERS

RH, RELATIVE HUMIDITY, %

EMPIRICAL VALUES FOR THE SOLUBILITY PARAMETERS

	a (GMS/CM^3)	b	a' (WT. % OF THE LAMINATE)	b'
NONPOSTCURED	.00058	1	.0117	1
POSTCURED	.00075	1	.0155	1

FICKIAN DIFFUSION

- Both absorption and desorption curves are linear in the initial state, i.e., $F \leq 0.6M_\infty$.
- Above the linear portions both absorption and desorption curves are concave to the abscissa axis until M_∞ is reached.
- A series of sorption curves for specimens at different thickness are superimposable if each curve is plotted in the form of a reduced sorption curve, i.e., F vs $\sqrt{t}/\ell$.
- If D_{ABS} is not equal to D_{DES}, then D is dependent upon concentration.

INTEGRAL CONJUGATE SORPTION FOR 7 PLY LAMINATES WITH NO PC

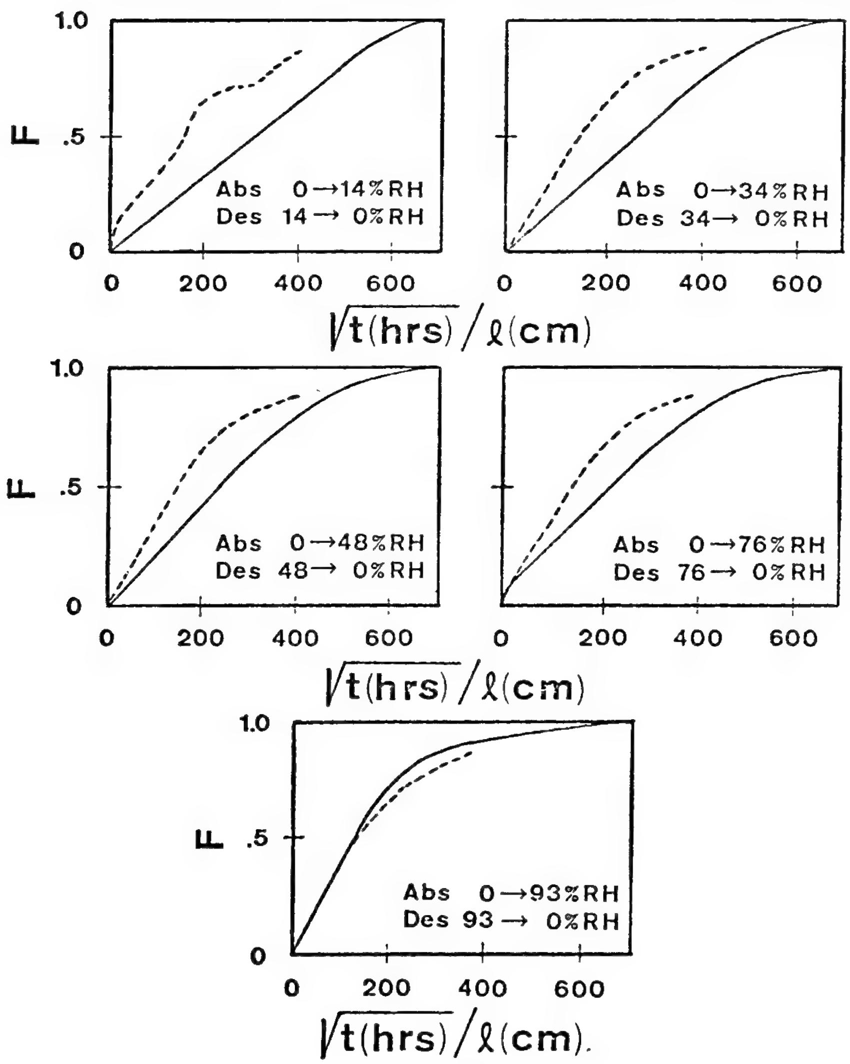

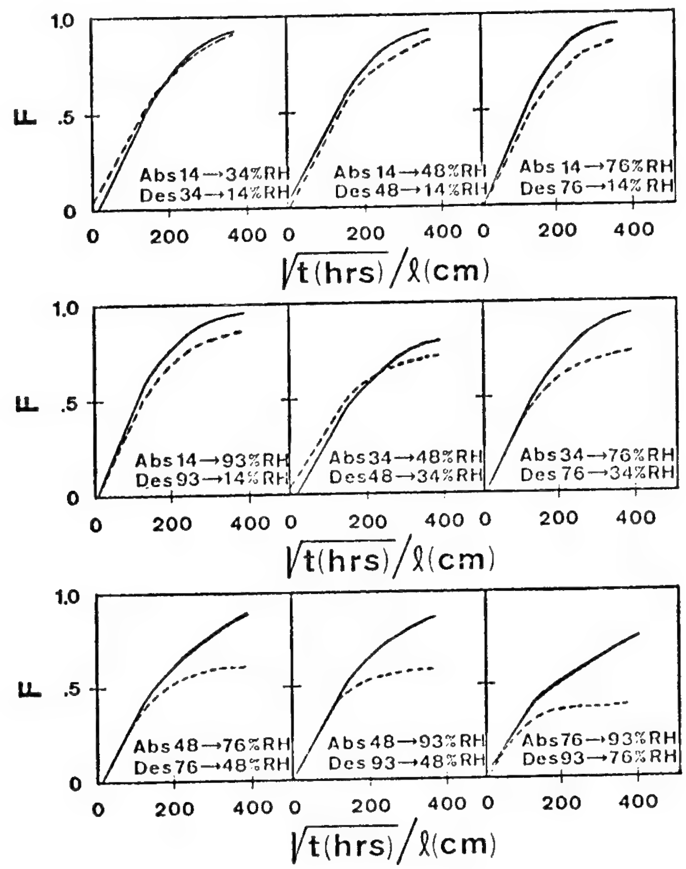

7 PLY LAMINATES WITH PC

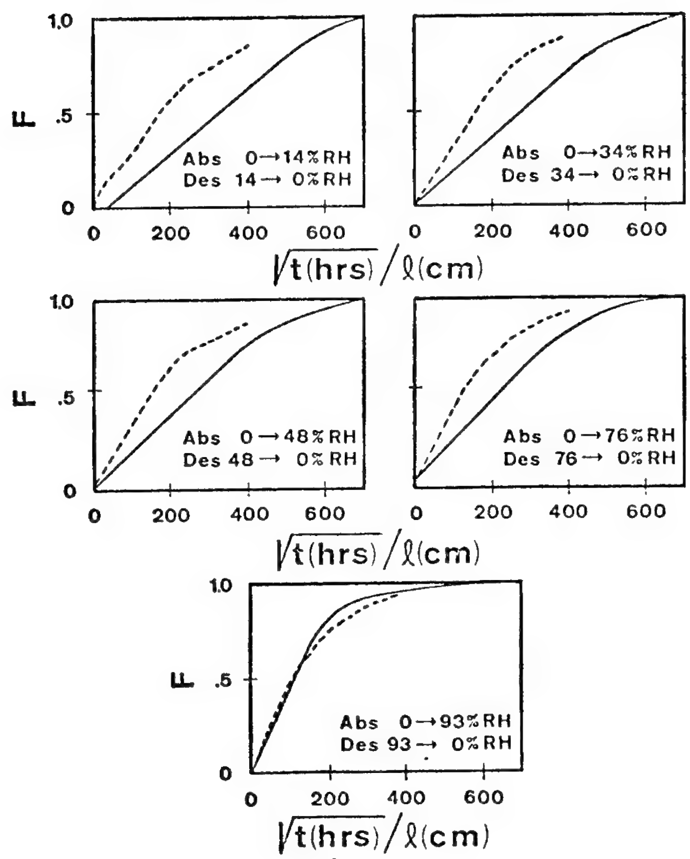

INTEGRAL REDUCED ABSORPTION FOR LAMINATES OF DIFFERENT THICKNESS

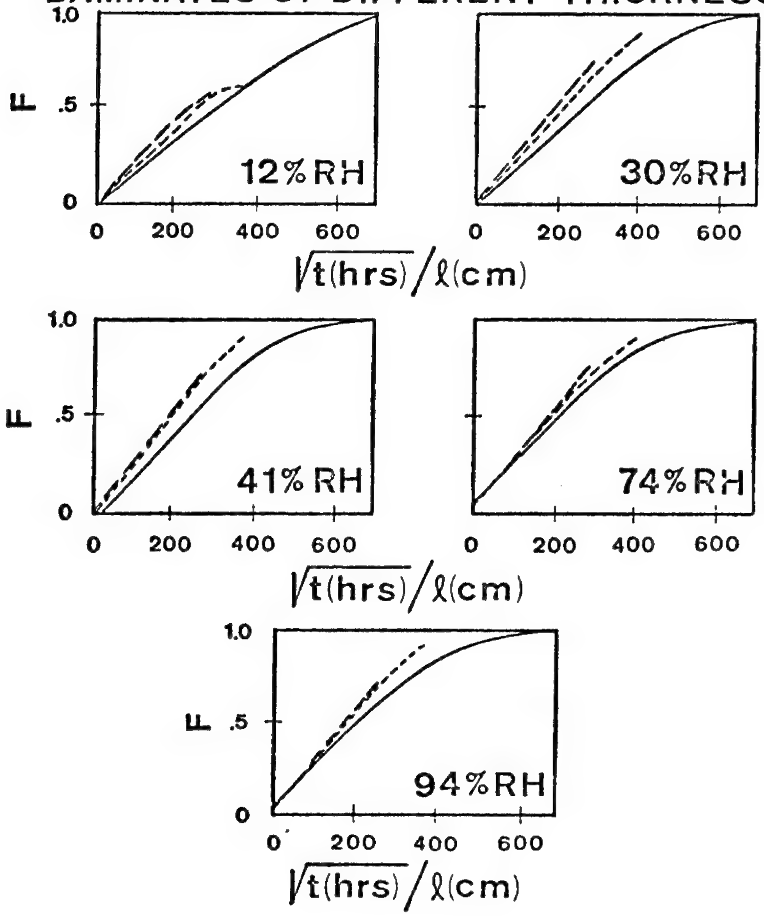

POSSIBLE PLY THICKNESS EFFECTS UPON DIFFUSIVITY

- Stress effects upon the mutual diffusion coefficient
- Stress effects upon the surface concentration of the penetrant
- Time dependent slow relaxation processes
- Anisotropic nature of the diffusion coefficient in fiberous resin matrix laminates, i.e., $D_{EDGE} \gg D_{SURFACE}$
  - Fiber obstruction would not explain the observed differences
  - Degradation of the fiber/resin interface by moisture (leading to rapid moisture penetration into the interior of the laminate) could result in $D_{EDGE} \gg D_{SURFACE}$.

APPARENT CONCENTRATION DEPENDENCE FOR DIFFUSION

- SINCE IN MANY OF THE REDUCED SORPTION PLOTS

$$D_{ABS} \neq D_{DES}$$

CONCENTRATION DEPENDENT DIFFUSION WOULD BE SUSPECTED OF OCCURING.

- THIS POSSIBILITY WAS EVALUATED USING THE METHOD OF BARRIER AND BROOK.

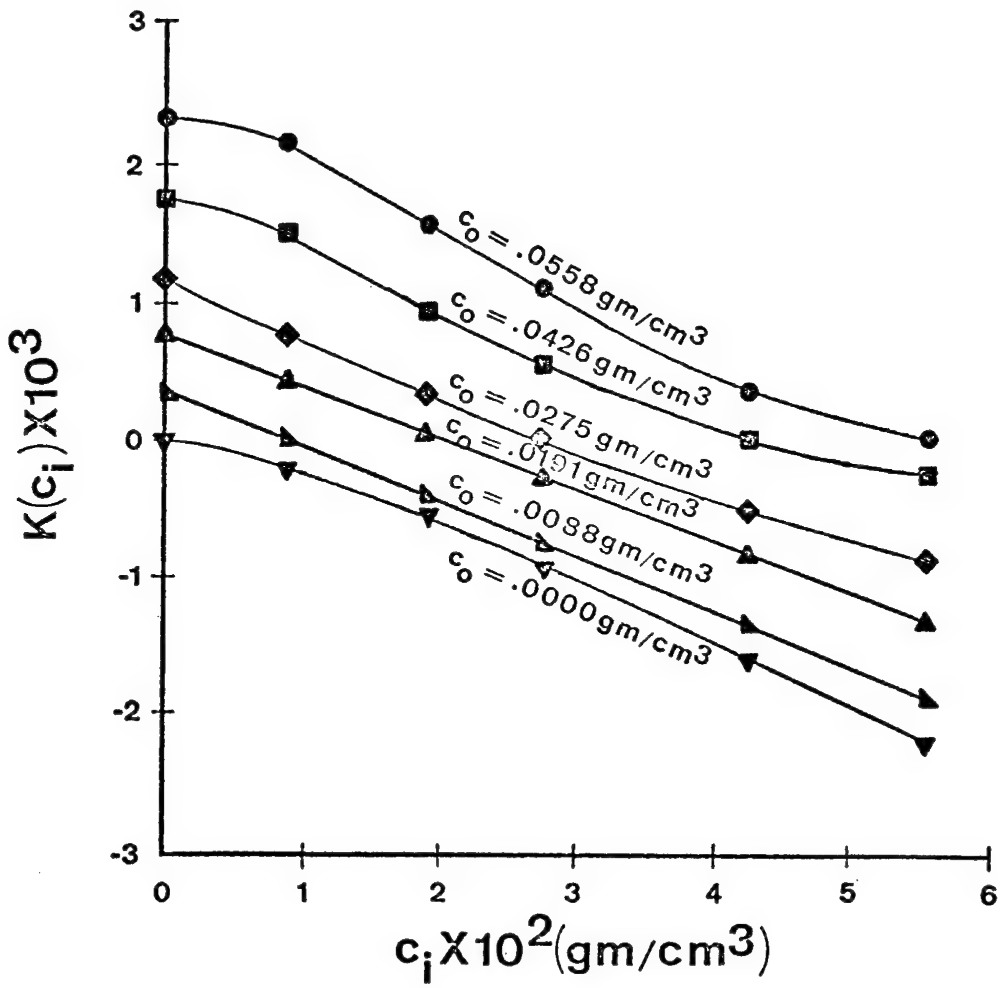

ARRHENIUS PLOT OF MOISTURE ABSORPTION IN T300/5208 LAMINATES

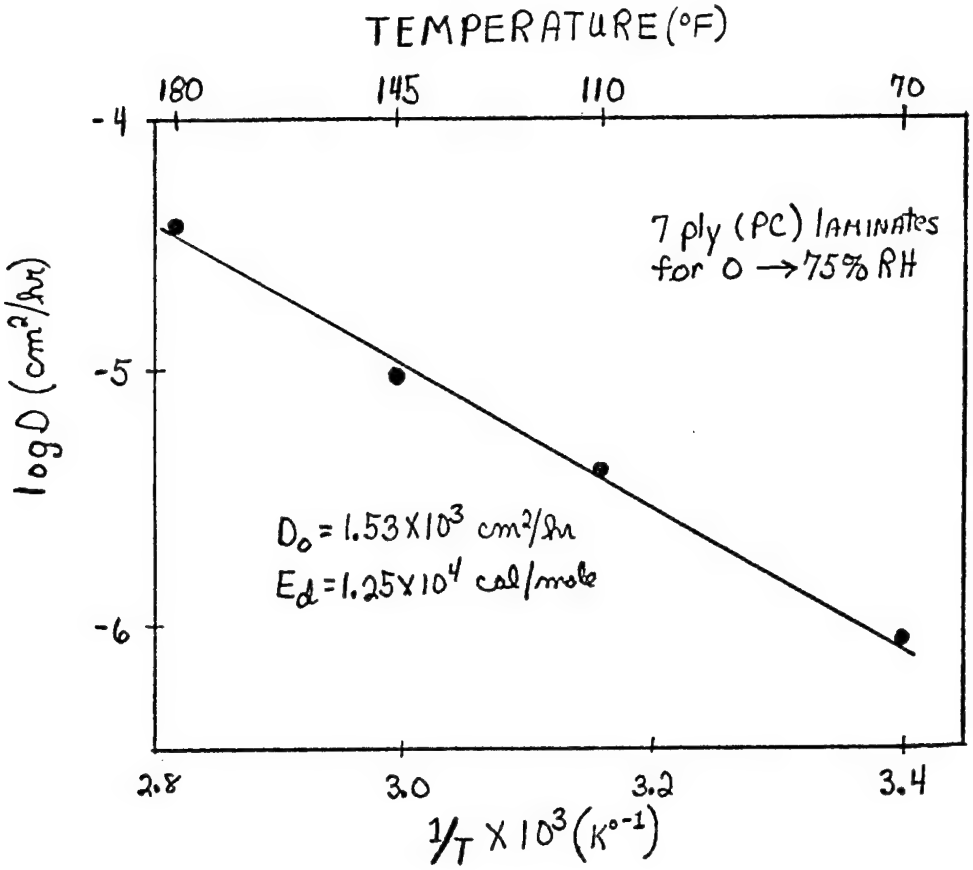

CONCLUSIONS

- NONFICKIAN ABSORPTION ANOMALIES WERE OBSERVED FOR T300/5208 SPECIMENS EXPOSED AT 180°F AND
  - FOR RH > 75% (POSTCURED SPECIMENS)
  - FOR ALL HUMIDITY CONDITIONS (NONPOSTCURED SPECIMENS).
- EQUILIBRIUM SOLUBILITY OF MOISTURE IN T300/5208 LAMINATES IS EFFECTED BY THE DEGREE OF CURE OF THE MATERIAL.
- EQUILIBRIUM MOISTURE SOLUBILITY IS LINEARLY RELATED TO RELATIVE HUMIDITY IN T300/5208 LAMINATES.
- NONFICKIAN DIFFUSION ANOMALIES WERE OBSERVED FOR INTERVAL SORPTION EXPERIMENTS.
- THE EQUILIBRIUM MOISTURE SOLUBILITY OF NONPOSTCURED SPECIMENS IS INDEPENDENT OF TESTING TEMPERATURE. FOR POSTCURED SPECIMENS THERE IS A DEFINITE TREND TOWARD LOWER EQUILIBRIUM MOISTURE CONTENT WITH INCREASING TESTING TEMPERATURE.

FRACTURE AND FATIGUE OF BI-MATERIALS

J. MAR

MASSACHUSETTS INSTITUTE OF TECHNOLOGY

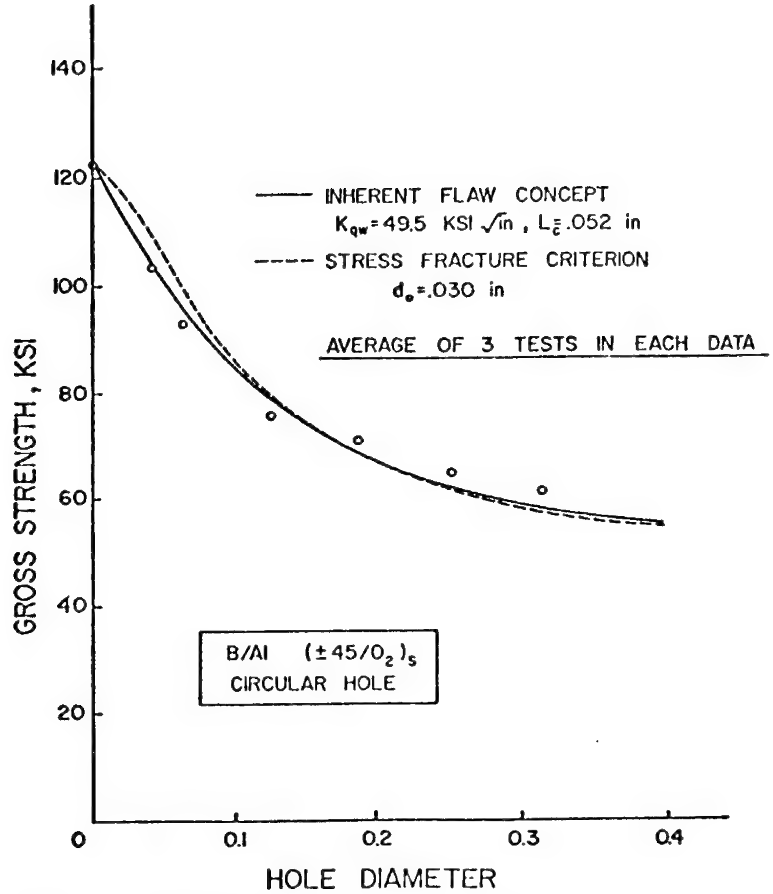

FIGURE 1 CORRELATION WITH WEK AND WN MODELS

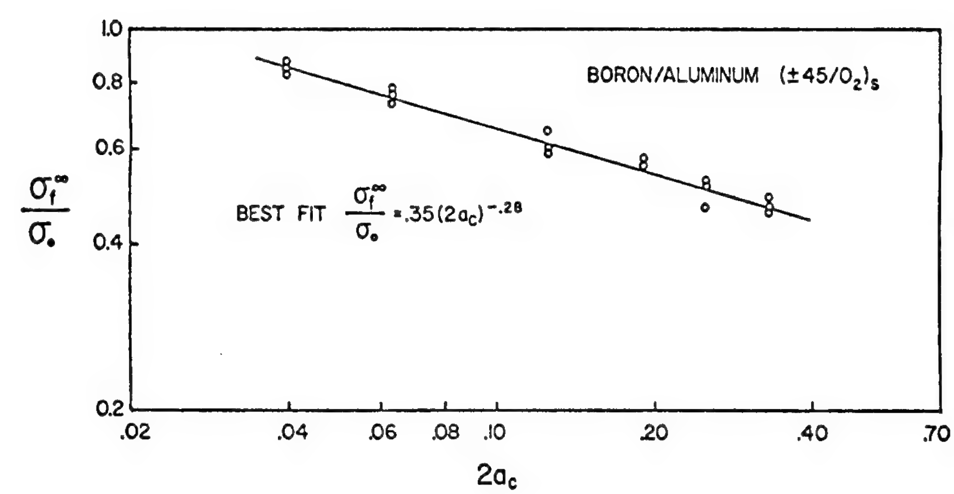

FIGURE 2 CORRELATION OF SPECIMENS WITH HOLES

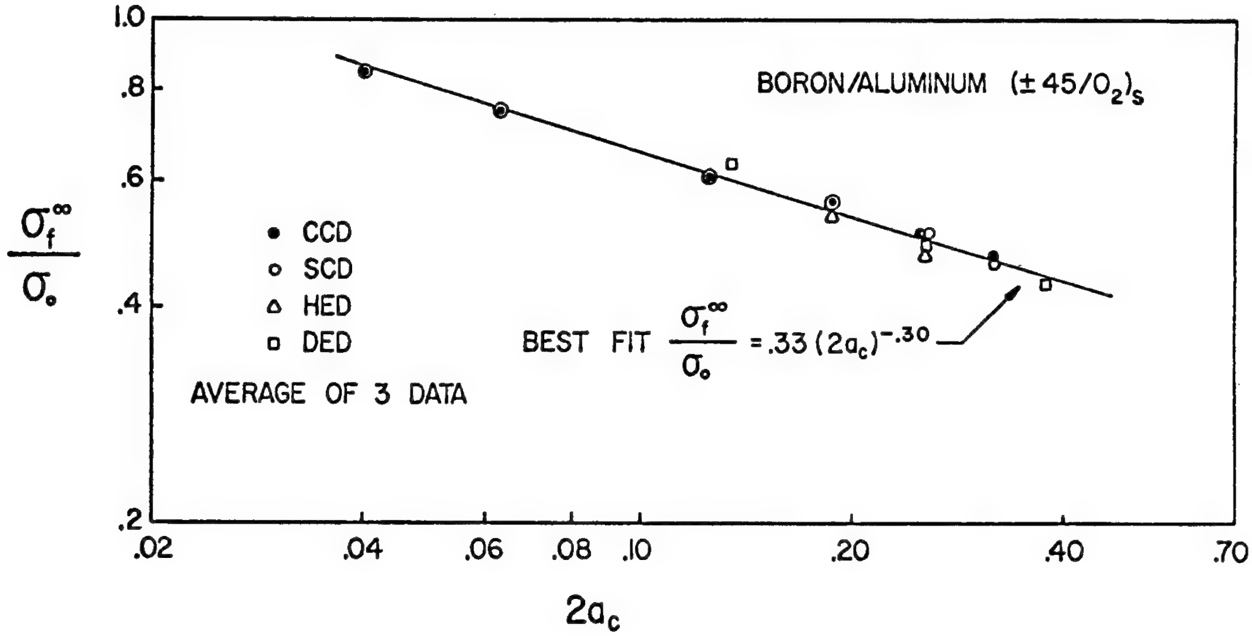

FIGURE 3 CORRELATION OF ALL SPECIMENS

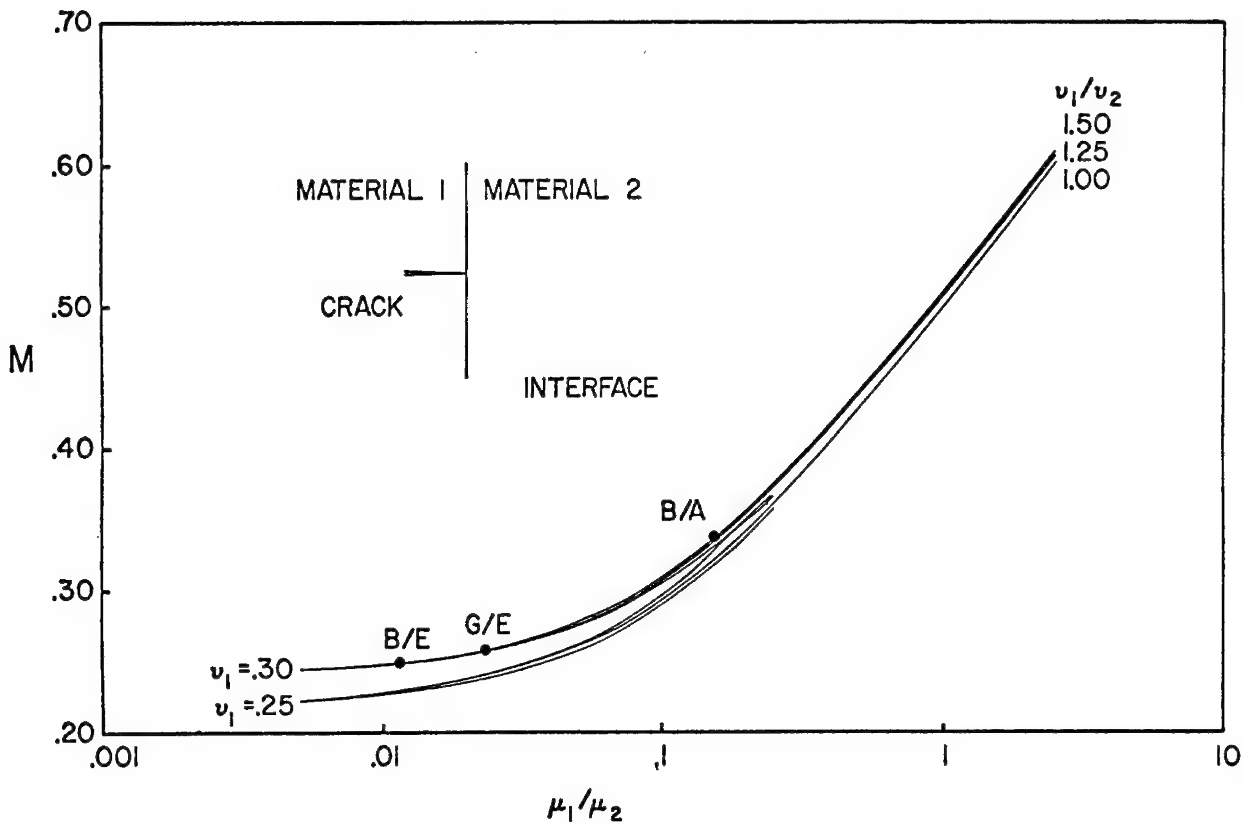

FIGURE 4 VALUES OF "M"

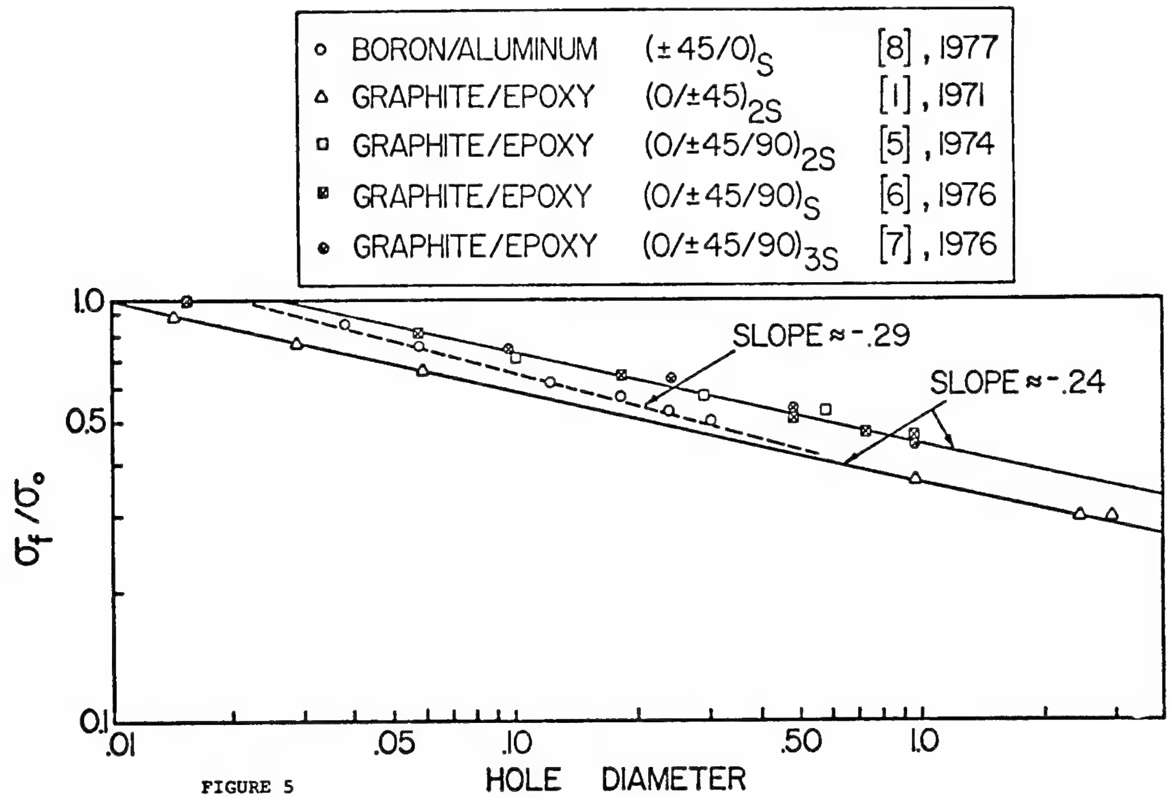

FIGURE 5

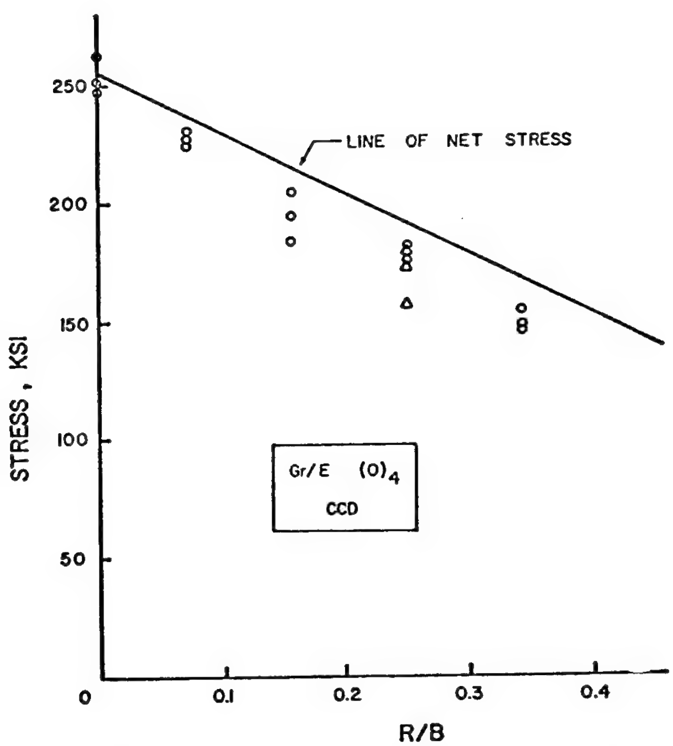

FIGURE 6 Strength Reduction of $(0)_4$ CCD Graphite/Epoxy Specimens

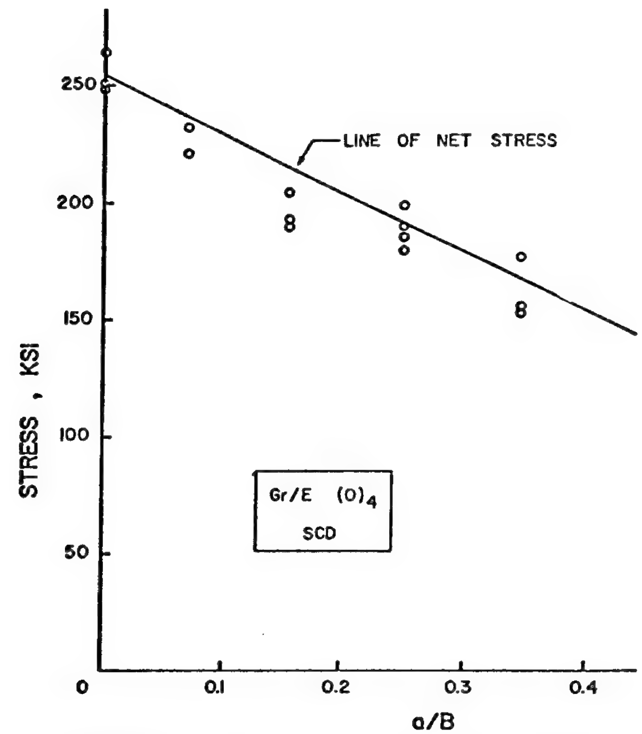

FIGURE 7 Strength Reduction of $(0)_4$ SCD Graphite/Epoxy Specimens

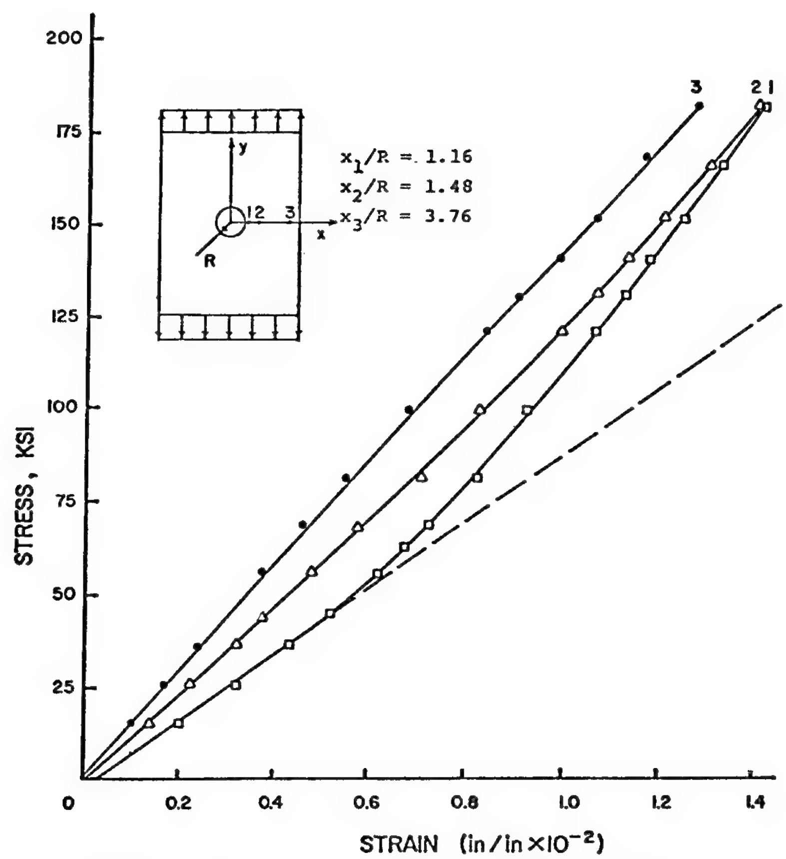

FIGURE 8 Strain Distribution for Graphite/Epoxy CCD Specimens

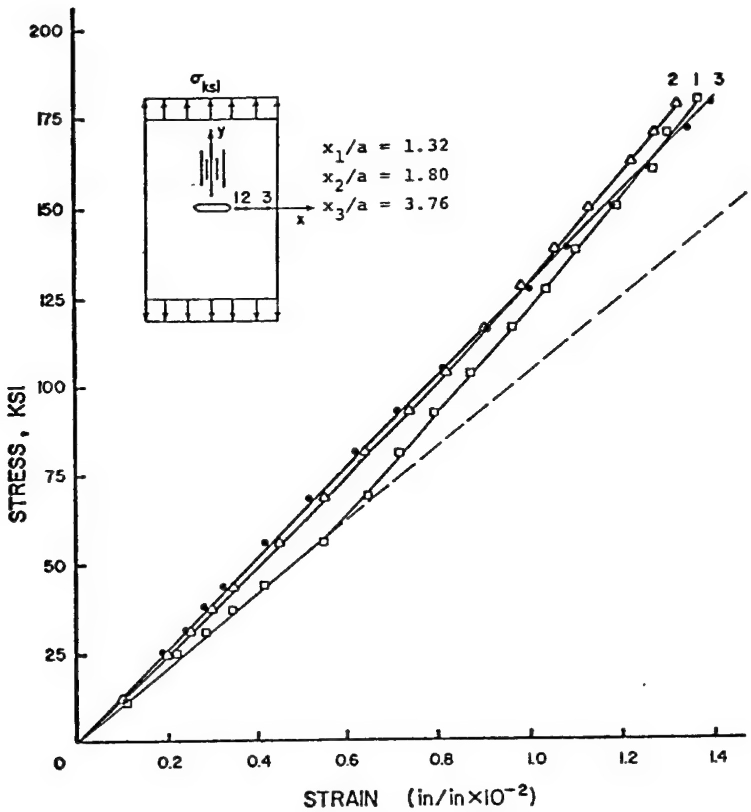

FIGURE 9 Strain Distribution for Graphite/Epoxy SCD Specimen

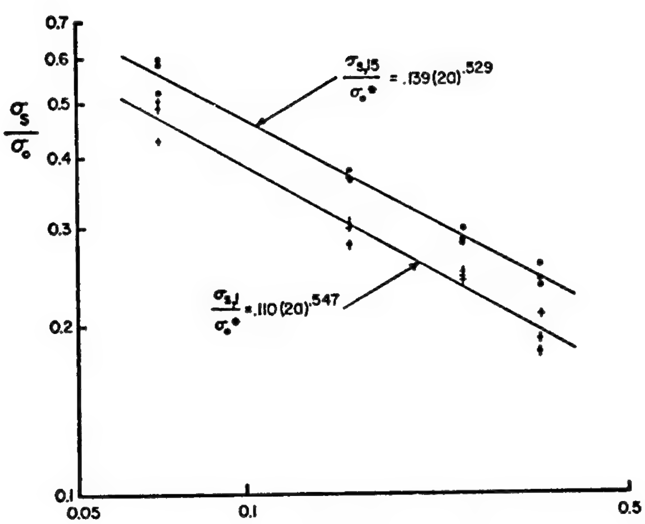

FIGURE 10 2a DISCONTINUITY LENGTH

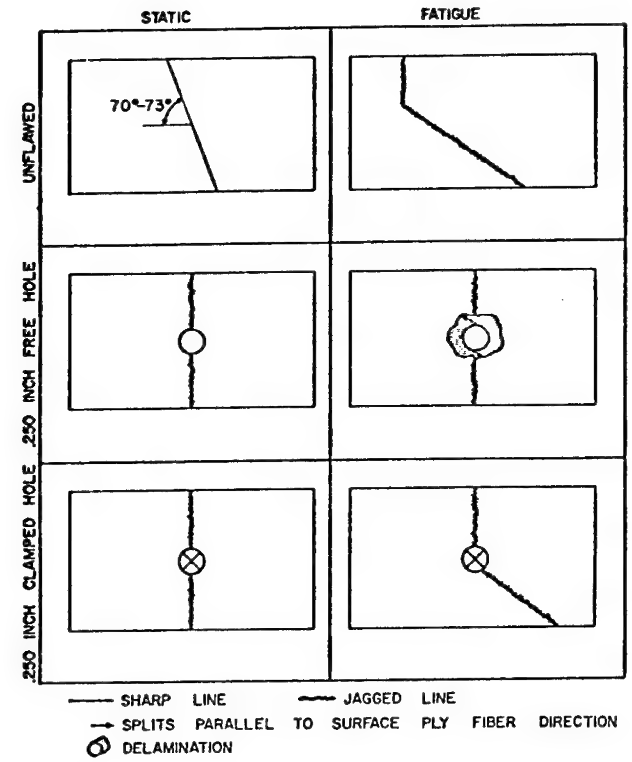

FIGURE 11 Schematic representation of failure modes - 'A' laminate.

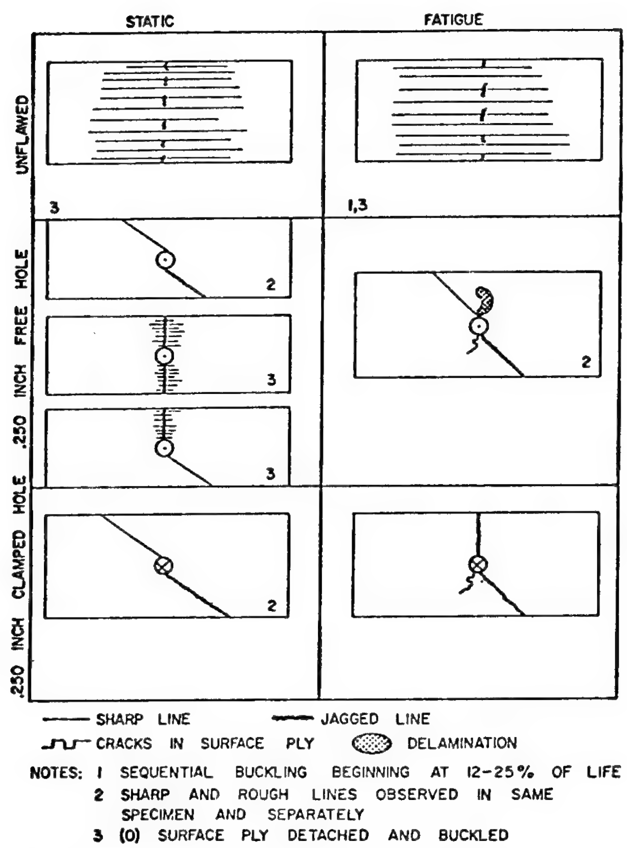

FIGURE 12 Schematic representations of failure modes - 'B' laminate.

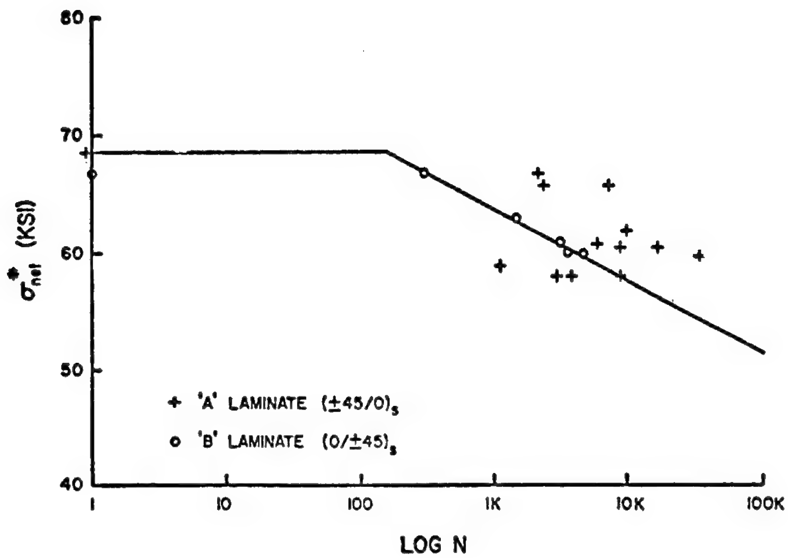

FIGURE 13 Free hole: 'A' laminate vs. 'B' laminate

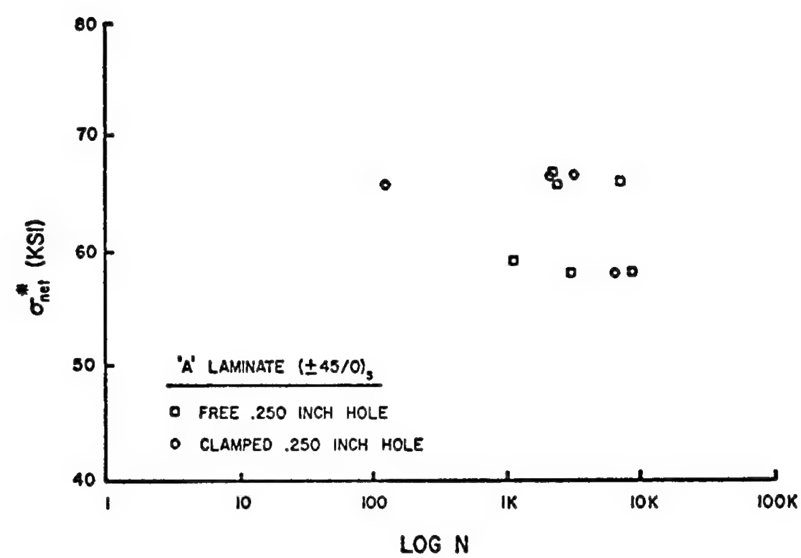

FIGURE 14 'A' laminate: Free hole vs. Clamped hole

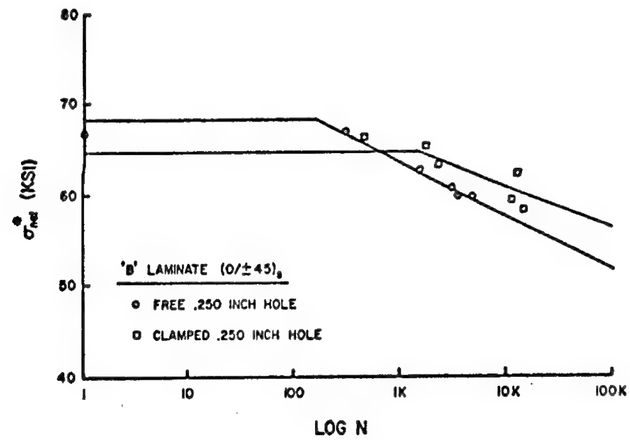

FIGURE 15 'B' laminate: Free hole vs. Clamped hole

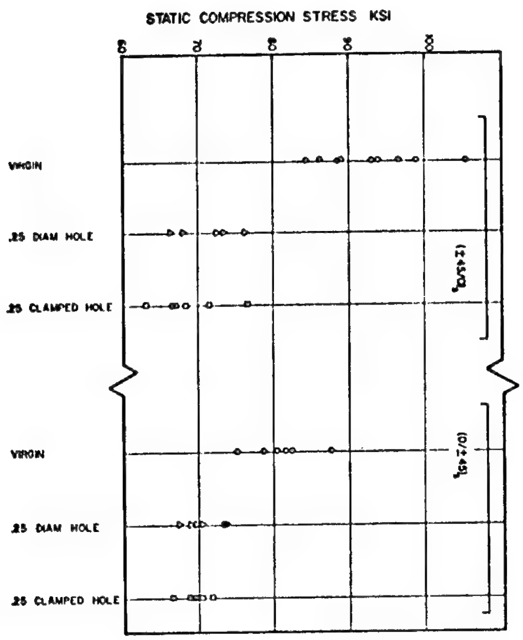

FIGURE 16

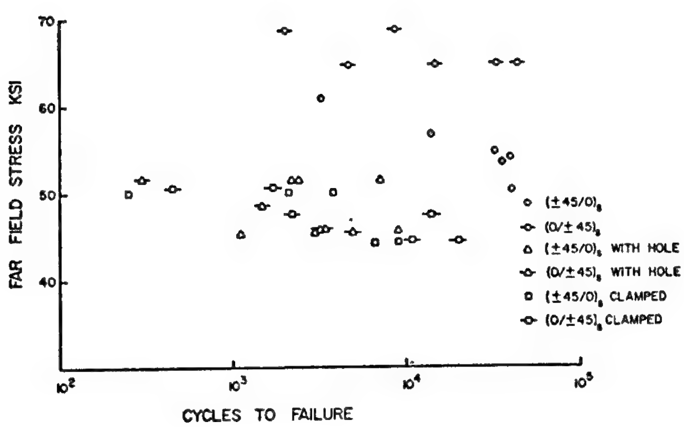

FIGURE 17

STRUCTURAL INTEGRITY OF COMPOSITES RESEARCH

by

G. P. SENDECKYJ

STRUCTURAL INTEGRITY BRANCH

STRUCTURAL MECHANICS DIVISION

AIR FORCE FLIGHT DYNAMICS LABORATORY

Subject . . . . Serial Number . . . .

STRUCTURAL INTEGRITY RESEARCH (COMPOSITES ACTIVITIES)

DURABILITY OF COMPOSITES

- DAMAGE ACCUMULATION IN NOTCHED $(0/\pm 45/90)_{2S}$ GRAPHITE-EPOXY LAMINATES (G.P. SENDECKYJ)
- EFFECT OF CYCLE SHAPE ON FATIGUE BEHAVIOR OF COMPOSITES (G.P SENDECKYJ)
- IMPROVED TAB DESIGN VERIFICATION FOR FATIGUE TESTING OF COMPOSITES (G.P. SENDECKYJ)
- FATIGUE SPECTRUM EFFECTS IN COMPOSITES (G.P. SENDECKYJ)

STRENGTH AND DAMAGE TOLERANCE OF COMPOSITES

- VERIFICATION OF MULTI-AXIAL LAMINATE STRENGTH CRITERION (R.S. SANDHU)
- OFF-AXIS TENSION TEST FOR SHEAR CHARACTERIZATION OF COMPOSITES (R.S. SANDHU AND G.P. SENDECKYJ)
- CRACK ARRESTMENT CONCEPTS (G.P. SENDECKYJ)

DIELECTRIC SPECTRUM ANALYSIS AS MOISTURE CONTENT INDICATOR FOR COMPOSITES (G.P. SENDECKYJ)

Subject .... Serial Number ....

DAMAGE ACCUMULATION IN COMPOSITES

OBJECTIVE:

- DOCUMENT FATIGUE INDUCED DAMAGE ACCUMULATION PROCESS IN COMPOSITES

APPROACH:

- PERIODICALLY NDI TEST SPECIMENS DURING FATIGUE TESTING

STATUS:

- $(0/\pm 45/90)_{2S}$ GRAPHITE-EPOXY SPECIMENS WITH CIRCULAR HOLES HAVE ABOUT 100 HOURS OF FATIGUE LOADING ON THEM
- STUDY IS CONTINUING

PAYOFF:

- RATIONAL BASIS FOR FATIGUE LIFE PREDICTION METHODOLOGY

FATIGUE DAMAGE GROWTH

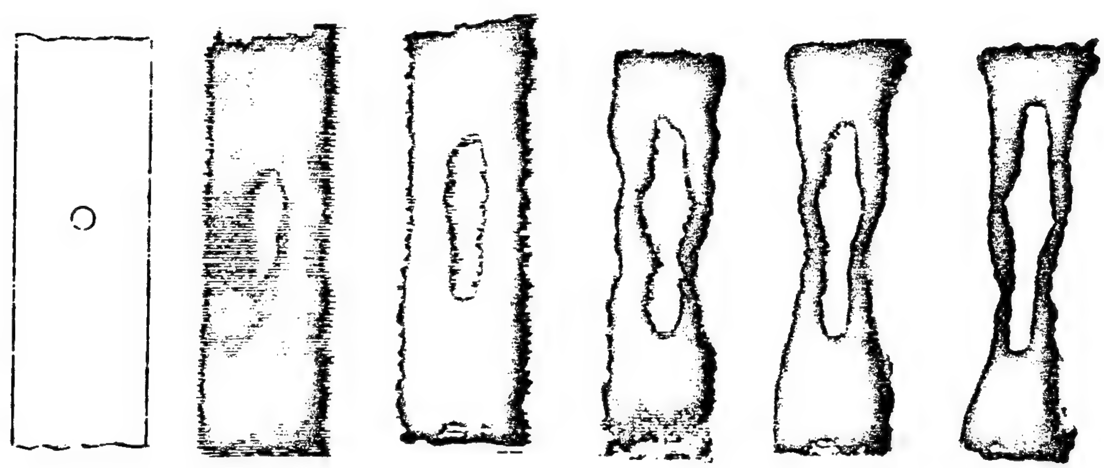

N = 0 8416 21456 30489 39509 52673

P_{MAX} = 3300 LB CYCLES TO FAILURE, N = 56122

MATERIAL: $(0/\pm 45/90)_{S2}$ GRAPHITE-EPOXY

EFFECT OF CYCLE SHAPE ON FATIGUE BEHAVIOR

PROBLEM:

- EFFECTS OF LOADING CYCLE SHAPE / FREQUENCY PARAMETERS ON FATIGUE LIFE OF COMPOSITES ARE NOT UNDERSTOOD

OBJECTIVE:

- ASSESS EFFECT OF CYCLE SHAPE PARAMETERS SUCH AS
  - TIME AT LOAD
  - LOADING RATE

APPROACH:

- GENERATE S-N CURVES USING DIFFERENT LOADING WAVE SHAPES
- ANALYZE DATA FOR TIME AT LOAD EFFECTS

STATUS:

- TESTING OF $(0/\pm 45)_{S4}$ GRAPHITE-EPOXY LAMINATES COMPLETED
- TEST DATA ANALYZED
- PAPER IN PREPARATION

PAYOFF:

- RATIONAL BASIS FOR ACCELERATED FATIGUE TESTING OF COMPOSITES

TIME AT LOAD EFFECT IN COMPOSITES

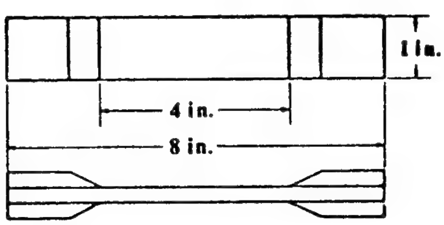

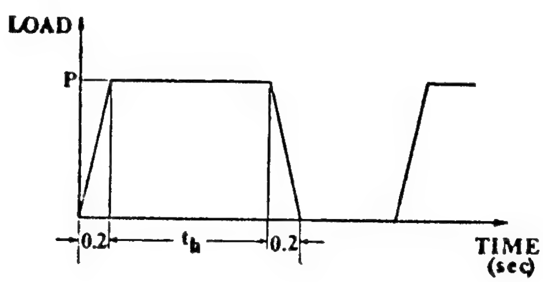

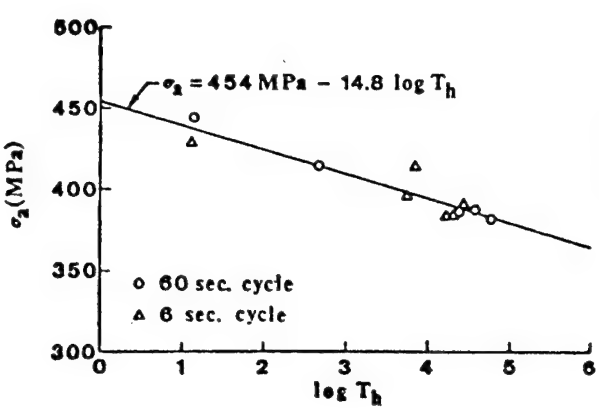

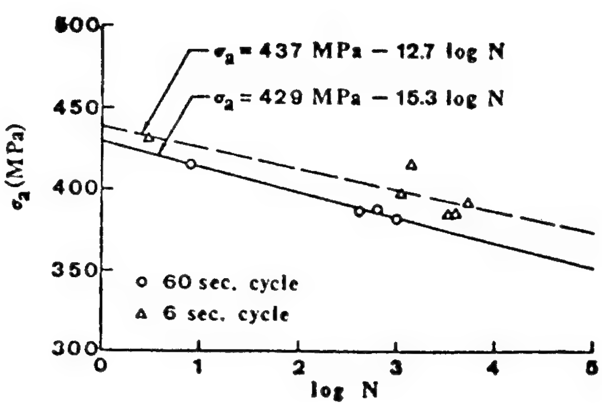

EFFECT OF CYCLE SHAPE ON FATIGUE BEHAVIOR

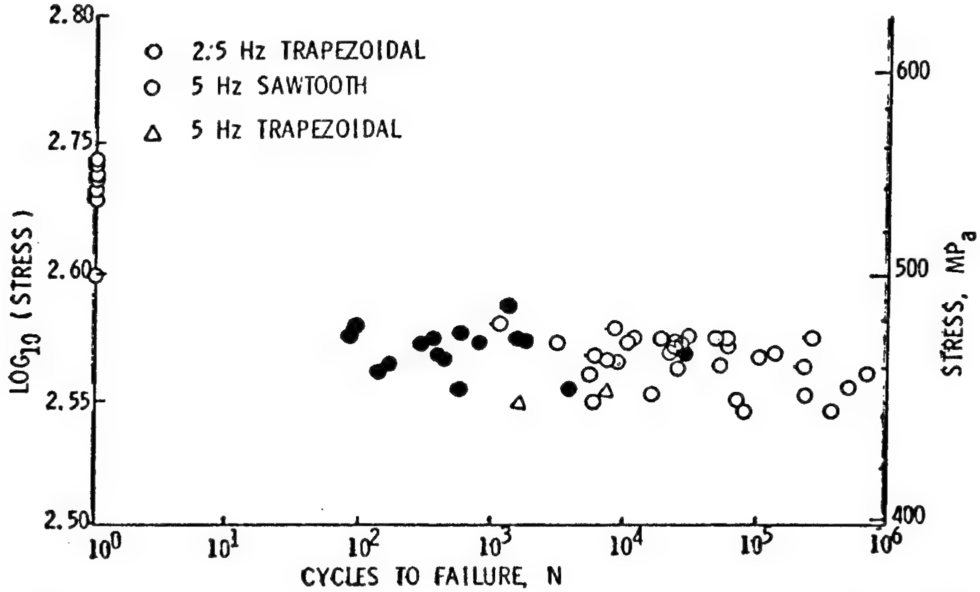

Subject . . . .   Serial Number . . . .

IMPROVED TAB DESIGN VERIFICATION

PROBLEM:

- STANDARD TAPERED TABS CAUSE DELAMINATION AT TAPER UNDER FATIGUE LOADING

OBJECTIVE:

- DEVELOP AND EXPERIMENTALLY VERIFY IMPROVED LOAD INTRODUCTION TAB DESIGN

APPROACH:

- CONDUCT STATIC AND FATIGUE TESTS ON SPECIMENS WITH STANDARD TAPERED TAB AT ONE END AND NEW TAB AT OTHER END

STATUS:

- IMPROVED TAB DESIGN (PARTIALLY BONDED, SQUARE-ENDED TABS) VERIFIED FOR $(\pm 45)_{4S}$, $(90/\pm 45/0)_{2S}$ AND $(0/\pm 45)_T$ GRAPHITE-EPOXY SPECIMENS
- DOCUMENTATION IN PREPARATION

PAYOFF:

- FEWER TAB FAILURES IN FATIGUE

IMPROVED TAB DESIGN VERIFICATION

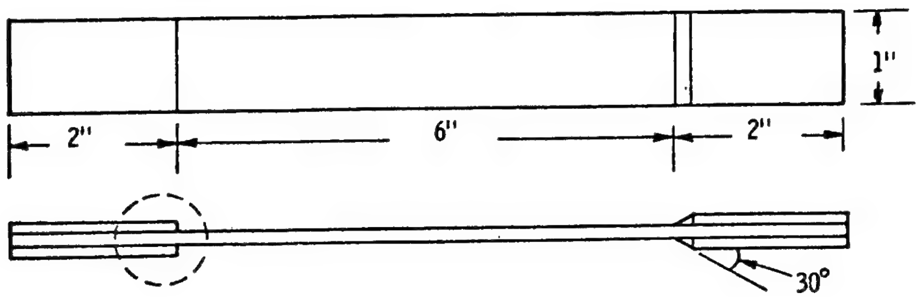

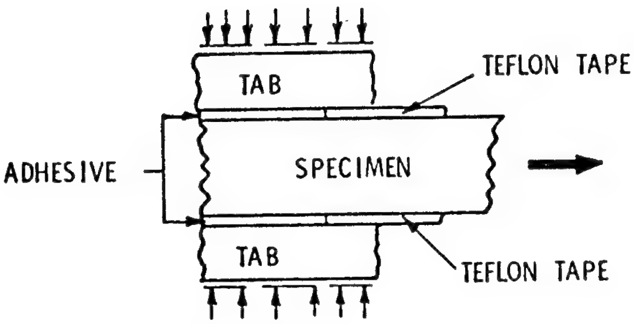

NOTE: NO UNBALANCED MOMENT AT TEST SECTION END OF TAB TO CAUSE DELAMINATION

TAB DESIGN VERIFICATION - $(\pm45)_{4S}$ GRAPHITE/EPOXY

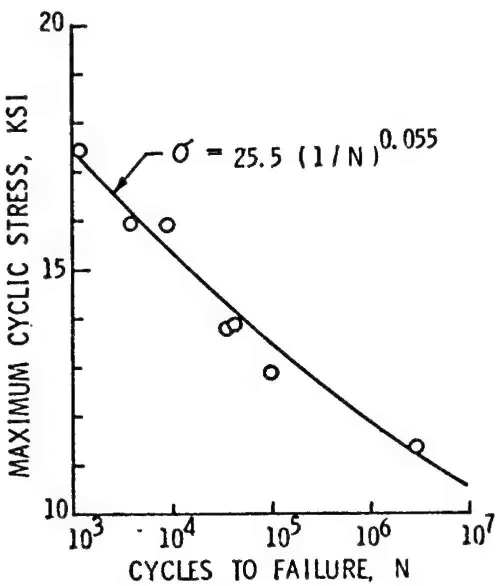

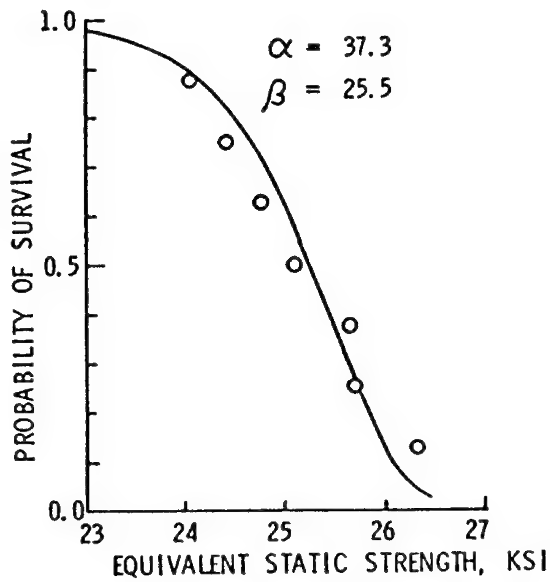

Serial Number ....

TAB DESIGN VERIFICATION - $(90/\pm45/0)_{2S}$ GRAPHITE/EPOXY

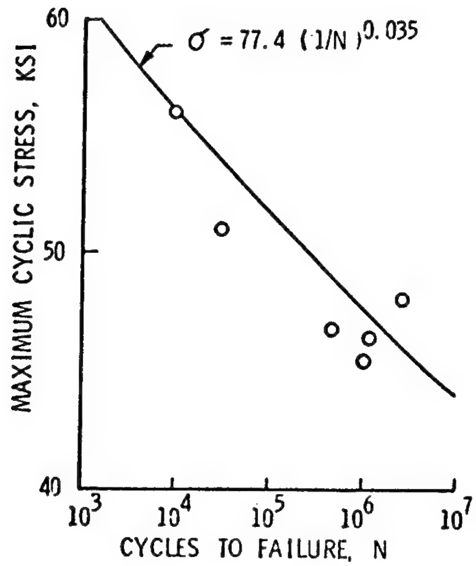

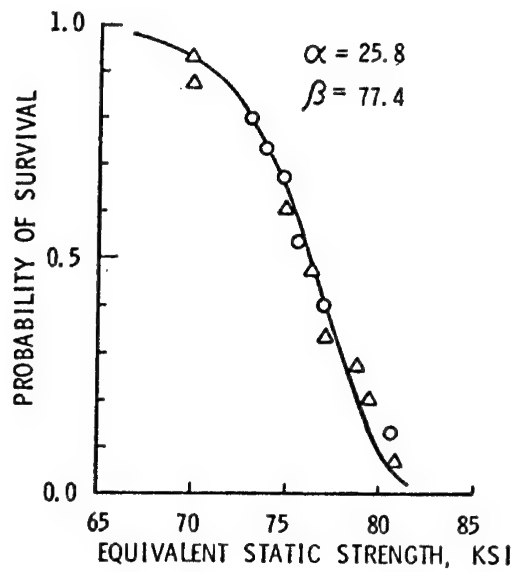

Subject ....

Serial Number ....

TAB DESIGN VERIFICATION - $(0/\pm45)_T$ GRAPHITE/EPOXY

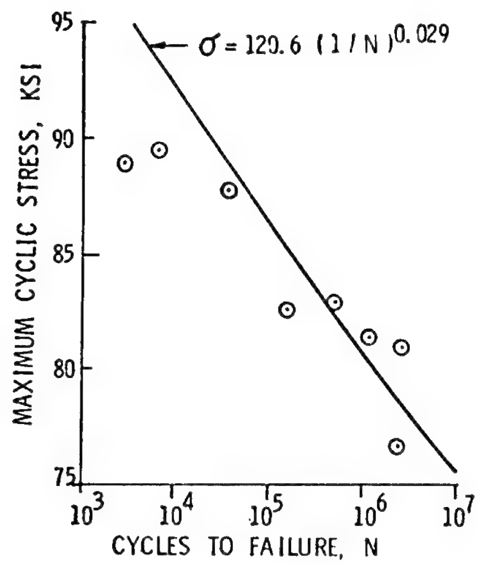

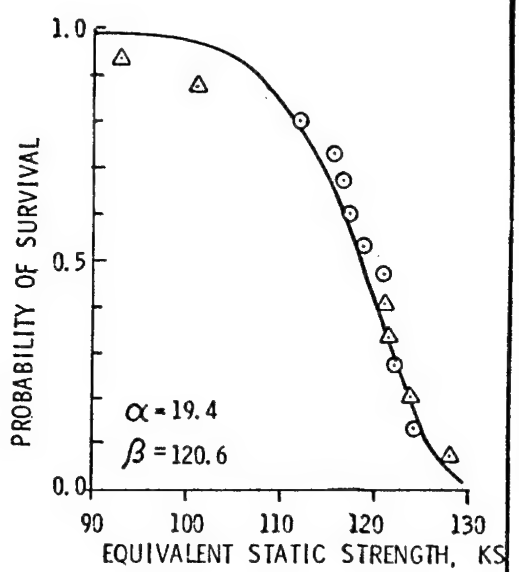

Subject .... Serial Number ....

FATIGUE SPECTRUM EFFECTS IN COMPOSITES

PROBLEM:

- LACK OF METHODOLOGY FOR PREDICTING FATIGUE LIFE UNDER SPECTRUM LOADING

OBJECTIVE:

- DEVELOP METHODOLOGY FOR PREDICTING FATIGUE LIVES UNDER SPECTRUM LOADING
- VERIFY METHODOLOGY EXPERIMENTALLY
- ASSESS EFFECT OF FIBER AND POROSITY CONTENT

APPROACH:

- CONDUCT CONSTANT LOAD AMPLITUDE FATIGUE TESTS AT FOUR STRESS LEVELS TO DEVELOP BASELINE DATA AND ASSESS EFFECT OF FIBER AND POROSITY CONTENT
- REPEAT LOWER STRESS LEVEL FATIGUE TESTS WITH PERIODIC NONDESTRUCTIVE INSPECTION USING TBE ENHANCED X-RAY RADIOGRAPHY TO DOCUMENT DAMAGE ACCUMULATION PROCESS AND ASSESS EFFECT OF PERIODIC NDI
- CONDUCT MULTI LOAD LEVEL AND SPECTRUM FATIGUE TESTS TO SUPPORT METHODOLOGY DEVELOPMENT

Subject .... Serial Number ....

FATIGUE SPECTRUM EFFECTS IN COMPOSITES (CONT'D)

STATUS:

- 283 $(\pm 45)_{4,5'}$ GRAPHITE-EPOXY SPECIMENS (15 TO 16 PER PANEL) FABRICATED
- PANEL QUALITY ASSESSED
- BASELINE TESTING STARTED

PAYOFF:

- RATIONAL METHODOLOGY FOR PREDICTING FATIGUE LIFE OF COMPOSITES UNDER SPECTRUM LOADING

Subject . . . .   Serial Number . . . .

$(\pm 45)_{4S}$ GRAPHITE/EPOXY - PANEL COMPOSITION

PANEL NUMBER	DENSITY (gm / cc)	RESIN CONTENT		FIBER CONTENT	VOID CONTENT
		BY WEIGHT	BY VOLUME	BY VOLUME	BY VOLUME
1 TO 2	1.590	26.7%	33.6%	65.6%	0.8%
3 TO 6	1.583	29.3	36.7	62.9	0.4
7 TO 10	1.597	28.5	36.0	64.1	-0.1
11 TO 14	1.577	26.7	33.2	65.0	1.8
15 TO 18	1.590	26.3	33.1	65.8	1.1

RESIN DENSITY = 1.265 gm / cc

FIBER DENSITY = 1.78 gm/cc

VERIFICATION OF MULTI-AXIAL LAMINATE STRENGTH CRITERIA

PROBLEM:

- POST FIRST PLY FAILURE MODELING OF LAMINATE BEHAVIOR IS INACCURATE
- ULTIMATE STRENGTH PREDICTIONS FOR LAMINATES ARE QUESTIONABLE, ESPECIALLY UNDER COMPLEX LOADING CONDITIONS

OBJECTIVE:

- VERIFY IN-HOUSE GENERATED PROGRAM FOR PREDICTING STRESS-STRAIN CURVES AND ULTIMATE STRENGTH OF LAMINATES FROM LAMINA DATA
- EXPLORE FAILED PLY UNLOADING MODELS

APPROACH:

- EXPERIMENTALLY, OBTAIN STRESS-STRAIN CURVES TO FAILURE COMPARE EXPERIMENTAL DATA WITH PREDICTIONS

STATUS:

- TESTING COMPLETED
- DATA BEING ANALYZED
- DOCUMENTATION IN PREPARATION

PAYOFF:

- RATIONAL BASIS FOR STRENGTH CRITICAL DESIGN

Subject ....   Serial Number ....

THEORY - EXPERIMENT COMPARISON

$(\pm 45 / 0_2 / \pm 45 / 90_2)_S$ GRAPHITE - EPOXY LAMINATE

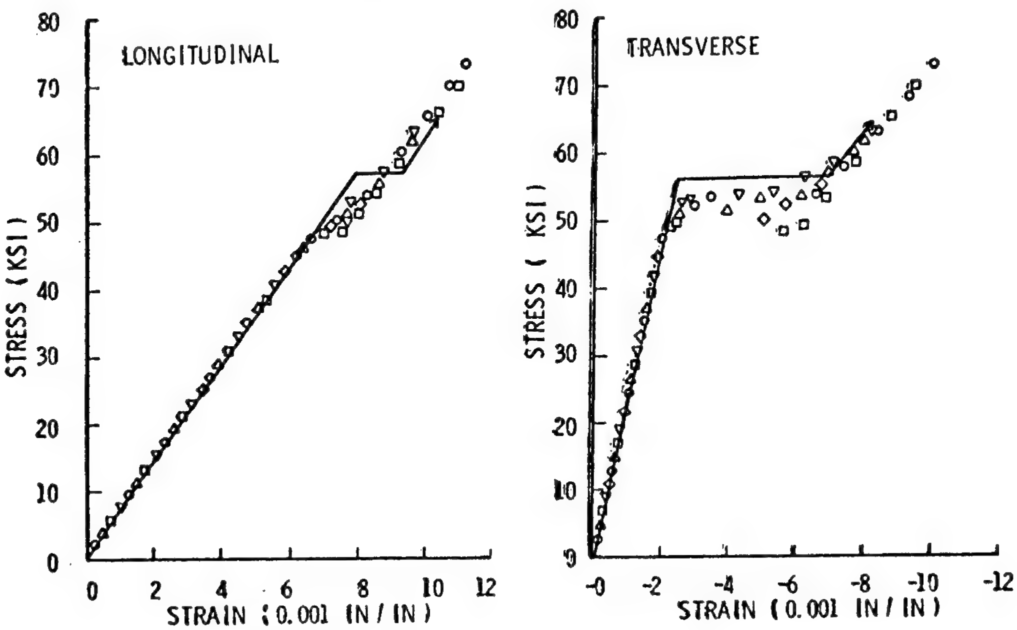

OFF-AXIS TENSION TEST FOR SHEAR CHARACTERIZATION OF UNIDIRECTIONAL COMPOSITES

PROBLEM:

- LACK OF GOOD TEST METHOD FOR BASIC SHEAR PROPERTIES OF UNI-DIRECTIONAL FIBER-REINFORCED COMPOSITES
- LACK OF QUALITY OFF-AXIS STRENGTH DATA

OBJECTIVE:

- VERIFY TEST METHOD PROPOSED BY NASA / LeRC
- GENERATE QUALITY OFF-AXIS STRENGTH DATA

APPROACH:

- TEST OFF-AXIS TENSION SPECIMENS WITH TWO LOAD INTRODUCTION TAB DESIGNS FOR A SERIES OF OFF-AXIS ANGLES
- COMPARE TEST DATA WITH PREDICTIONS

STATUS:

- 0 DEGREE TENSION AND COMPRESSION TEST COMPLETED
- OFF-AXIS SPECIMENS WITH TAB DESIGN "A" INSTRUMENTED AND COMMITTED TO TESTING
- OFF-AXIS SPECIMENS WITH TAB DESIGN "B" BEING FABRICATED

Serial Number . . . .

OPTIMUM OFF-AXIS ANGLES

- ANGLE FOR MAXIMUM SHEAR STRESS CONTRIBUTION TO FAILURE:

  $$\tan\theta = \sqrt{F_2 / F_1}$$

- FOR STRENGTH CRITERION OF THE FORM

  $$(\sigma_1 / F_1)^2 + (\sigma_T / F_2)^2 - A\,\sigma_L\,\sigma_T + (\sigma_{LT} / F_{12})^2 = 1$$

- NOTE: THIS OPTIMUM ANGLE HOLDS FOR MOST OTHER TYPES OF STRENGTH CRITERIA

- ANGLE FOR WHICH TRANSVERSE STRAIN IS ZERO:

  $$\tan\theta = \sqrt{\nu_{LT}\, E_T / E_L} = \sqrt{\nu_{TL}}$$

- NOTE: OFF-AXIS ANGLES IN TEST PROGRAM SPAN BOTH OPTIMALITY CONDITIONS

Serial Number . . . .

OFF-AXIS TENSION TEST FOR SHEAR CHARACTERIZATION OF UNIDIRECTIONAL COMPOSITES

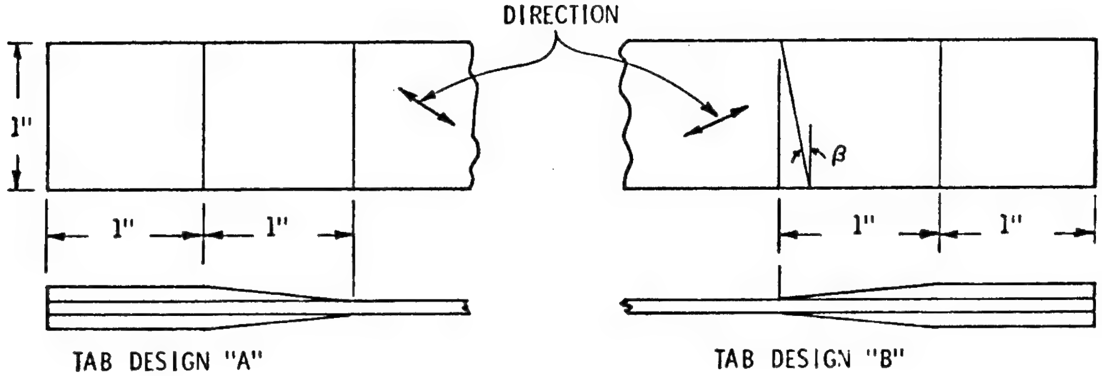

NOTE: ANGLE β OPTIMIZED FOR TEST SECTION STRESS UNIFORMITY

CRACK ARRESTMENT CONCEPTS

PROBLEM:

- COMPOSITES ARE BRITTLE AND SUSCEPTIBLE TO FRACTURE INITIATING FROM DAMAGE SITES

OBJECTIVE:

- DEVELOP CONCEPTS FOR CRACK ARRESTMENT IN COMPOSITES
- VERIFY CONCEPTS BY EXPERIMENT

APPROACH:

- GENERATE BASIC STRENGTH AND FRACTURE DATA FOR HYBRIDS USED IN CRACK ARRESTMENT PANELS
- TEST CRACK ARRESTMENT PANELS

STATUS:

- STRENGTH AND FRACTURE TESTS FOR SIX HYBRIDS COMPLETED - DATA BEING ANALYZED
- CRACK ARRESTMENT PANEL TESTING INITIATED - TAB FAILURE ENCOUNTERED - TAB FAILURE PROBLEM BEING INVESTIGATED

PAYOFF:

- MORE DAMAGE TOLERANT COMPOSITE STRUCTURES

DIELECTRIC SPECTRUM ANALYSIS AS MOISTURE CONTENT INDICATOR FOR COMPOSITES

PROBLEM:

- ABSORBED MOISTURE DEGRADES MATRIX DOMINATED PROPERTIES OF COMPOSITES
- HOW TO NONDESTRUCTIVELY DETERMINE MOISTURE CONTENT IN SERVICE

OBJECTIVE:

- DETERMINE WHETHER DIELECTRIC SPECTRUM CHANGES CAN BE USED TO NONDESTRUCTIVELY MEASURE MOISTURE CONTENT AND / OR STATE OF DAMAGE IN COMPOSITES

APPROACH:

- DETERMINE COMPLEX DIELECTRIC CONSTANT AS FUNCTION OF FREQUENCY FOR:
  - UNDAMAGED AND DAMAGED (CRAZED) SPECIMENS
  - SPECIMENS WITH DIFFERENT MOISTURE CONTENTS AND PROFILES

STATUS:

- TESTING OF GLASS / EPOXY SPECIMENS COMPLETED TEST RESULTS ARE BEING ANALYZED AND DOCUMENTED
- EXPERIMENTAL TECHNIQUE MODIFIED FOR GRAPHITE / EPOXY TESTING
- GRAPHITE / EPOXY TESTING INITIATED

PAYOFF:

- PROCEDURE FOR IN-SERVICE, NONDESTRUCTIVE MOISTURE CONTENT MONITORING

DIELECTRIC SPECTRUM ANALYSIS AS MOISTURE CONTENT INDICATOR FOR COMPOSITE

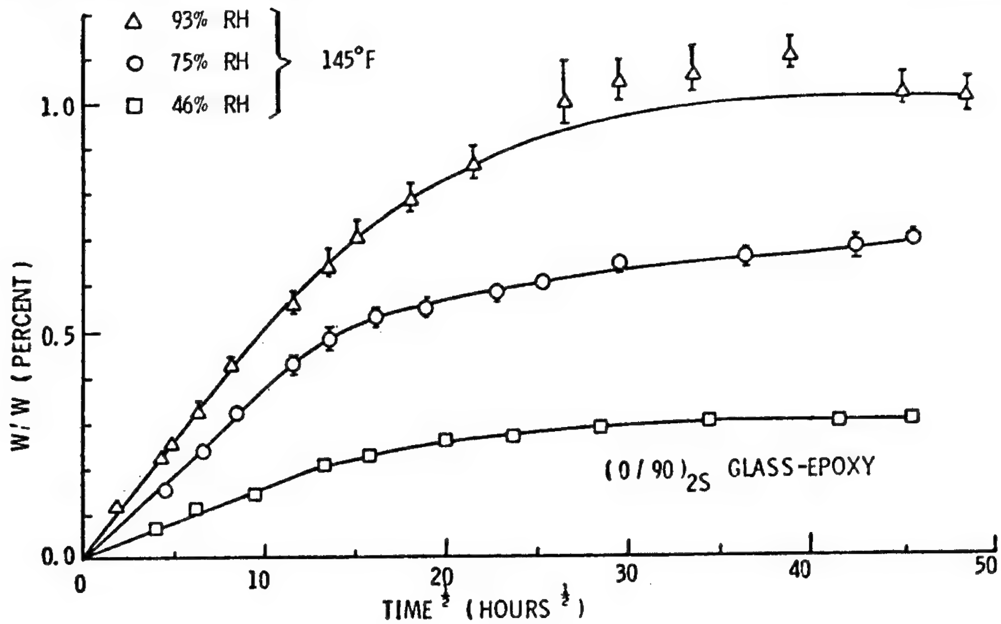

DIELECTRIC SPECTRUM ANALYSIS AS MOISTURE CONTENT INDICATOR FOR COMPOSITE

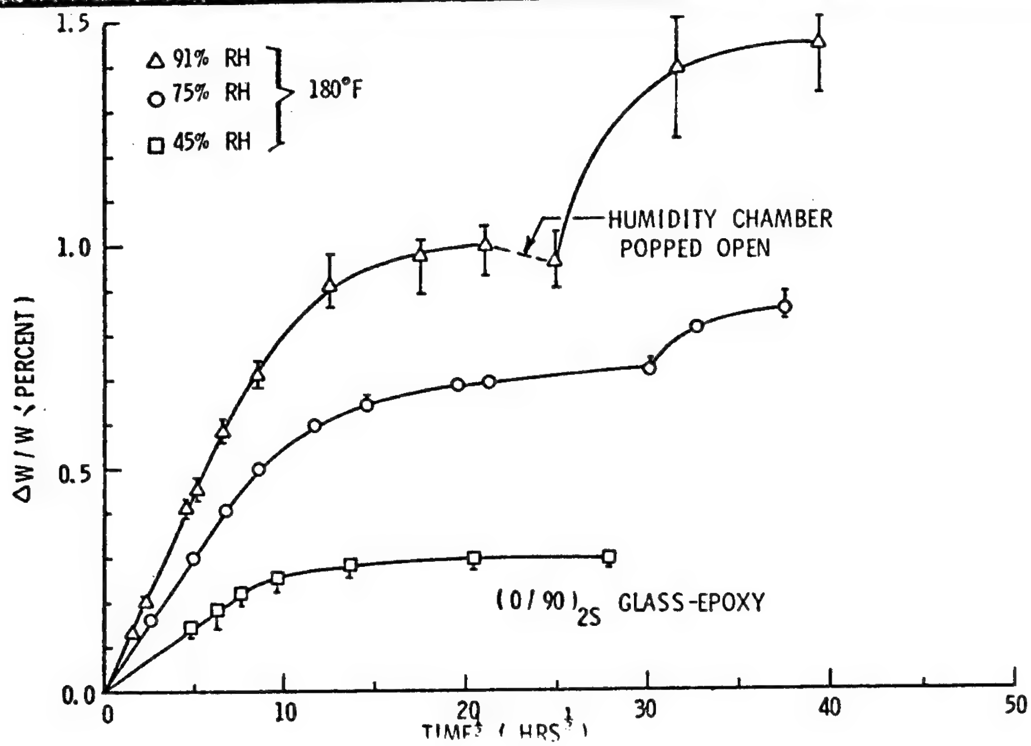

DIELECTRIC SPECTRUM ANALYSIS AS MOISTURE CONTENT INDICATOR FOR COMPOSITES

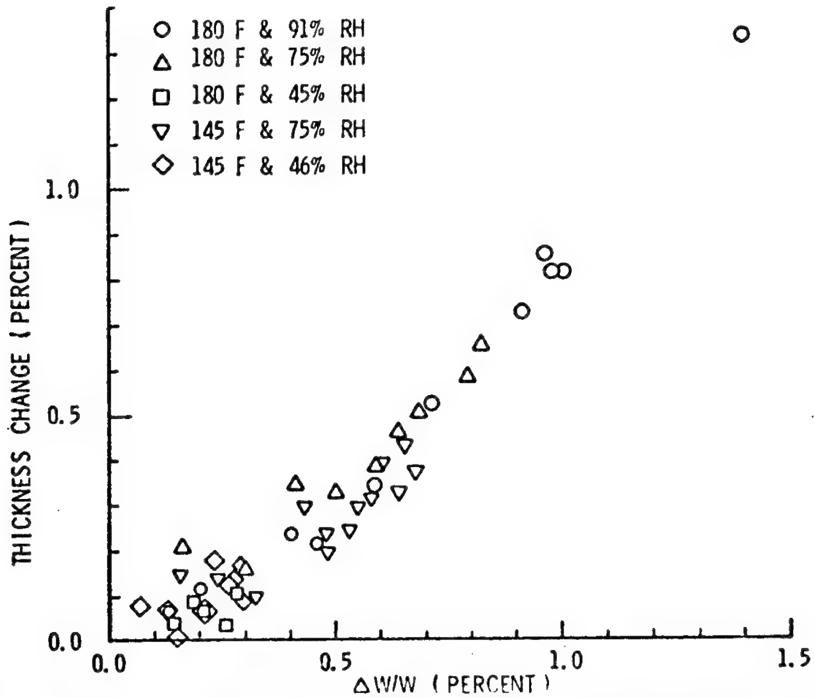

DIELECTRIC CONSTANT vs MOISTURE CONTENT

$(0/90)_{2S}$ SCOTCHPLY 1003

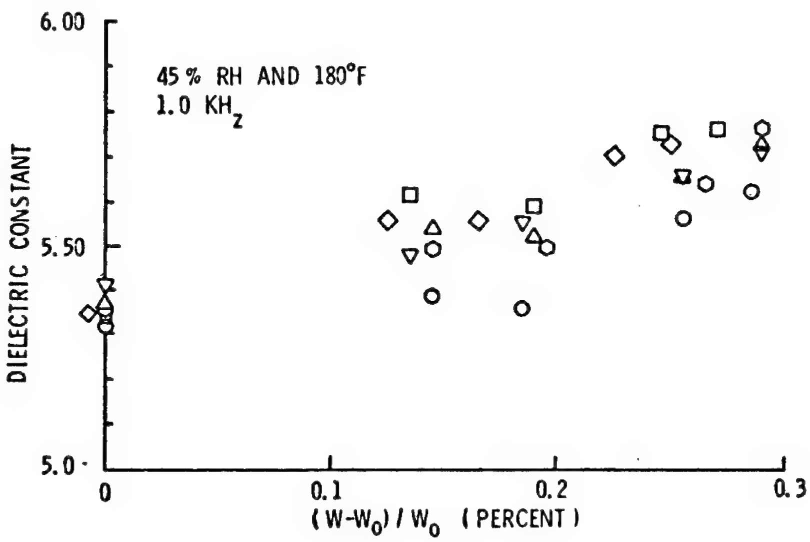

Statistical Failure Analysis of Composite Materials

by

P. C. Chou
A. S. D. Wang
J. Awerbuch

Drexel University

Objectives

(1) To study fatigue failure of composite materials by utilizing statistical methods, assumed failure models, and limited experimentation.

(2) To verify the "matrix-degradation" model of fatigue failure in unidirectional composites.

(3) To develop the "in-series, in-parallel" model of fatigue failure.

Progress to date

1. Unidirectional graphite/epoxy specimens prepared. Limited number of static and fatigue tension tests completed.

2. A few methods of estimating population distribution from test data that contain suspended specimens are studied. These include the modified ranking increment method, the cumulative hazard method, and the hazard rate method. These methods are applied to existing fatigue data.

3. The in-series model (weakest link) is applied to tension specimens. The long specimen is considered as a number of short ones arranged in series. Wide metal specimen treated as a series of narrow ones arranged in series is also considered.

4. Residual stress distribution based on existing test data is studied.

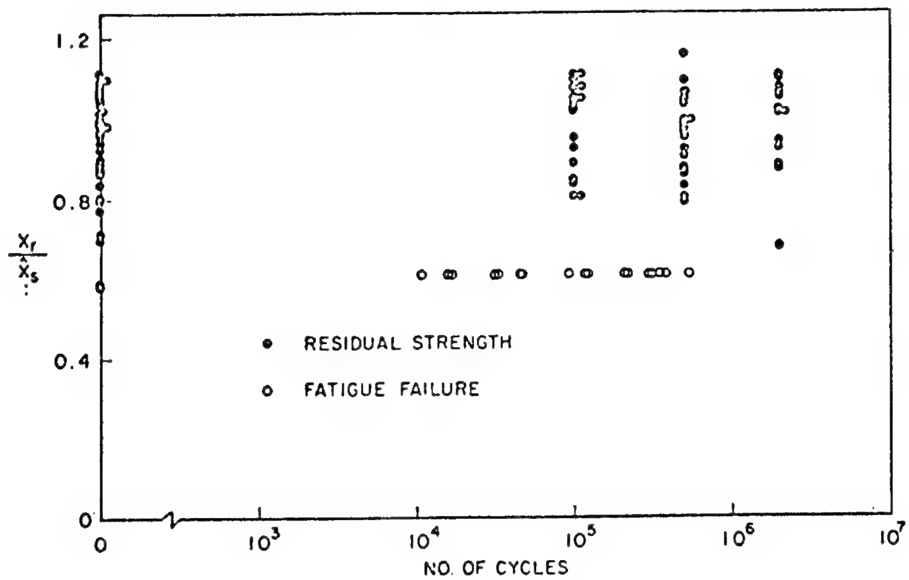

Static and Fatigue Strength Data

(Presented by J. Awerbuch and H. T. Hahn at ASTM Fatigue Symposium 1976)

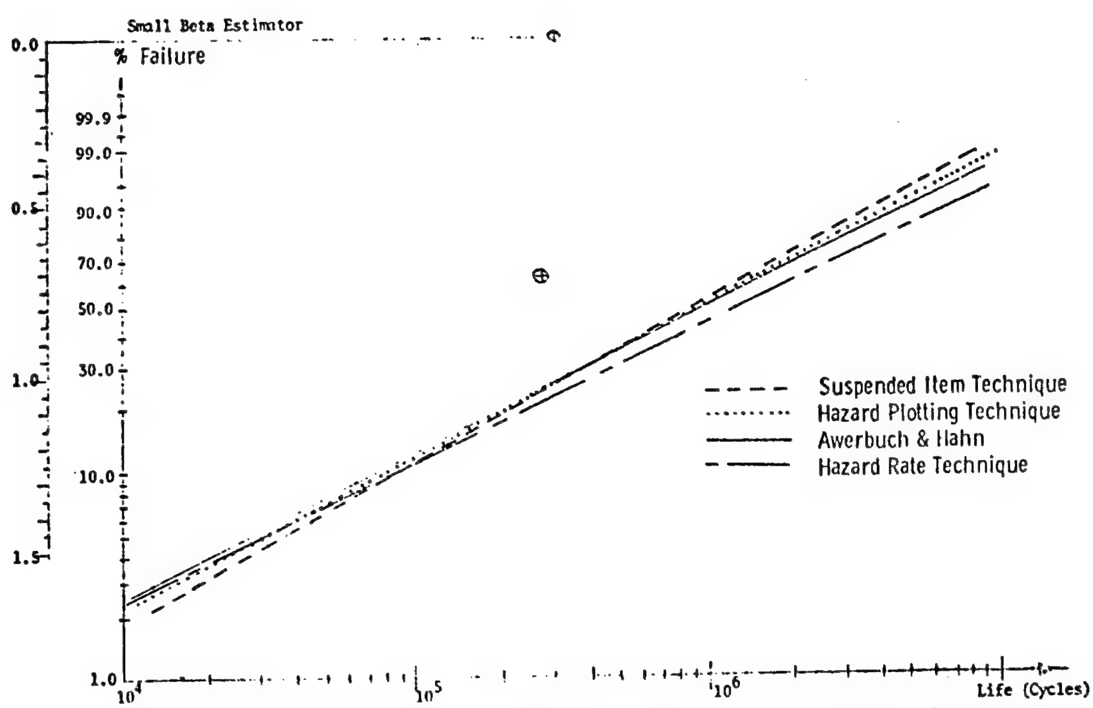

Comparison of Several Techniques to Analyze Fatigue Data Containing Non Failed Specimens
(Weibull Coordinates)

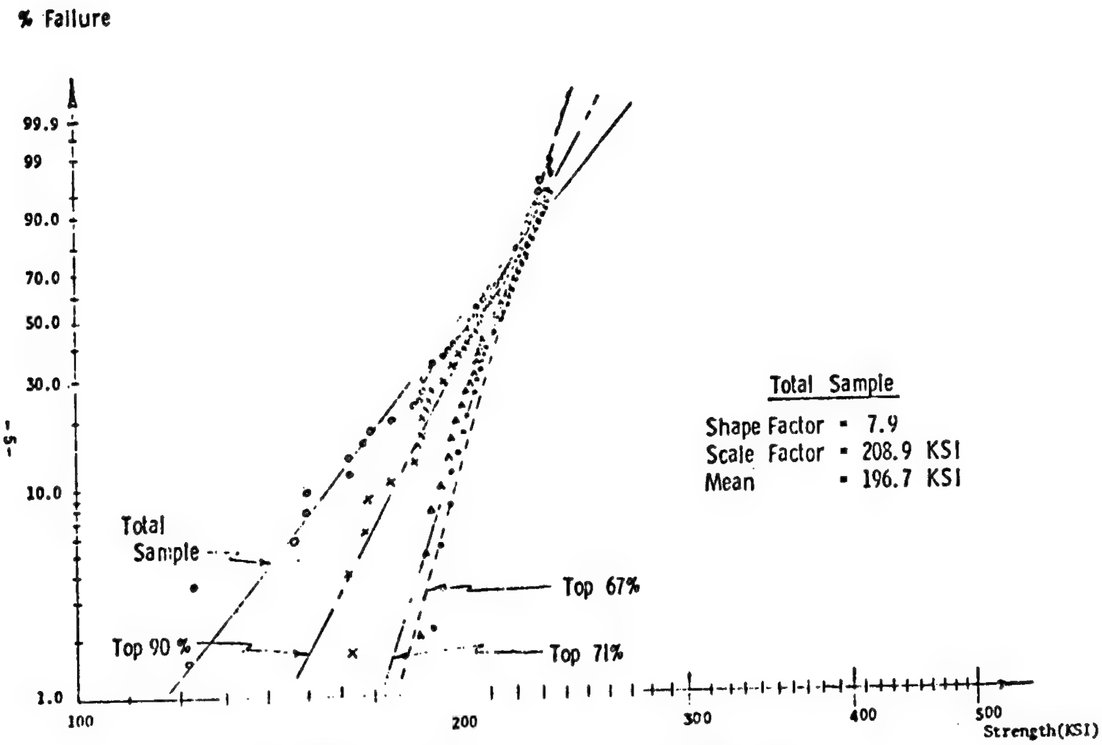

Distribution of the Static Strength for 6 Inch Specimens
(Weibull Coordinates)

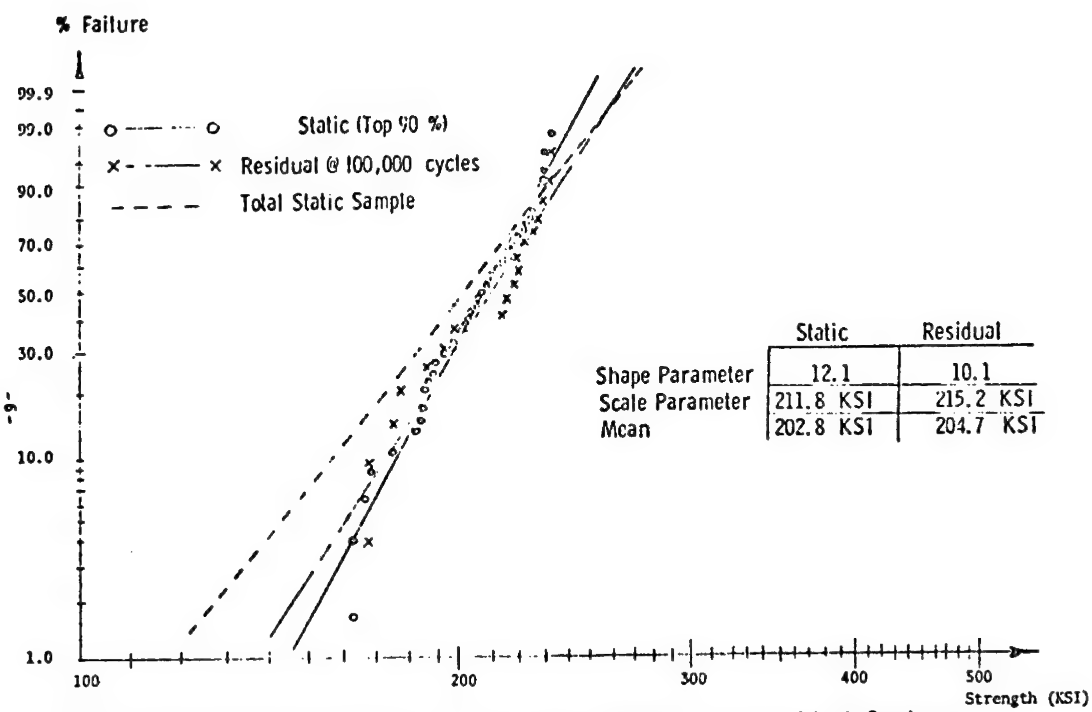

Comparison of Static (top 90 %) and Residual Strengths at 100,000 Cycles for 6 Inch Specimens
(Weibull Coordinates)

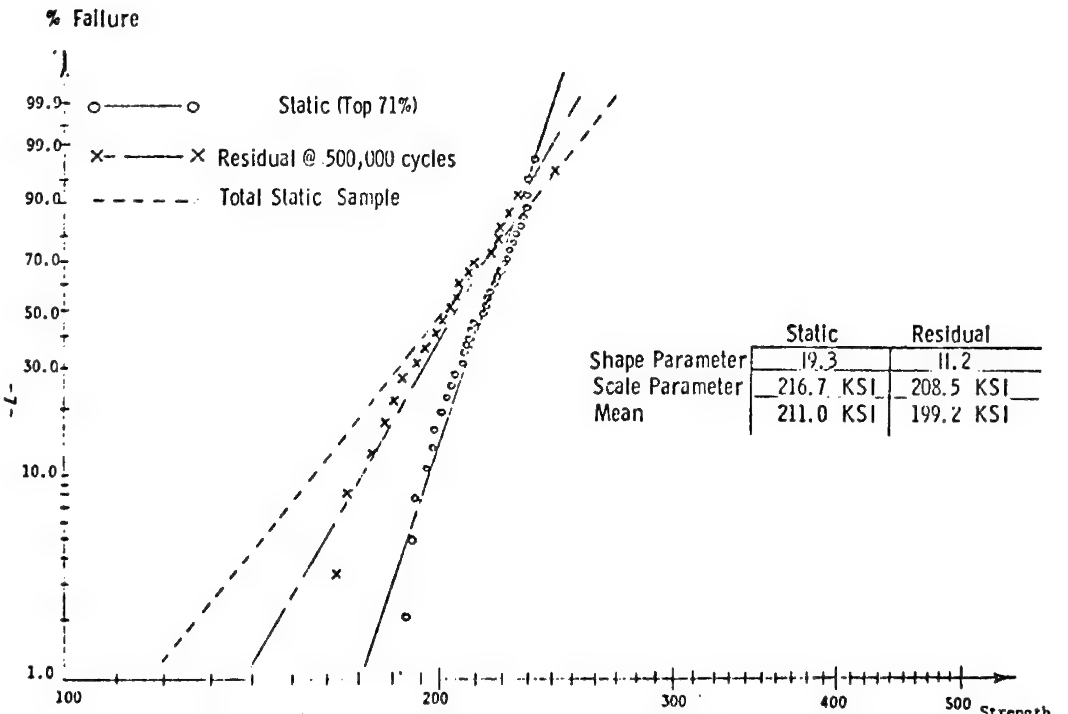

	Static	Residual
Shape Parameter	19.3	11.2
Scale Parameter	216.7 KSI	208.5 KSI
Mean	211.0 KSI	199.2 KSI

Comparison of Static (Top 71%) and Residual Strengths at 500,000 Cycles for 6 Inch Specimens (Weibull Coordinates)

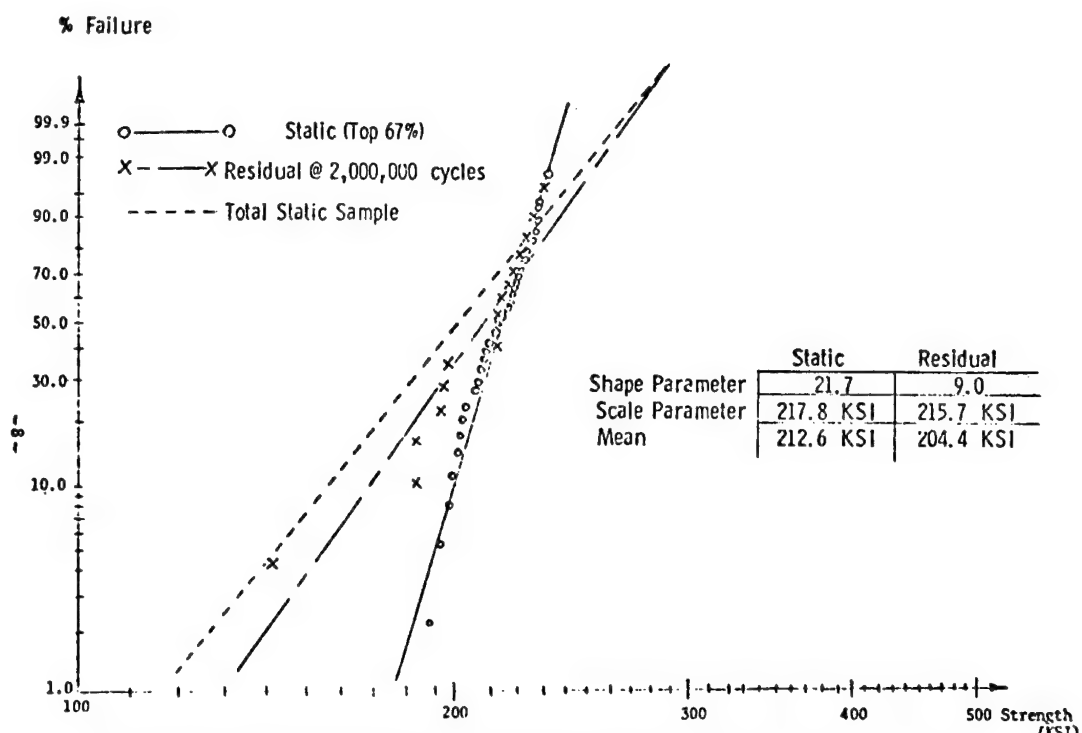

	Static	Residual
Shape Parameter	21.7	9.0
Scale Parameter	217.8 KSI	215.7 KSI
Mean	212.6 KSI	204.4 KSI

Comparison of Static (Top 67%) and Residual Strengths at 2,000,000 Cycles for 6 Inch Specimens (Weibull Coordinates)

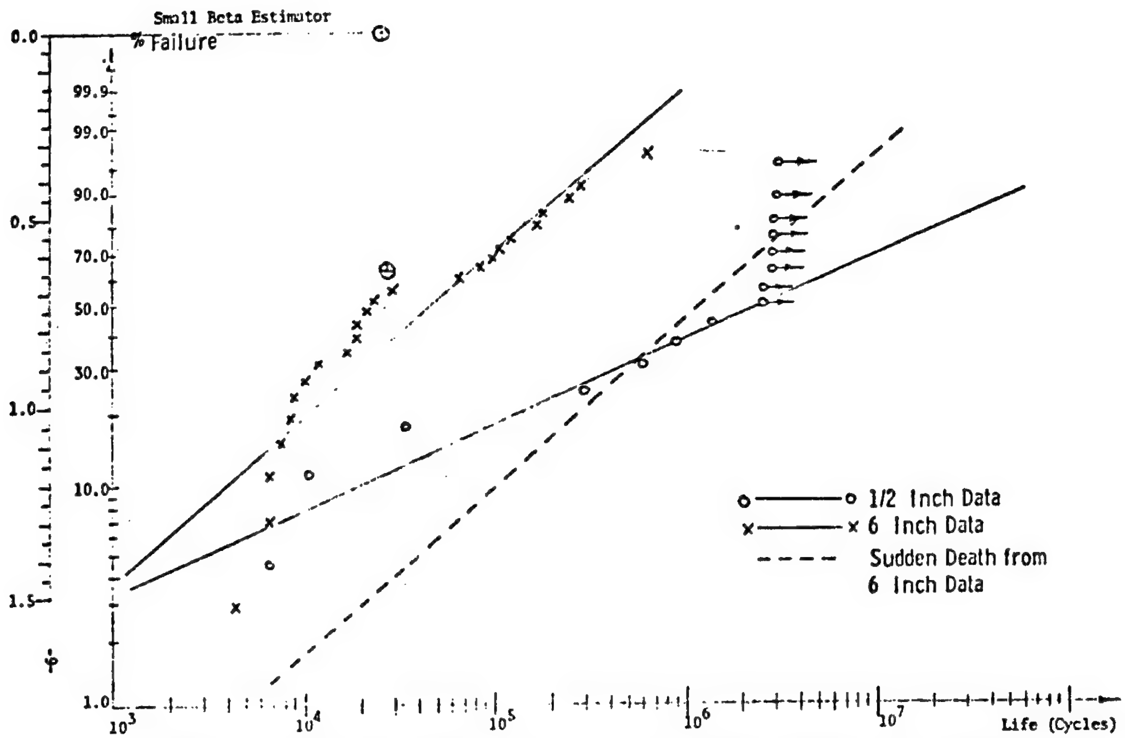

Applicability of In-Series Model to 6 Inch and 1/2 Inch Specimens Under Dynamic Loading (Weibull Coordinates)

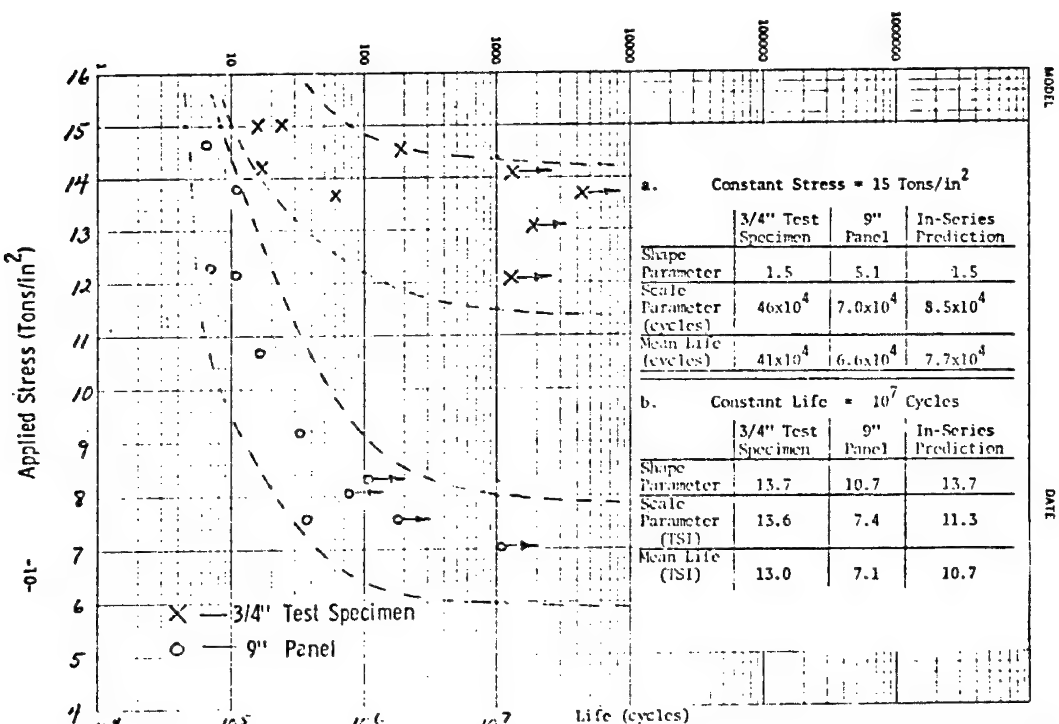

a. Constant Stress = 15 Tons/in^2

	3/4" Test Specimen	9" Panel	In-Series Prediction
Shape Parameter	1.5	5.1	1.5
Scale Parameter (cycles)	46×10^4	7.0×10^4	8.5×10^4
Mean Life (cycles)	41×10^4	6.6×10^4	7.7×10^4

b. Constant Life = 10^7 Cycles

	3/4" Test Specimen	9" Panel	In-Series Prediction
Shape Parameter	13.7	10.7	13.7
Scale Parameter (TSI)	13.6	7.4	11.3
Mean Life (TSI)	13.0	7.1	10.7

Scale Effect in Fatigue of Aluminum (Data from Phillips & Fenner)

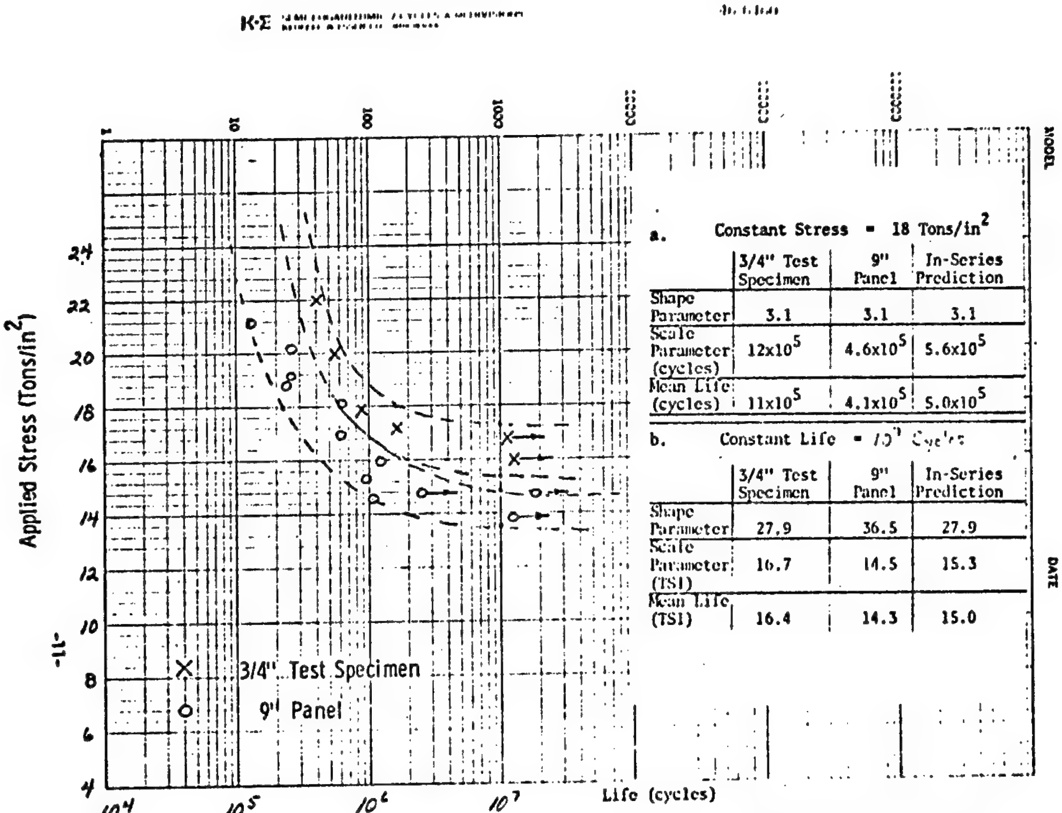

a. Constant Stress = 18 Tons/in^2

	3/4" Test Specimen	9" Panel	In-Series Prediction
Shape Parameter	3.1	3.1	3.1
Scale Parameter (cycles)	12×10^5	4.6×10^5	5.6×10^5
Mean Life (cycles)	11×10^5	4.1×10^5	5.0×10^5

b. Constant Life = 10^7 Cycles

	3/4" Test Specimen	9" Panel	In-Series Prediction
Shape Parameter	27.9	36.5	27.9
Scale Parameter (TSI)	16.7	14.5	15.3
Mean Life (TSI)	16.4	14.3	15.0

Scale Effect in Fatigue of Mild Steel (Data from Philips & Fenner)

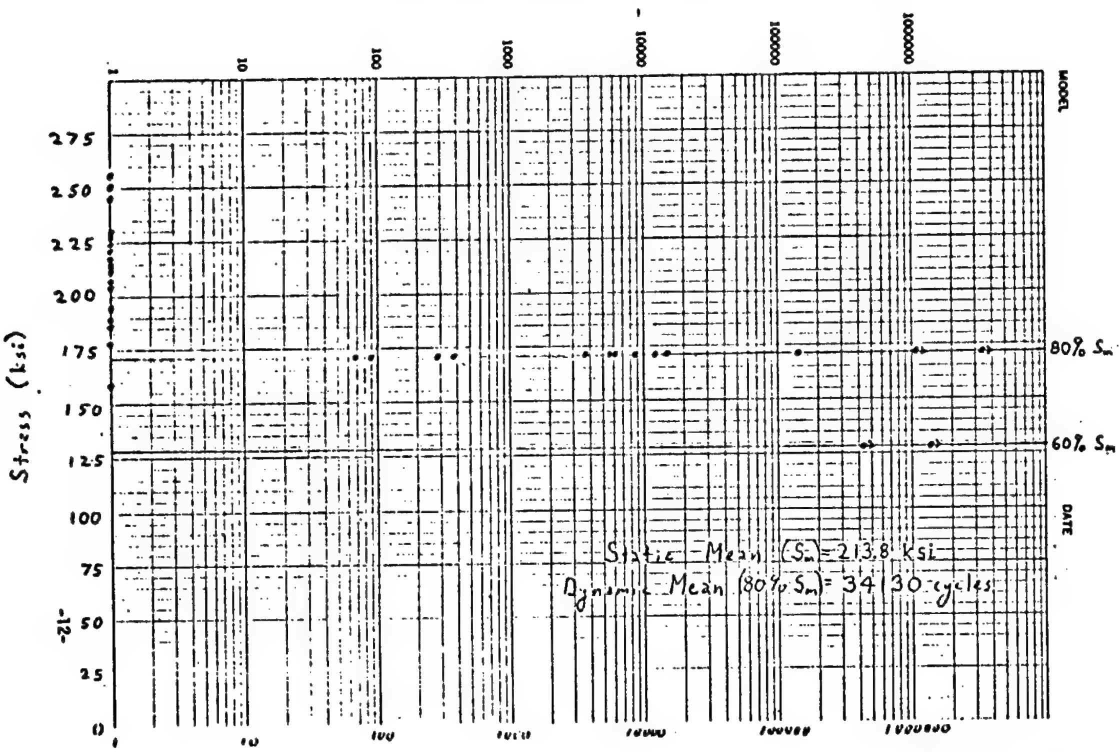

S-N Plot for A.E Data Cycles

Graphite epoxy (0° - 6 ply)

Fatigue Specimen 80% S_m , $S_m = 213.8$ ksi
Graphite epoxy (0°-6 ply)

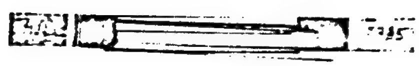

Fatigue Specimen 80% S_m , $S_m = 213.8$ ksi
Graphite epoxy (0°-6 ply).

Fatigue Specimen 80% S_m , $S_m = 213.8$ ksi
No failure 1,066,623 cycles
Graphite epoxy (0°- 6ply)

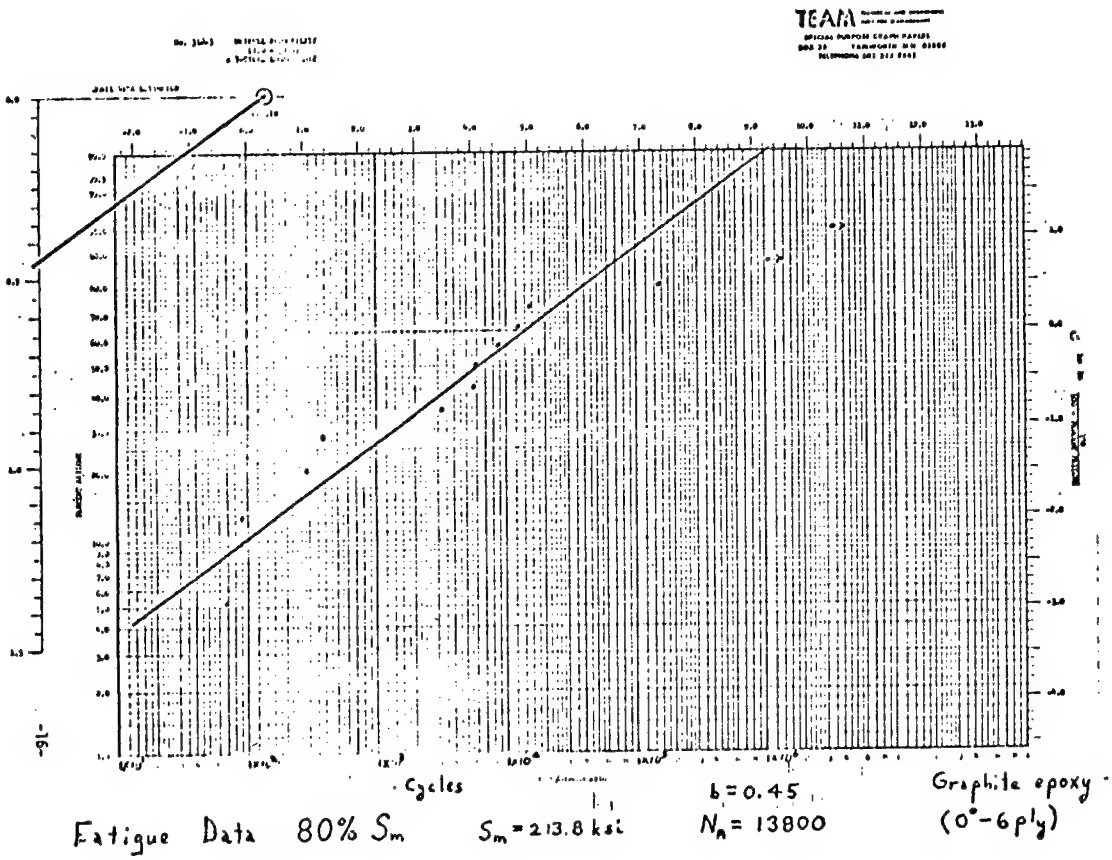

Preliminary Conclusions

1. Residual strength distribution has larger, not smaller, scatter than static strength, if proper method of comparison is used.

2. Hazard-rate method can best demonstrate the failure mode in fatigue.

3. Fatigue life distribution of small specimens can be used to predict that of larger ones, if the "statistical arrangement" is in-series.

4. At a constant fatigue stress level that is higher than the lowest static strength specimen, the fatigue life distribution must include failure at very low cycles.

CHARACTERIZATION OF COMPOSITE PROPERTIES USING TUBULAR SPECIMENS

H. T. HAHN AND J. ERIKSON

OBJECTIVE:

TO CHARACTERIZE MECHANICAL BEHAVIOR OF COMPOSITE LAMINATES UNDER COMBINED LOADINGS.

- ELASTIC MODULI
- FAILURE ENVELOPE
- STRENGTH DISTRIBUTION
- NONLINEAR STRESS-STRAIN RELATIONSHIP

APPROACH:

- TUBULAR SPECIMENS UNDER AXIAL AND TORSIONAL LOADINGS
- COMPARISON BETWEEN TENSION COMPLIANCES AND COMPRESSION COMPLIANCES
- APPLICATION OF INVARIANTS
- POLYNOMIAL CRITERION FOR MATRIX/INTERFACE-CONTROLLED FAILURE
- WEIBULL DISTRIBUTION FOR STRENGTH
- NORMALIZED STRENGTH PARAMETER

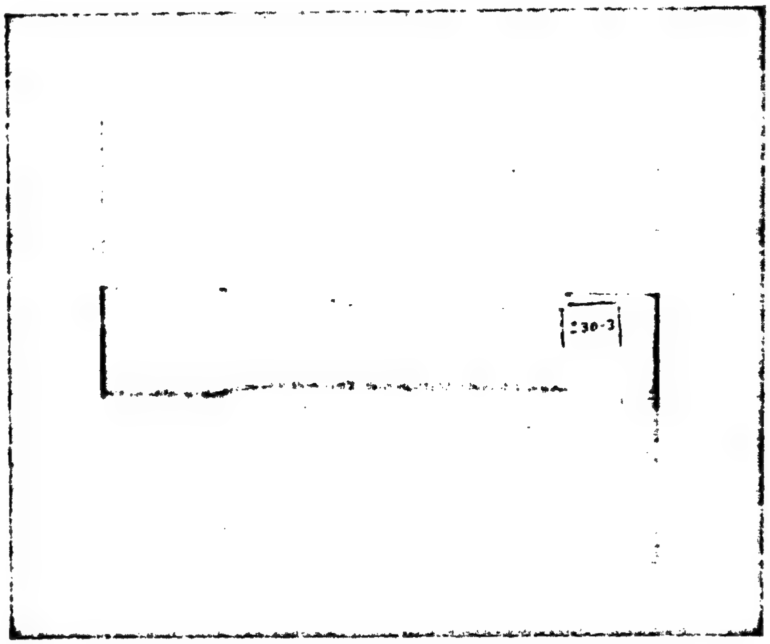

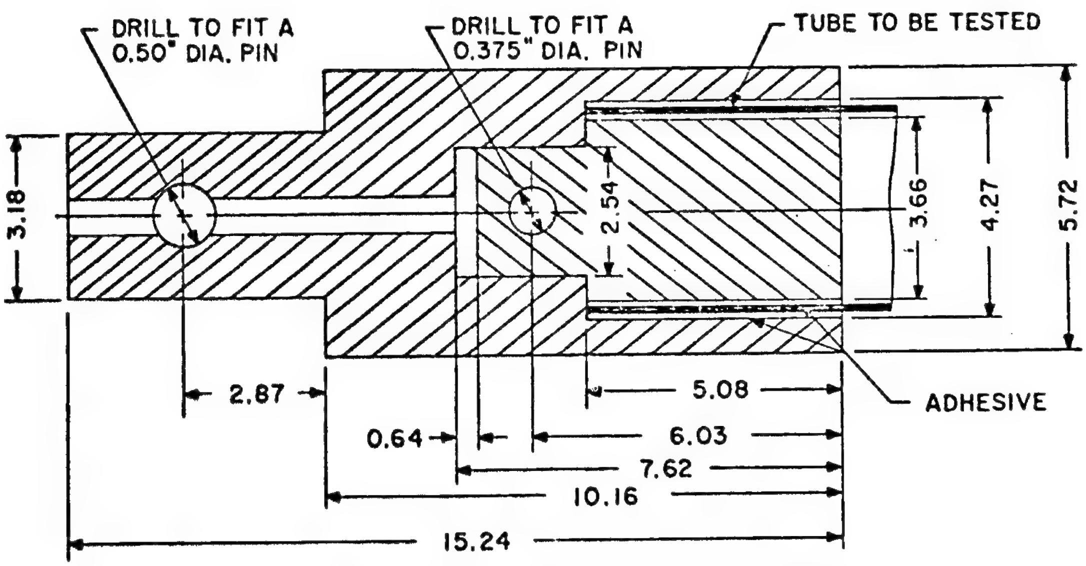

ALL DIMENSIONS IN cm UNLESS OTHERWISE MENTIONED

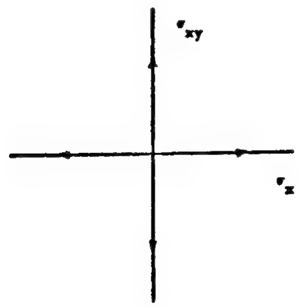

$$e_x = S'_{11}\sigma_x + S'_{16}\sigma_{xy}$$

$$e_y = S'_{21}\sigma_x + S'_{26}\sigma_{xy}$$

$$e_{xy} = S'_{61}\sigma_x + S'_{66}\sigma_{xy}$$

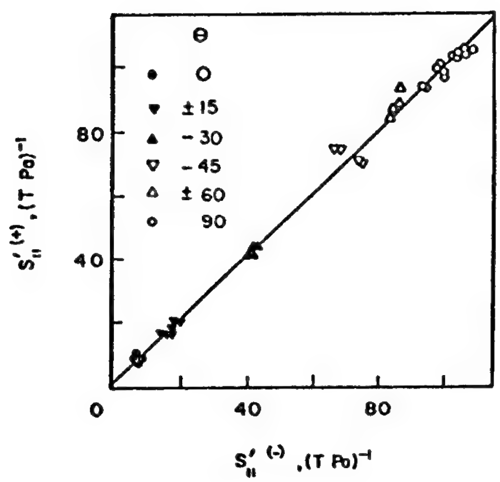

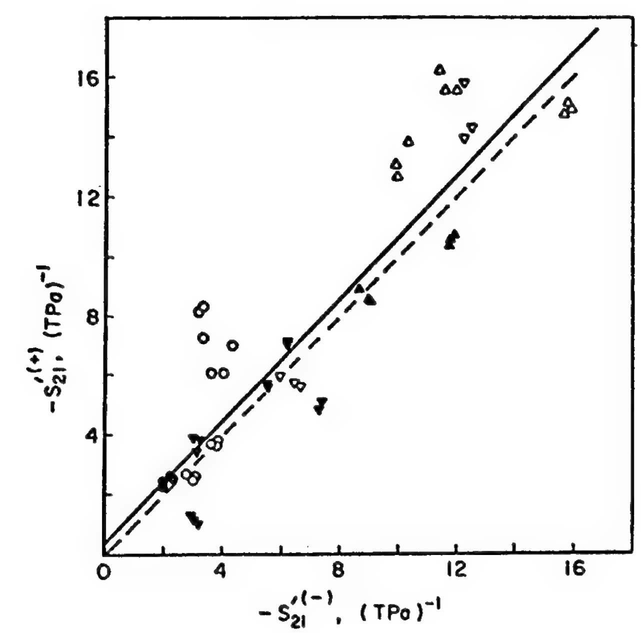

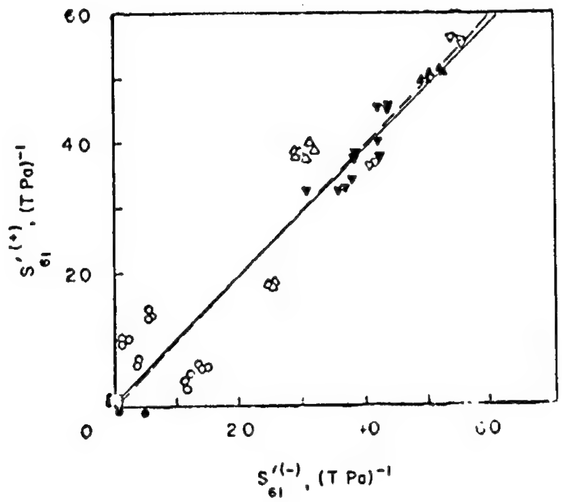
60
40
20
0
20
40
60
$S'^{(+)}_{61}$, (T Pa)$^{-1}$
$S'^{(-)}_{61}$, (T Pa)$^{-1}$

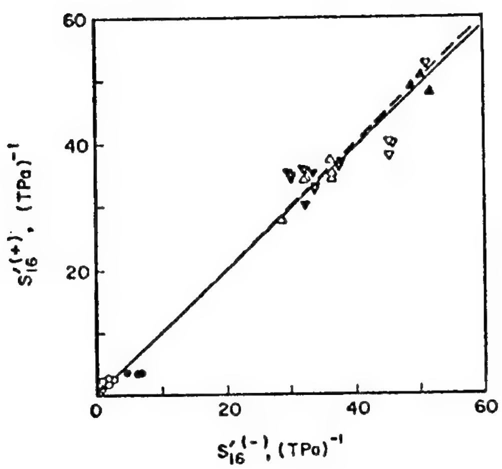
60
40
20
0
20
40
60
$S'^{(+)}_{16}$, (TPa)$^{-1}$
$S'^{(-)}_{16}$, (TPa)$^{-1}$

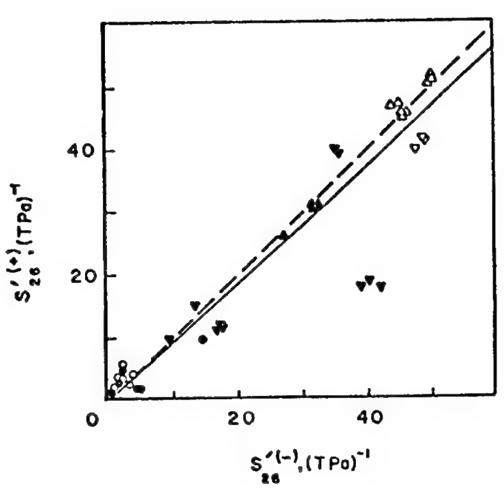
40
20
0
20
40
$S'^{(+)}_{26}$, (TPa)$^{-1}$
$S'^{(-)}_{26}$, (TPa)$^{-1}$

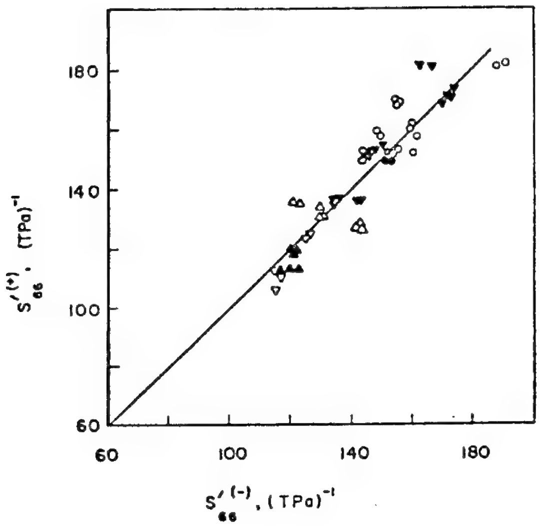

TABLE PARAMETERS a and b

	S'_{11}	$-S'_{12}$	S'_{61}	S'_{16}	S'_{26}	S'_{66}	S'_{61} vs. S'_{16}
a	0.984	1.026	0.975	0.980	0.936	1.006	0.950
b, $(TPa)^{-1}$	0.945	0.333	0.412	0.065	-0.480	-0.611	3.497
r	0.9974	0.9152	0.9599	0.9930	0.9557	0.9595	0.9683

$$S'^{(+)}_{ij} = aS'^{(-)}_{ij} + b$$

TABLE AVERAGE INVARIANTS AND AVERAGE COMPLIANCES

	$\bar{I}_1$	$\bar{I}_2$	$\bar{R}_1$	$\bar{R}_2$
Ave., $(TPa)^{-1}$	26.43	34.63	46.22	5.510
C.V., %	8.96	5.29	5.49	17.50

$\bar{S}_{11}$ $(TPa)^{-1}$	$\bar{S}_{12}$ $(TPa)^{-1}$	$\bar{S}_{22}$ $(TPa)^{-1}$	$\bar{S}_{66}$ $(TPa)^{-1}$
9.33	-2.69	101.77	160.56

$$I_1 = (S'_{11} + S'_{22} + 2S'_{12}) / 4$$

$$I_2 = (S'_{11} + S'_{22} - 2S'_{12} + S'_{66}) / 8$$

$$R_1 = [(-S'_{11} + S'_{22})^2 + (S'_{16} + S'_{26})^2]^{1/2} / 2$$

$$R_2 = [(S'_{11} + S'_{22} - 2S'_{12} - S'_{66})^2 + 4(S'_{26} - S'_{16})^2]^{1/2} / 8$$

$$\bar{S}_{11} = \bar{I}_1 + \bar{I}_2 - \bar{R}_1 - \bar{R}_2$$

$$\bar{S}_{22} = \bar{I}_1 + \bar{I}_2 + \bar{R}_1 - \bar{R}_2$$

$$\bar{S}_{12} = \bar{I}_1 - \bar{I}_2 + \bar{R}_2$$

$$\bar{S}_{66} = 4\bar{I}_2 + 4\bar{R}_2 .$$

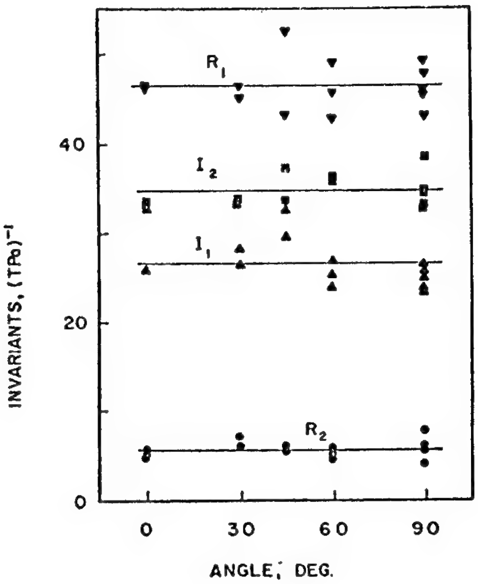

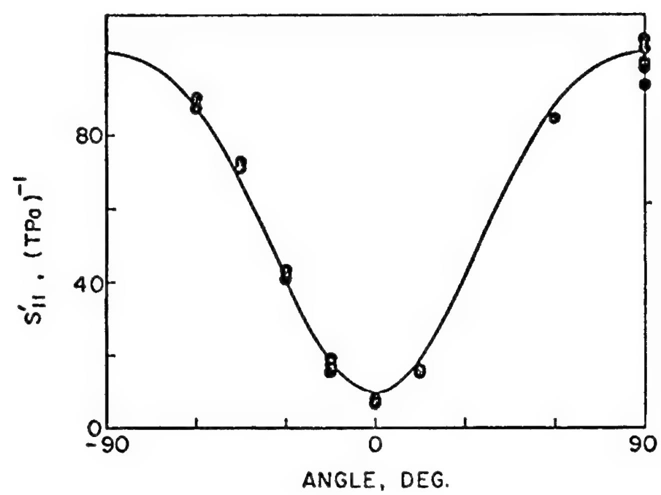

ELASTIC BEHAVIOR UNDER COMBINED LOADINGS

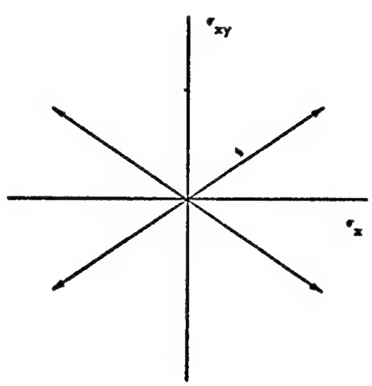

$$\epsilon_x/\sigma_x = S'_{11} + S'_{16}\sigma_{xy}/\sigma_x$$

$$\epsilon_y/\sigma_x = S'_{12} + S'_{26}\sigma_{xy}/\sigma_x$$

$$\epsilon_{xy}/\sigma_x = S'_{16} + S'_{66}\sigma_{xy}/\sigma_x$$

$$\epsilon_x/\sigma_{xy} = S'_{11}\sigma_x/\sigma_{xy} + S'_{16}$$

$$\epsilon_y/\sigma_{xy} = S'_{12}\sigma_x/\sigma_{xy} + S'_{26}$$

$$\epsilon_{xy}/\sigma_{xy} = S'_{16}\sigma_x/\sigma_{xy} + S'_{66}$$

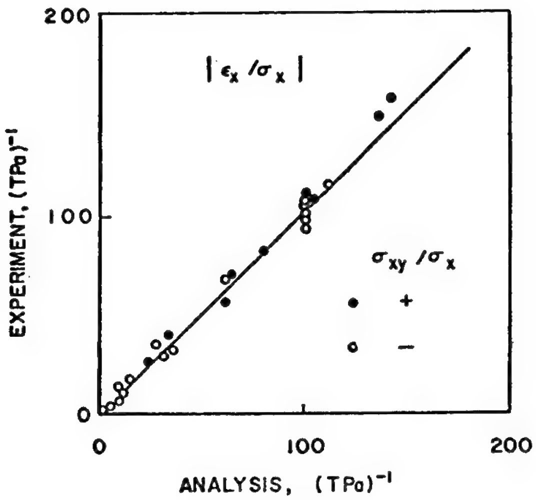

STRENGTH

$$f(\sigma_2, \sigma_6) = F_2\sigma_2 + F_{22}\sigma_2^2 + F_{66}\sigma_6^2 = 1 .$$

$$F_2 = 3.376 \times 10^{-2} (MPa)^{-1} ,$$

$$F_{22} = 4.721 \times 10^{-4} (MPa)^{-2} ,$$

$$F_{66} = 2.384 \times 10^{-4} (MPa)^{-2} .$$

$$R = \exp\left[-\left(\frac{f - f_{min}}{\hat{f}} \right)^{a} \right] .$$

$$a = 3.055 \quad , \quad \hat{f} = 1.5265$$

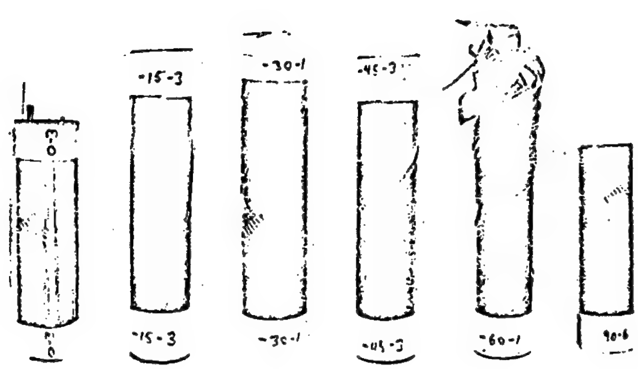

Figure Failure Modes of Composite Tubes

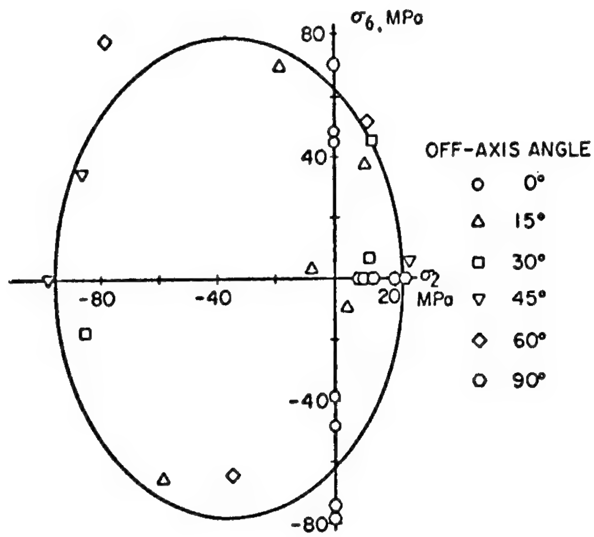

σ_6, MPa
80
40
-40
-80
-80
-40
20
σ_2 MPa
OFF-AXIS ANGLE
0°
15°
30°
45°
60°
90°

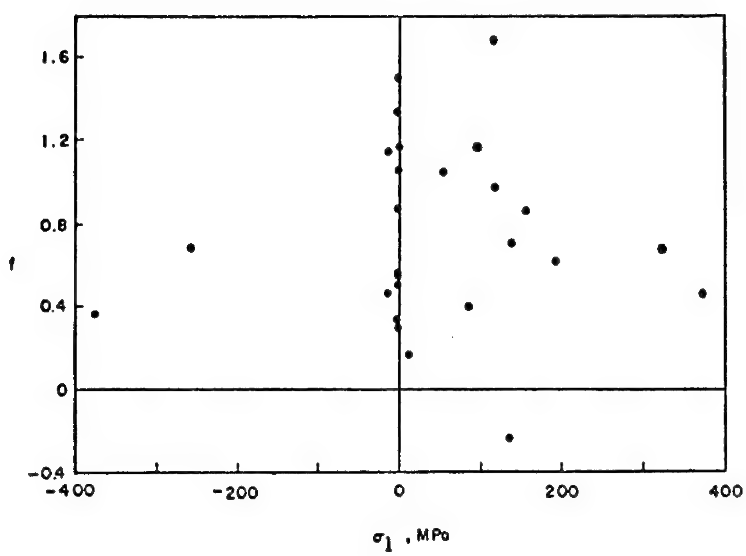

1.6
1.2
0.8
0.4
0
-0.4
f
-400
-200
0
200
400
σ_1, MPa

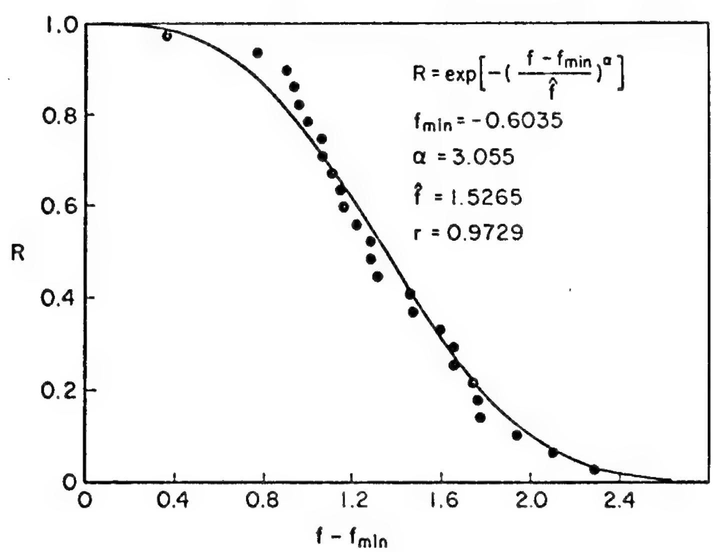

1.0
0.8
0.6
0.4
0.2
0
R
0
0.4
0.8
1.2
1.6
2.0
2.4
$f - f_{min}$
$R = \exp\left[-\left(\frac{f - f_{min}}{\hat{f}}\right)^{\alpha}\right]$
$f_{min} = -0.6035$
$\alpha = 3.055$
$\hat{f} = 1.5265$
$r = 0.9729$

SIZE EFFECT

$$S = \frac{\text{DISTANCE TO DATA POINT}}{\text{DISTANCE TO FAILURE ENVELOPE}}$$

$$R = \exp\left(-\left(s/\hat{s}\right)^{\alpha}\right)$$

FOR SHORT SPECIMENS

$$\hat{s}' = \hat{s}\,(8/3)^{1/4.7451} = 1.23\,\hat{s}$$

$$\hat{F}_2' = \hat{F}_2 / 1.23$$

$$\hat{F}_{22}' = \hat{F}_{22} / 1.23^2$$

$$\hat{F}_{66}' = \hat{F}_{66} / 1.23^2$$

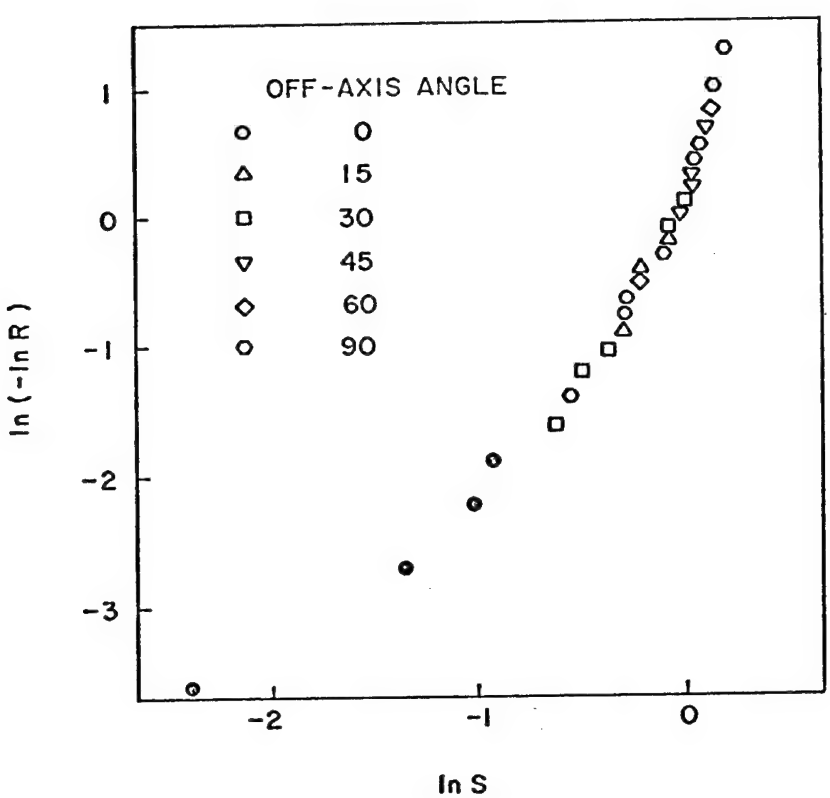

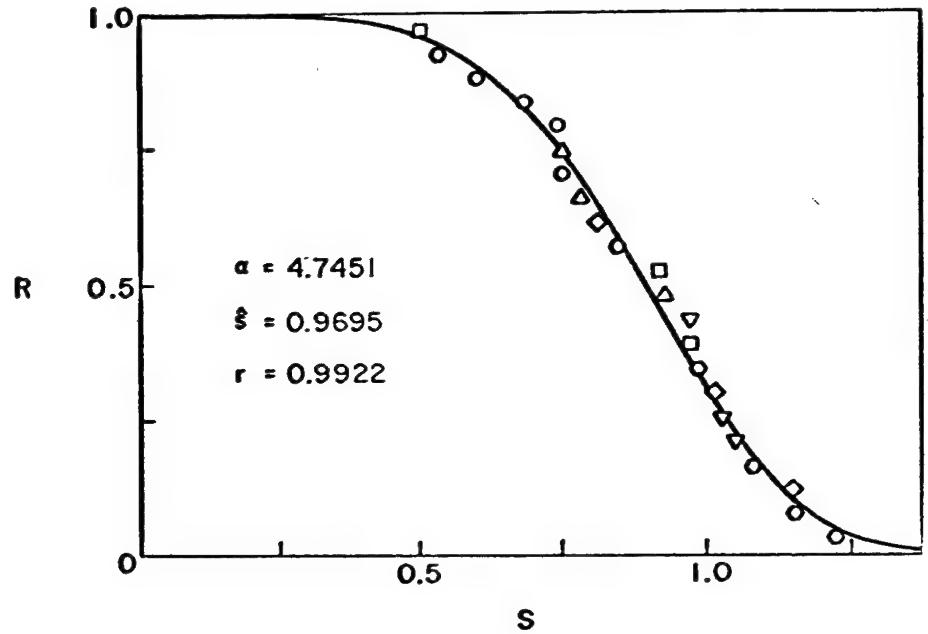

1.0
R
0.5
0
0.5
1.0
S
α = 4.7451
ŝ = 0.9695
r = 0.9922

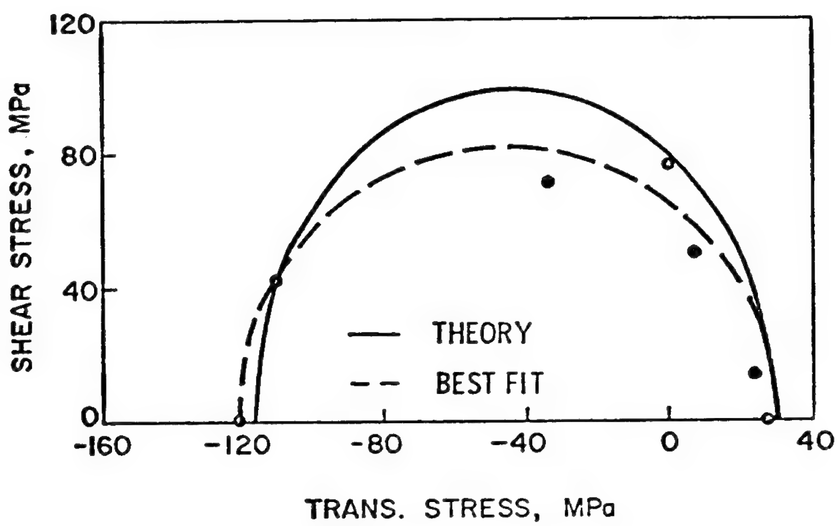

120
80
40
0
SHEAR STRESS, MPa
THEORY
BEST FIT
-160
-120
-80
-40
0
40
TRANS. STRESS, MPa

MATERIALS SCIENCES CORPORATION

EFFECTS OF ENVIRONMENT, AND DAMPING AND COUPLING PROPERTIES OF COMPOSITE LAMINATES ON PANEL FLUTTER

(AFOSR CONTRACT F44620-76-C-0080)

SAILENDRA N. CHATTERJEE
AND
SATISH V. KULKARNI

OBJECTIVES

I. DEVELOP EPOXY-MATRIX COMPOSITE LAMINATE CONSTITUTIVE RELATIONS WHICH ACCOUNT FOR THE EFFECTS OF LAMINAE STACKING SEQUENCE, TRANSVERSE SHEAR DEFORMATION, AND TIME-DEPENDENT BEHAVIOR IN A FORM THAT IS APPLICABLE TO STRUCTURAL DYNAMICS.

II. EXTEND CONSTITUTIVE RELATIONS UNDER "I", TO CONSIDER EFFECTS OF MOISTURE ABSORPTION AND ELEVATED TEMPERATURE ON EPOXY-MATRIX ADVANCED COMPOSITES.

III. EVALUATE DAMPING CHARACTERISTICS OF COMPOSITE PANELS USING CONSTITUTIVE THEORY DEVELOPED.

IV. PERFORM PANEL FLUTTER ANALYSIS USING LINEAR PISTON THEORY AERODYNAMICS AND THE CONSTITUTIVE THEORY DEVELOPED. QUANTITATIVELY EVALUATE COMPOSITE MATERIAL AND DESIGN FACTORS WHICH HAVE MAJOR INFLUENCE ON PANEL FLUTTER.

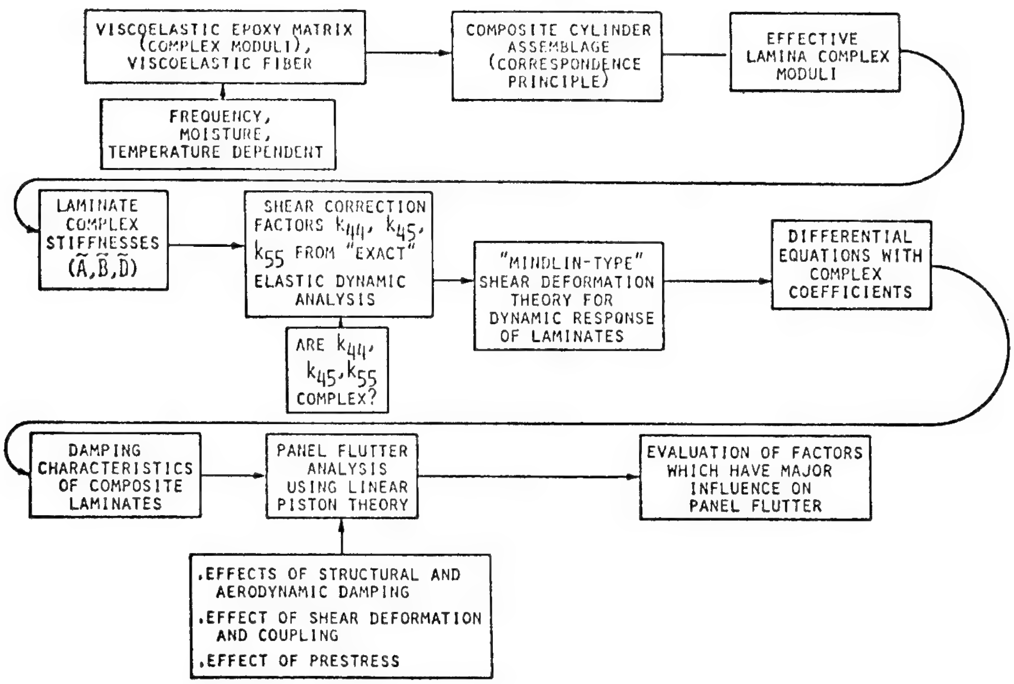

VARIOUS MODULES IN THE COMPOSITE LAMINATE PANEL FLUTTER PROBLEM

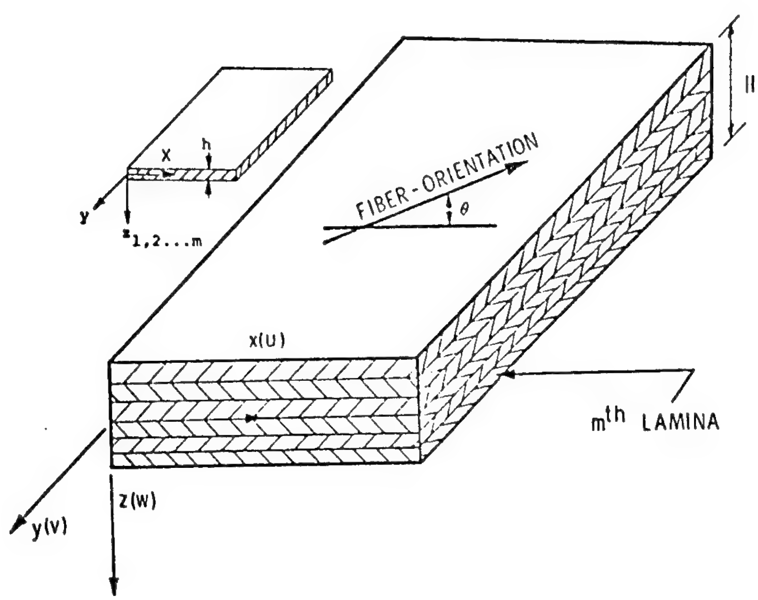

Composite Lamina/Laminate Coordinate Systems

DAMPING EFFECTS

EFFECTIVE COMPLEX MODULI OF LAMINA

- CONSTITUTIVE RELATIONS FOR CONSTITUENTS ARE KNOWN FROM DYNAMIC EXPERIMENTS
- DYNAMIC CORRESPONDENCE PRINCIPLE AND ELASTIC COMPOSITE CYLINDER ASSEMBLAGE SOLUTION ARE USED FOLLOWING HASHIN

EXAMPLE:

$$\tilde{G}_A^* = \tilde{G}_A^M \frac{V^M \tilde{G}_A^M + (1 + V^F)\tilde{G}_A^F}{(1 + V^F)\tilde{G}_A^M + V^M \tilde{G}_A^F}$$

$\sim$ INDICATES COMPLEX MODULI
M INDICATES MATRIX
F INDICATES FIBER

LAMINATE COMPLEX STIFFNESSES

- OBTAINED FROM LAMINA EFFECTIVE COMPLEX MODULI (OR COMPLIANCES) AND ASSUMED DISPLACEMENT (OR STRESS) FIELD

EXAMPLE:

$$\tilde{A}_{IJ}, \tilde{B}_{IJ}, \tilde{D}_{IJ} = \int_{-H/2}^{H/2} \tilde{Q}_{IJ}(1, z, z^2)dz \qquad (I,J = 1,2,6)$$

$\tilde{Q}_{IJ}$ ARE PLANE STRESS REDUCED STIFFNESSES

$$\tilde{A}_{IJ} = k'_{IJ} H^2 \left[\int_{-H/2}^{H/2} \tilde{S}_{IJ}\, dz\right]^{-1} = k_{IJ} \left[\int_{-H/2}^{H/2} \tilde{C}_{IJ}\, dz\right] \quad (I,J = 4,5)$$

K_{IJ} ARE SHEAR CORRECTION FACTORS BASED ON CONSTANT TRANSVERSE SHEAR STRAIN
K'_{IJ} ARE SHEAR CORRECTION FACTORS BASED ON CONSTANT TRANSVERSE SHEAR STRESS

TRANSVERSE SHEAR DEFORMATION EFFECTS

- IMPORTANCE OF THESE EFFECTS ON LAMINATE STATIC AND DYNAMIC RESPONSE IS WELL KNOWN
- DETERMINE THE SHEAR CORRECTION FACTORS (K_{IJ} OR K'_{IJ}) AS A FUNCTION OF STACKING SEQUENCE AND LAMINATE CONSTRUCTION FROM "EXACT" ELASTIC ANALYSIS

$$A_{44,55} = I' (\omega_1^2 + \omega_2^2) \pm [I'^2(\omega_1^2 - \omega_2^2)^2 - 4A_{45}^2]^{1/2}$$

$\omega_{1,2}$ ARE THICKNESS SHEAR CUTOFF FREQUENCIES FROM "EXACT" ANALYSIS

$$I' = I - R^2/P$$

$$P, R, I = \int_{H/2}^{H/2} \rho(1, z, z^2)dz$$

- CROSSTERM A_{45} ESTIMATED FROM SHEAR FORCE - AVG. ROTN. RELATION FROM FIRST U/V DOMINATED MODES

SHEAR CORRECTION FACTORS FOR A SYMMETRIC CROSS PLY LAMINATE WITH EQUAL PERCENTAGE OF 0° AND 90° LAYERS

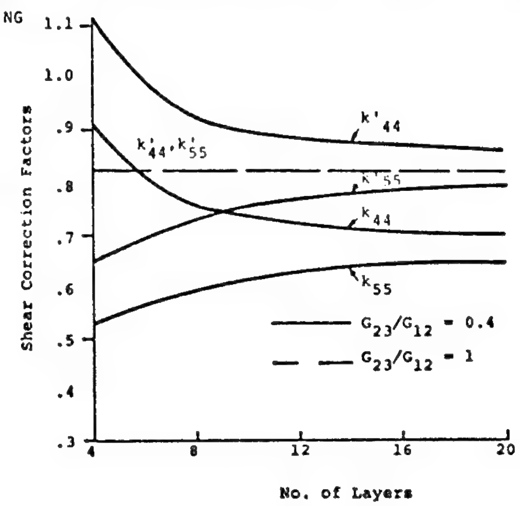

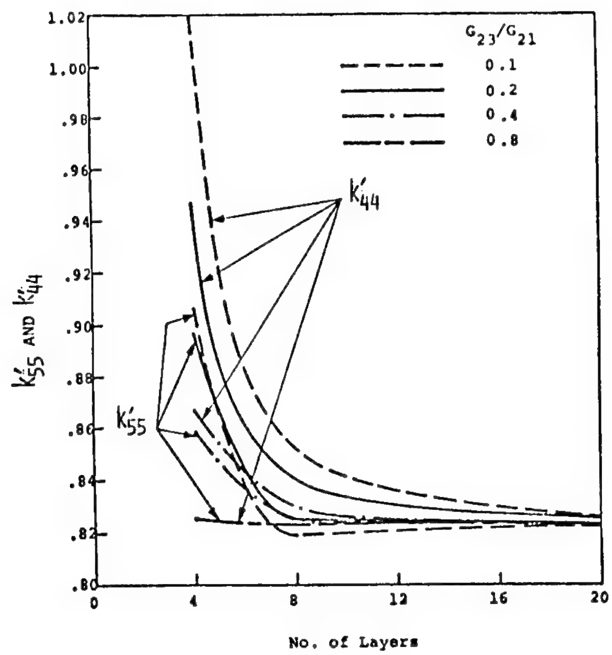

SHEAR CORRECTION FACTORS K'_{44} AND K'_{55} FOR $[\pm 30°]_s$ LAMINATE

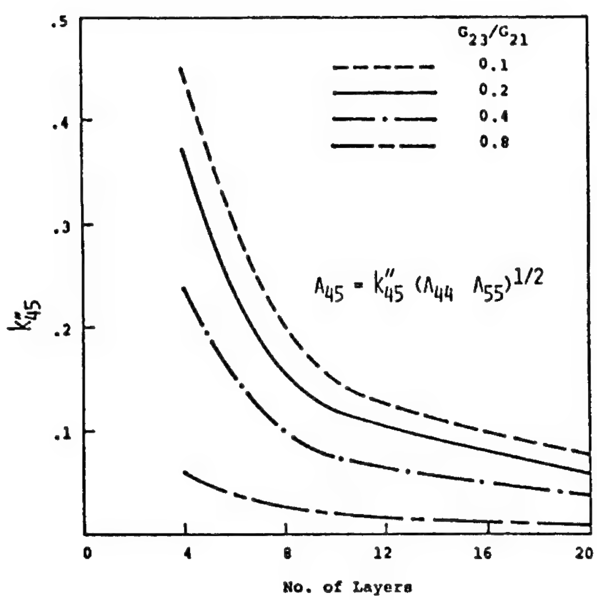

SHEAR CORRECTION FACTOR K''_{45} FOR $[\pm 30°]_s$ LAMINATE

OBSERVATIONS

- FOR NON-HOMOGENEOUS LAMINATES, SHEAR CORRECTION FACTORS CAN BE SIGNIFICANTLY DIFFERENT FROM THE CLASSICAL VALUE OF $\pi^2/12$.
- HOWEVER, SHEAR CORRECTION FACTORS K'_{44} AND K'_{55} APPROACH $\pi^2/12$ FOR LARGE NUMBER OF LAYERS (SHEAR CORRECTION FACTORS K_{44} AND K_{55} DO NOT.)
- ESTIMATES OF THE SHEAR CORRECTION FACTOR K'_{45} OBTAINED FOR THE FIRST TIME.

MOISTURE/TEMPERATURE EFFECTS

OBSERVATIONS

- EFFECT OF MOISTURE/TEMPERATURE IS TO ALTER LAMINA/LAMINATE COMPLEX MODULI (PARTICULARLY THOSE WHICH ARE MATRIX CONTROLLED).
- PLASTICIZING EFFECT OF MOISTURE/TEMPERATURE REDUCES THE STORAGE MODULUS AND INCREASES THE LOSS FACTOR (FOR EXAMPLE, MECHANICAL DAMPING INDEX PEAKS WHEN THE RELATIVE RIGIDITY DROPS AT $T = T_G$ FOR AN EPOXY; HOWEVER, DATA FOR COMPLEX DYNAMIC PROPERTIES OF EPOXIES/LAMINA FOR DIFFERENT MOISTURE CONTENTS AND TEMPERATURES ARE LACKING).

APPROACH

- LAMINA DIFFUSIVITIES OBTAINED FROM TEST DATA OR ANALYTICALLY FROM CONSTITUENT DIFFUSIVITIES
- DETERMINE THROUGH-THE-THICKNESS TRANSIENT/STEADY STATE MOISTURE DISTRIBUTION IN A LAMINATE FROM 1-D DIFFUSION EQUATIONS - NUMERICAL SOLUTION EMPLOYING FINITE DIFFERENCE AND PREDICTOR CORRECTOR TECHNIQUE - TEMPERATURE AND MOISTURE DEPENDENT DIFFUSIVITIES
- DETERMINE EFFECT OF MOISTURE AND TEMPERATURE DISTRIBUTION ON LAMINATE PROPERTIES USING APPROPRIATE KNOCK DOWN OR SHIFT FACTORS FOR STORAGE AND LOSS MODULI. EFFECTS OF NONSYMMETRIC TEMPERATURE/MOISTURE DISTRIBUTION ON SYMMETRIC LAMINATE PROPERTIES ARE CONSIDERED

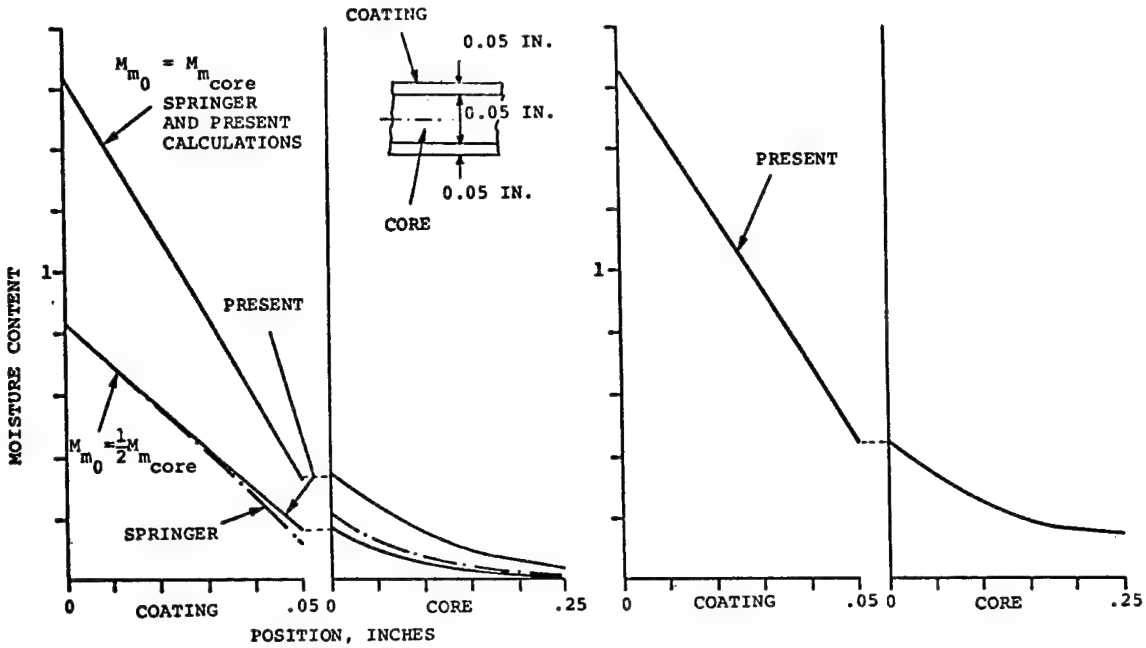

MOISTURE DISTRIBUTION, 3000 DAYS

75°F, 82% R.H.

MOISTURE DISTRIBUTION, 6000 DAYS

75°F, 82% R.H.

MOISTURE DISTRIBUTION IN A COATED COMPOSITE

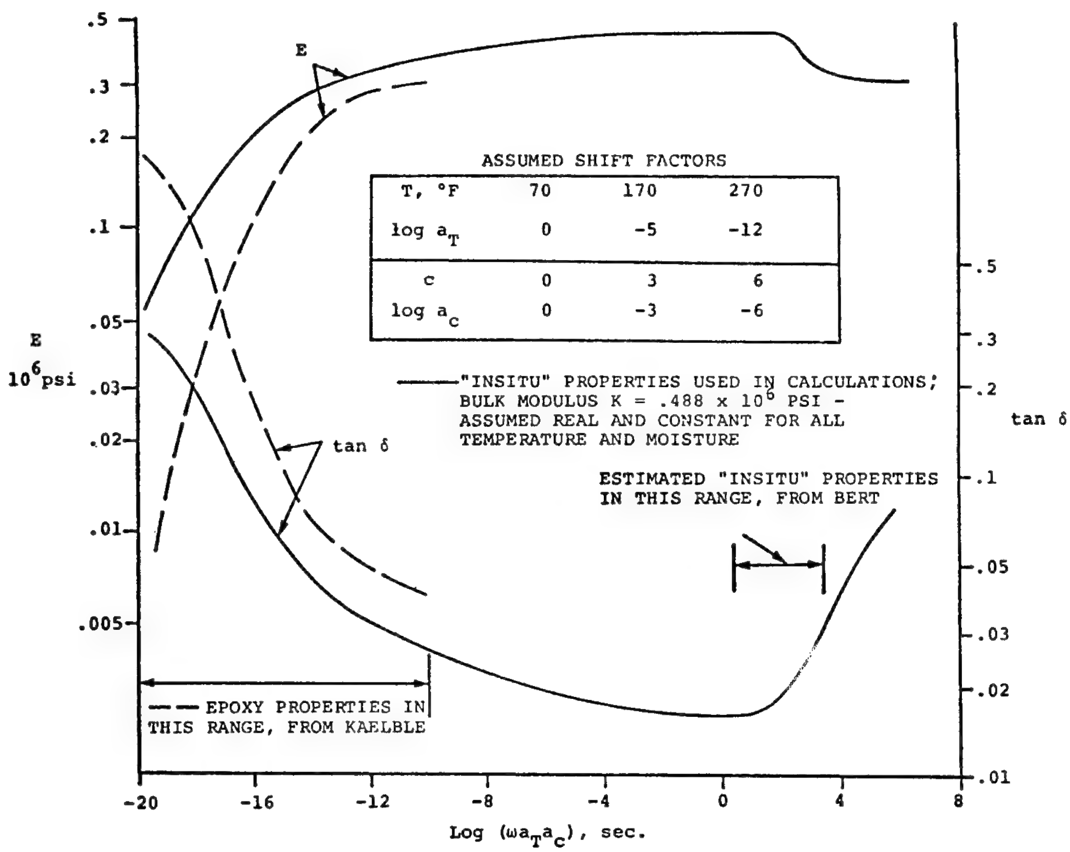

T, °F	70	170	270
log a_T	0	-5	-12
c	0	3	6
log a_c	0	-3	-6

MASTER CURVE FOR DYNAMIC PROPERTIES OF EPOXY - REFERENCE TEMPERATURE = 70°F

PANEL FLUTTER

SOLVE THE CYLINDRICAL BENDING FLUTTER PROBLEM USING GALERKIN PROCEDURE TO DETERMINE ENVIRONMENTAL EFFECTS, SPAN TO DEPTH RATIO (SHEAR DEFORMATION), AERODYNAMIC DAMPING, PRESTRESS. EXAMPLES: NO PRESTRESS, NO AERODYNAMIC DAMPING, GRAPHITE/EPOXY LAMINATES

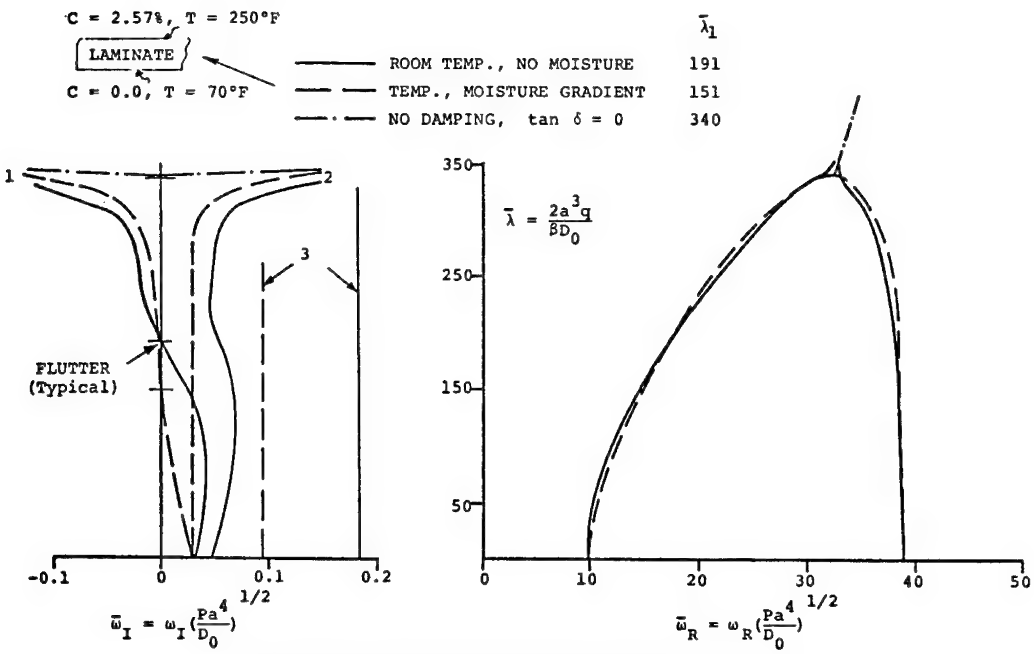

FREQUENCY SPECTRUM FOR $(0/90/0/90)_s$ CROSS PLY LAMINATE a/h = 60

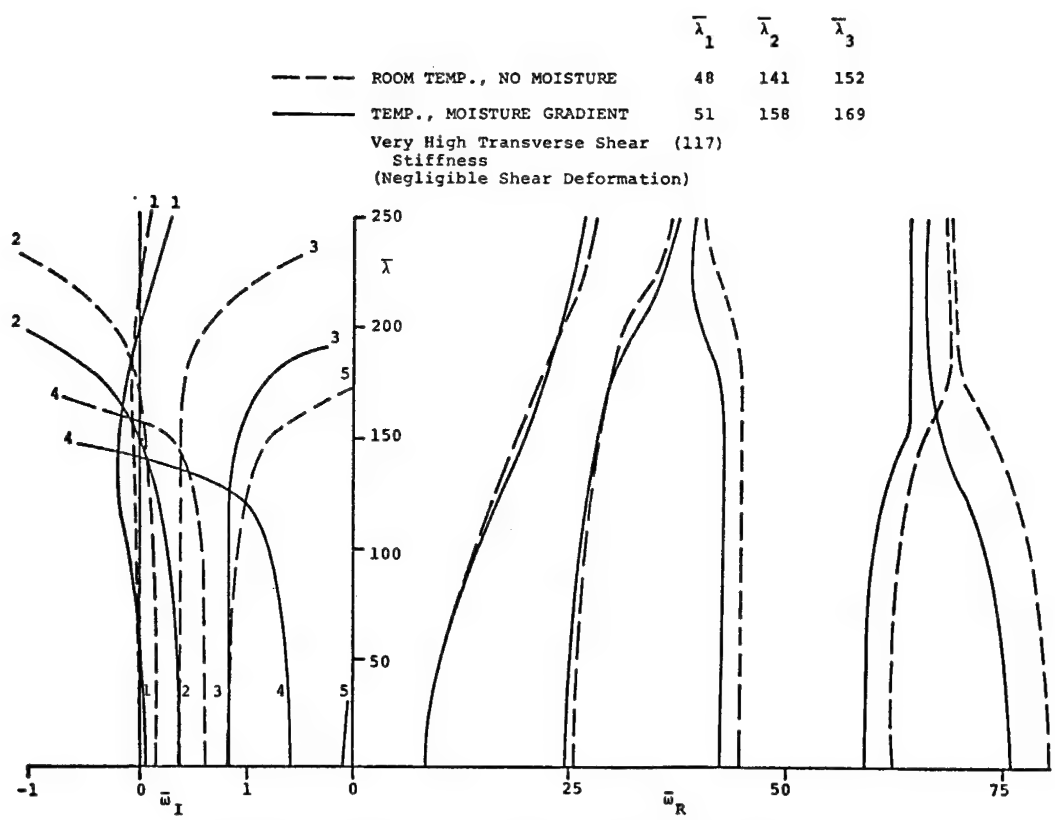

FREQUENCY SPECTRUM FOR $(0/90/0/90)_s$ CROSS PLY LAMINATE a/h = 10

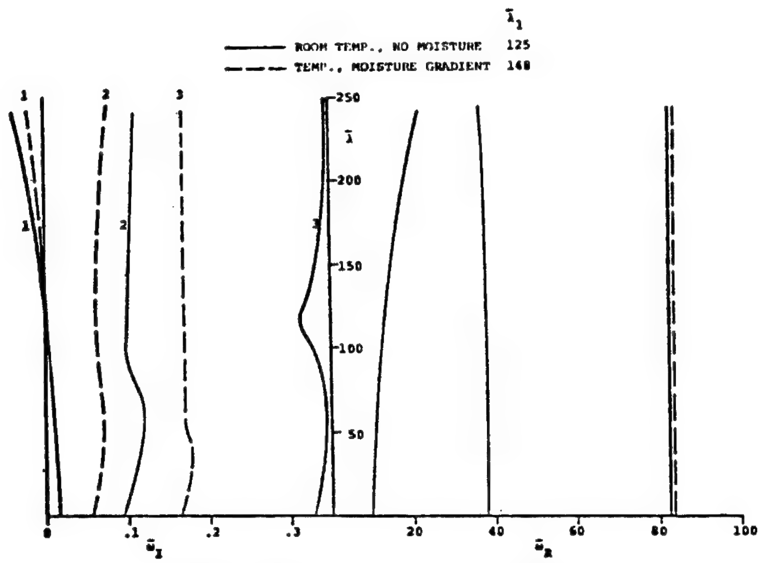

FREQUENCY SPECTRUM FOR $(+45/-45/0_2/90)_s$ LAMINATE a/h = 40

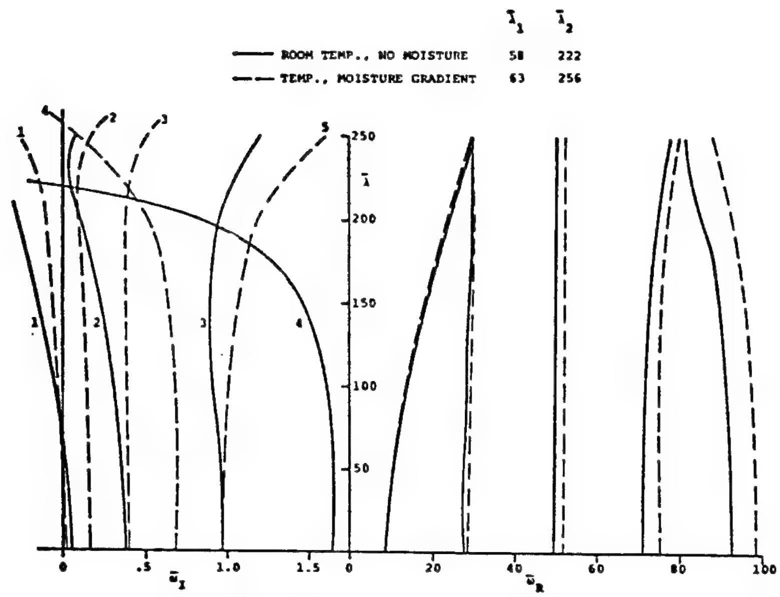

FREQUENCY SPECTRUM FOR $(+45/-45/0_2/90)_s$ LAMINATE a/h = 10

OBSERVATIONS

- DAMPING REDUCES THE CRITICAL FLUTTER SPEED
- SHEAR DEFORMATION HAS A SIGNIFICANT EFFECT ON THE CRITICAL FLUTTER SPEED, ESPECIALLY FOR SMALLER a/h RATIOS
- CONSIDERATION OF MOISTURE AND TEMPERATURE GRADIENT MAY INCREASE OR DECREASE THE CRITICAL FLUTTER SPEED
  - RESULTS ARE STRONGLY DEPENDENT ON THE MASTER CURVE FOR DYNAMIC PROPERTIES AND SHIFT FACTORS FOR TEMPERATURE AND MOISTURE

DEFECT - PROPERTY RELATIONSHIPS IN COMPOSITE MATERIALS

INVESTIGATORS
E. G. HENNEKE II, K. L. REIFSNIDER, W. W. STINCHCOMB
VIRGINIA POLYTECHNIC INSTITUTE & STATE UNIVERSITY
BLACKSBURG, VIRGINIA

OBJECTIVES:

1. TO IDENTIFY THE PRECISE NATURE OF DAMAGE DEVELOPMENT IN QUASI-ISOTROPIC GRAPHITE-EPOXY LAMINATES UNDER VARIOUS LOAD HISTORIES.

2. TO DETERMINE THE PHYSICAL PARAMETERS WHICH LEAD TO A LOSS OF STRENGTH AND/OR LIFE.

3. TO ESTABLISH THE MECHANICS OF THE INDIVIDUAL AND COMBINED ACTION OF THESE PARAMETERS AS THEY INFLUENCE MECHANICAL RESPONSE.

4. TO ADDRESS THE QUESTION OF HOW THESE FINDINGS CAN BEST BE DESCRIBED BY ANALYSIS.

INVESTIGATIVE PROGRAM:

TYPE I MATERIAL - $[0,\pm45,90]_S$, AS3501 GRAPHITE-EPOXY
- INSTRUMENTED TENSILE TESTS
- LAMINATE THEORY CALCULATIONS - FAILURE PREDICTIONS
- SEM AND LIGHT MICROSCOPE STUDIES
- ACOUSTIC EMISSION AND ULTRASONIC ATTENUATION STUDIES
- FATIGUE LOADING
- VIDEO AND THERMOGRAPHIC STUDIES
- SECTIONING STUDIES

TYPE II MATERIALS - $[0,90,\pm45]_S$, AS3501 GRAPHITE-EPOXY
- INSTRUMENTED TENSILE TESTS
- LAMINATE ANALYSIS AND 3-D FEM - FAILURE PREDICTIONS
- SEM AND LIGHT MICROSCOPE STUDIES
- ACOUSTIC EMISSION AND ULTRASONIC ATTENUATION STUDIES
- INSTRUMENTED FATIGUE LOADING
- VIDEO, CINE, AND THERMOGRAPHIC STUDIES
- SECTIONING STUDIES

GENERAL
- LOAD HISTORY STUDIES
- TRANSVERSE CRACK AND DELAMINATION INVESTIGATION - INITIATION, GROWTH AND FRACTURE
- TECHNIQUE DEVELOPMENT - ULTRASONIC ATTENUATION, THERMOGRAPHY, REPLICATION
- ANALYSIS EVALUATION AND DEVELOPMENT

EARLIER FINDINGS: (QUASI-STATIC LOADING)

1. CRACKS APPEAR AT LEVELS OF LOAD AS LOW AT 1/3 OF ULTIMATE FRACTURE LOAD, CORRESPONDING TO THE LEVEL PREDICTED IF THERMAL RESIDUAL STRESSES ARE INCLUDED.

2. THE GRADUAL DEVELOPMENT OF CRACKS IN THE WEAKEST PLY (FIRST PLY FAILURE) OCCURS OVER A RANGE OF STRESS BOUNDED ABOVE BY A STRESS LEVEL WHICH APPROXIMATELY CORRESPONDS TO THE "KNEE" IN THE LOAD-EXTENSION CURVE.

3. THE STRENGTH OF THE $[0°, 90°, \pm 45°]_s$ LAMINATES IS SOMEWHAT GREATER THAN THE $[0°, \pm 45°, 90°]_s$ LAMINATES.

4. CRACKS DO PROPAGATE FROM ONE LAYER TO ANOTHER, AND ACROSS THE WIDTH OF PLATE SPECIMENS.

5. CRACK FORMATION AND GROWTH IN THE INTERIOR OF A SPECIMEN CAN BE DETECTED BY NDT; ULTRASONIC METHODS APPEAR TO BE BEST SUITED FOR THAT PURPOSE.

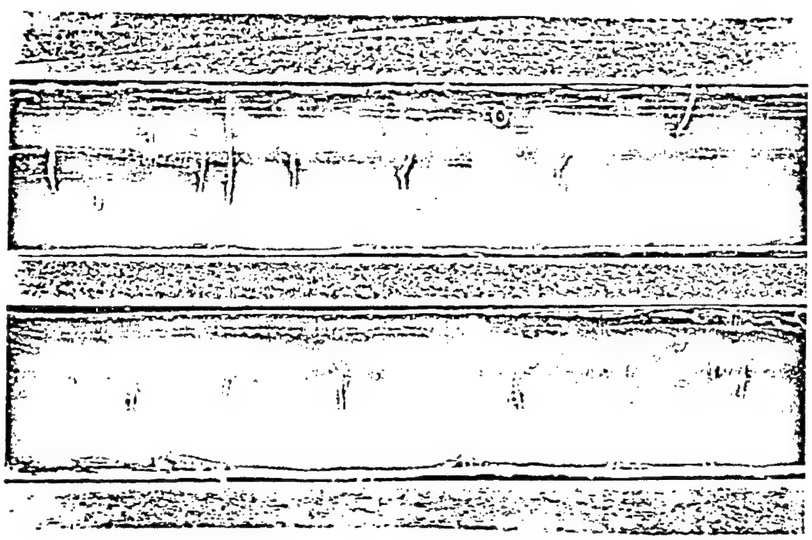

Figure 4. Cracks in type I specimen loaded to 2228 lb.; edge and 0.1 in. section

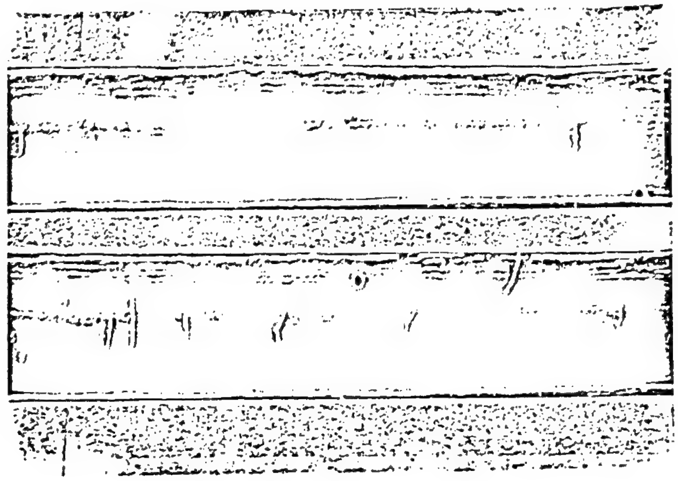

Figure 5. Edge cracks in same specimen as in Figure 4 at 1500 and 2228 lb. static loads

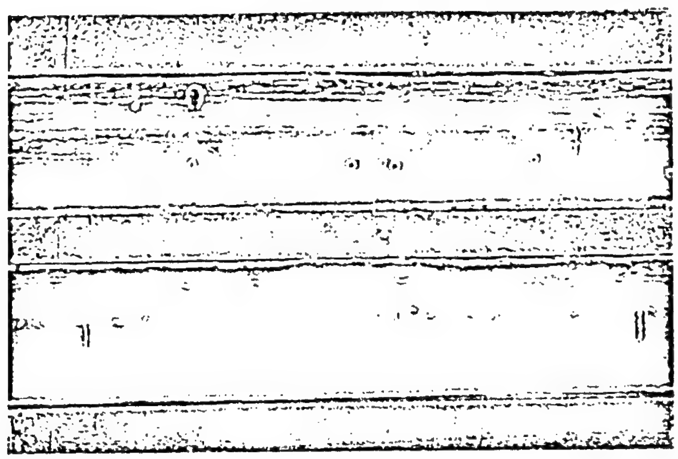

Figure 6. Edge cracks in same specimen as in Figure 4 at 1000 and 1500 lb. static loads

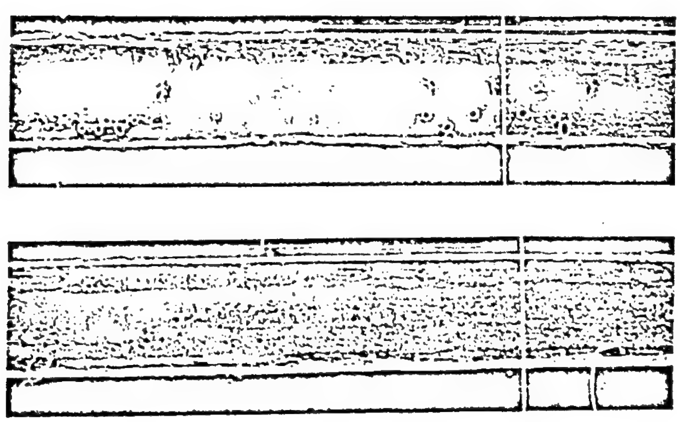

Figure 7. Cracks in a type II specimen statically loaded to 2500 lb at one edge and at a 0.04 in. section

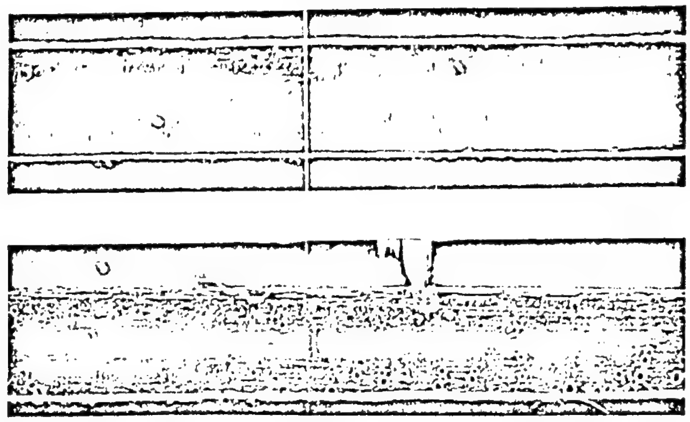

Figure 8. Other edge and corresponding section of specimen shown in Figure 7

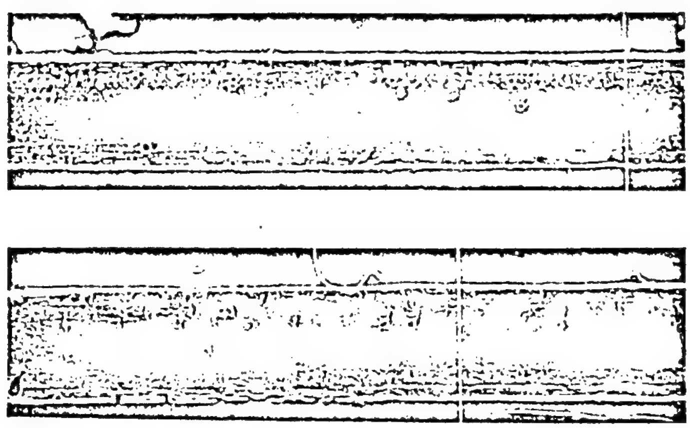

Figure 9. Both outer edges of specimen shown in Figure 7 loaded to a static level of 1500 lb.

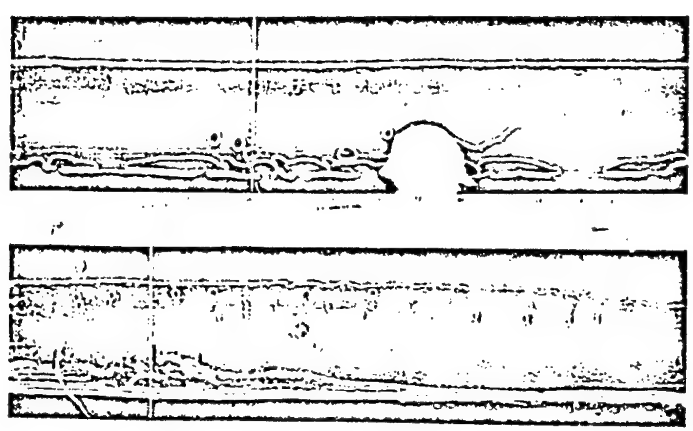

Figure 10. Outer edges of specimen shown in Figure 7 loaded to a static level of 1000 lb.

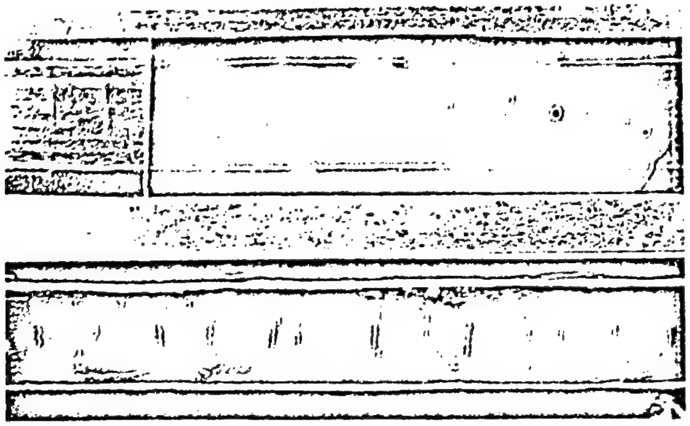

Figure 11. A type I specimen cyclically loaded to a maximum stress of 40 ksi (R = 0.1) for one million cycles. Cracks are shown at sections which are 0.045 and 0.090 in. from the specimen centerline

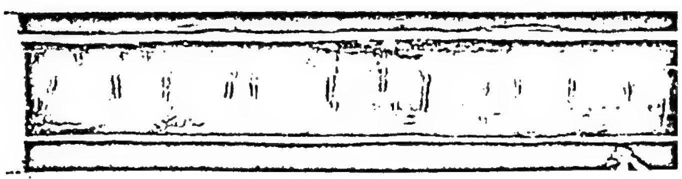

Figure 12. Cracks found in sections of specimen shown in Figure 11 which were 0.09 and 0.135 in. from the specimen centerline

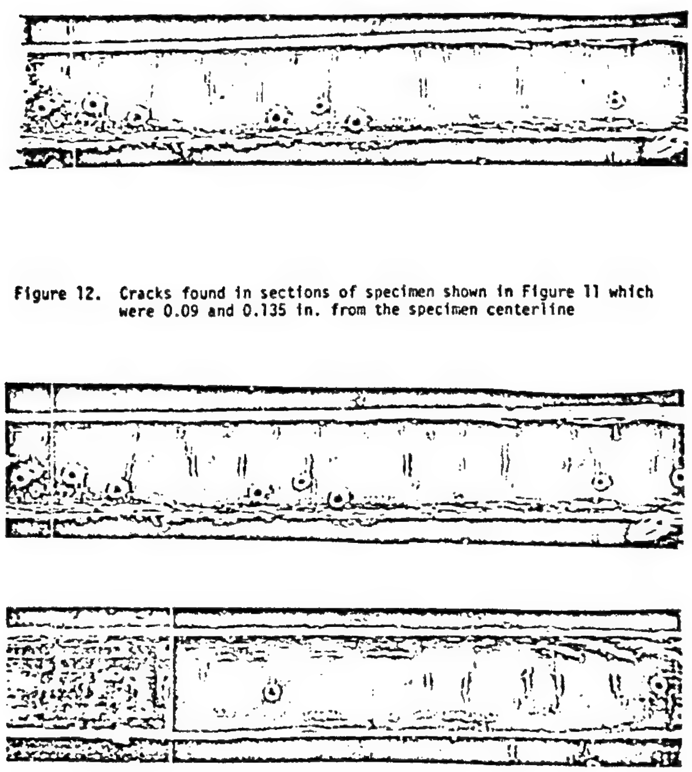

Figure 13. Cracks found in sections of specimen shown in Figure 11 which were 0.135 and 0.225 in. from the specimen centerline

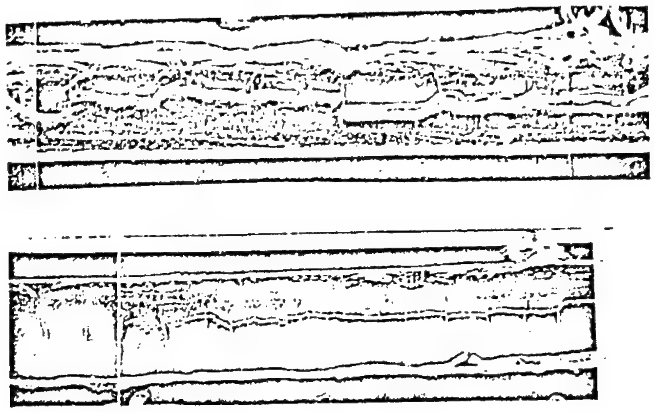

Figure 14. Cracks found in sections of specimen shown in Figure 11 which were 0.27 in. from the specimen centerline compared to the outside edge of that specimen

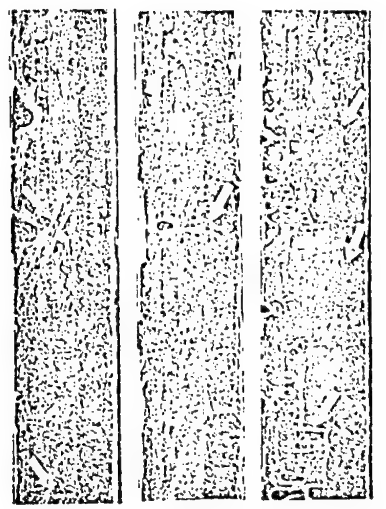

a) Static b) 50 Cycles c) 10,000 Cycles

Replicas of 1600 lb, Type I Specimen

Fig. 15.

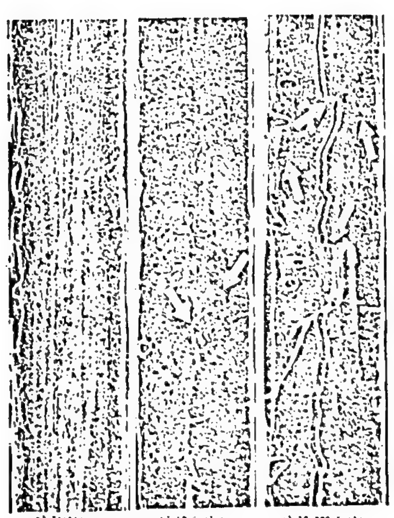

a) Static b) 50 Cycles c) 10,000 Cycles

Replicas of 2000 lb, Type I Specimen

Fig. 16.

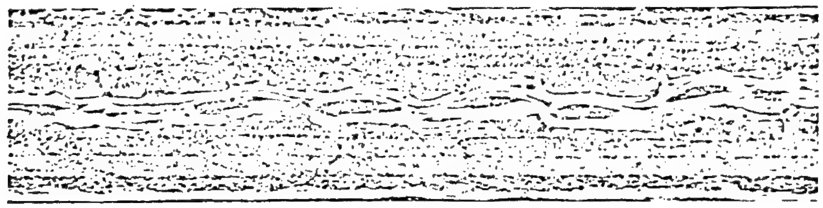

a) Static

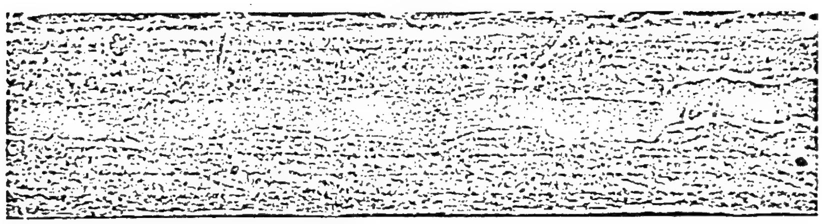

b) 50 Cycles

Fig. 17. Replicas of 2700 lb, Type I Specimen

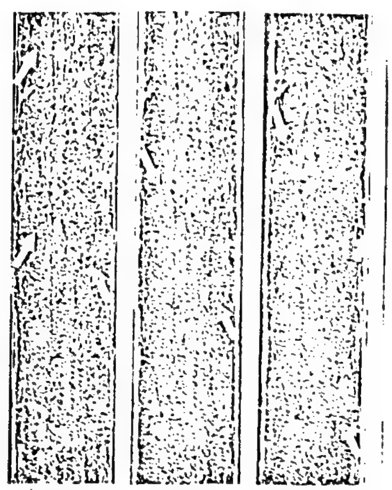

a) Static b) 50 Cycles c) 10 000 Cycles

Replicas of 1600 lb, Type II Specimen

Fig. 18.

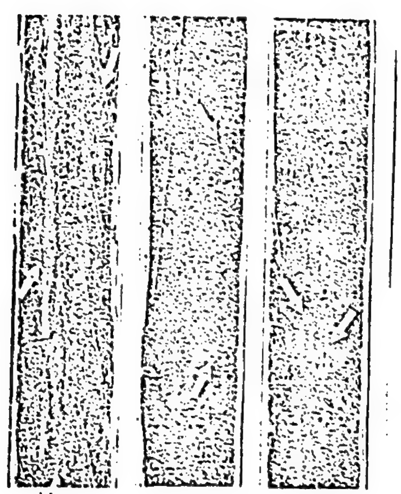

a) Static b) 50 Cycles c) 10 000 Cycles

Replicas of 2000 lb, Type II Specimen

Fig. 19.

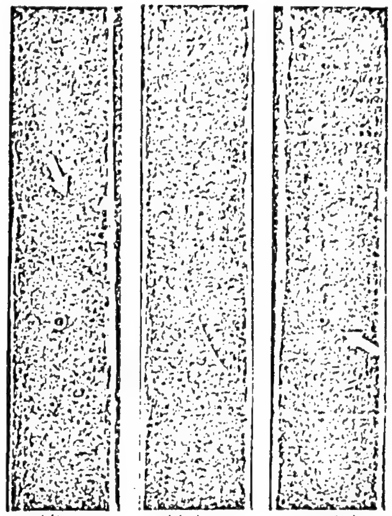

Replicas of 2700 lb, Type II Specimen

Fig. 20

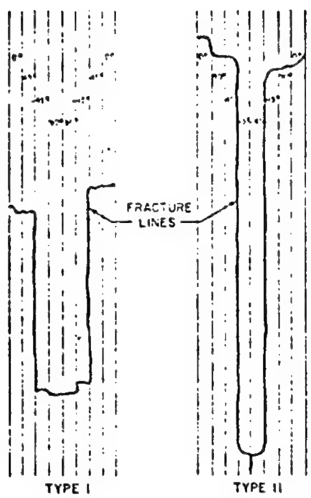

Typical Edge View Fracture Patterns for Type I and Type II Specimens

Fig. 21.

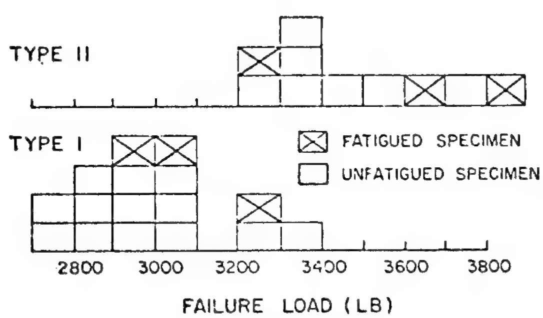

Distribution of Failure Loads for Type I and Type II Specimens

Fig. 22.

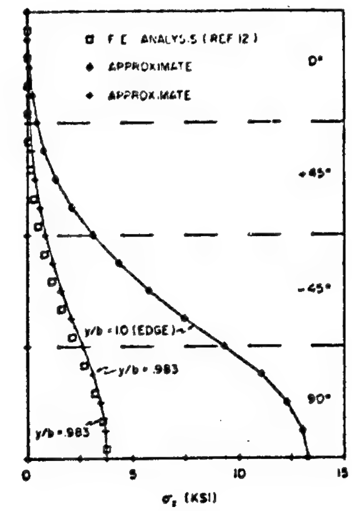

Interlaminar Normal Stress, σ_z, Through-the-Thickness Distribution for a Type I Specimen with 2000 lb Axial Load

Fig. 23.

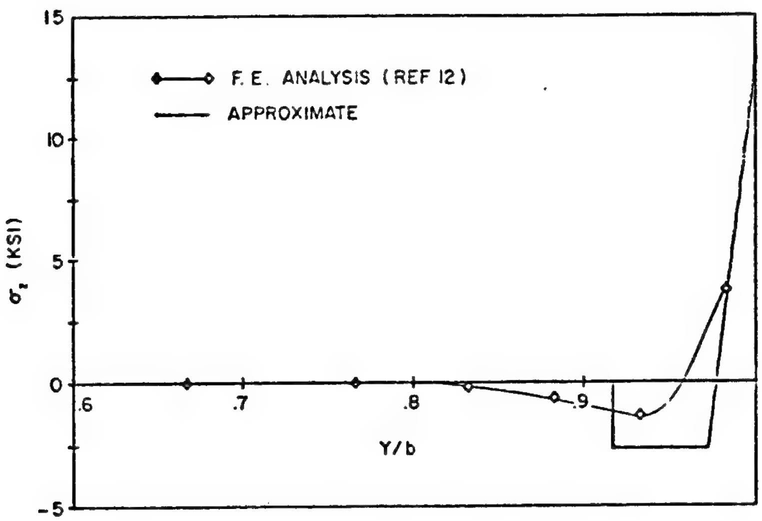

Fig. 24. Interlaminar Normal Stress, σ_z, Through-the-Width Distribution for a Type I Specimen with 2000 lb Axial Load

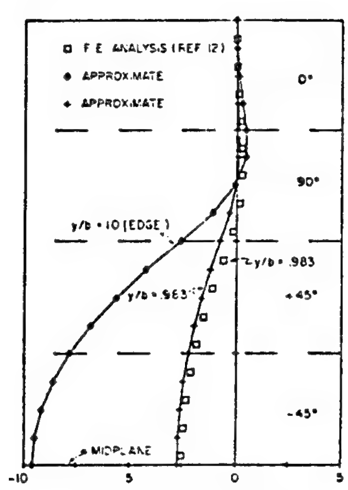

Interlaminar Normal Stress, σ_z, Through-the-Thickness Distribution for a Type II Specimen with 2000 lb Axial Load

Fig. 25

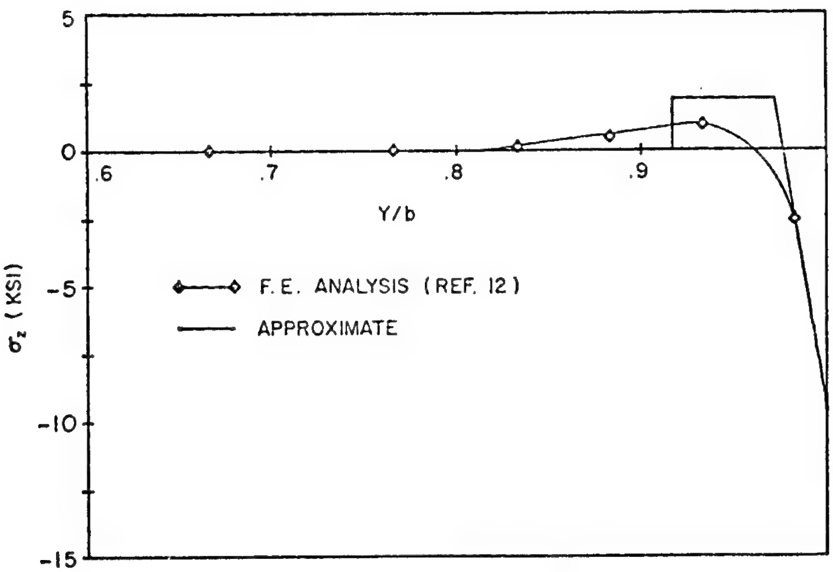

Fig. 26. Interlaminar Normal Stress, σ_z, Through-the-Width Distribution for a Type II Specimen for a Type II Specimen with 2000 lb Axial Load

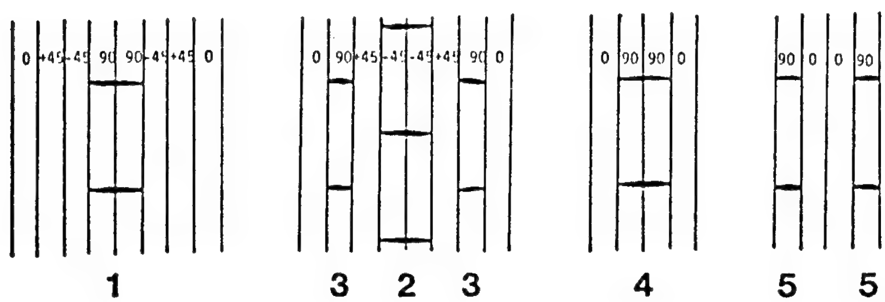

Fig. 27. Five cases of equilibrium crack spacing analyzed

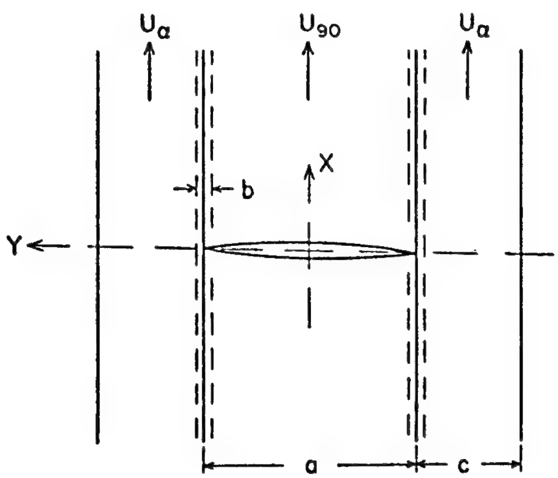

Fig. 28. Schematic diagram of a cracked laminate

TABLE I

Specimen Type	Predicted Crack Spacing (mm)	Observed Crack Spacing (mm)
Cracks in center two 90° plies of $[0,\pm45,90]_s$ laminate	0.76 0.76	Static 1.51-0.62 Fatigue 1.44-0.47
Cracks in two center 45° plies of $[0,90,\pm45]_s$ laminate	1.21	1.25-0.995
Cracks in single 90° plies of $[0,90,\pm45]_s$ laminate	0.411	0.423-0.241
Cracks in two center 90° plies of $[0,90]_s$ laminate	0.882	1.087-0.532
Cracks in outside 90° plies of $[90,0]_s$ laminate	1.66	1.73-0.775

Fig. 29. Table comparing experimental results with analytical predictions of equilibrium crack spacings for five laminates

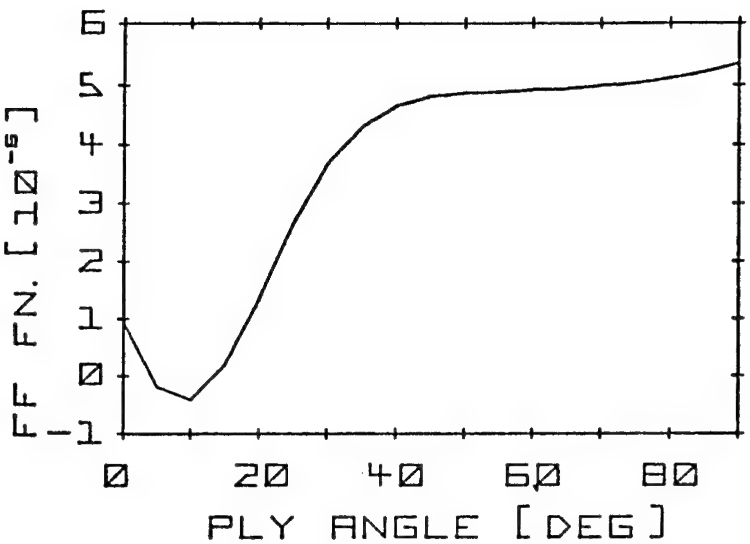

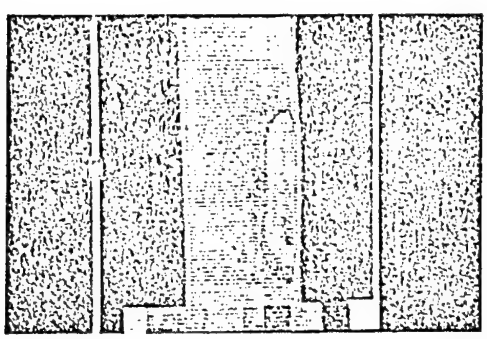

Figure 31. Thermogram of Group 1, first specimen after static loading, frequency one.

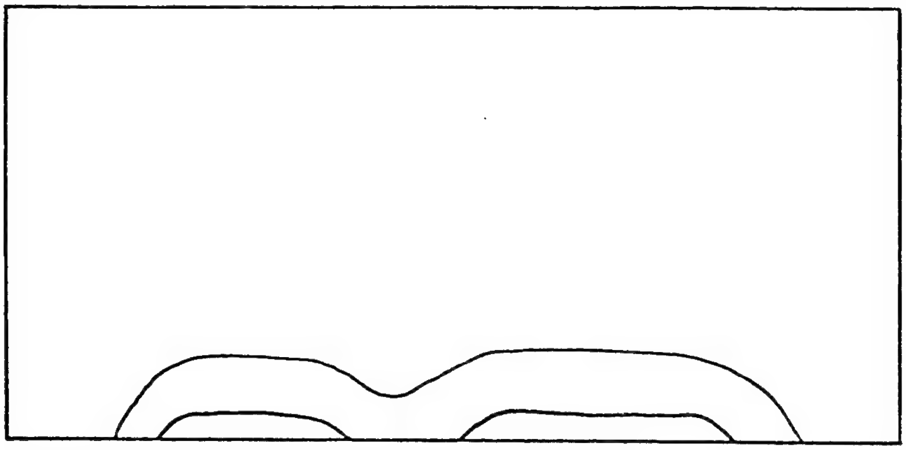

Figure 32. Computer generated thermogram of Group 1, first specimen, frequency one.

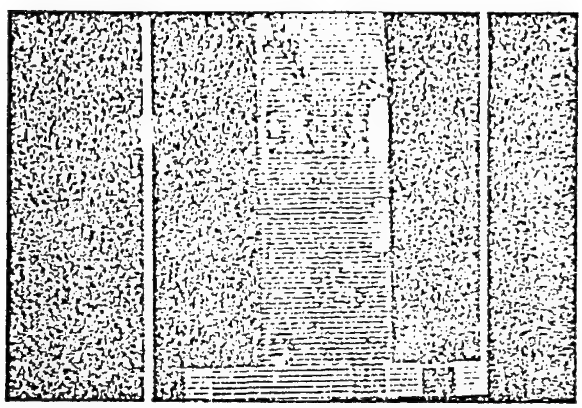

Figure 33. Thermogram of Group 1, first specimen after static loading, frequency two.

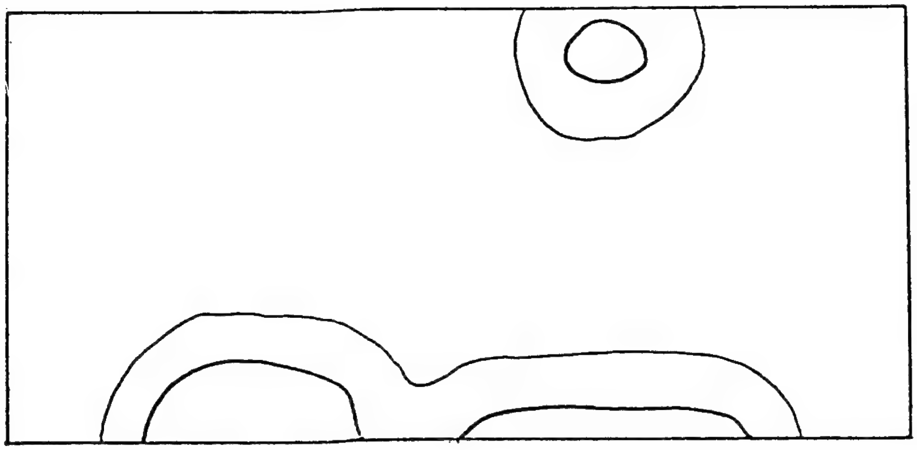

Figure 34. Computer generated thermogram for Group 1, first specimen, frequency two.

CURRENT FINDINGS

1. DAMAGE IN THESE LAMINATES CONSISTS OF THE DEVELOPMENT OF EQUILIBRIUM SPACINGS OF CRACKS IN EACH PLY BY MEANS OF CRACK INITIATION AND GROWTH OVER A SIGNIFICANT LOAD RANGE OR NUMBER OF CYCLES OF LOAD APPLICATION. THESE EQUILIBRIUM SPACINGS CAN BE PREDICTED BY ANALYSIS.
2. INITIAL CRACKS DO NOT APPEAR TO BE OF ANY SPECIAL CONSEQUENCE.
3. INTERLAMINAR STRESSES DO INFLUENCE DAMAGE INITIATION, GROWTH AND INTERACTION, AS EVIDENCED BY A DEPENDENCE OF FAILURE STRENGTH AND DAMAGE MODES ON STACKING SEQUENCE.
4. THE DIFFERENCE IN THE STRESS STATE AT THE EDGE AND INTERIOR OF THE LAMINATES IS REFLECTED IN DISTINCTIVE DAMAGE FEATURES SUCH AS EDGE DELAMINATION, ANGULAR CRACKING OF 45° PLIES AT THE EDGE, AND SOMEWHAT HIGHER CRACK DENSITIES IN THE INTERIOR IN SOME CASES.
5. CYCLED LOADING INCREASES THE DENSITY OF CRACKS IN A GIVEN PLY COMPARED TO A SINGLE APPLICATION OF LOAD TO THE SAME LEVEL. THE MODE OF FAILURE UNDER CYCLIC LOADING IS NOT IDENTICAL TO STATIC FAILURE MODES UNDER OTHERWISE IDENTICAL CONDITIONS.
6. NONDESTRUCTIVE TEST METHODS SUCH AS STIFFNESS DETERMINATION, VIDEO-THERMOGRAPHY AND MEASUREMENT OF ULTRASONIC ATTENUATION CONTINUE TO BE VERY USEFUL TECHNIQUES FOR THE DETECTION AND INVESTIGATION OF DAMAGE DEVELOPMENT.

LOCKHEED PALO ALTO RESEARCH LABORATORY

COMPUTER ANALYSIS OF SHELLS AND COMPOSITES

AFOSR Contract F49620-77-C-0122
Monitor - W. Walker
Period - 9/77 to 5/79

- Analysis of Shells and Panels (D. Bushnell)
- Hygrothermal Effects in Composite Laminates (F. Crossman)

HYGROTHERMAL EFFECTS

OBJECTIVES

- Develop Hygrothermal-Viscoelastic Finite Element and Plane Stress (Lamination Theory) Models
- Analyze The Influence of Hygrothermal History on Laminate Mechanical Response as a Function of Distance From Free Edges.

APPROACH

1. Computational Development
   - Coupled Analysis of Diffusion (Moisture Sorption or Heat Conduction) and Mechanical Response
   - Viscoelastic, Generalized Plane Strain Finite Element Model of Laminate Free Edges.
   - Moisture Altered Viscoelastic Constitutive Equations For Plane Stress and Finite Element Models.
2. Analysis
   - Determine Alteration of Internal Residual Stresses Due to Hygrothermal Exposure.
   - Determine Alteration of Laminate Free Edge Stresses Due to Hygrothermal History.
   - Examine the Combined Effects of Mechanical and Hygrothermal Loading.

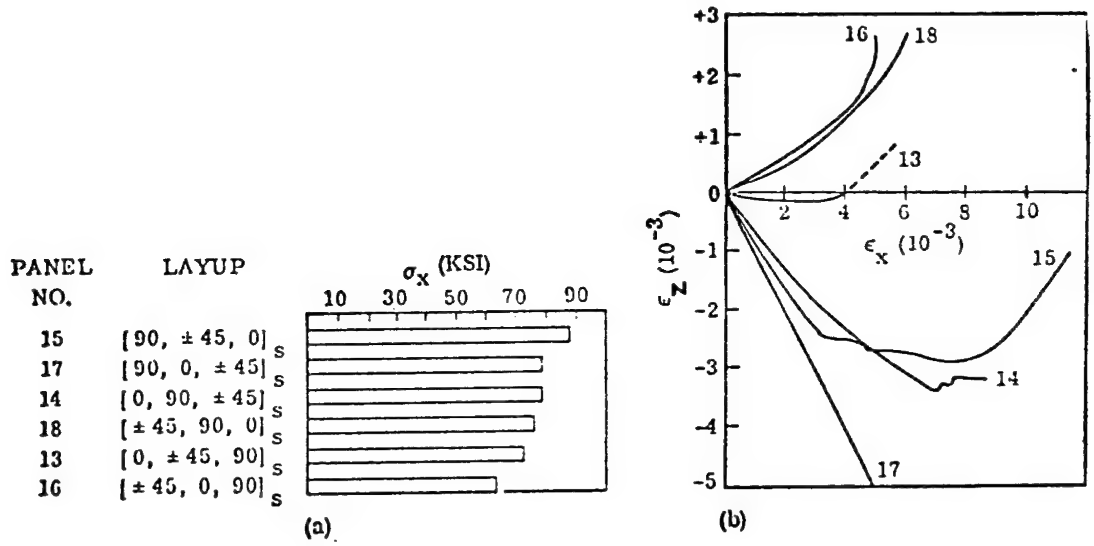

Figure 1 (a) Tensile Strength of QI T300/934 Laminates
(b) Through Thickness Strain at Free Edge vs. Applied Tensile Strain ϵ_x

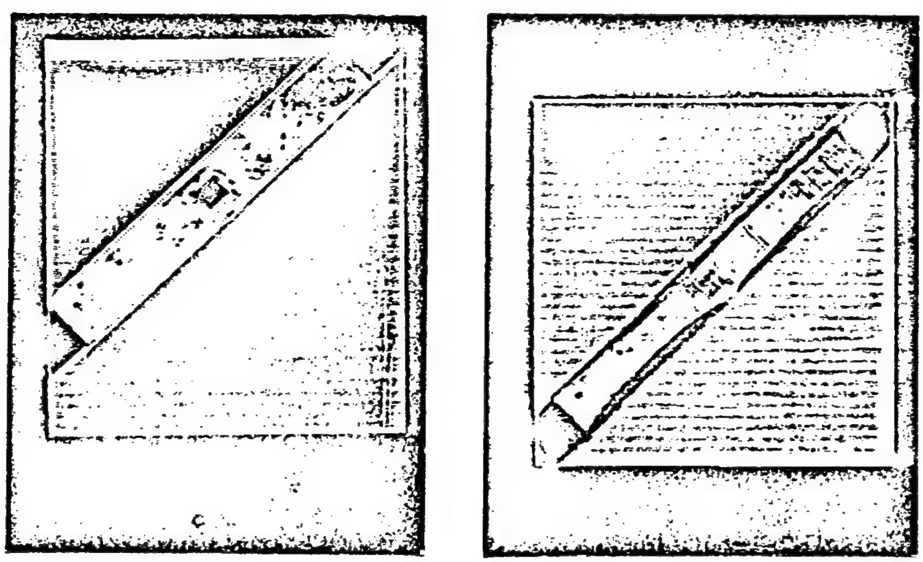

(a) (b)

Figure 2 Acoustic Transmission Image of $(\pm 45,0,90)_s$ T300/934
(a) Before Loading
(b) After Loading to 90 percent of UTS

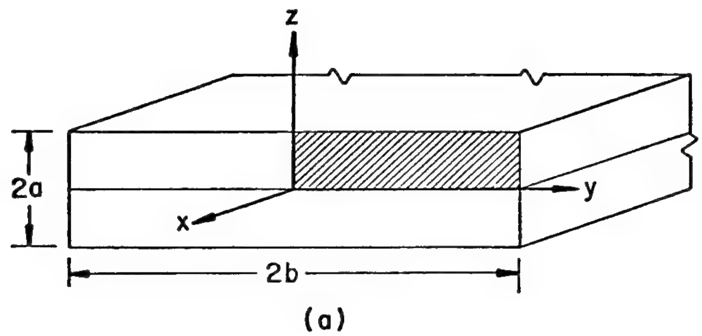

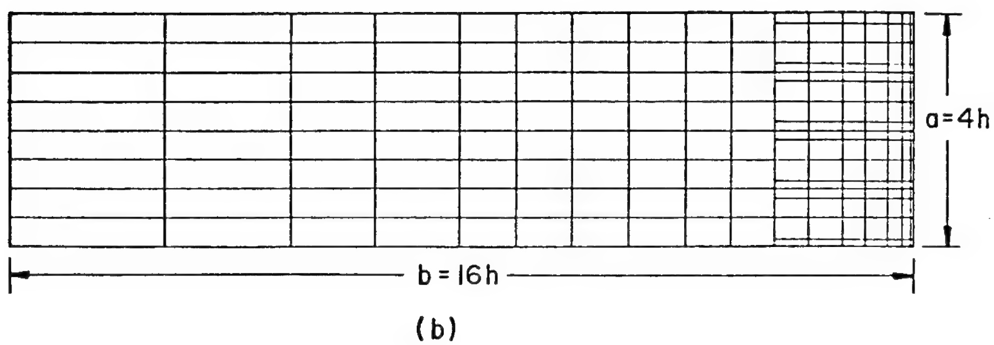

Figure 3 (a) Geometry of Symmetric Laminate
(b) Finite Element Gridwork (226 Nodes)

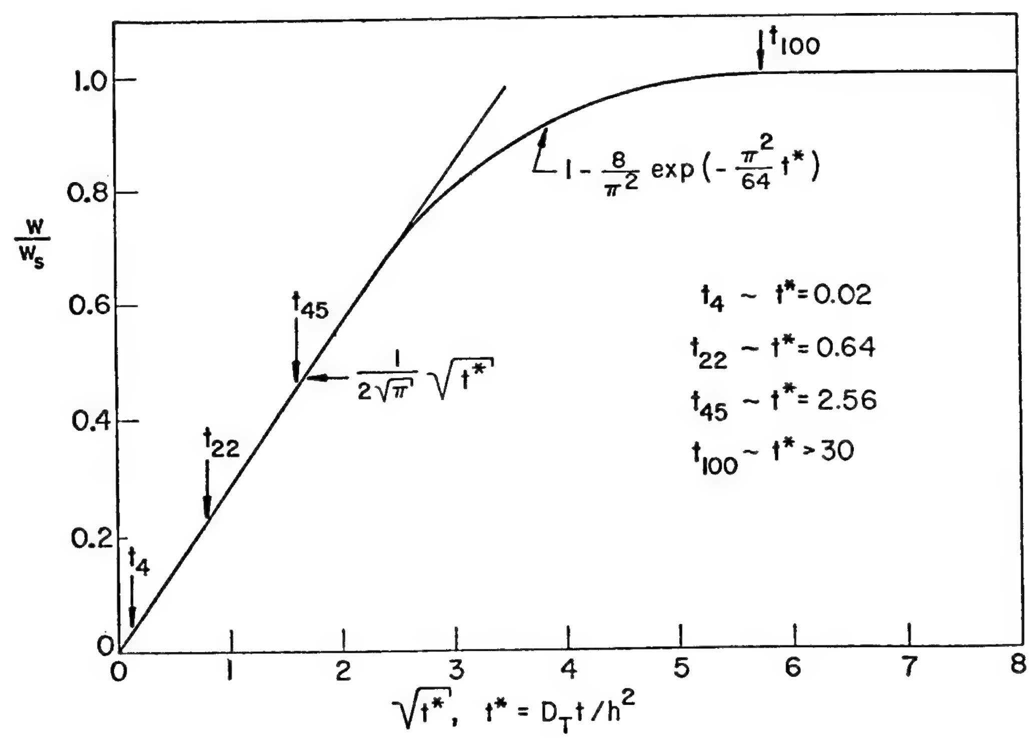

Figure 4 Normalized Moisture Content vs. Absorption Time

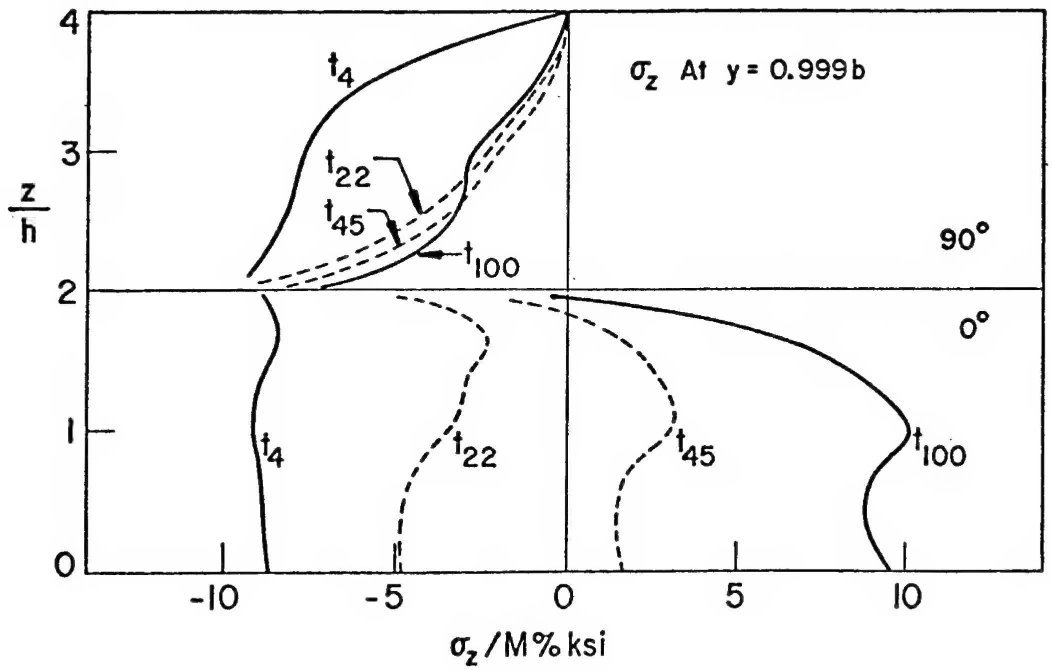

Figure 5 Through Thickness Distribution of σ_z Near The Free Edge of a $(90/0)_s$ Laminate At Various Absorption Times

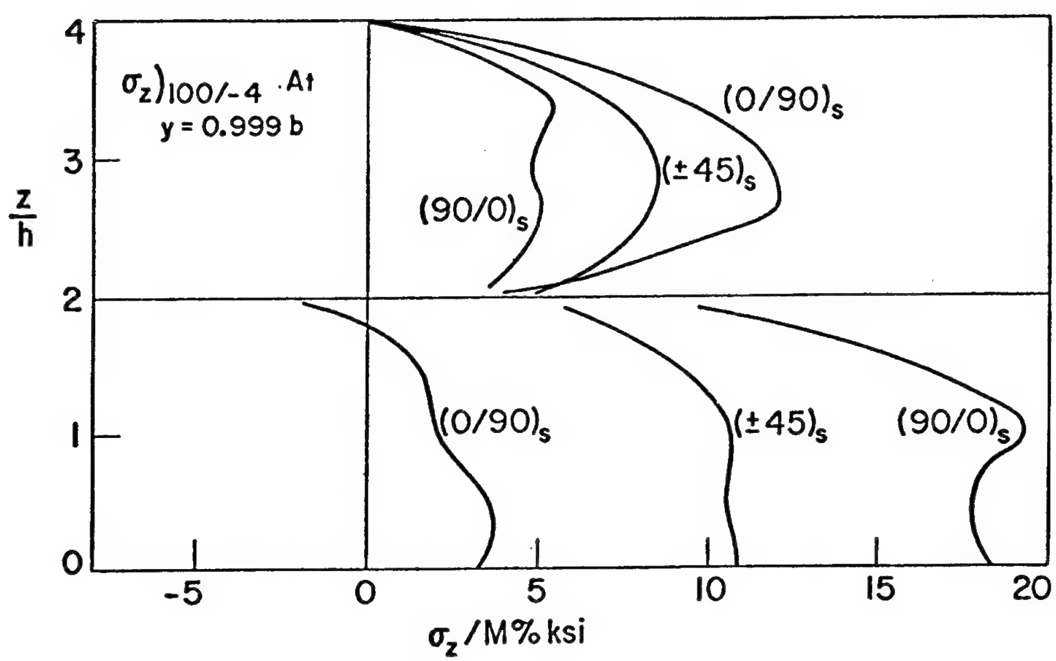

Figure 6 Through Thickness Distribution of σ_z Near the Free Edge of $(0/90)_s$, $(90/0)_s$ and $(\pm 45)_s$ Laminates After Short Time Desorption Following Full Saturation

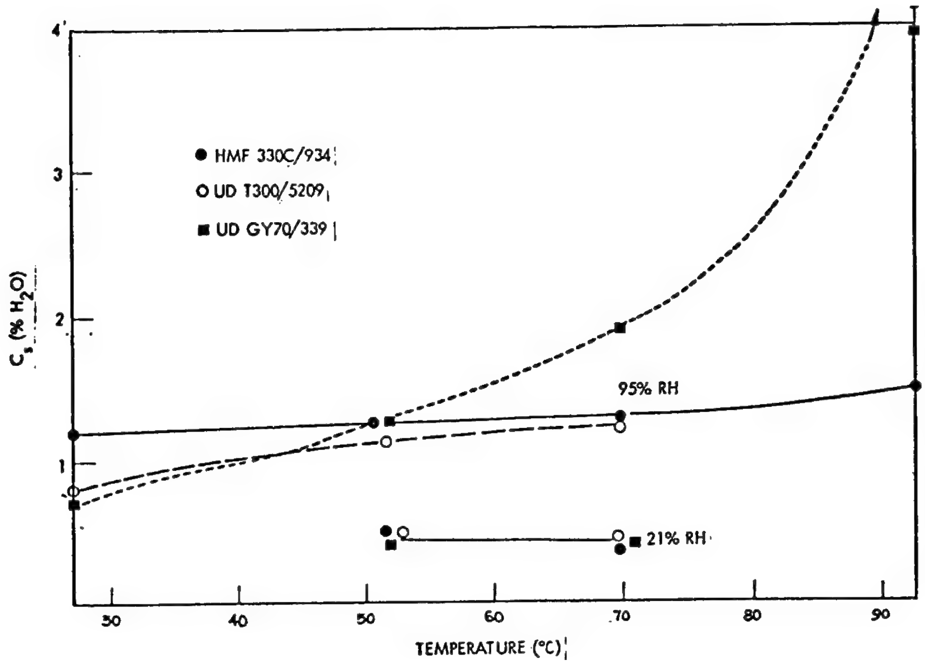

Figure 7 Equilibrium Absorbed Moisture Content C_s vs. Exposure Temperature and Humidity

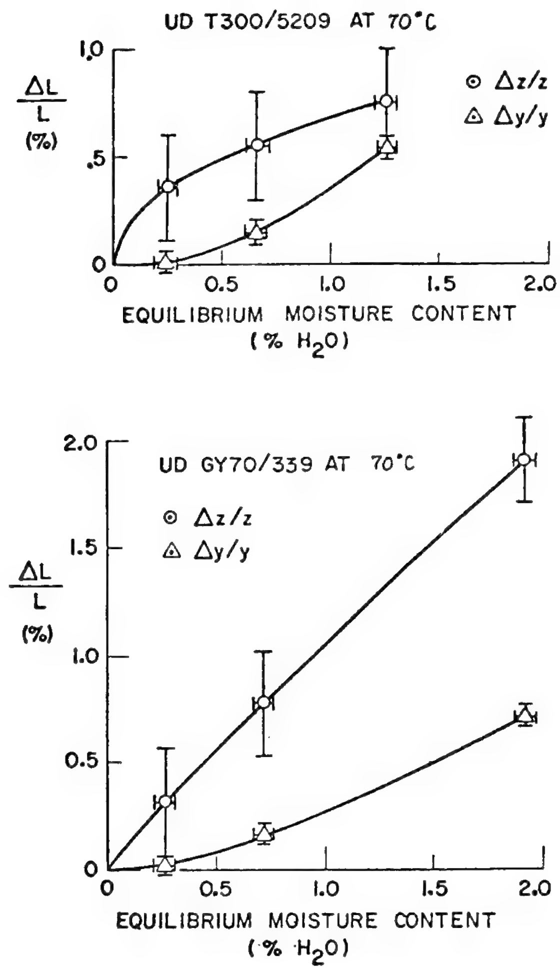

Figure 8 Dimensional Changes in Unidirectional T300/5209 and GY70/339 Brought to Equilibrium Moisture Contents at 70°C

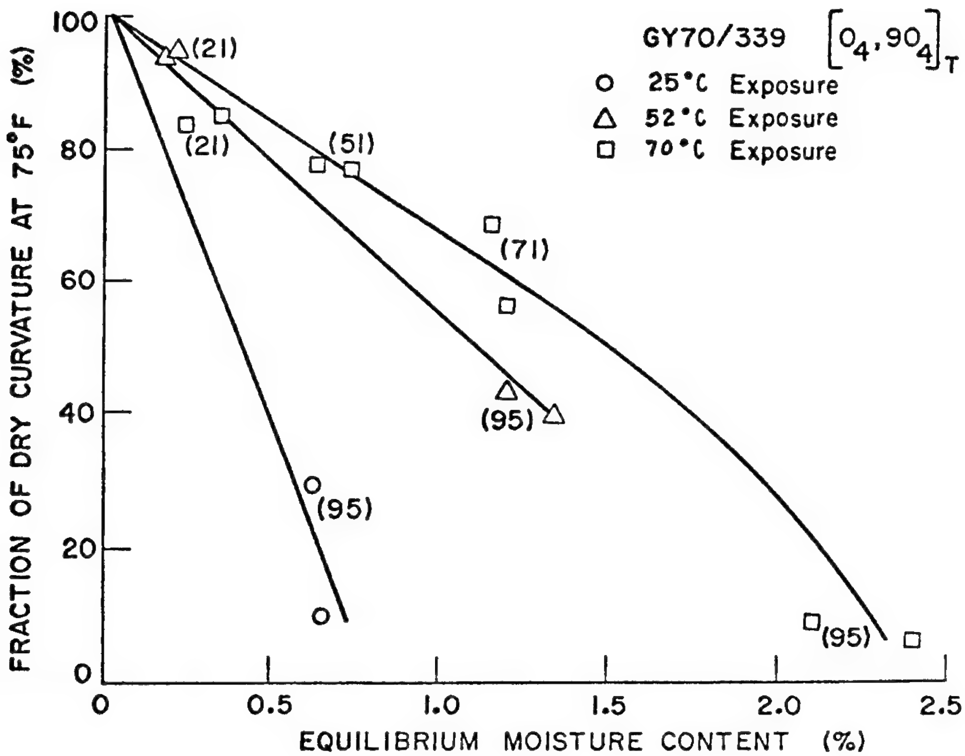

Figure 9 Moisture Induced Alteration of Internal Stresses in Non-symmetric Crossplied Laminates Exposed to Equilibrium Moisture Contents At Constant Temperature-Humidity. Relative Humidity of Exposure Given in Parentheses

VISCOELASTIC ANALYSIS

$$\bar{\sigma}(t) = \int_{0^+}^{t} \tilde{Q}(t-\tau)\, \dot{\bar{\varepsilon}}(\tau)\, d\tau$$

Integrating by parts and using $\bar{\varepsilon}(0^-) = \bar{0}$ gives

$$\bar{\sigma}(t) = \tilde{Q}(0)\, \bar{\varepsilon}(t) + \int_{0^+}^{t} \dot{\tilde{Q}}(t-\tau)\, \bar{\varepsilon}(\tau)\, d\tau$$

Choosing an exponental series to describe the relaxation functions

$$\tilde{Q}(t) = \tilde{Q}(o) - \sum_{\ell=1}^{L} \tilde{F}_\ell \,(1-\exp(-\lambda_\ell t))$$

Then the convolution integral is simplified to the degenerate form.

$$\bar{\sigma}(t) = \tilde{Q}(o)\, \bar{\varepsilon}(t) - \sum_{\ell=1}^{L} \lambda_\ell \tilde{F}_\ell \exp(-\lambda_\ell t) \int_{0^+}^{t} \exp(\lambda_\ell \tau)\bar{\varepsilon}(t)d\tau$$

The integral is now easily updated at each time step and does not involve integration over the entire loading history at each time step.

TEMPERATURE AND MOISTURE ALTERED VISCOELASTICITY

$$\bar{\sigma}(t) = \tilde{Q}(0,T,M)\,\bar{\varepsilon}(t) + \int_{0^+}^{t} \dot{\tilde{Q}}(\zeta-\zeta',T,M)\,\bar{\varepsilon}(\tau)\,d\tau$$

where

$$\zeta = \int_0^t \frac{d\xi}{a(T,M)} \qquad \zeta' = \int_0^t \frac{d\xi}{a(T,M)}$$

ζ is the reduced or modified time

$a(T,M)$ is the time-temperature-moisture horizontal shift function

$\tilde{Q}(0,T,M)$ defines the vertical shift in relaxation functions.

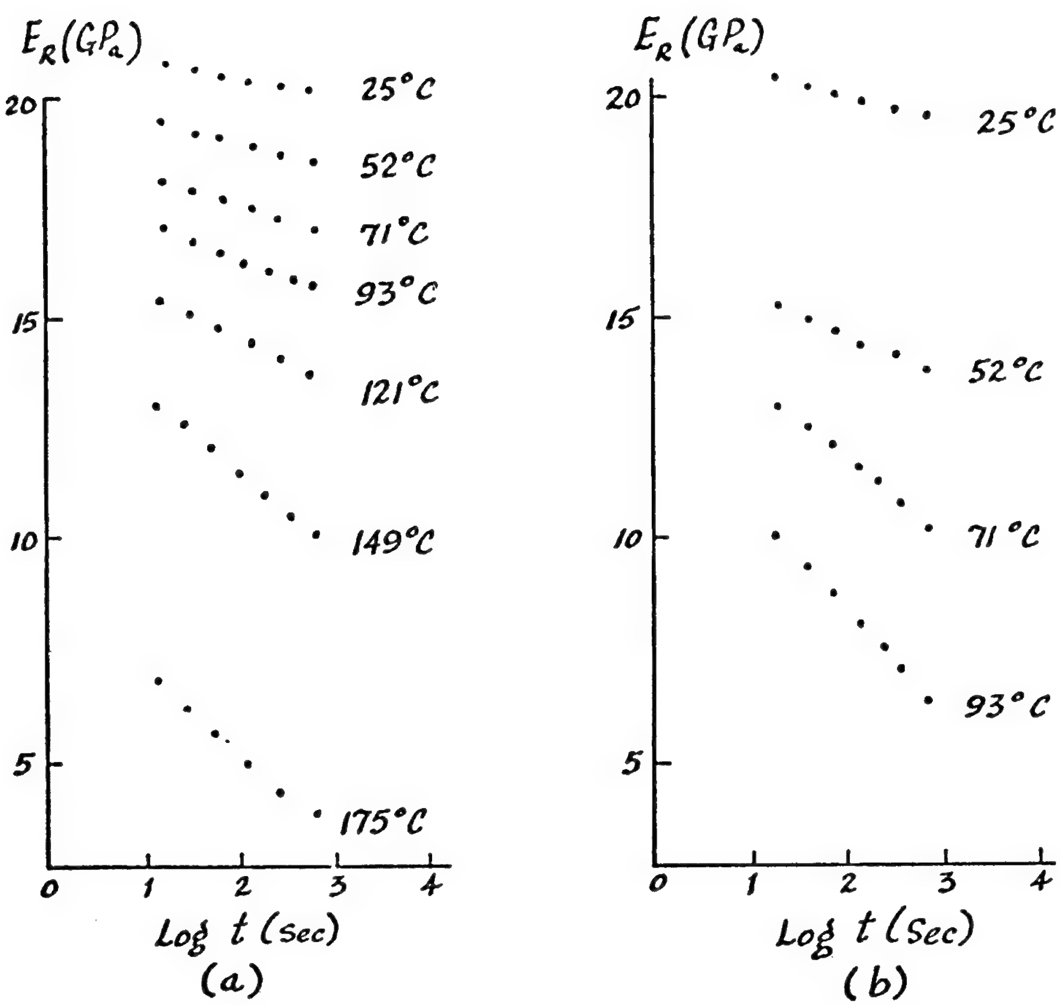

Figure 10 Relaxation Modulus of $(\pm 45)_s$ HMF330C/934 Laminates at Moisture Contents of (a) .14 percent, (b) 1.40 percent

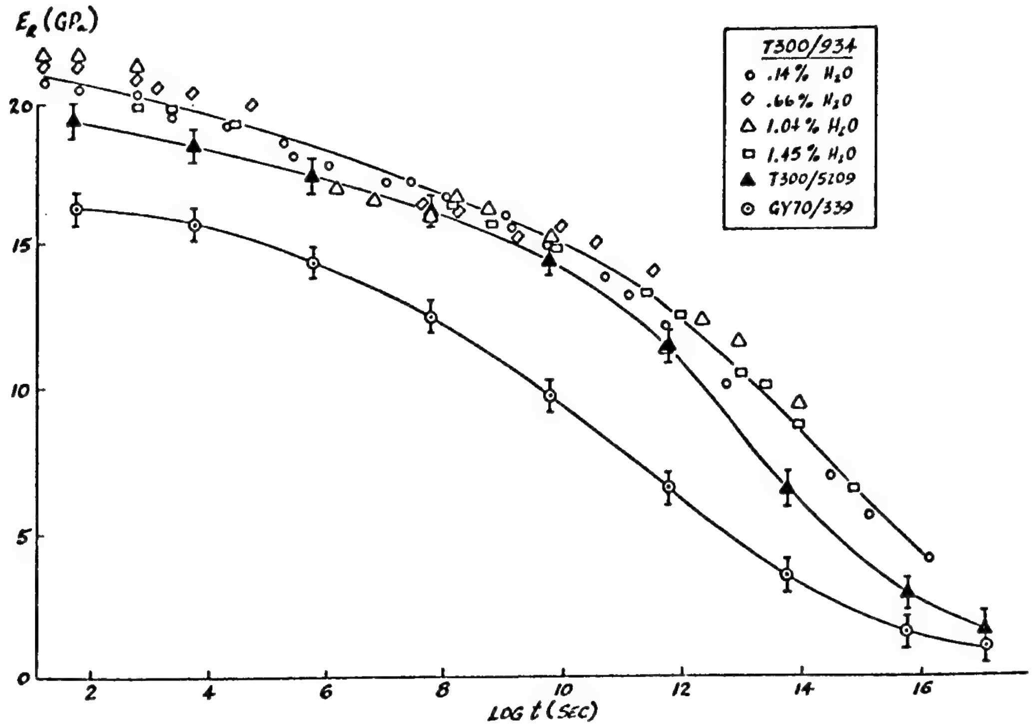

Figure 11 Master Relaxation Modulus vs. Time Obtained by Horizontal Shifting of Short-Time Relaxation Data Obtained at Several Temperatures and Moisture Contents

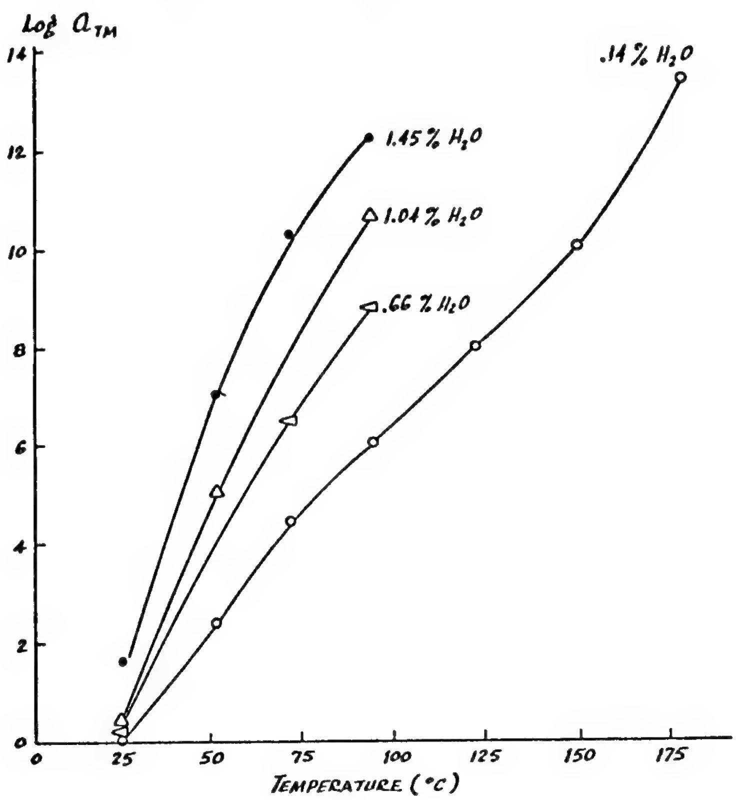

Figure 12 Time-Temperature/Moisture Shift Factor for HMF330C/934

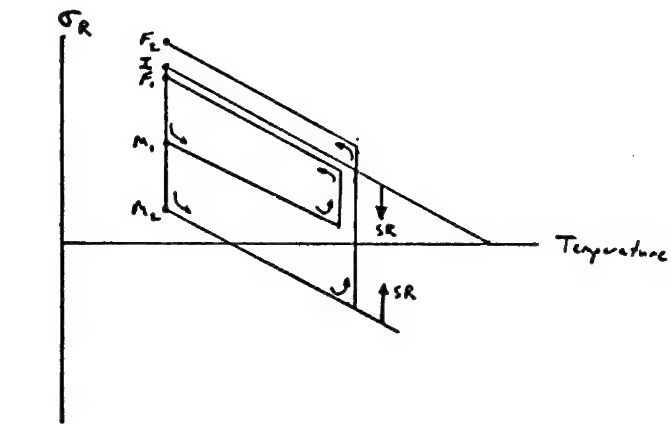

Figure 13 Alteration of Residual Stresses Under Hygrothermal Cycling

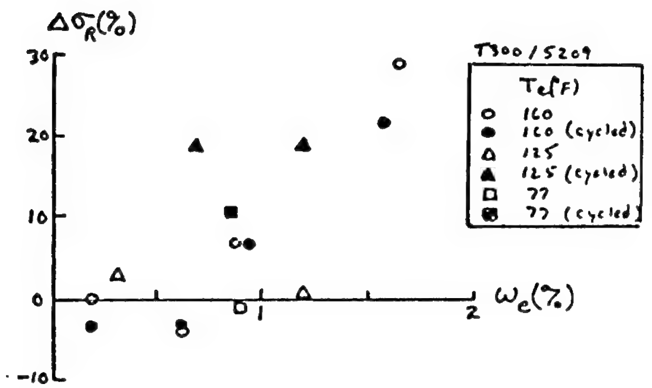

Figure 14 Altered Residual Stresses in Dry GY70/339 and T300/5209 $(0_4,90_4)_T$ Laminates After Hygrothermal Cycling. Specimens Previously Exposed to Equilibrium Moisture Content We at Three Temperatures (See Legend). Some Specimens Then Cycled 10 Times From 77 to 160°F. All Specimens Then Dried at 125°F.

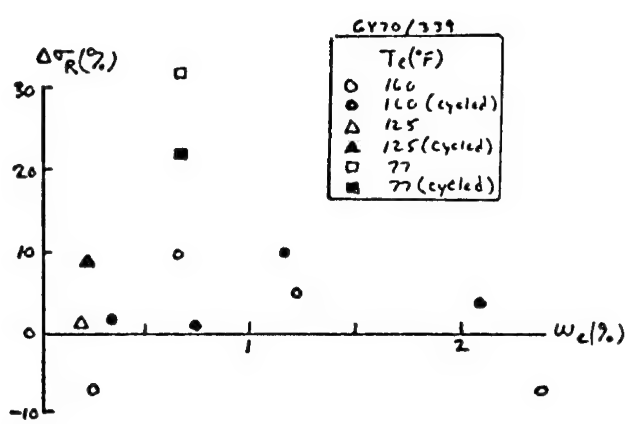

SPECTRUM LOAD/ENVIRONMENT INTERACTION EFFECTS IN ADVANCED FIBER REINFORCED LAMINATE

PROGRAM INITIATION APRIL 1, 1977

Edward M. Wu

Lawrence Livermore Laboratory
Fiber Composites and Mechanics

PROGRAM GUIDELINE AND MILESTONES

- Laminate time-dependent strength from lamina behavior

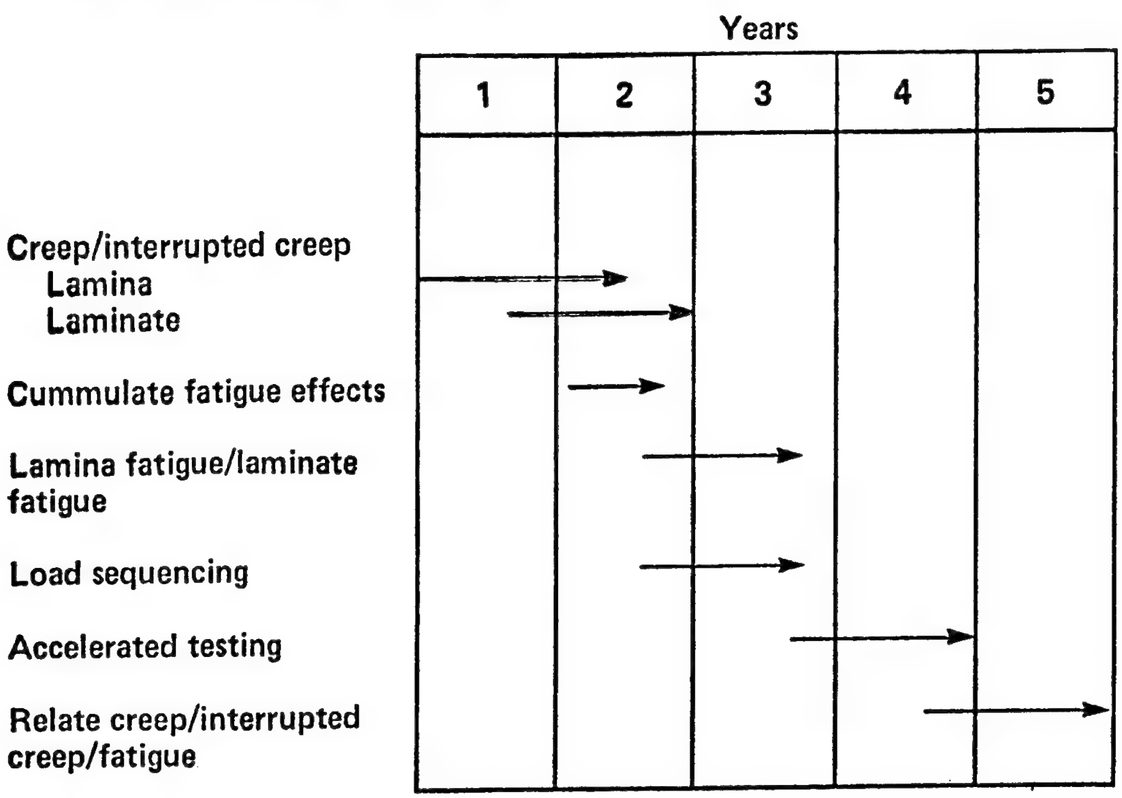

Deformation and strength under time-varying load histories and environment

Data generation:

- Service spectrum AFFDL (Sendeckyj)
- Creep/interrupted creep LLL (Wu)

Theory development: AFFDL/LLL

PROGRAM SCOPE

I. Environmental effects on creep rupture
   a) σ_L + , –
   b) σ_T + , –
   c) σ_S

II. Environment effects on fatigue (lamina, laminate)
   cummulative effects of
   a) Time at load
   b) Time at rest
   c) Rise and fall time

III. Spectrum load/environment effects
   Matrix dominated laminates
   Fiber dominated laminates

PROGRAM SPECIFICS

- Load-deformation constitutive relations
- Damage parameter identification
- Comprehensive instrumentation
- Adequate data base

LOAD-DEFORMATION RELATION

$$\epsilon = \frac{1}{E}\sigma \qquad \text{Static}$$

$$\epsilon(t) = \int_{t_o}^{t} J(t-\tau)\frac{d\sigma}{dt}\,dt \qquad \text{Time dependent}$$

Need to
- Record $\epsilon(t)$, $\sigma(t)$
- Establish limit of linearity
- Quantitatively determine $J(t)$, E^*

DAMAGE PARAMETER IDENTIFICATION

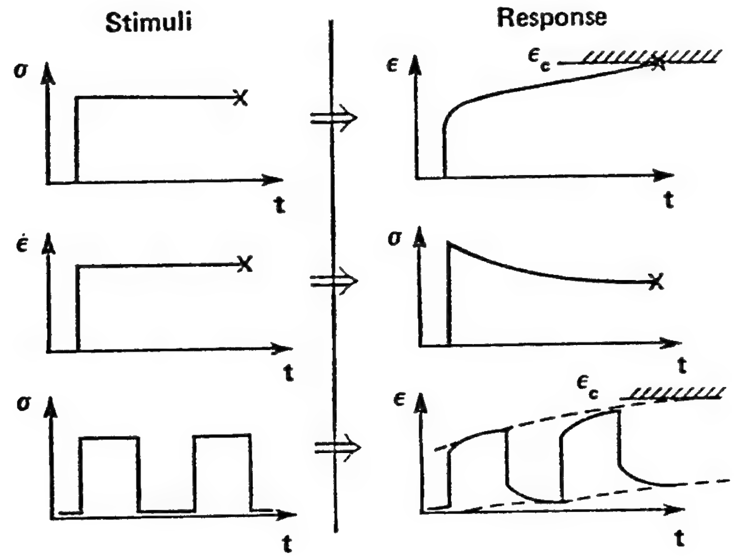

Objective: Estimation of long-term performance (life)

Operations:
- Damage parameter identification
- Sensitivity consideration

SENSITIVE DAMAGE PARAMETER ESSENTIAL FOR LIFE-ESTIMATE

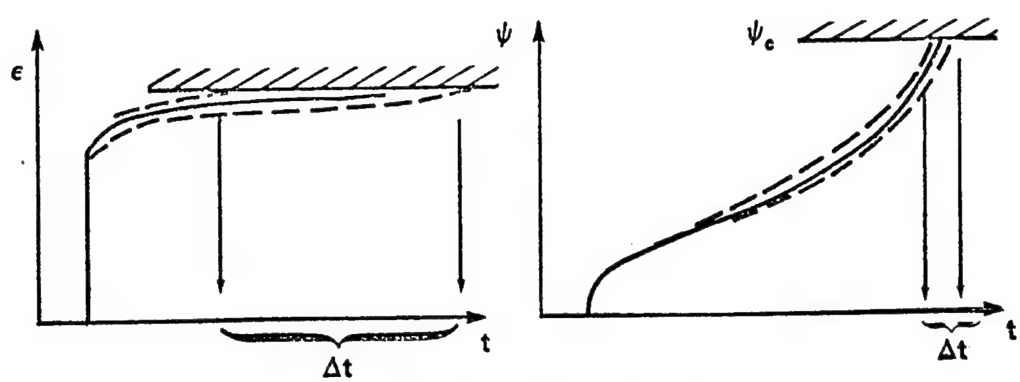

Damage function $\psi\ (\sigma(t), \epsilon(t), t, \theta)$

$$\psi = \int_{t_0}^{t} f(\sigma, \epsilon, t, \theta)\ dt$$

Need comprehensive instrumentation

DEFORMATION AND STRENGTH UNDER TIME-VARYING HISTORY

- Comprehensive instrumentation

$\epsilon_T = \epsilon_L + \epsilon_{NL}$ Input stimuli: stress

$\sigma_T = \sigma_L + \sigma_{NL}$ Input stimuli: strain

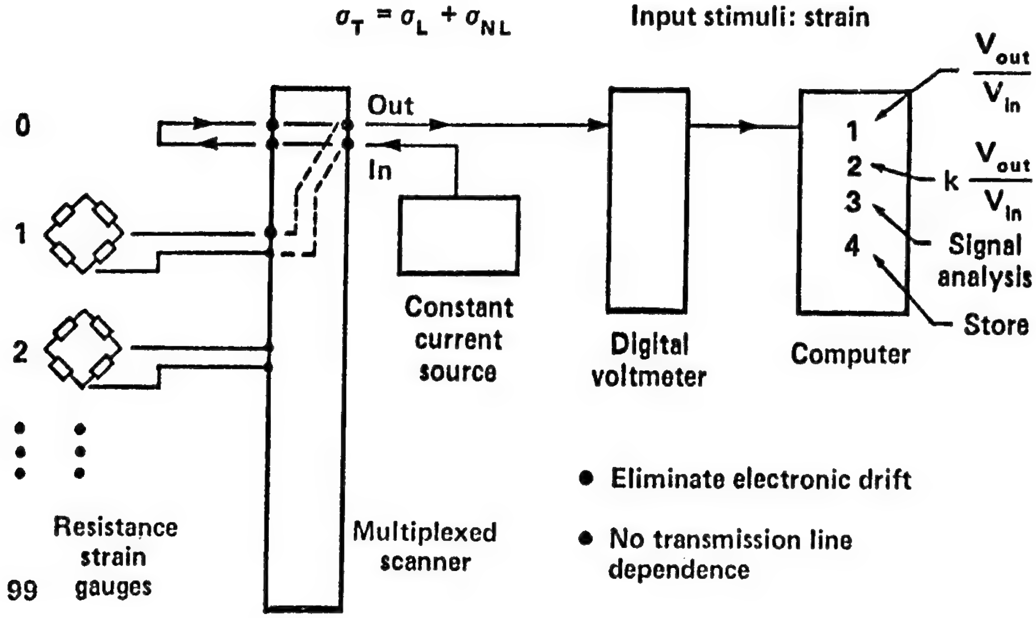

- Eliminate electronic drift
- No transmission line dependence

MECHANICAL TESTING

- Creep/interrupted creep

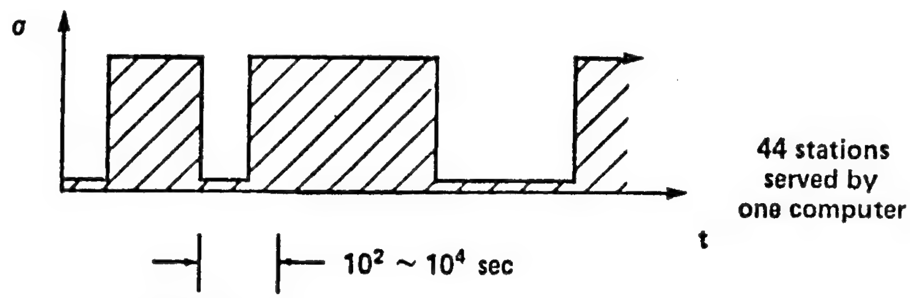

(i) Cummulative damage
(ii) History effect

- Servo-hydraulic machines

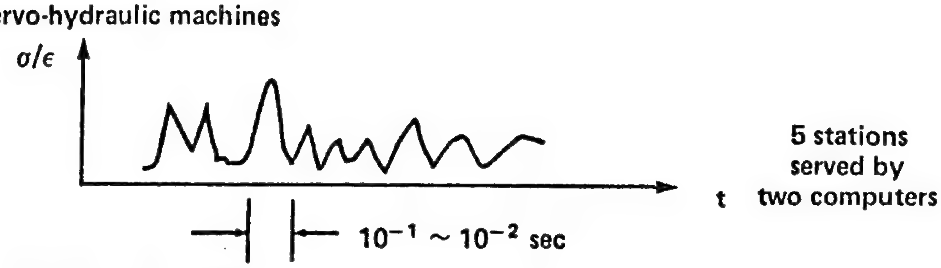

(i) Frequency effect

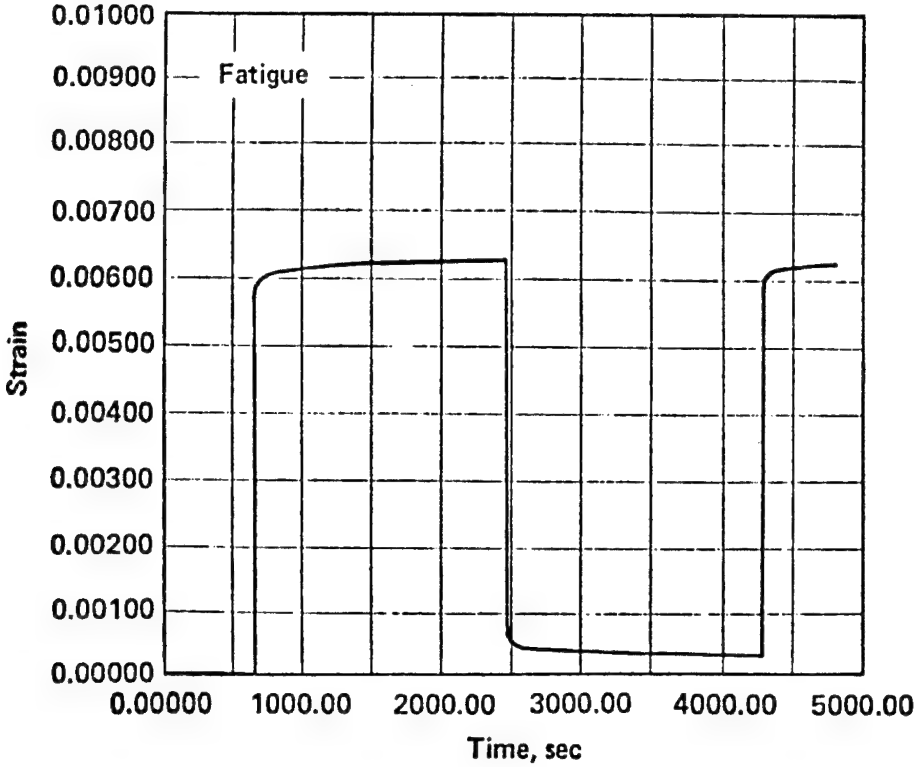
Fatigue
Strain
0.01000
0.00900
0.00800
0.00700
0.00600
0.00500
0.00400
0.00300
0.00200
0.00100
0.00000
0.00000
1000.00
2000.00
3000.00
4000.00
5000.00
Time, sec

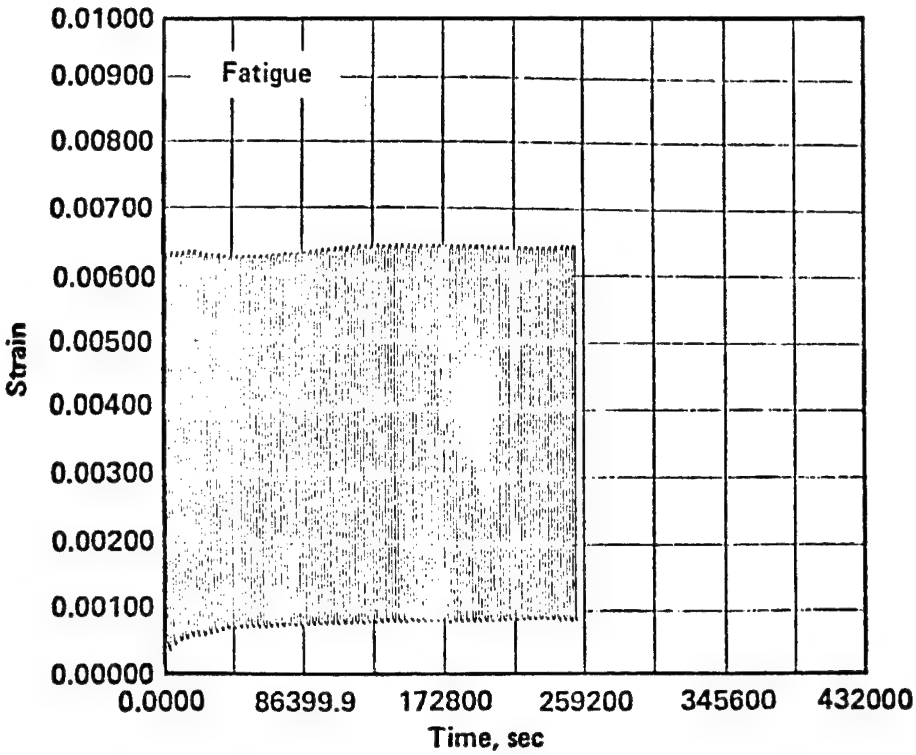
Fatigue
Strain
0.01000
0.00900
0.00800
0.00700
0.00600
0.00500
0.00400
0.00300
0.00200
0.00100
0.00000
0.0000
86399.9
172800
259200
345600
432000
Time, sec

WEAR OF MATERIALS UNDER REPEATED NORMAL AND SLIDING IMPACT

S. L. RICE
UNIVERSITY OF CONNECTICUT

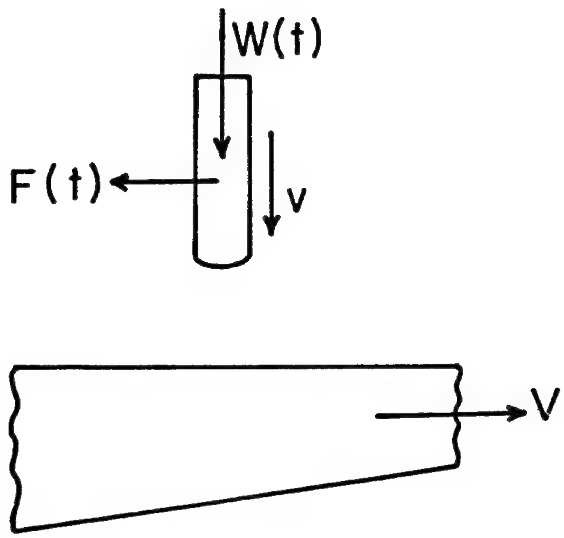

IMPACT
WEAR

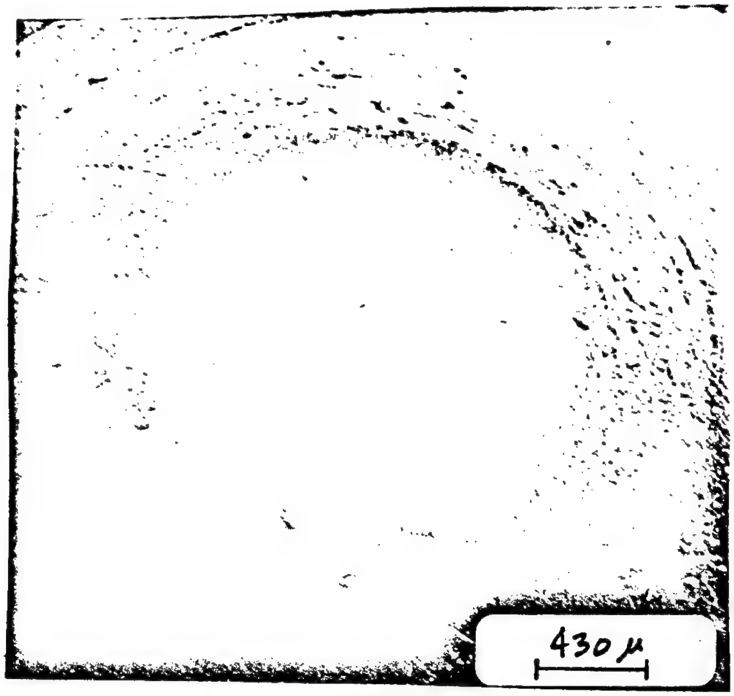
430 μ

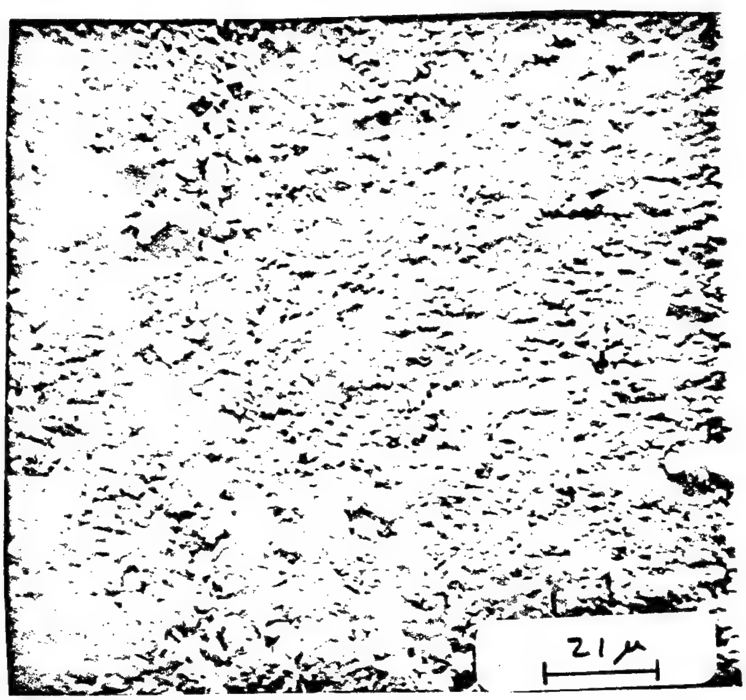
21 μ

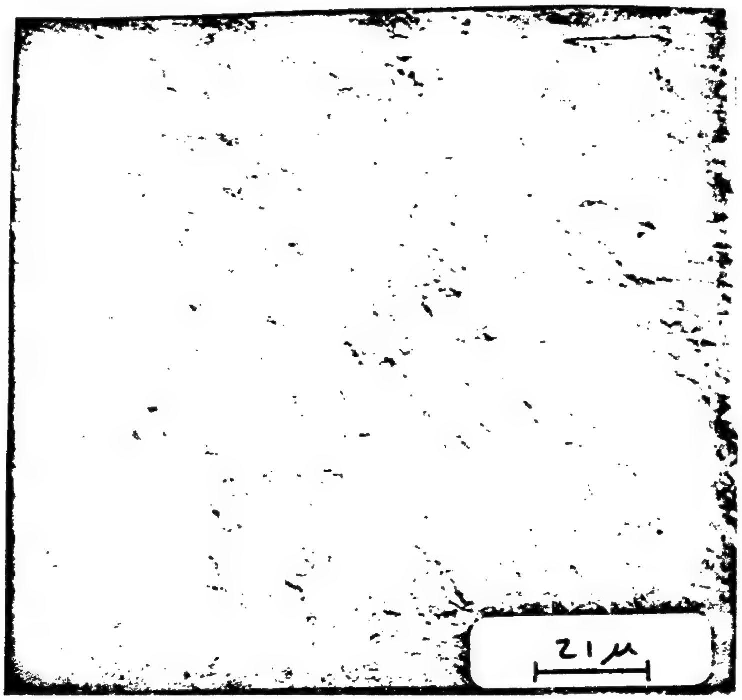
21μ


15μ


11 μ

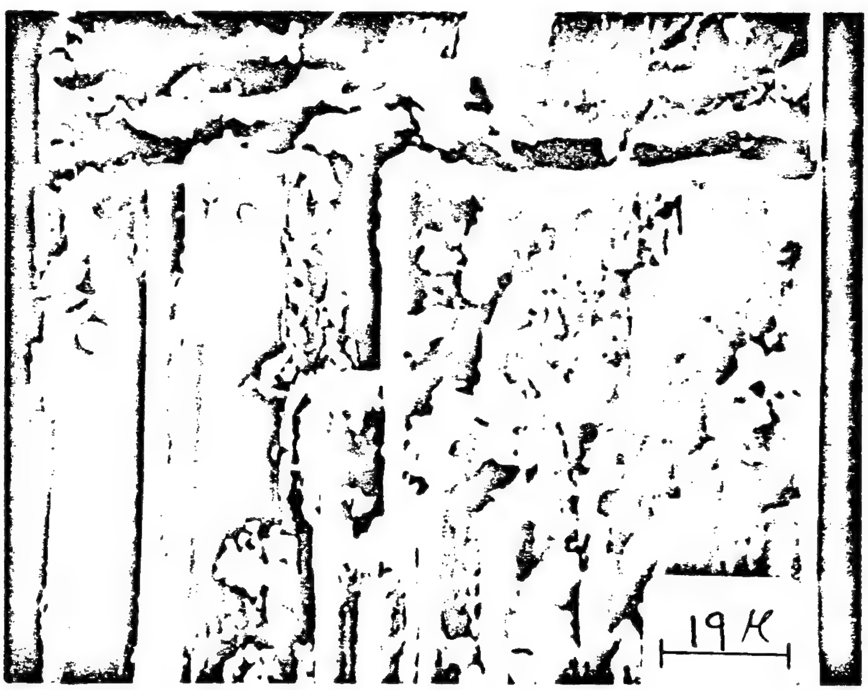
19 μ

EVALUATION OF THE EMBEDDED SPAR

COMPOSITE DESIGN CONCEPT

J.W. Gillespie, Jr.

R. B. Pipes

University of Delaware

Center for Composite Materials

AFFDL/University Design

Program

OBJECTIVES

- DEVELOP DESIGN INFORMATION FOR ADVANCED COMPOSITE STRUCTURAL CONCEPTS FOR CURRENT AND FUTURE AIR FORCE SYSTEM
- FOSTER ACTIVITIES IN THE UNIVERSITY COMMUNITY DIRECTED AT THE DEVELOPMENT OF STRUCTURES DESIGN EXPERTISE IN ADVANCED COMPOSITES
- CONTRIBUTE TO THE DEVELOPMENT OF DESIGNERS TRAINED IN ADVANCED COMPOSITES IN ORDER TO FULFILL FUTURE AIR FORCE SYSTEMS DEVELOPMENT REQUIREMENTS

APPROACH

- DESIGN CONCEPT STUDY
  - PRELIMINARY DESIGN
  - DETAILED DESIGN
- INDUSTRIAL CONSULTATION
  - STUDENT / DESIGNER CONTACT
  - DIRECTION
  - CRITICISM
- CONCEPT FABRICATION
  - HANDS ON EXPERIENCE
  - DESIGN / FABRICATION INTERACTION
- CONCEPT TESTS
  - ACTUAL STRUCTURE/PAPER DESIGN
  - FAILURE MODE
  - DESIGN/ACTUAL STRENGTH
- DOCUMENTATION
  - AIR FORCE REPORT
  - MASTER'S THESIS

DESIGN CONCEPT

- WING SKIN SPAR ATTACHMENTS
- F-14, F-15, AND F-16 EMPENNAGE STRUCTURE
- EMBEDDED SPAR CONCEPT
  - NO BONDING / FATIGUE
  - NO BOLTING / STRESS CONCENTRATIONS
- COST SAVING
- RISK / EXPERIENCE BASE

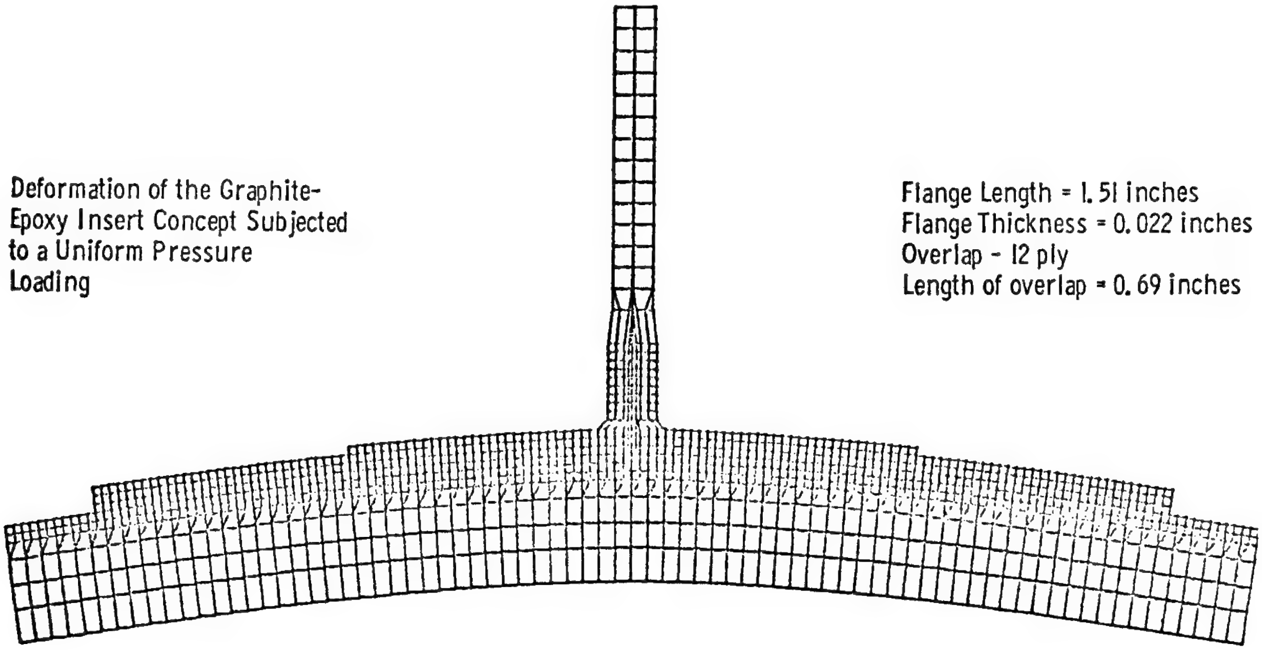

Material Properties for Finite Element Model

	Adhesive	Titanium	Unidirectional Graphite-Epoxy
Ey (Msi)	0.5	16.0	19.9
Ez (Msi)	0.5	16.0	1.4
Ex (Msi)	0.5	16.0	1.4
νzy	0.3	0.34	0.015
νxy	0.3	0.34	0.015
νxz	0.3	0.34	0.300
Gyz (Msi)	0.6	6.0	0.6
αy $(10^{-6}/^{o}F)$	20.0	4.9	- .21
αz $(10^{-6}/^{o}F)$	20.0	4.9	20.0
αx $(10^{-6}/^{o}F)$	20.0	4.9	16.0

Material Properties for Finite Element Model

Wingskin 1

	Mtl. 1 $(0/\pm45/0)_4$	Mtl. 2 $(\pm45)_2(0/\pm45/0)_2$	Mtl. 4 $(\pm45)_4$	Mtl. 7 $(\pm45)_4$	Mtl. 6 $(0/\pm45/0)$
Ey (Msi)	3.3	3.2	2.3	1.4	2.7
Ez (Msi)	1.4	1.4	1.4	2.3	1.4
Ex (Msi)	11.3	6.7	2.3	2.3	11.2
νzy	0.092	0.080	0.034	0.057	0.125
νxy	0.681	0.741	0.788	0.057	0.591
νxz	0.085	0.072	0.057	0.788	0.0850
Gyz (Msi)	0.6	0.6	0.6	0.6	0.6
αy $(10^{-6}/^{o}F)$	4.8	3.7	1.04	20.00	6.59
αz $(10^{-6}/^{o}F)$	20.0	20.00	20.00	1.04	20.00
αx $(10^{-6}/^{o}F)$	- 0.49	- 0.24	1.04	1.04	- 0.29

Material Properties for Finite Element Model

Wingskin 2

	Mtl. 2 $(\pm45/90_2)(0/\pm45/0)_3$	Mtl. 1 $(0/\pm45/0)_2$	Mtl. 6 $(0/\pm45/0)$	Mtl. 10 $(\pm45/90_2)$	Mtl. 4 $(\pm45)_4$	Mtl. 7 $(\pm45)_4$
Ey (Msi)	4.5	3.2	2.7	5.8	2.3	1.4
Ez (Msi)	1.4	1.4	1.4	1.4	1.4	2.3
Ex (Msi)	8.7	11.3	11.2	2.0	2.3	2.3
νzy	0.064	0.093	0.125	0.02	0.034	0.057
νxy	0.438	0.677	0.591	0.235	0.788	0.057
νxz	0.154	0.085	0.085	0.215	0.057	0.788
Gyz (Msi)	0.6	0.6	0.6	0.6	0.6	0.6
αy $(10^{-6}/^{o}F)$	3.1	4.9	6.6	0.19	1.04	20.0
αz $(10^{-6}/^{o}F)$	20.0	20.0	20.0	20.0	20.0	1.04
αx $(10^{-6}/^{o}F)$	- .11	- .48	- .29	8.06	1.04	1.04

Strength Allowables

	X_1^T (Ksi)	X_1^C (Ksi)	X_2^T (Ksi)	X_2^C (Ksi)	X_3^T (Ksi)	X_3^C (Ksi)	S_6 (Ksi)	S_4 (Ksi)
Unidirectional AS-3501-6 Graphite-Epoxy	180	180	8	30	8	30	12	12
±45 Graphite-Epoxy Laminates	22	22	22	22	8	30	12	12
0/±45/0 Graphite-Epoxy Laminates	102	102	20	38	8	30	12	12
$\pm 45/90_2$ Graphite-Epoxy Laminates	20	38	102	102	8	30	12	12

Ultimate Adhesive Shear Strength $F^{SU}_{Adhesive}$ = 4 Ksi

Comparison of Stress Levels for the No-Insert Concept* for Wingskin's 1 and 2

Position	Wingskin 1			Wingskin 2		
	$\frac{\sigma_3}{P}$	$\frac{\sigma_2}{P}$	$\frac{\sigma_{23}}{P}$	$\frac{\sigma_3}{P}$	$\frac{\sigma_2}{P}$	$\frac{\sigma_{23}}{P}$
Second row from top of wingskin in Material 6 at center of wingskin	22.9	120.6	0.5	23.4	101.6	4.4
First row from top of wingskin at center of wingskin (Wingskin 1 -Material 6, Wingskin 2-Material 10)	23.1	171.8	3.4	25.0	285.9	2.1
Adjacent to Web in Material 4 (First row of overlap)	32.6	124.8	1.4	32.7	104.0	1.5
Adjacent to Web in Material 4 (Second row of overlap)	42.3	149.9	12.7	39.9	125.2	13.1
Adjacent to Web in Material 7 (Second row of overlap)	110.3	26.6	2.8	94.8	29.3	2.6

*12 ply overlap
Length of overlap = .69 inches

Comparison of Stress Levels for the No-Insert Concept for Wingskin's 1 and 2

Position	Wingskin 1 $\frac{\sigma_3}{P}$	Wingskin 1 $\frac{\sigma_2}{P}$	Wingskin 1 $\frac{\sigma_{23}}{P}$	Wingskin 2 $\frac{\sigma_3}{P}$	Wingskin 2 $\frac{\sigma_2}{P}$	Wingskin 2 $\frac{\sigma_{23}}{P}$
Adjacent to Web in Material 4 (Third row of overlap)	43.7	206.5	33.4	175.4	41.3	30.8
Adjacent to Web in Material 7 (Third row of overlap)	103.9	22.9	10.4	90.2	26.9	9.0

Thermal Stresses in the Embedded Spar Concepts

Position	No Insert $\frac{\sigma_3}{\Delta T}$	No Insert $\frac{\sigma_2}{\Delta T}$ $[\frac{psi}{^oF}]$	No Insert $\frac{\sigma_{23}}{\Delta T}$	Titanium Insert $\frac{\sigma_3}{\Delta T}$	Titanium Insert $\frac{\sigma_2}{\Delta T}$ $[\frac{psi}{^oF}]$	Titanium Insert $\frac{\sigma_{23}}{\Delta T}$	Graphite-Epoxy Insert $\frac{\sigma_3}{\Delta T}$	Graphite-Epoxy Insert $\frac{\sigma_2}{\Delta T}$ $[\frac{psi}{^oF}]$	Graphite-Epoxy Insert $\frac{\sigma_{23}}{\Delta T}$
Center of Flange in Adhesive (Top)				3.4	11.5	4.3			
Adjacent to Web in Material 4 (First row of overlap)	0.7	-11.0	3.6	1.0	- 7.6	7.0	-0.6	2.3	2.5
Adjacent to Web in Adhesive (First row of overlap)				7.4	- 5.7	3.6			
Adjacent to Web in Material 4 (Second row of overlap)	3.5	- 0.4	5.0	4.7	1.5	6.6	2.2	9.1	3.4
Adjacent to Web in Material 7 (Second row of overlap)	-6.1	- 9.8	5.3	-4.4	-11.8	4.9	6.0	-13.8	3.1
Adjacent to Web in Adhesive (Second row of overlap)				9.2	2.1	2.8			

*Flange Thickness = .088 inches
Flange Length = 1.51 inches
12 Ply Overlap
Length of Overlap = .69 inches

Summary of Test Results

	Number of Specimens	Average Failure Load (lb/in)	Specific Failure Load (in^{-1})	Failure Mode
		Wingskin 1		
Titanium Flange Thickness (inches)				
0.036	1	598	6,308	Adhesive failure at center of flange on bottom surface
0.054	2	846	8,668	Adhesive failure at base of spar
		Wingskin 2		
0.00	5	767	9,411	Interlaminar failure at base of spar
0.036	5	817	8,618	Adhesive failure at center of flange on bottom surface
0.054	6	830	8,504	Adhesive failure at base of spar
0.078	7	1,116	10,679	Interlaminar-adhesive failure at base of spar
Graphite-Epoxy Flange Thickness (inches)				
0.088	2	861	9,685	Interlaminar Failure at base of spar

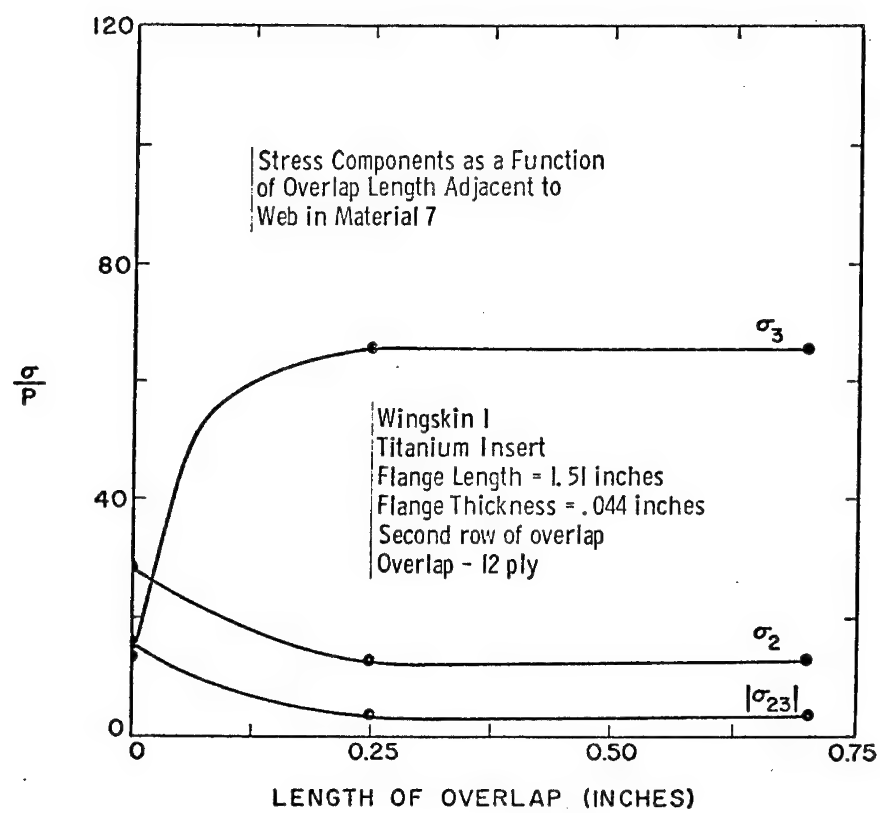

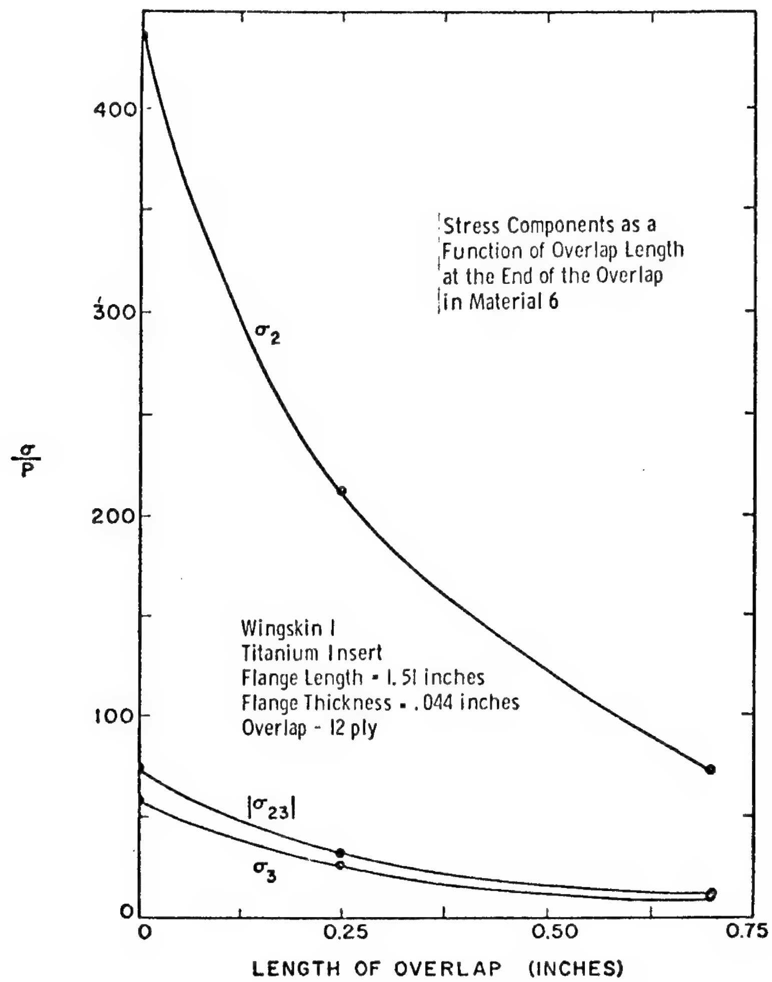

Stress Components as a Function of Overlap Length at the End of the Overlap in Material 6
Wingskin I
Titanium Insert
Flange Length = 1.51 inches
Flange Thickness = .044 inches
Overlap - 12 ply
σ_2
$|\sigma_{23}|$
σ_3
$\frac{\sigma}{P}$
0
100
200
300
400
0
0.25
0.50
0.75
LENGTH OF OVERLAP (INCHES)

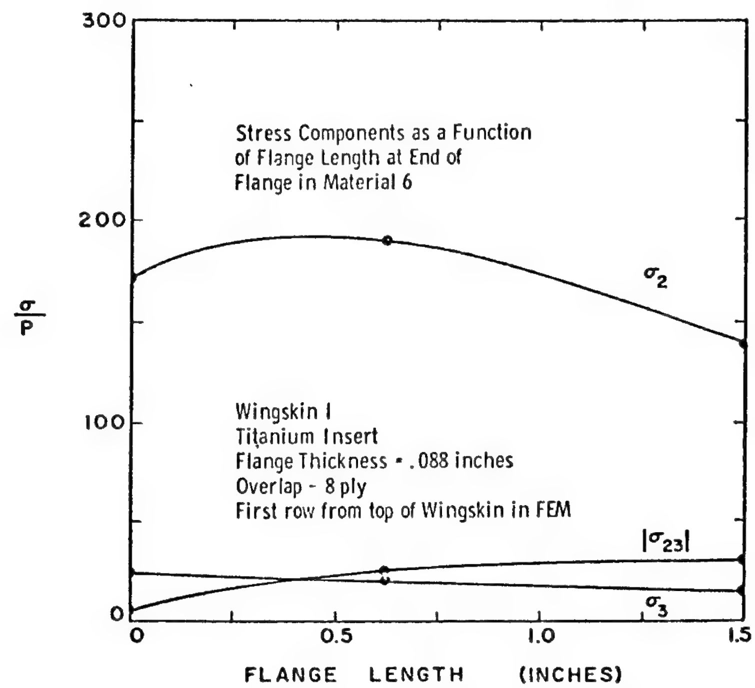

Stress Components as a Function of Flange Length at End of Flange in Material 6
Wingskin I
Titanium Insert
Flange Thickness = .088 inches
Overlap - 8 ply
First row from top of Wingskin in FEM
σ_2
$|\sigma_{23}|$
σ_3
$\frac{\sigma}{P}$
0
100
200
300
0
0.5
1.0
1.5
FLANGE LENGTH (INCHES)

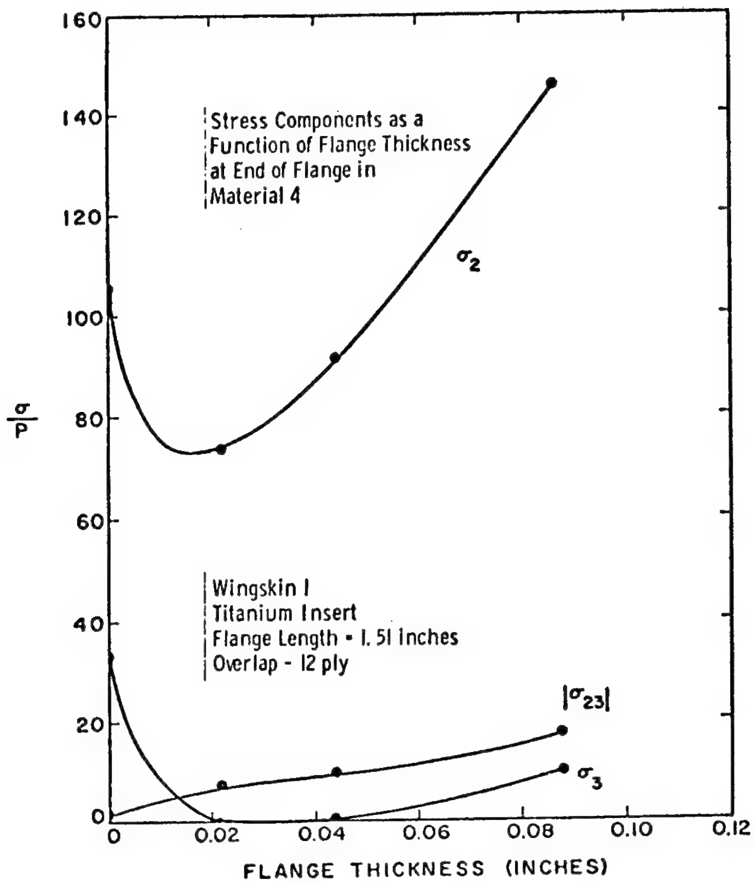
Stress Components as a
Function of Flange Thickness
at End of Flange in
Material 4
Wingskin I
Titanium Insert
Flange Length = 1.51 inches
Overlap - 12 ply
σ_2
$|\sigma_{23}|$
σ_3
$\frac{\sigma}{p}$
0
20
40
60
80
100
120
140
160
0
0.02
0.04
0.06
0.08
0.10
0.12
FLANGE THICKNESS (INCHES)

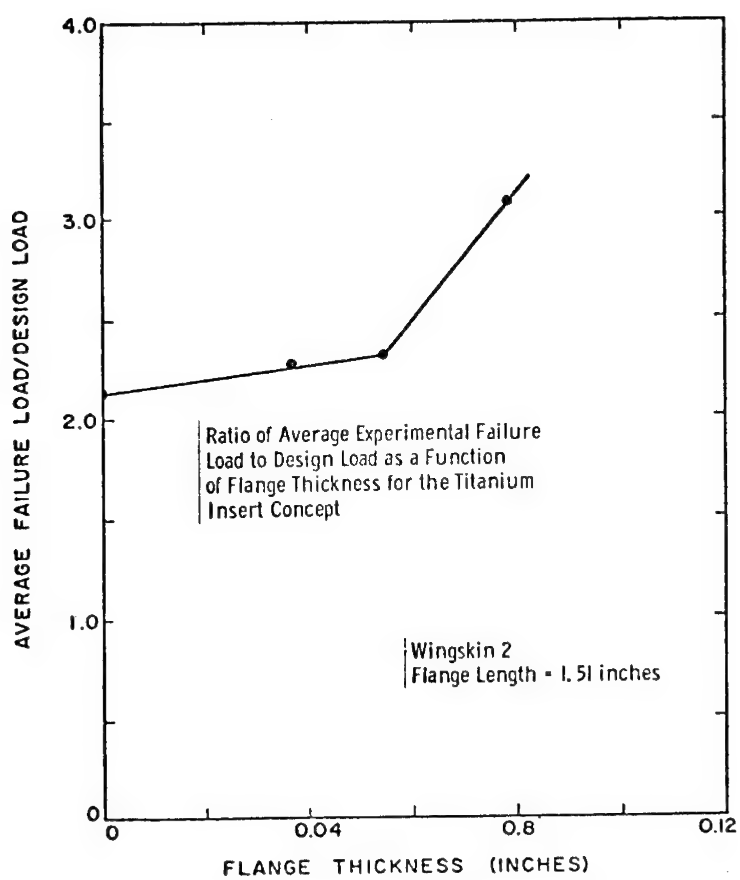
Ratio of Average Experimental Failure
Load to Design Load as a Function
of Flange Thickness for the Titanium
Insert Concept
Wingskin 2
Flange Length = 1.51 inches
AVERAGE FAILURE LOAD/DESIGN LOAD
0
1.0
2.0
3.0
4.0
0
0.04
0.8
0.12
FLANGE THICKNESS (INCHES)

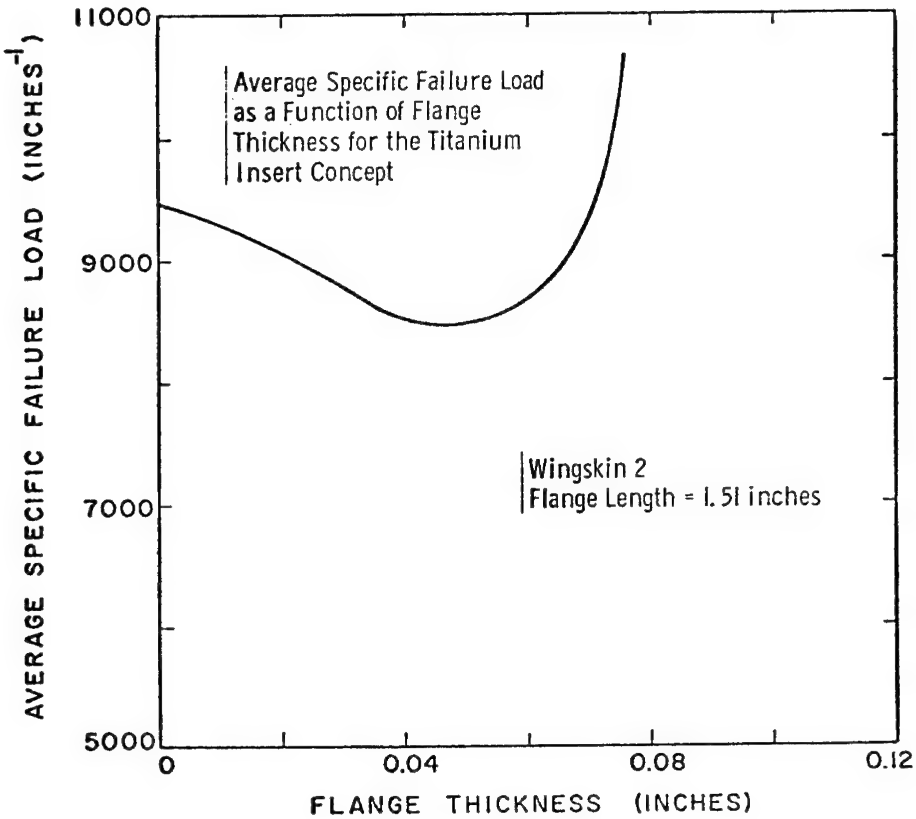
Average Specific Failure Load
as a Function of Flange
Thickness for the Titanium
Insert Concept
Wingskin 2
Flange Length = 1.51 inches
AVERAGE SPECIFIC FAILURE LOAD (INCHES^{-1})
11000
9000
7000
5000
0
0.04
0.08
0.12
FLANGE THICKNESS (INCHES)

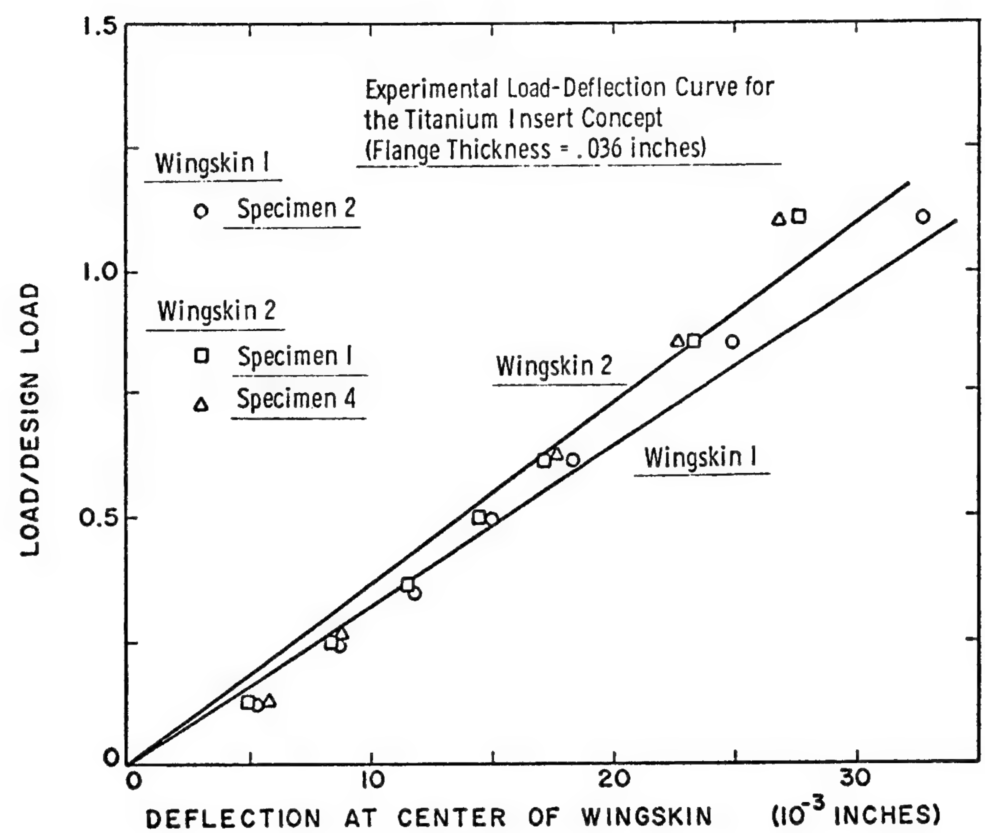
Experimental Load-Deflection Curve for
the Titanium Insert Concept
(Flange Thickness = .036 inches)
Wingskin 1
Specimen 2
Wingskin 2
Specimen 1
Specimen 4
Wingskin 2
Wingskin 1
LOAD/DESIGN LOAD
1.5
1.0
0.5
0
0
10
20
30
DEFLECTION AT CENTER OF WINGSKIN (10^{-3} INCHES)

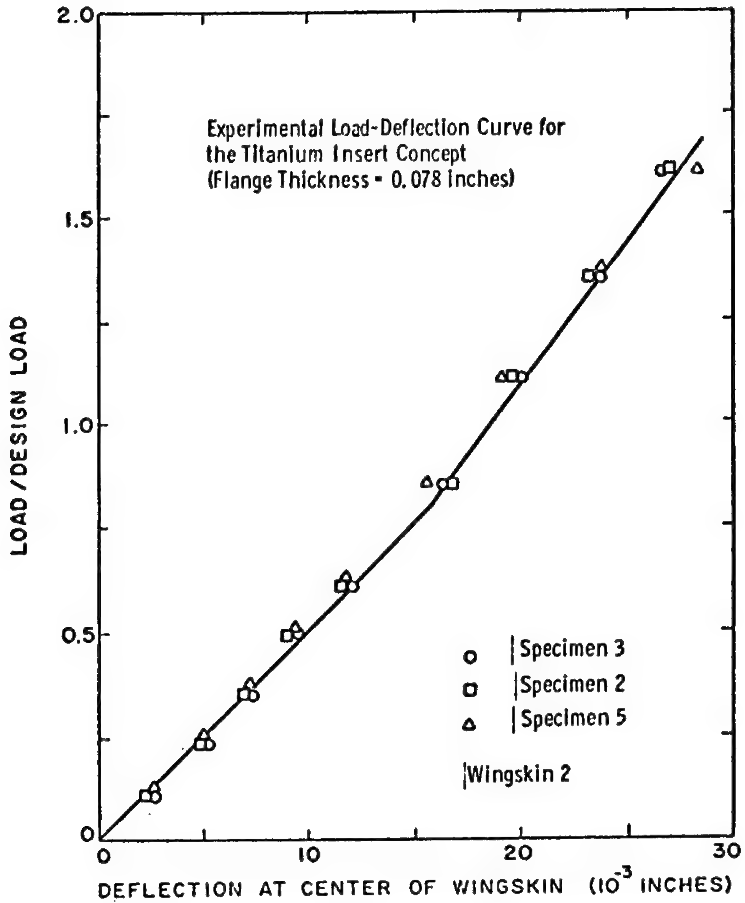

Experimental Load-Deflection Curve for
the Titanium Insert Concept
(Flange Thickness = 0.078 inches)
Specimen 3
Specimen 2
Specimen 5
Wingskin 2
LOAD/DESIGN LOAD
DEFLECTION AT CENTER OF WINGSKIN (10^{-3} INCHES)

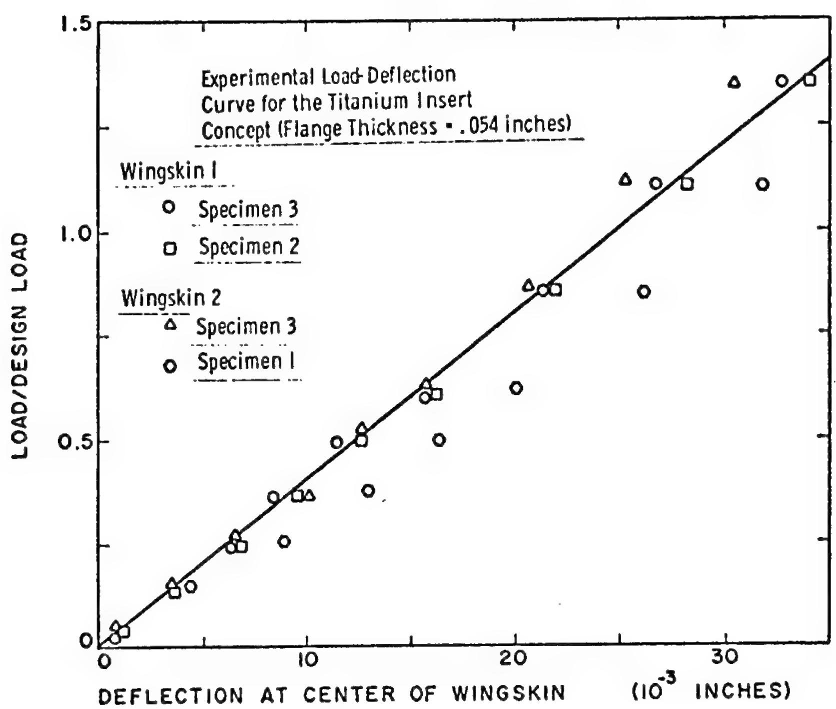

Experimental Load-Deflection
Curve for the Titanium Insert
Concept (Flange Thickness = .054 inches)
Wingskin 1
Specimen 3
Specimen 2
Wingskin 2
Specimen 3
Specimen 1
LOAD/DESIGN LOAD
DEFLECTION AT CENTER OF WINGSKIN (10^{-3} INCHES)

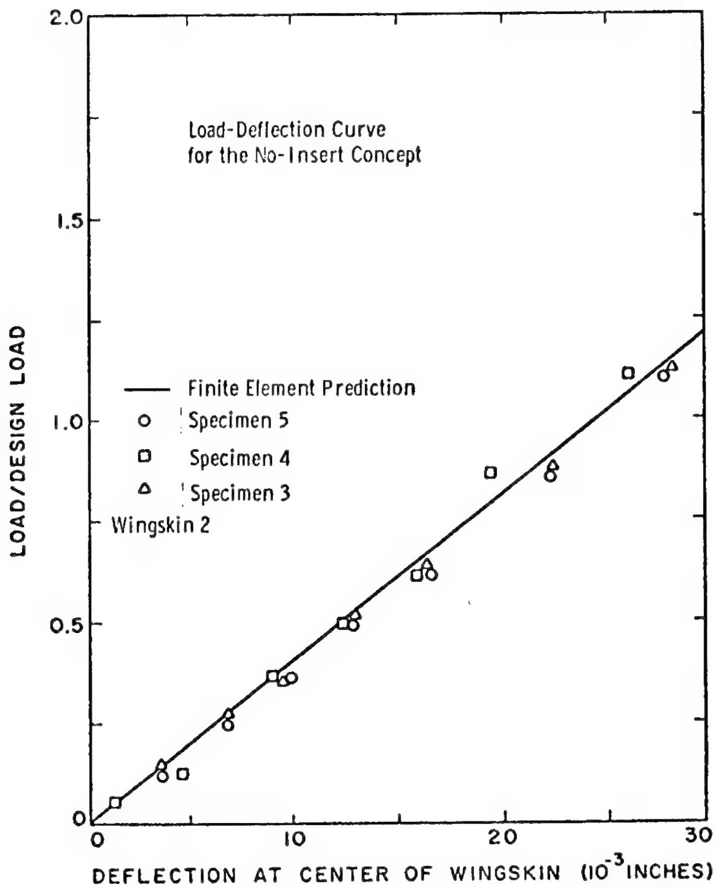

Load-Deflection Curve
for the No-Insert Concept
Finite Element Prediction
Specimen 5
Specimen 4
Specimen 3
Wingskin 2
LOAD/DESIGN LOAD
2.0
1.5
1.0
0.5
0
0
10
20
30
DEFLECTION AT CENTER OF WINGSKIN (10^{-3} INCHES)

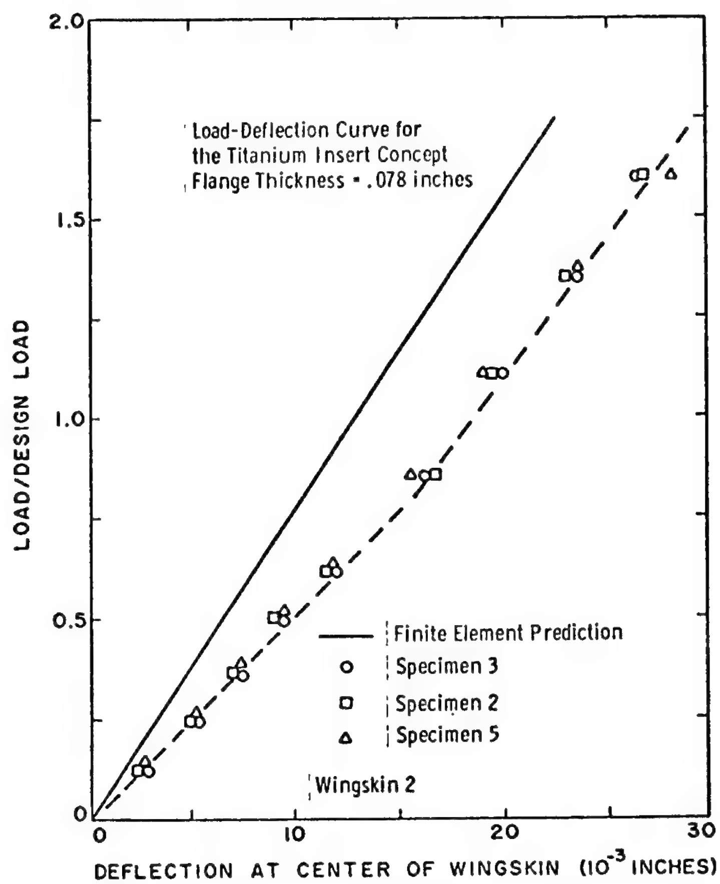

Load-Deflection Curve for
the Titanium Insert Concept
Flange Thickness = .078 inches
Finite Element Prediction
Specimen 3
Specimen 2
Specimen 5
Wingskin 2
LOAD/DESIGN LOAD
2.0
1.5
1.0
0.5
0
0
10
20
30
DEFLECTION AT CENTER OF WINGSKIN (10^{-3} INCHES)

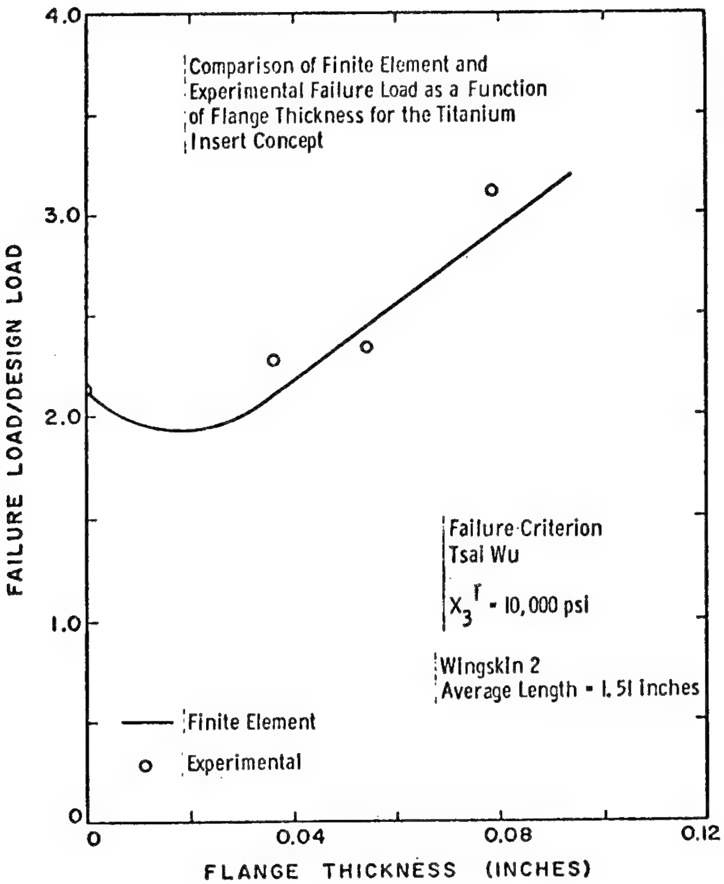
Comparison of Finite Element and Experimental Failure Load as a Function of Flange Thickness for the Titanium Insert Concept
Failure Criterion
Tsai Wu
X_3^T = 10,000 psi
Wingskin 2
Average Length = 1.51 inches
Finite Element
Experimental
FAILURE LOAD/DESIGN LOAD
FLANGE THICKNESS (INCHES)
4.0
3.0
2.0
1.0
0
0
0.04
0.08
0.12

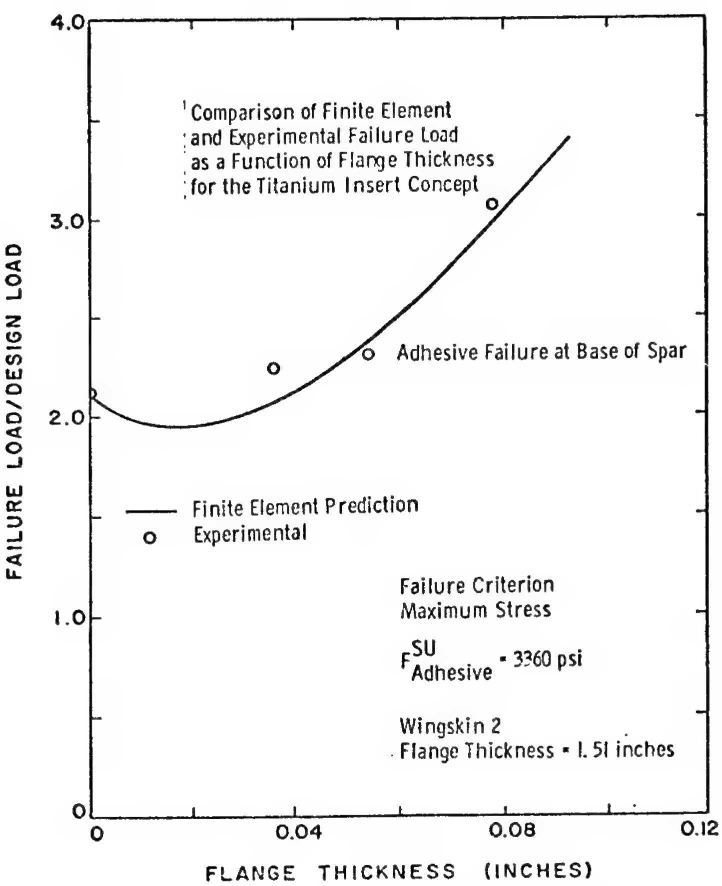
Comparison of Finite Element and Experimental Failure Load as a Function of Flange Thickness for the Titanium Insert Concept
Adhesive Failure at Base of Spar
Finite Element Prediction
Experimental
Failure Criterion
Maximum Stress
$F^{SU}_{Adhesive}$ = 3360 psi
Wingskin 2
Flange Thickness = 1.51 inches
FAILURE LOAD/DESIGN LOAD
FLANGE THICKNESS (INCHES)
4.0
3.0
2.0
1.0
0
0
0.04
0.08
0.12

DYNAMIC RESPONSE OF COMPOSITE
MATERIALS AND STRUCTURES

BY

GEORGE HERRMANN
DIVISION OF APPLIED MECHANICS
STANFORD UNIVERSITY
STANFORD, CALIFORNIA

UNDER

AFOSR SPONSORSHIP

OBJECTIVES

GENERAL: MORE COMPLETE UNDERSTANDING OF DYNAMIC BEHAVIOR OF COMPOSITE MATERIALS, WITH EMPHASIS ON PERIODICALLY-LAYERED COMPOSITES.

SPECIFIC: 1. WAVE PROPAGATION AND VIBRATION OF LAYERED ELASTIC COMPOSITES IN ANTI-PLANE STRAIN AND IN PLANE STRAIN. "EXACT" TREATMENT IN BODIES OF INFINITE EXTENT.

2. BASED ON KNOWLEDGE ACQUIRED IN (1), DEVELOP APPROXIMATE THEORIES WHICH WOULD PERMIT STUDY OF STRUCTURAL ELEMENTS (BOUNDED BODIES) SUBJECTED TO DYNAMIC LOADS.

REMARK: "EXACT" TREATMENT INVOLVES EQUATIONS WITH VARIABLE COEFFICIENTS. APPROXIMATE THEORIES INVOLVE EQUATIONS WITH CONSTANT COEFFICIENTS, BUT WITH MICROSTRUCTURE.

Recent Accomplishments and Current Activities

1. Exact treatment of waves in anti-plane strain.
2. Exact treatment of waves in plane strain.
3. Novel approximate theory for motions normal to the layering in anti-plane strain. Effective Dispersion Theory
4. New types of surface waves in composites.
5. Composite beams subjected to moving loads.

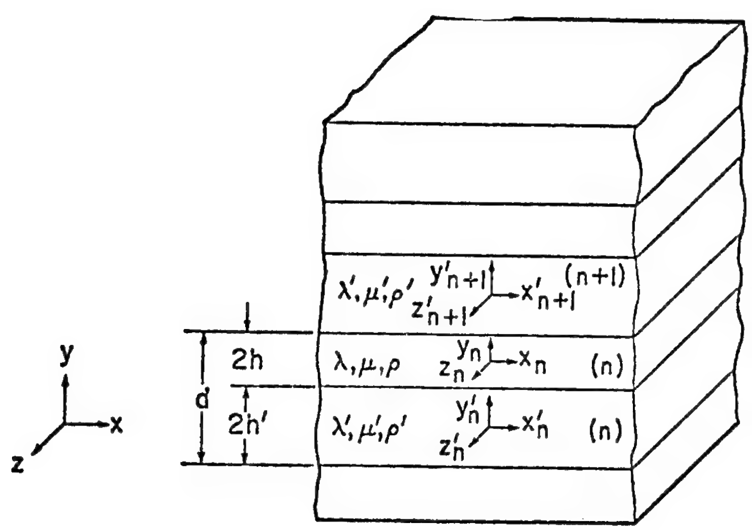

Fig. 1 Geometry of layered composites

$$
\begin{vmatrix}
e^{-\frac{i\pi\alpha}{2}} & e^{\frac{i\pi\alpha}{2}} & -e^{\frac{i\pi\epsilon\alpha'}{2}} & -e^{-\frac{i\pi\epsilon\alpha'}{2}} \\
\gamma\alpha\, e^{-\frac{i\pi\alpha}{2}} & -\gamma\alpha\, e^{\frac{i\pi\alpha}{2}} & -\alpha' e^{\frac{i\pi\epsilon\alpha'}{2}} & \alpha' e^{-\frac{i\pi\epsilon\alpha'}{2}} \\
e^{\frac{i\pi\alpha}{2}} & e^{-\frac{i\pi\alpha}{2}} & -e^{-\frac{i\pi\epsilon\alpha'}{2}} e^{i\pi(1+\epsilon)\eta} & -e^{\frac{i\pi\epsilon\alpha'}{2}} e^{i\pi(1+\epsilon)\eta} \\
\gamma\alpha\, e^{\frac{i\pi\alpha}{2}} & -\gamma\alpha\, e^{-\frac{i\pi\alpha}{2}} & -\alpha' e^{-\frac{i\pi\epsilon\alpha'}{2}} e^{i\pi(1+\epsilon)\eta} & \alpha' e^{\frac{i\pi\epsilon\alpha'}{2}} e^{i\pi(1+\epsilon)\eta}
\end{vmatrix} = 0
$$

$$\epsilon = \frac{h'}{h} \qquad \zeta = \frac{2h}{\pi} k_z$$

$$\gamma = \frac{\mu}{\mu'} \qquad \alpha = \sqrt{\Omega^2 - \zeta^2}$$

$$\eta = \frac{2h}{\pi} k_y \qquad \alpha' = \sqrt{\sigma^2\Omega^2 - \zeta^2}$$

$$\Omega = \frac{2h\omega}{\pi\sqrt{\mu/\rho}} \qquad \sigma^2 = \mu\rho'/\mu'\rho$$

$$4\gamma\alpha\alpha' \cos \pi\eta(1+\epsilon) + (\gamma\alpha - \alpha')^2 \cos \pi(\alpha - \epsilon\alpha') - (\gamma\alpha + \alpha')^2 \cos \pi(\alpha + \epsilon\alpha') = 0$$

DISPERSION EQUATION FOR ANTI-PLANE STRAIN

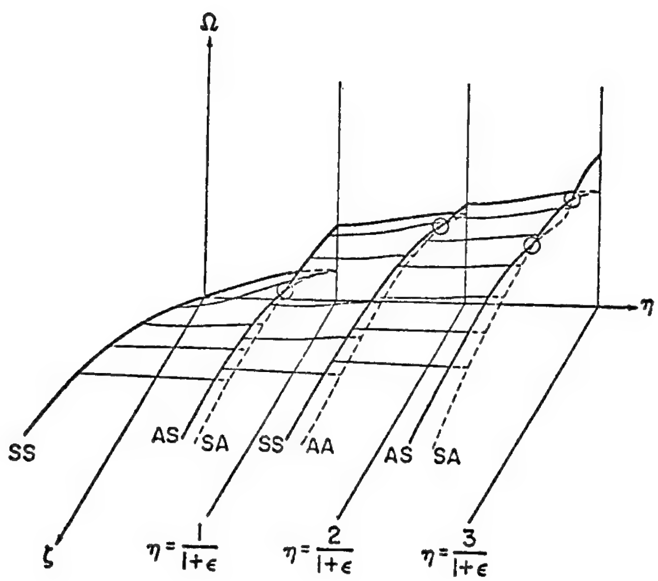

FIG. 2 ANTIPLANE STRAIN DISPERSION SURFACE ON THE EXTENDED ZONE SCHEME

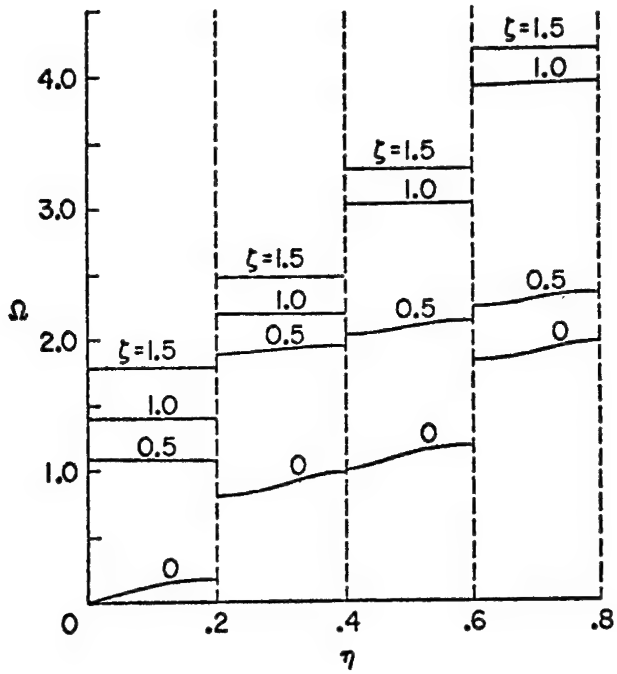

Fig. 3. Curves of constant ζ on the antiplane strain dispersion surface.

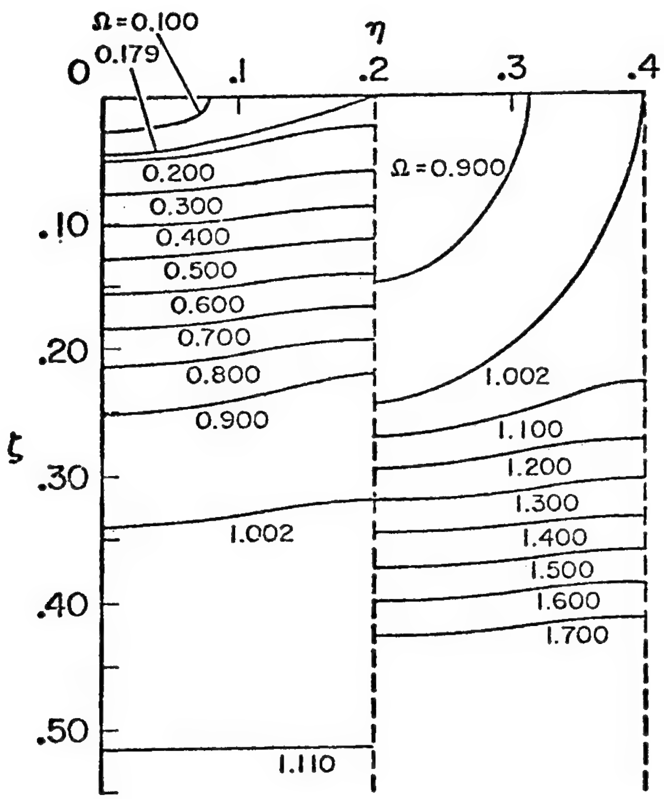

Fig. 4 Curves of constant Ω on the anti-plane strain dispersion surface

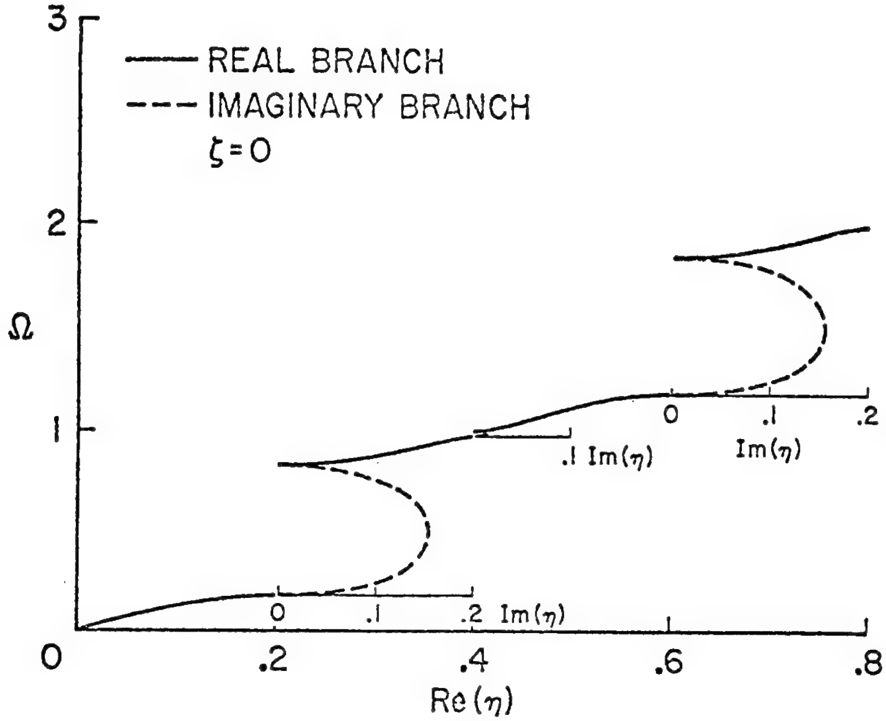

FIG. 5 ANTI-PLANE STRAIN DISPERSION SURFACE IN THE $\zeta = 0$ PLANE, WITH COMPLEX BRANCHES.

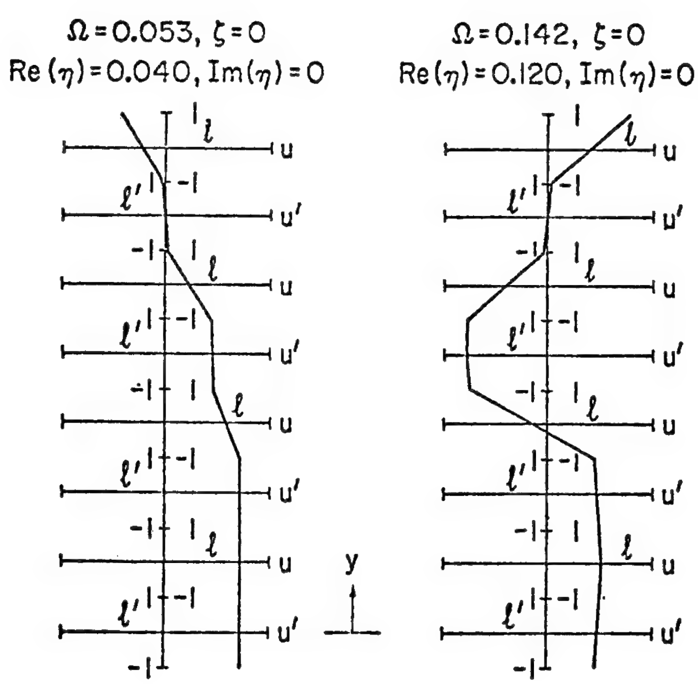

FIG. 6 MODE SHAPES AT TWO POINTS IN THE FIRST BRILLOUIN ZONE ($\zeta = 0$).

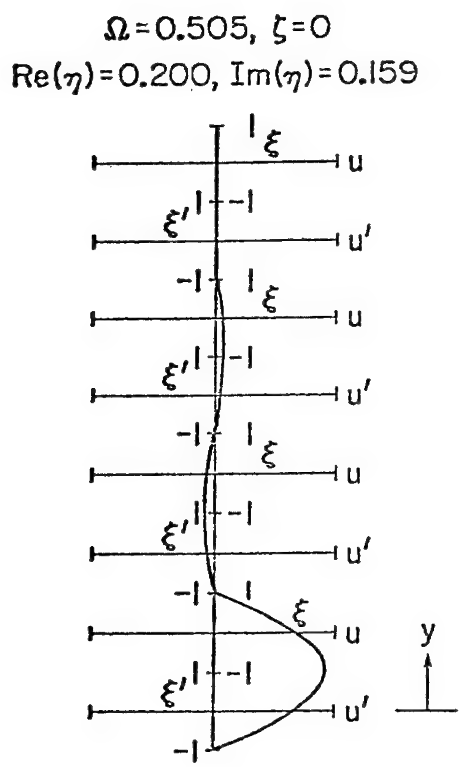

FIG. 7 MODE SHAPE AT A POINT IN THE STOPPING BAND BETWEEN THE FIRST TWO BRILLOUIN ZONES ($\zeta = 0$) .

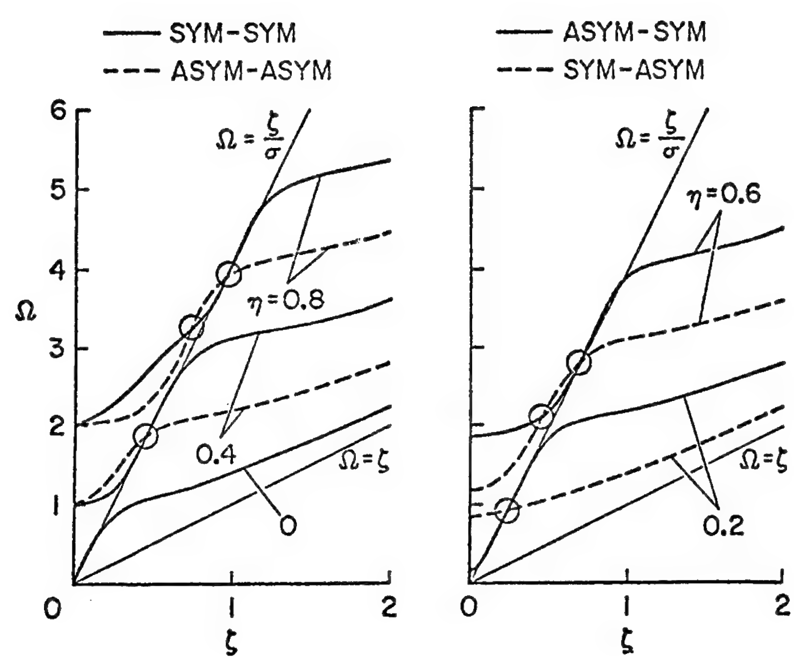

FIG. 8 SPECTRAL LINES CORRESPONDING TO MODES OF OPPOSITE SYMMETRY AT THE ENDS OF THE BRILLOUIN ZONES.

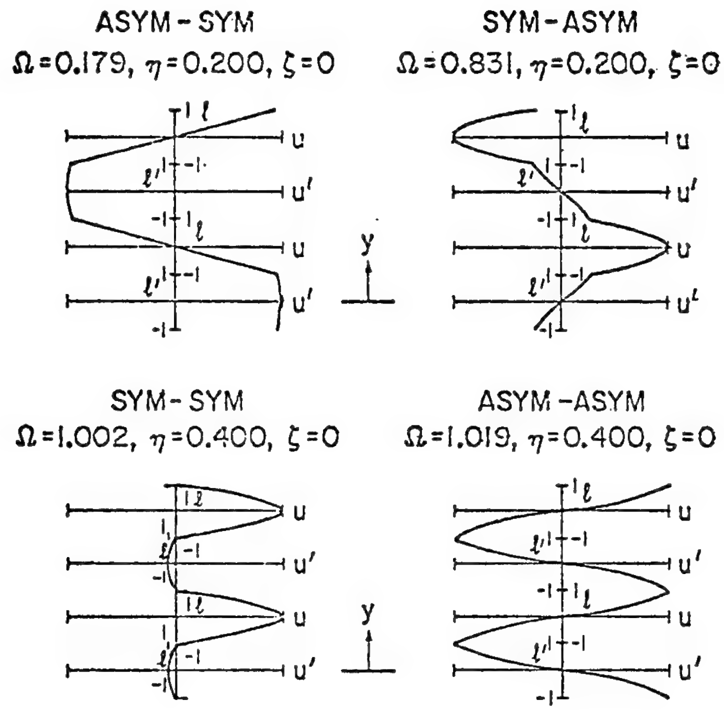

FIG. 9 MODE SHAPES AT POINTS ON THE ENDS OF BRILLOUIN ZONES ($\zeta = 0$) .

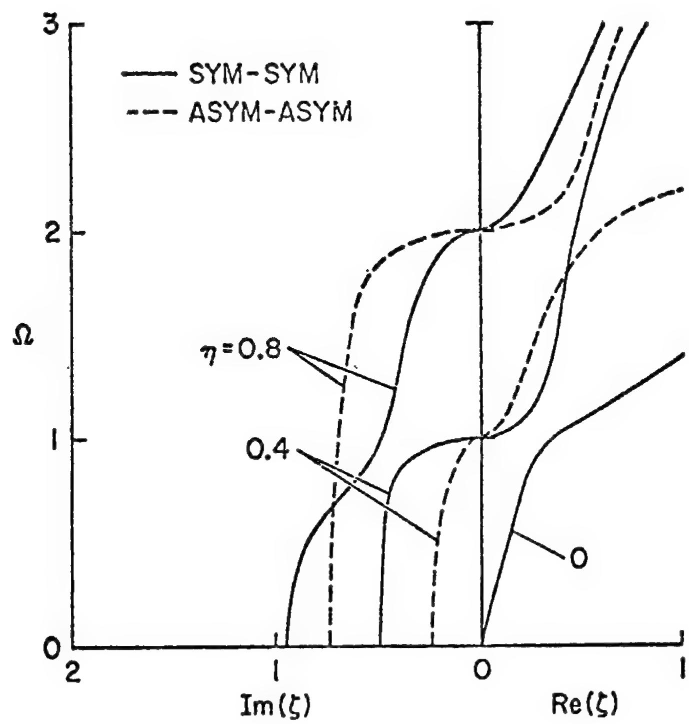

FIG. 10 CURVES OF CONSTANT η AT THE ENDS OF THE BRILLOUIN ZONES, WITH COMPLEX BRANCHES (SYMMETRIC-SYMMETRIC AND ANTISYMMETRIC-ANTISYMMETRIC MODES SHOWN ONLY).

$$
\begin{vmatrix}
\zeta p^- & \zeta p^+ & \alpha q & -\alpha q^+ & -\zeta r^+ & -\zeta r^- & -\alpha' s^+ & \alpha' s^- \\
\beta p^- & -\beta p^+ & -\zeta q^- & -\zeta q^+ & -\beta' r^+ & \beta' r^- & \zeta s^+ & \zeta s^- \\
2\gamma\beta\zeta p^- & -2\gamma\beta\zeta p^+ & \gamma(\alpha^2-\zeta^4)q^- & \gamma(\alpha^2-\zeta^4)q^+ & -2\beta'\zeta r^+ & 2\beta'\zeta r^- & -(\alpha'^2-\zeta^2)s^+ & -(\alpha'^2-\zeta^2)s^- \\
\gamma(\alpha^2-\zeta^2)p^- & \gamma(\alpha^2-\zeta^2)p^+ & -2\gamma\alpha\zeta q^- & 2\gamma\alpha\zeta q^+ & -(\alpha'^2-\zeta^2)r^+ & -(\alpha'^2-\zeta^2)r^- & 2\alpha'\zeta s^+ & -2\alpha'\zeta s^- \\
\zeta p^+ & \zeta p^- & \alpha q^+ & -\alpha q^- & -\zeta r^- t & -\zeta r^+ t & -\alpha' s^- t & \alpha' s^+ t \\
\beta p^+ & -\beta p^- & -\zeta q^+ & -\zeta q^- & -\beta' r^- t & \beta' r^+ t & \zeta s^- t & \zeta s^+ t \\
2\gamma\beta\zeta p^+ & -2\gamma\beta\zeta p^- & \gamma(\alpha^2-\zeta^2)q^+ & \gamma(\alpha^2-\ ^2)q^- & -2\beta'\zeta r^- t & 2\beta'\zeta r^+ t & -(\alpha'^2-\zeta^2)s^- t & -(\alpha'^2-\zeta^2)s^+ t \\
\gamma(\alpha^2-\zeta^2)p^+ & \gamma(\alpha^2-\zeta^2)p^- & -2\gamma\alpha\zeta q^+ & 2\gamma\alpha\zeta q^- & -(\alpha\ ^2-\zeta^2)r^- t & -(\alpha'^2-\zeta^2)r^+ t & 2\alpha'\zeta s^- t & -2\alpha'\zeta s^+ t
\end{vmatrix} = 0
$$

where $p^{\pm} = e^{\pm i\pi\beta/2}$, $q^{\pm} = e^{\pm i\pi\alpha/2}$, $r^{\pm} = e^{\pm i\pi\epsilon\beta'/2}$, $s^{\pm} = e^{\pm i\pi\epsilon\alpha'/2}$, $t = e^{i\pi(1+\epsilon)2}$,

$\epsilon = h'/h$; $\gamma = \mu/\mu'$; $\eta = 2hk_y/\pi$; $\beta^2 = \Omega^2/\delta - \zeta^2$; $\beta'^2 = \sigma^2\Omega^2/\delta' - \zeta^2$; $\delta' = 2(1 - \nu')/(1 - 2\nu')$.

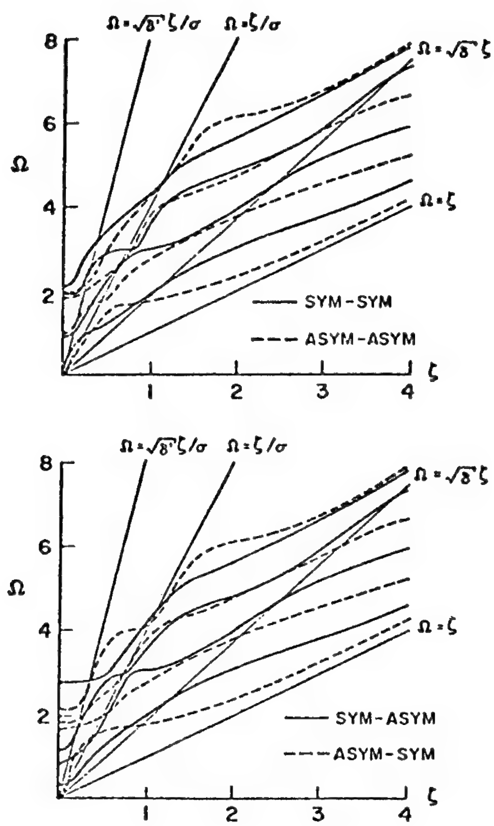

FIG. 11 SPECTRAL LINES CORRESPONDING TO MODES OF OPPOSITE SYMMETRY, AT THE ENDS OF THE BRILLOUIN ZONES FOR PLANE STRAIN.

Effective Dispersion Theory

Assumed displacements

$$u(y,t) = u_0(y,t)\big|_{y_N=0} + y_N\psi(y,t)\big|_{y_N=0}$$

$$u^*(y,t) = u_0(y,t)\big|_{y_N^*=0}$$

Generalized strain

$$e_{12} = u_{0,y}$$

$$\gamma_{21} = u_{0,y} - \psi$$

$$\rho_{221} = \frac{\partial}{\partial y}(\gamma_{21}) = u_{0,yy} - \psi_{,y}$$

$$\kappa_{221} = \psi_{,y}$$

Strain energy

$$V = \frac{1}{2}c_1 e_{12}^2 + c_2 e_{12}\gamma_{21} + \frac{1}{2}c_3\gamma_{21}^2 + \frac{1}{2}c_4\kappa_{221}^2 + c_5\kappa_{221}\rho_{221} + \frac{1}{2}c_6\rho_{221}^2$$

$$= \frac{1}{2}(c_1 + 2c_2 + c_3)u_{0,y}^2 - (c_2 + c_3)\psi u_{0,y} + \frac{1}{2}c_3\psi^2$$

$$+ \frac{1}{2}(c_4 - 2c_5 + c_6)\psi_{,y}^2 + (c_5 - c_6)u_{0,yy}\psi_{,y} + \frac{1}{2}c_6 u_{0,yy}^2$$

$$a_1 = c_1 + 2c_2 + c_3 \;;\; a_2 = -c_6 \;;\; a_3 = c_2 + c_3 \;;$$

$$a_4 = c_5 - c_6 \;;\; a_5 = c_3 \;;\; a_6 = -c_4 + 2c_5 - c_6$$

Modified strain energy

$$V = \frac{1}{2}a_1 u_{0,y}^2 - \frac{1}{2}a_2 u_{0,yy}^2 - a_3 u_{0,y}\psi + a_4 u_{0,yy}\psi_{,y}$$

$$+ \frac{1}{2}a_5\psi^2 - \frac{1}{2}a_6\psi_{,y}^2$$

Kinetic energy

$$T = \frac{1}{2}b_1\dot{u}_0^2 + \frac{1}{2}b_2\dot{\psi}^2$$

Equations of motion

$$b_1\ddot{u}_0 - a_1 u_{0,yy} - a_2 u_{0,yyyy} + a_3\psi_{,y} + a_4\psi_{,yyy} = 0$$

$$b_2\ddot{\psi} - a_3 u_{0,y} - a_4 u_{0,yyy} + a_5\psi + a_6\psi_{,yy} = 0$$

Dispersion equation

$$\alpha\omega^4 + (\beta k^4 + \gamma k^2 + \delta)\,\omega^2 + \xi k^2 + \theta k^4 + k^6 = 0$$

$$\alpha = \frac{b_1 b_2}{a_2 a_6 - a_4^2} \; ; \quad \beta = \frac{a_2 b_2}{a_2 a_6 - a_4^2} \; ; \quad \gamma = \frac{a_6 b_1 - a_1 b_2}{a_2 a_6 - a_4^2}$$

$$\delta = -\frac{a_5 b_1}{a_2 a_6 - a_4^2} \; ; \quad \xi = \frac{a_1 a_5 - a_3^2}{a_2 a_6 - a_4^2} \; ; \quad \theta = \frac{2a_3 a_4 - a_1 a_6 - a_2 a_5}{a_2 a_6 - a_4^2}$$

Equations to determine coefficients

$$\left.\frac{d\omega}{dk}\right|_{\substack{\omega=0\\ k=0}} = c_g \; ; \quad \omega\Big|_{k=k_B} = \omega_B \; ; \quad \omega\Big|_{k=k_B} = \omega_D$$

$$\left.\frac{d\omega}{dk}\right|_{\substack{\omega=\omega_B\\ k=k_B}} = 0 \; ; \quad \left.\frac{d\omega}{dk}\right|_{\substack{\omega=\omega_D\\ k=k_B}} = 0$$

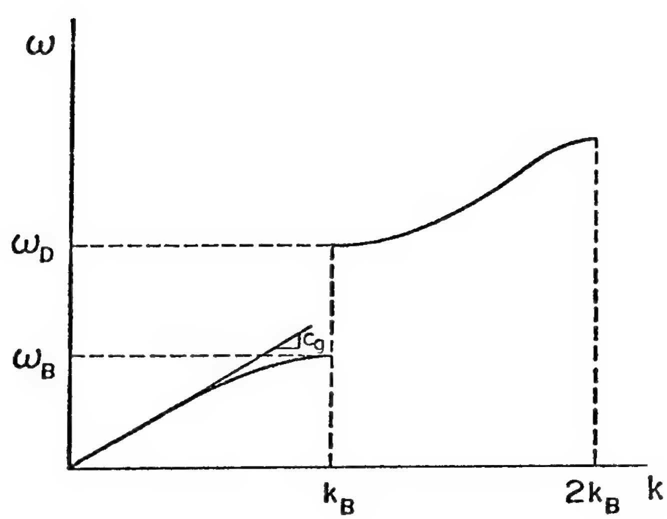

Fig. 12 Parameters of exact solution used in effective dispersion theory.

COEFFICIENTS OF DISPERSION EQUATION

$$\alpha = -\frac{k_B^4}{\omega_B^2\omega_D^2}\left(\theta + 2k_B^2\right)$$

$$\beta = \frac{1}{k_B^2}\left[\left(\frac{2}{c_g^2} + Rk_B^2\right)\theta + \frac{3k_B^2}{c_g^2} + 2Rk_B^4\right]$$

$$\delta = \frac{k_B^2}{c_g^2}\left(2\theta + 3k_B^2\right)$$

$$\xi = -k_B^2\left(2\theta + 3k_B^2\right)$$

$$\gamma = -2\left[\left(\frac{2}{c_g^2} + Rk_B^2\right)\theta + \frac{3k_B^2}{c_g^2} + 2Rk_B^4\right]$$

where

$$R = -\frac{\left(\omega_B^2 + \omega_D^2\right)}{\omega_B^2\omega_D^2}$$

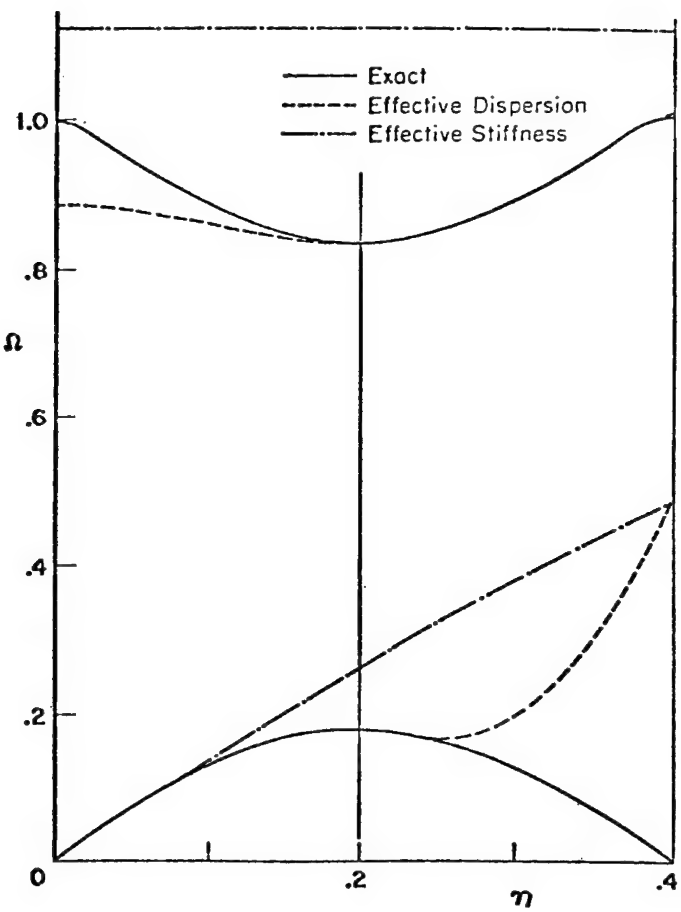

FIG. 13 SPECTRUM OF EFFECTIVE DISPERSION THEORY OVER THE FIRST TWO BRILLOUIN ZONES (REAL BRANCHES).

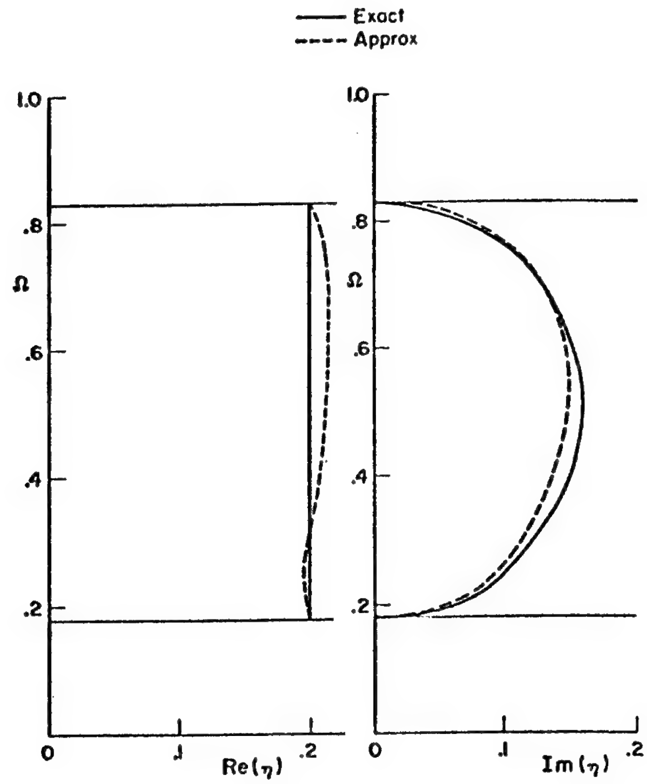

FIG. 14 COMPLEX BRANCH BETWEEN THE FIRST TWO BRILLOUIN ZONES.

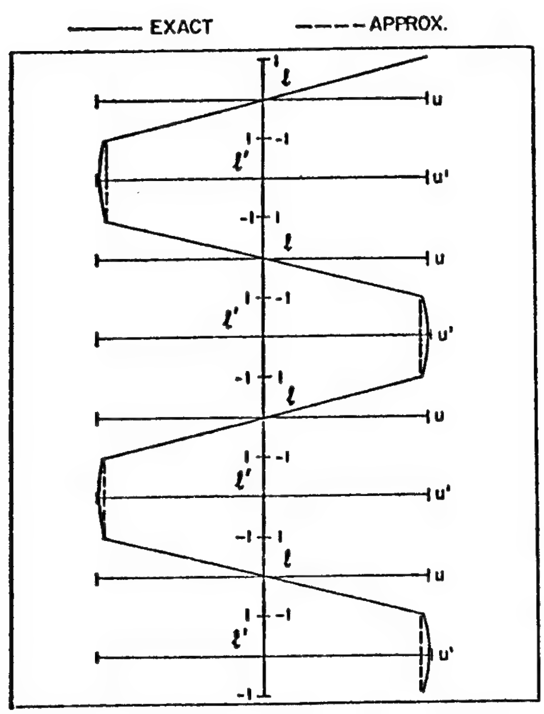

FIG. 15 EFFECTIVE DISPERSION MODE SHAPES AND EXACT MODE SHAPES AT THE RIGHT-HAND END OF THE FIRST BRILLOUIN ZONE.

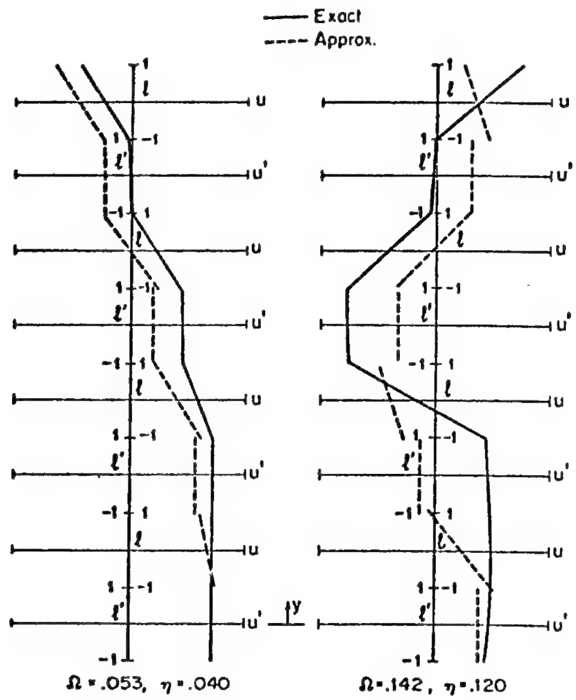

FIG. 16 EFFECTIVE DISPERSION MODE SHAPES AND EXACT MODE SHAPES AT TWO POINTS IN THE INTERIOR OF THE FIRST BRILLOUIN ZONE.

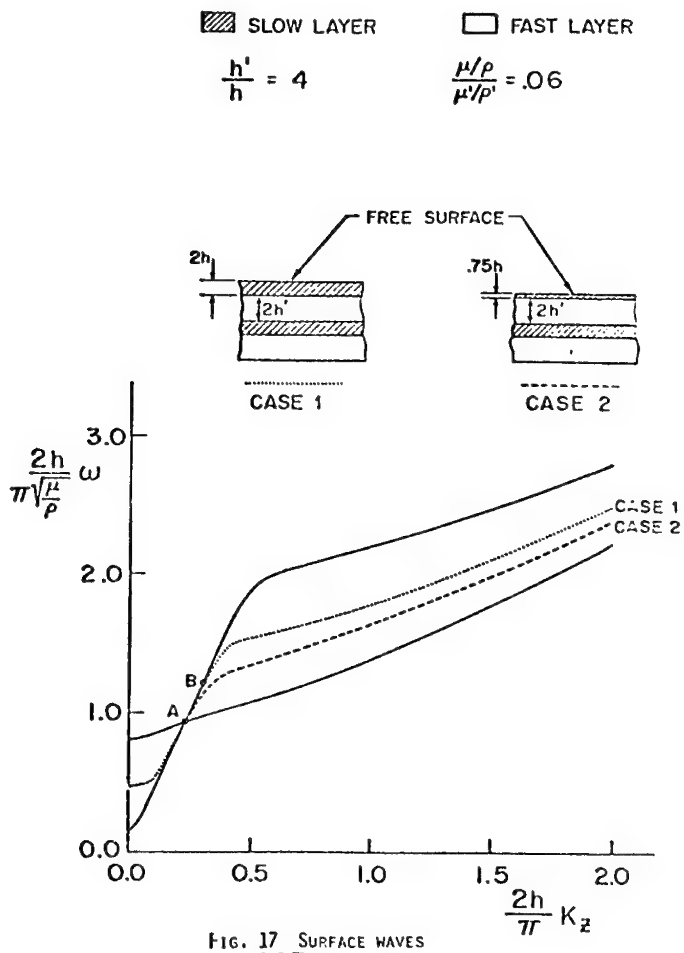

FIG. 17 SURFACE WAVES

EFFECT OF COMPRESSIVE LOADING ON THE FATIGUE LIFETIME OF GRAPHITE/EPOXY LAMINATES

PRINCIPAL INVESTIGATOR: J. T. RYDER

AIR FORCE PROJECT ENGINEER: J. M. WHITNEY

LOCKHEED-CALIFORNIA COMPANY

PURPOSE - PROGRAM I (FEB. 1975 TO DEC. 1976)

- o BUILD STATISTICAL DATA BASE
- o EVALUATE WEAR-OUT MODEL
- o EVALUATE EFFECT OF COMPRESSION FATIGUE

PURPOSE - PROGRAM 2 (MAY 1977 TO AUG. 1979)

- EFFECT OF A CIRCULAR HOLE
- EFFECT OF ENVIRONMENT

PROGRAM DEFINITION

TWO LAMINATES

LAMINATE 1: $25\%\ 0^0$ FIBERS
16 PLIES
$(0/+45/90/-45_2/90/45/0)_2$
QUASI - ISOTROPIC

LAMINATE 2: $66.7\%\ 0^0$ FIBERS
24 PLIES
$(0/+45/0_2/-45/0_2/+45/0_2/-45/0)_2$

TESTING

- STATIC TENSION, COMPRESSION
- S-N CURVE, T-T, C-T
- EVALUATE FATIGUE SCATTER
- MINIMUM TWENTY TESTS AT EACH STRESS LEVEL
- RESIDUAL STRENGTH
  - FATIGUE CYCLE 40 COUPONS AT STRESS LEVELS CHOSEN
  - FAIL HALF TENSION AND COMPRESSION
  - ORIGINAL STRENGTH DISTRIBUTION

MATERIAL: (934/T300)

CURE CYCLE: 350^0F CURE FOR 2 HOURS

CONDITIONING:
1. 72 HOURS AT 72 ± 2^0F, $40 \pm 10\%$ R.H.
2. TO EQUILIBRIUM WT. GAIN AT 180 ± 2^0F $90 \pm 5\%$ R.H.

TEST ENVIRONMENT:
1. 72 ± 2^0F, $40 \pm 10\%$ R.H.
2. 180 ± 2^0F, $90 \pm 5\%$ R.H.

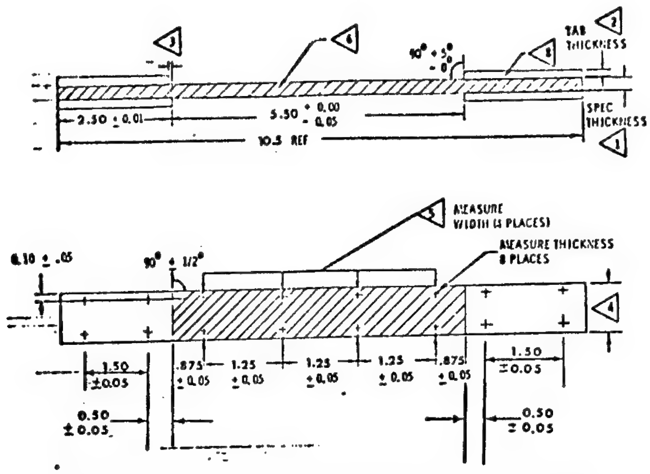

- SPECIMENS TO BE FLAT OVER THE ENTIRE 10.5 INCH LENGTH WITHIN 0.01 INCHES.
- TAB EDGES TO BE PARALLEL TO SIDES OF SPECIMEN WITHIN 0.02 INCHES. OVERHANG NOT TO EXCEED 0.15 INCHES.
- 7 THE TAB AND SPECIMEN BONDING SURFACES TO BE THOROUGHLY SOLVENT CLEANED USING METHYL-ETHYL-KETONE PRIOR TO BONDING. A 350°F CURING ADHESIVE IS TO BE USED AND MUST COVER ENTIRE SURFACE UNIFORMLY.
- WATER SPRAY MIST TO BE USED DURING SAWING OPERATIONS AND SOLUBLE OIL DURING GRINDING. MACHINED SURFACES TO BE RMS 50 OR BETTER. NO EDGE DAMAGE OR FIBER SEPARATION SHOULD BE VISIBLE.
- MEASURE SPECIMEN WIDTH 4 PLACES. WIDTH MUST NOT VARY BY MORE THAN 0.004 INCHES.
- SPECIMEN WIDTH TO BE 0.875 ± 0.005 INCHES.
- MISMATCH OF TABS FROM SIDE TO SIDE NOT TO EXCEED 0.01 INCHES.
- TABS TO BE CUT FROM AN 6 PLY LAMINATE FABRICATED FROM PREPREG OF 1581 GLASS FABRIC IN A 350°F CURING EPOXY. TAB PLUS ADHESIVE THICKNESS MUST NOT VARY SIDE OR END TO END BY MORE THAN 0.01 AS MEASURED 8 PLACES.
- SPECIMEN THICKNESS TO BE WITHIN ± 0.003 INCHES OF THE AVERAGE OF 8 THICKNESS MEASUREMENTS.

Figure 2. Specimen Configuration, Unnotched

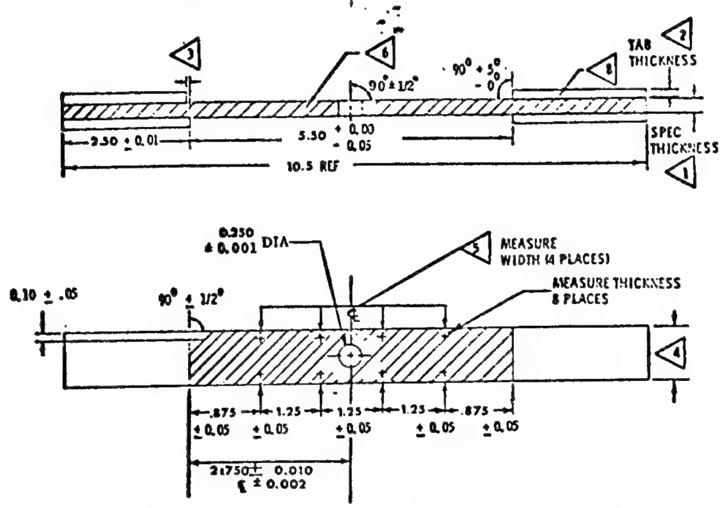

- SPECIMENS TO BE FLAT OVER THE ENTIRE 10.5 INCH LENGTH WITHIN 0.01 INCHES.
- TAB EDGES TO BE PARALLEL TO SIDES OF SPECIMEN WITHIN 0.02 INCHES. OVERHANG NOT TO EXCEED 0.15 INCHES.
- 7 THE TAB AND SPECIMEN BONDING SURFACES TO BE THOROUGHLY SOLVENT CLEANED USING METHYL-ETHYL-KETONE PRIOR TO BONDING. A 350°F CURING ADHESIVE IS TO BE USED AND MUST COVER ENTIRE SURFACE UNIFORMLY.
- WATER SPRAY MIST TO BE USED DURING SAWING OPERATIONS AND SOLUBLE OIL DURING GRINDING. MACHINED SURFACES TO BE RMS 50 OR BETTER. NO EDGE DAMAGE OR FIBER SEPARATION SHOULD BE VISIBLE.
- MEASURE SPECIMEN WIDTH 4 PLACES. WIDTH MUST NOT VARY BY MORE THAN 0.004 INCHES.
- SPECIMEN WIDTH TO BE 0.875 ± 0.005 INCHES.
- MISMATCH OF TABS FROM SIDE TO SIDE NOT TO EXCEED 0.01 INCHES.
- TABS TO BE CUT FROM AN 6 PLY LAMINATE FABRICATED FROM PREPREG OF 1581 GLASS FABRIC IN A 350°F CURING EPOXY. TAB PLUS ADHESIVE THICKNESS MUST NOT VARY SIDE OR END TO END BY MORE THAN 0.01 AS MEASURED 8 PLACES.
- SPECIMEN THICKNESS TO BE WITHIN ± 0.003 INCHES OF THE AVERAGE OF 8 THICKNESS MEASUREMENTS.

Figure 3. Specimen Configuration, Notched

FABRICATION

VARIATION IN AREA WITHIN GAGE LENGTH:	$< \pm$ 1.5%
PERCENT FIBER VOLUME:	60 to 65 %
VOIDS:	$\ll$ 1/2 %

- ONE BATCH OF PREPREG 12 IN. WIDE TAPE
- TWO HOUR SINGLE STAGE CURE
- E-GLASS TABS BONDED ON WITH FM400

TABLE 3-1. PROPOSED TEST MATRIX

TEST CATEGORY	TEST TYPE	LAMI-NATE	TESTING ENVIRONMENT	NUMBER OF STRESS LEVELS	NUMBER OF COUPON REPLICATIONS	TOTAL NO. OF TEST CONDITIONS
Material Characterization (Unnotched coupons)	Static Tension	1,2	D^a	T	5/panel (13 panels)	65
Effect of a Circular Hole (Notched Coupon)	Static	1	D,W^b	$2(T,C)^c$	20	80
	Fatigue Screen					
	T-T	1	D,W	8	3	48
	T-C	1	D,W	8	3	48
	Scatter					
	T-T	1	D,W	3	20	120^e
	T-C	1	D,W	3	20	120^e
	Residual Strength					
	T-T	1	D,W	$2(T,C) \times 2^d$	20	160
	T-C	1	D,W	$2(T,C) \times 2^d$	20	160
Effect of Environment on Unnotched Laminates (Unnotched Coupons)	Static	1,2	D,W	2(T,C)	20	160^f
	Fatigue Screen					
	T-T	1,2	D,W	8	3	96
	T-C	1,2	D,W	8	3	96
	Scatter					
	T-T	1,2	W	3	20	120^e
	T-C	1,2	W	3	20	120^e
	Residual Strength					
	T-T	1,2	W	$2(T,C) \times 2^d$	20	160
	T-C	1,2	W	$2(T,C) \times 2^d$	20	160

TABLE 3-1. PROPOSED TEST MATRIX (Continued)

TEST CATEGORY	TEST TYPE	LAMI-NATE	TESTING ENVIRONMENT	NUMBER OF STRESS LEVELS	NUMBER OF COUPON REPLICATIONS	TOTAL NO. OF TEST CONDITIONS
Static Scatter	Static	2	D	T	100	100[g]
Fatigue Threshold	Fatigue	1	D	2(T-T, T-C)	20	40[h]
					Total	1853

a D - $72^{\circ} \pm 2^{\circ}$F, 40 ±10% RH environment

b W - 180°F, 95% RH environment

c T - tension
C - compression

d Residual strength at two different lines will be determined.

e 18 of these coupons will be tested in the fatigue screening program

f Note that 40 of the tension tests will be tested in material characterization

g These tests include 20 coupons previously tested under Contract F33615-75-C-5118; the remaining 80 coupons will come from panels fabricated for the same contract

h These 40 coupons will come from panels fabricated under Contract F33615-75-C-5118

TABLE 10

SUMMARY OF STATIC TENSION TEST RESULTS

	Avg. Ultimate Stress, σ_{ult}, MPa (ksi)	Avg. Ultimate Strain, ϵ_{ult}, mm/mm in 50.8 mm	Avg. Initial Apparent Modulus of Elasticity, E_A, GPa (psi x 10^6)
LAMINATE 1	477 (69.2)[a] + 43 (6.2), 9% - 50 (7.2), 10%	0.0096 +0.0011, 11% -0.0010, 10%	52.7 (7.64) + 3.7 (0.54), 7% - 4.8 (0.69), 9%
LAMINATE 2	977 (141.7) +139 (20.1), 14% -140 (20.3), 14%	0.0092 +0.0009, 10% -0.0027, 29%	106 (15.4) + 20 (2.9), 19% - 13 (1.9), 12%

a - Based on minimum area

TABLE 3-1. PROPOSED TEST MATRIX (Continued)

TEST CATEGORY	TEST TYPE	LAMI-NATE	TESTING ENVIRONMENT	NUMBER OF STRESS LEVELS	NUMBER OF COUPON REPLICATIONS	TOTAL NO. OF TEST CONDITIONS
Static Scatter	Static	2	D	T	100	100[g]
Fatigue Threshold	Fatigue	1	D	2(T-T, T-C)	20	40[h]
					Total	1853

a D - $72^{\circ}\pm2^{\circ}$F, 40 ±10% RH environment

b W - 180°F, 95% RH environment

c T - tension
C - compression

d Residual strength at two different lines will be determined.

e 18 of these coupons will be tested in the fatigue screening program

f Note that 40 of the tension tests will be tested in material characterization

g These tests include 20 coupons previously tested under Contract F33615-75-C-5118: the remaining 80 coupons will come from panels fabricated for the same contract

h These 40 coupons will come from panels fabricated under Contract F33615-75-C-5118

TABLE 10

SUMMARY OF STATIC TENSION TEST RESULTS

	Avg. Ultimate Stress, σ_{ult}, MPa (ksi)	Avg. Ultimate Strain, ϵ_{ult}, mm/mm in 50.8 mm	Avg. Initial Apparent Modulus of Elasticity, E_A, GPa (psi x 10^6)
LAMINATE 1	477 (69.2)[a] + 43 (6.2), 9% - 50 (7.2), 10%	0.0096 +0.0011, 11% -0.0010, 10%	52.7 (7.64) + 3.7 (0.54), 7% - 4.8 (0.69), 9%
LAMINATE 2	977 (141.7) +139 (20.1), 14% -140 (20.3), 14%	0.0092 +0.0009, 10% -0.0027, 29%	106 (15.4) + 20 (2.9), 19% - 13 (1.9), 12%

a - Based on minimum area

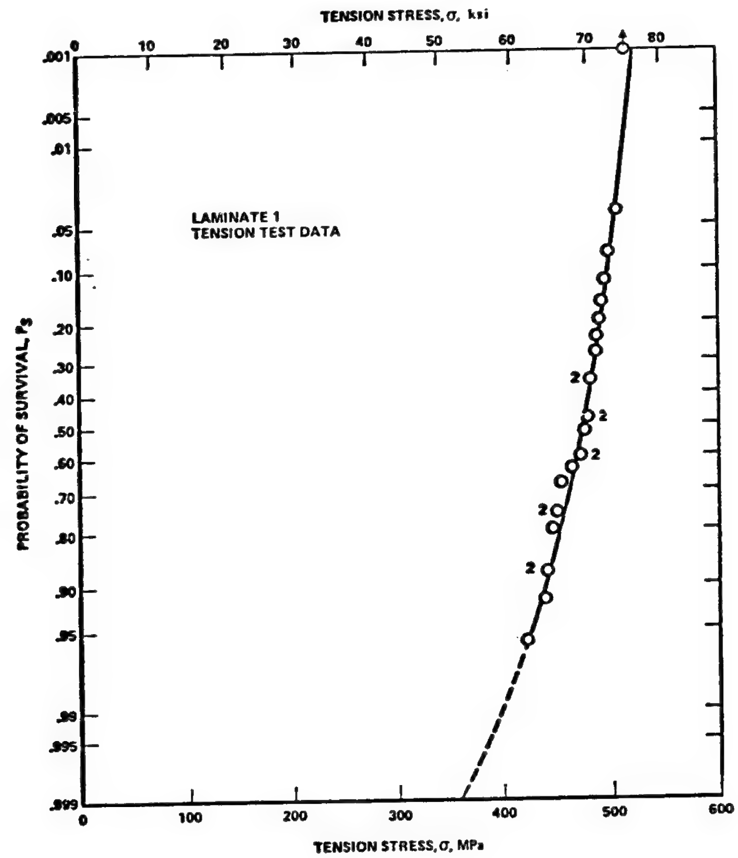
TENSION STRESS, σ, ksi
LAMINATE 1
TENSION TEST DATA
PROBABILITY OF SURVIVAL, P_S
TENSION STRESS, σ, MPa

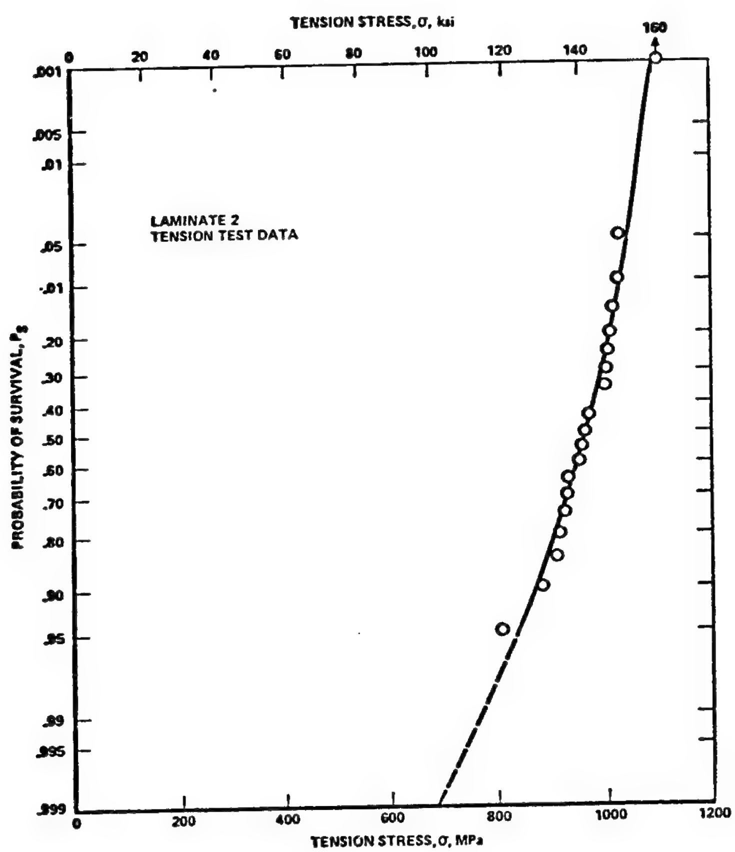
TENSION STRESS, σ, ksi
LAMINATE 2
TENSION TEST DATA
PROBABILITY OF SURVIVAL, P_S
TENSION STRESS, σ, MPa

TABLE 17

COMPARISON OF
STATIC COMPRESSION TEST RESULTS

	AVERAGE ULTIMATE STRESS, σ_{ult}, MPa (ksi)	AVERAGE ULTIMATE STRAIN, ϵ_{ult}, mm/mm in 50.8 mm	AVERAGE APPARENT MODULUS OF ELASTICITY, E_{avg}, GPa (psi x 10^6)
LAMINATE 1	481 (69.7)[a] +81 (11.8), 17% -82 (12.1), 17%	0.0110 +0.0022, 20% -0.0025, 23%	47.9 (6.95)[b] +2.0 (0.29), 4% -5.7 (0.83), 12%
LAMINATE 2	787 (114.2) +103 (15.0), 13% -70 (10.2), 9%	0.0098 +0.0014, 14% -0.0011, 11%	79.3 (11.5) +5.5 (0.8), 7% -3.4 (0.5), 4%

a - Based on minimum area

b - Average Initial Apparent Modulus of Elasticity

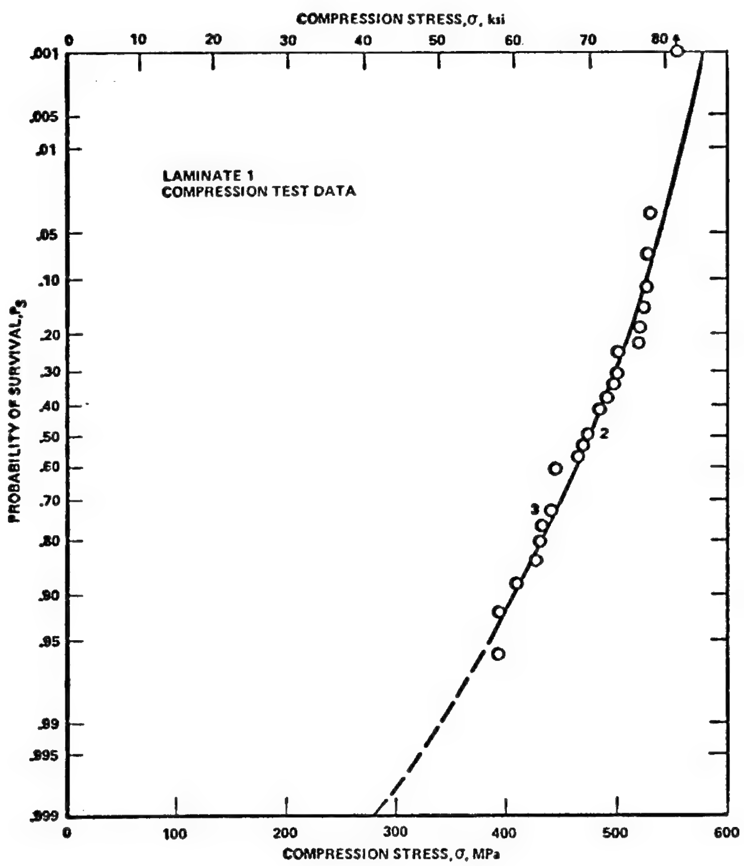

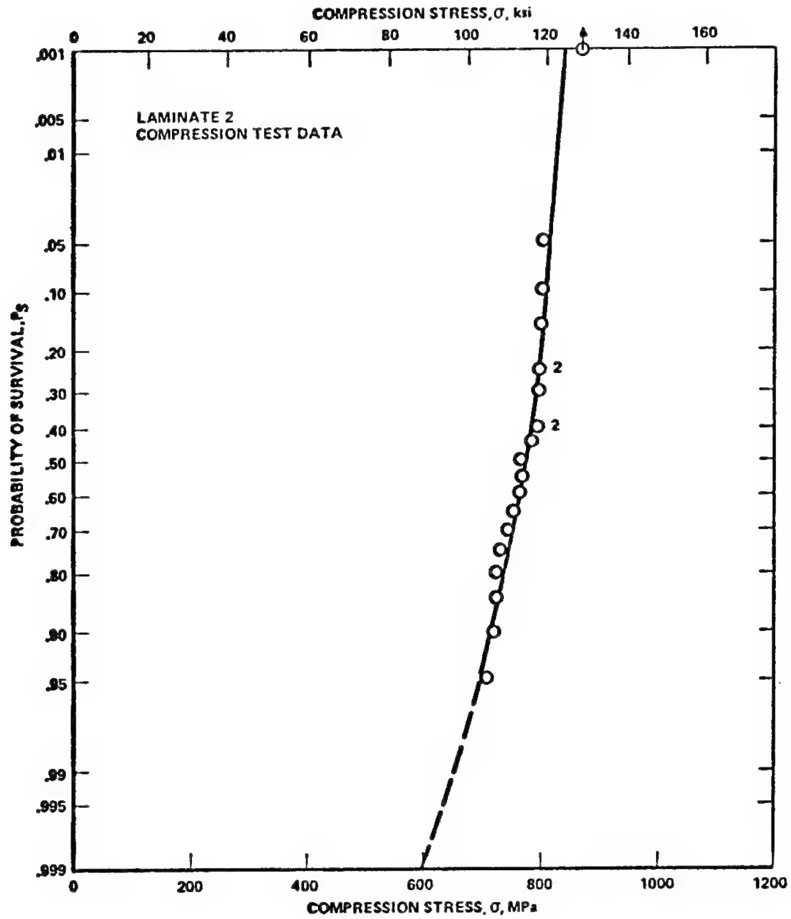
COMPRESSION STRESS, σ, ksi
LAMINATE 2
COMPRESSION TEST DATA
PROBABILITY OF SURVIVAL, P_S
COMPRESSION STRESS, σ, MPa

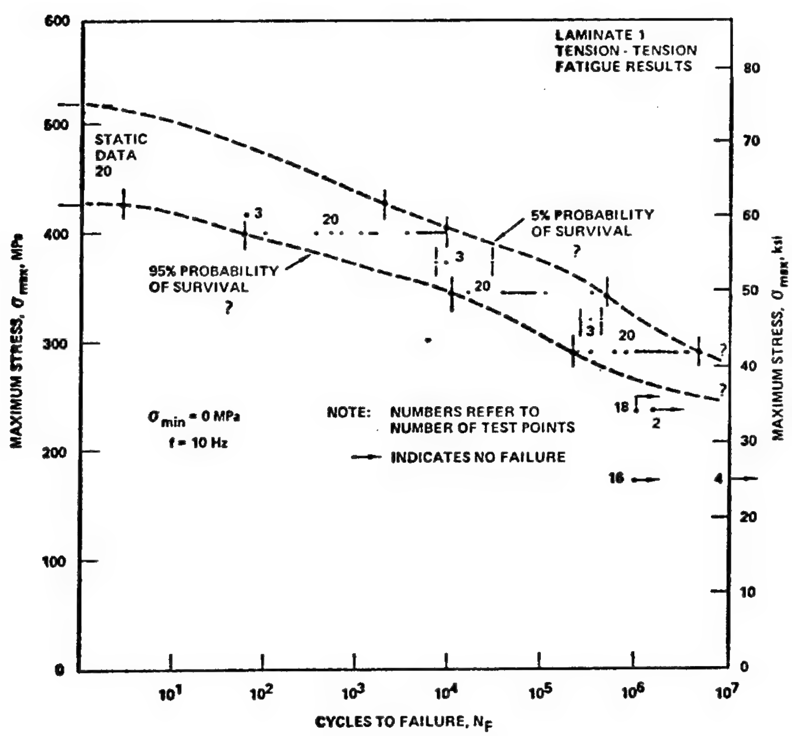
LAMINATE 1
TENSION - TENSION
FATIGUE RESULTS
STATIC
DATA
20
5% PROBABILITY
OF SURVIVAL
95% PROBABILITY
OF SURVIVAL
σ_{min} = 0 MPa
f = 10 Hz
NOTE: NUMBERS REFER TO
NUMBER OF TEST POINTS
INDICATES NO FAILURE
MAXIMUM STRESS, σ_{max}, MPa
MAXIMUM STRESS, σ_{max}, ksi
CYCLES TO FAILURE, N_F

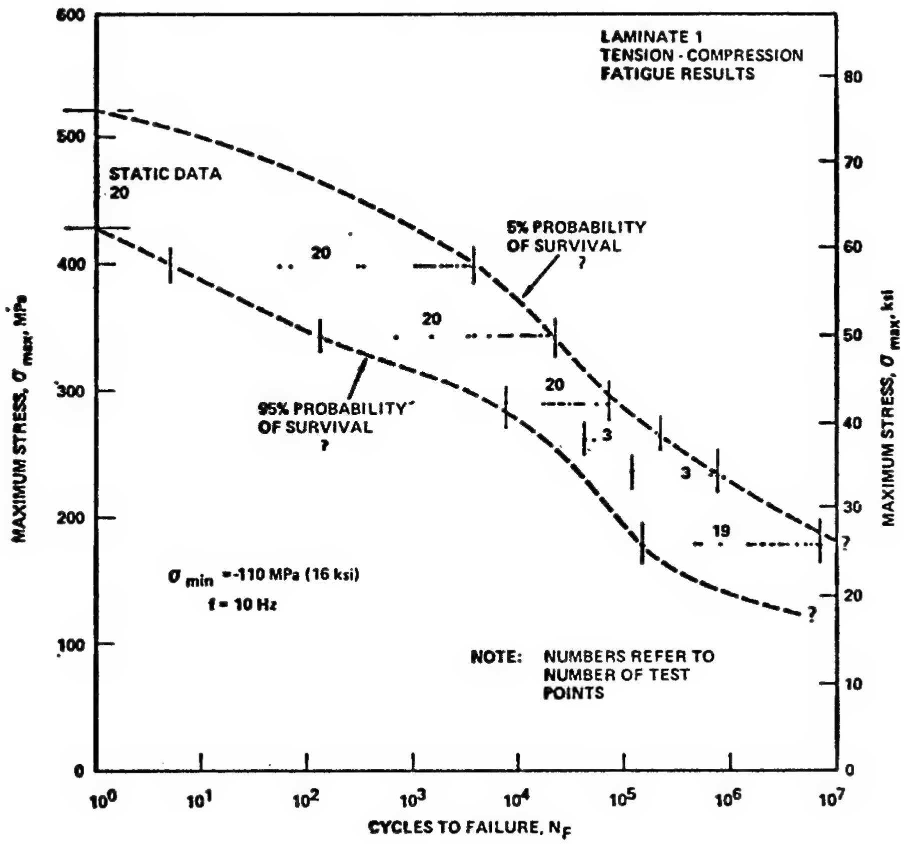
LAMINATE 1
TENSION - COMPRESSION
FATIGUE RESULTS
STATIC DATA
20
5% PROBABILITY
OF SURVIVAL
95% PROBABILITY
OF SURVIVAL
σ_{min} = -110 MPa (16 ksi)
f = 10 Hz
NOTE: NUMBERS REFER TO NUMBER OF TEST POINTS
MAXIMUM STRESS, σ_{max}, MPa
MAXIMUM STRESS, σ_{max}, ksi
CYCLES TO FAILURE, N_F

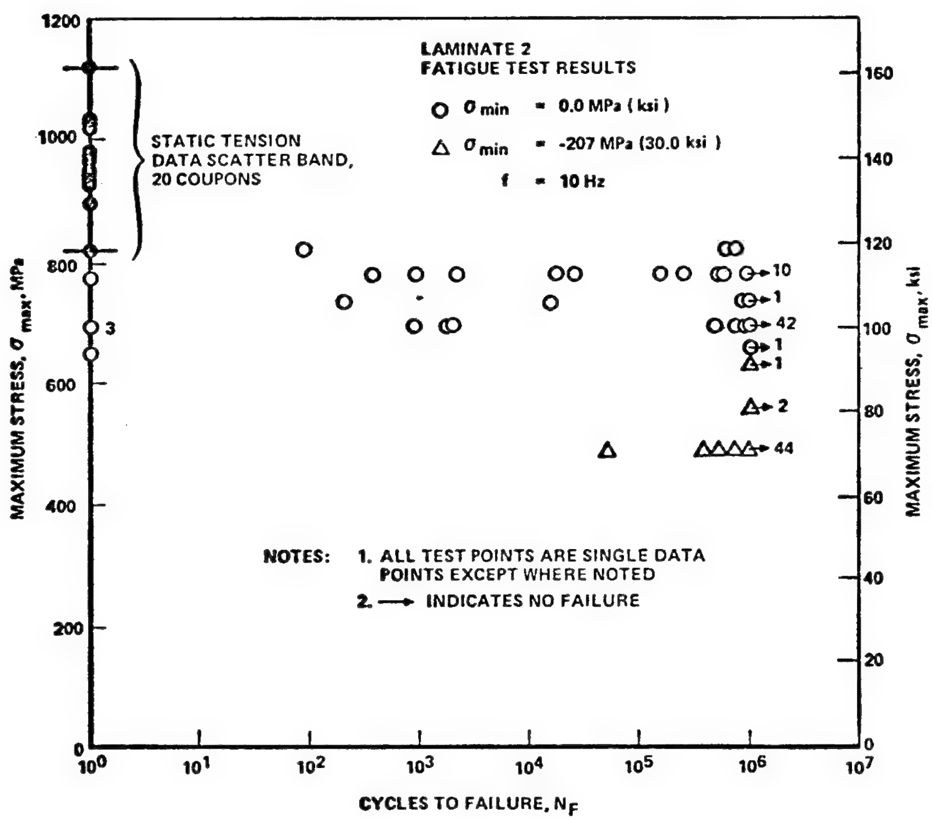
LAMINATE 2
FATIGUE TEST RESULTS
○ σ_{min} = 0.0 MPa (ksi)
△ σ_{min} = -207 MPa (30.0 ksi)
f = 10 Hz
STATIC TENSION
DATA SCATTER BAND,
20 COUPONS
NOTES: 1. ALL TEST POINTS ARE SINGLE DATA POINTS EXCEPT WHERE NOTED
2. ⟶ INDICATES NO FAILURE
MAXIMUM STRESS, σ_{max}, MPa
MAXIMUM STRESS, σ_{max}, ksi
CYCLES TO FAILURE, N_F

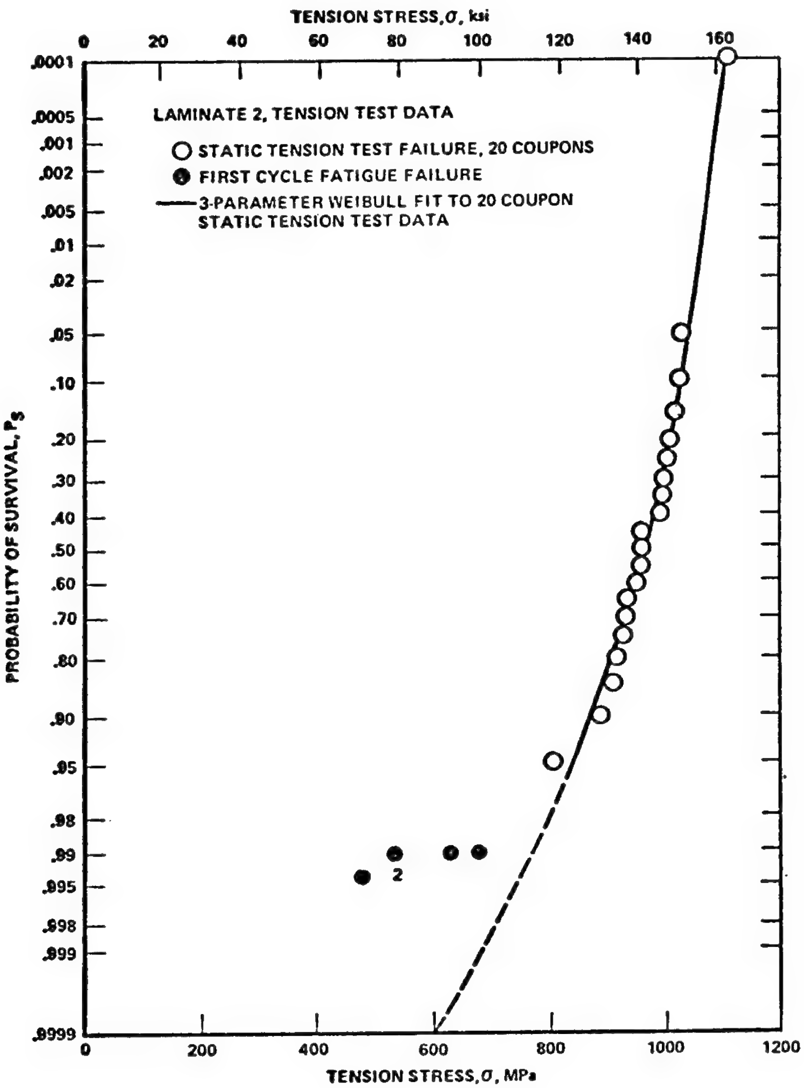

RESIDUAL STRENGTH STUDY - LAMINATE 1

- COUPONS FATIGUED TO $P_{.90}$ AT EACH σ LEVEL
- FAILED COUPONS REPLACED
- 40 COUPONS/σ LEVEL, 1/2 T AND 1/2 C
- FAILURE MODE SAME AS PREVIOUS T AND C, DISSIMILAR TO FATIGUE

TABLE 28

SUMMARY OF RESIDUAL STRENGTH TESTS FOR LAMINATE 1

(20 Coupons/Test Condition)

Fatigue Stress Levels, MPa (ksi)	Weibull Parameters k	e	v	Correlation Coefficient, R	Average Ultimate Stress, σ_{avg}, MPa (ksi)	Average Ultimate Strain, ϵ_{avg}, mm/mm in 50.8 mm	Average Apparent Modulus, E_{avg}, GPa (psi x 10^6)
Tension Test Results Before Fatigue	24.18	-0.0753	70.50	0.9995	477(69.2)	0.0096	52.7(7.64)
	24.12	0	70.57	0.9995			
290 to 0 (42 to 0)	12.12	-0.6276	64.52	0.9958	430(62.4)	0.0090	47.2(6.84)
	11.88	0	65.04	0.9957			
345 to 0 (50 to 0)	12.85	-0.1688	67.31	0.9987	449(65.1)	0.0093	48.3(7.01)
	12.78	0	64.45	0.9987			
290 to -110 (42 to -16)	18.51	-0.0608	68.43	0.9995	463(67.2)	0.0094	49.4(7.17)
	18.48	0	68.49	0.9995			
345 to -110 (50 to -16)	18.34	-0.1326	69.26	0.9992	467(67.7)	0.0095	49.2(7.13)
	18.27	0	69.38	0.9992			
Compression Test Results Before Fatigue	12.09	-0.4572	72.19	0.9973	480(69.7)	0.0110	47.9(6.95)
	11.94	0	72.53	0.9973			
290 to 0 (42 to 0)	7.22	-0.6574	60.15	0.9962	394(57.2)	0.0098	43.9(6.37)
	7.07	0	60.52	0.9961			
345 to 0 (50 to 0)	13.02	-0.2053	65.62	0.9988	439(63.7)	0.0111	45.8(6.64)
	12.94	0	65.79	0.9988			
290 to -110 (42 to -16)	12.54	-0.2387	67.26	0.9982	450(65.3)	0.0108	45.9(6.66)
	12.46	0	67.45	0.9982			
345 to -110 (50 to -16)	14.74	-0.5418	70.34	0.9969	473(68.6)	0.0110	45.9(6.66)
	14.52	0	70.82	0.9969			

TABLE 30

SUMMARY OF RESIDUAL STRENGTH TESTS FOR LAMINATE 2

(20 Coupons/Test Condition)

Type of Static Test, T-Tension C-Compression	Fatigue Stress Level, MPa (ksi)	Weibull Parameters k	e	v	Average Ultimate Stress, σ_{avg}, MPa (ksi)	Average Ultimate Strain, ϵ_{avg}, mm/mm in 50.8 mm	Average Apparent Modulus, E_{avg}, GPa (psi x 10^6)	Secant Modulus at 483 MPa (70 ksi) E_{sec}, GPa (psi x 10^6)
T	Tensile Test Results Before Fatigue	18.87	-0.4304	144.41	977(141.7)	.0092	106 (15.4)	-
	689 to 0 (100 to 0)	17.19	-0.3926	146.81	989(143.5)	.0092	108 (15.7)	-
	483 to -207 (70 to -30)	21.57	-0.1409	146.42	991(143.7)	.0094	105 (15.3)	-
C	Compression Test Results Before Fatigue	25.02[a]	-0.2592	115.82	787(114.2)	.0098	79.3 (11.5)	86.2(12.50)
		19.79[b]	-0.4902	115.97	782(113.4)	.0093	83.4 (12.1)	91.0(13.21)
	689 to 0 (100 to 0)	9.30	-1.6398	103.07	665(99.3)	.0078	87.6 (12.7)	92.9(13.46)
	483 to -207 (70 to -30)	9.32	-4.8439	102.60	681(98.8)	.0079	86.7 (12.6)	92.9(13.50)

a - Tested 3-76

b - Tested 10-76

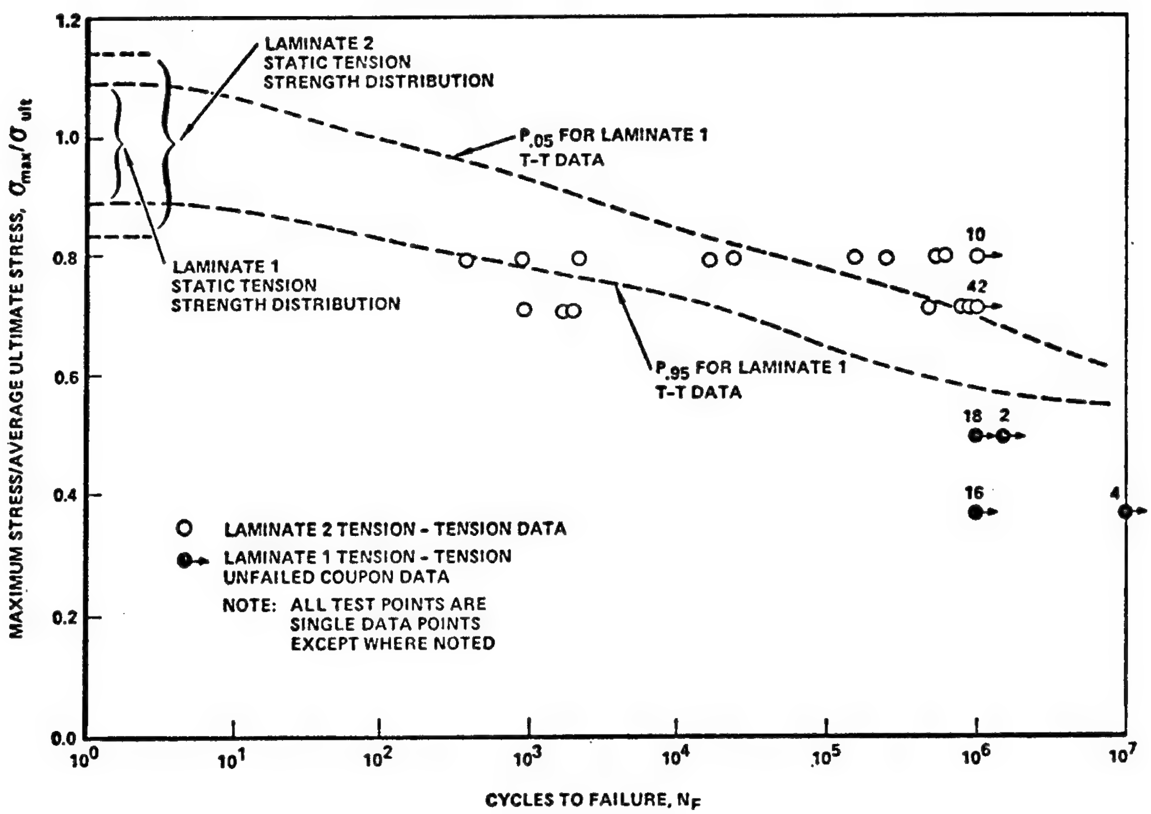

LAMINATE 2
STATIC TENSION
STRENGTH DISTRIBUTION
P.05 FOR LAMINATE 1
T-T DATA
LAMINATE 1
STATIC TENSION
STRENGTH DISTRIBUTION
P.95 FOR LAMINATE 1
T-T DATA
LAMINATE 2 TENSION - TENSION DATA
LAMINATE 1 TENSION - TENSION
UNFAILED COUPON DATA
NOTE: ALL TEST POINTS ARE
SINGLE DATA POINTS
EXCEPT WHERE NOTED
10
42
18
2
16
4
MAXIMUM STRESS/AVERAGE ULTIMATE STRESS, σmax/σult
CYCLES TO FAILURE, NF

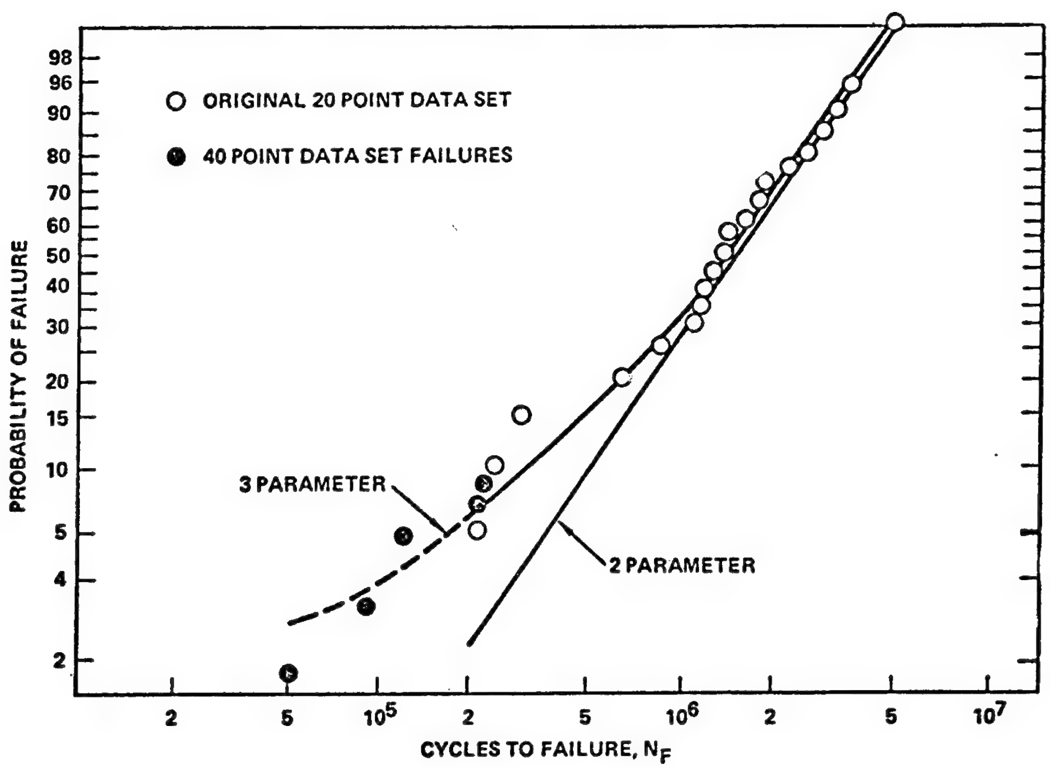

ORIGINAL 20 POINT DATA SET
40 POINT DATA SET FAILURES
3 PARAMETER
2 PARAMETER
PROBABILITY OF FAILURE
CYCLES TO FAILURE, NF

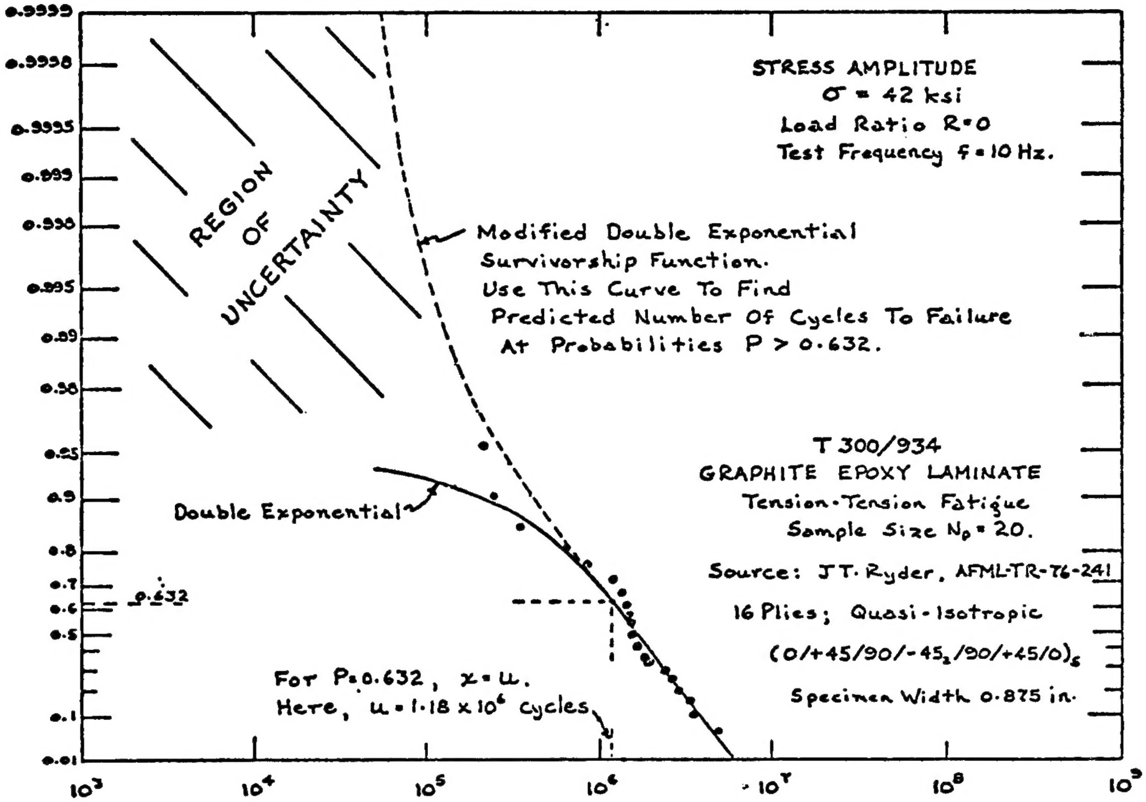
STRESS AMPLITUDE
σ = 42 ksi
Load Ratio R=0
Test Frequency f = 10 Hz.
REGION OF UNCERTAINTY
Modified Double Exponential Survivorship Function. Use This Curve To Find Predicted Number Of Cycles To Failure At Probabilities P > 0.632.
T 300/934
GRAPHITE EPOXY LAMINATE
Tension-Tension Fatigue
Sample Size Np = 20.
Source: J.T. Ryder, AFML-TR-76-241
16 Plies; Quasi-Isotropic
(0/+45/90/-45₂/90/+45/0)s
Specimen Width 0.875 in.
Double Exponential
For P=0.632, x=u.
Here, u=1.18 x 10⁶ cycles.
0.632

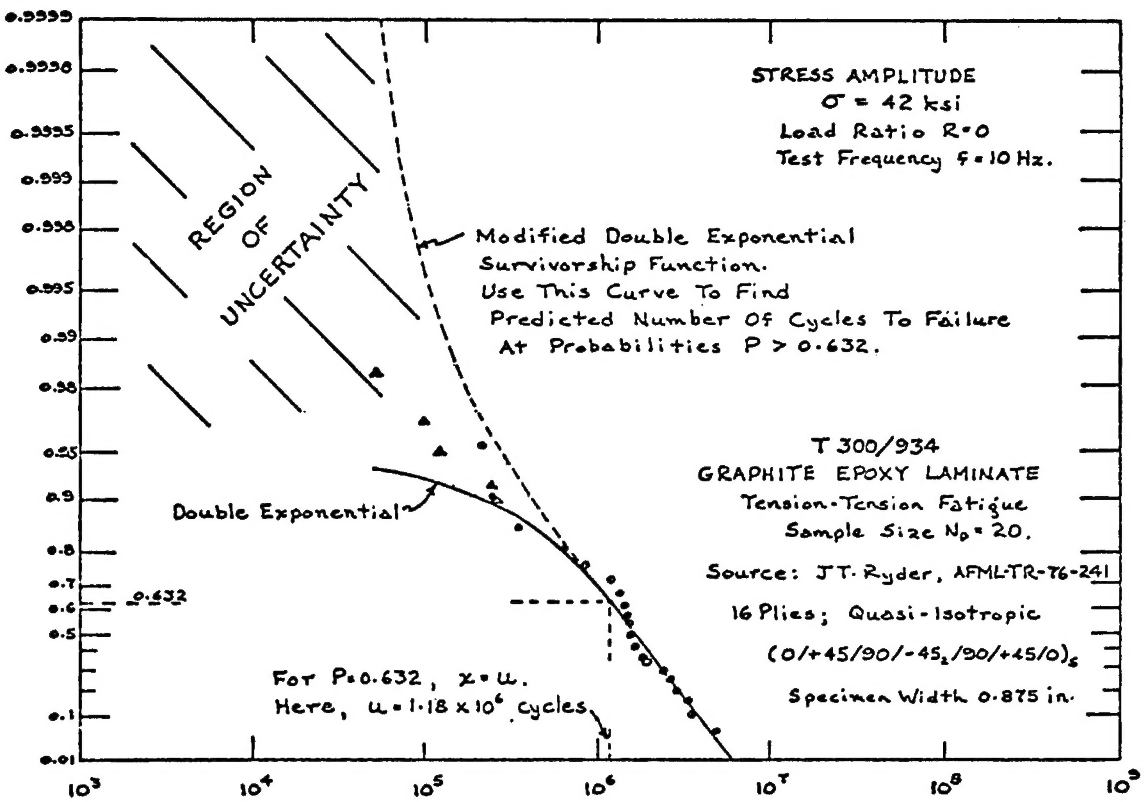
STRESS AMPLITUDE
σ = 42 ksi
Load Ratio R=0
Test Frequency f = 10 Hz.
REGION OF UNCERTAINTY
Modified Double Exponential Survivorship Function. Use This Curve To Find Predicted Number Of Cycles To Failure At Probabilities P > 0.632.
T 300/934
GRAPHITE EPOXY LAMINATE
Tension-Tension Fatigue
Sample Size Np = 20.
Source: J.T. Ryder, AFML-TR-76-241
16 Plies; Quasi-Isotropic
(0/+45/90/-45₂/90/+45/0)s
Specimen Width 0.875 in.
Double Exponential
For P=0.632, x=u.
Here, u=1.18 x 10⁶ cycles.
0.632

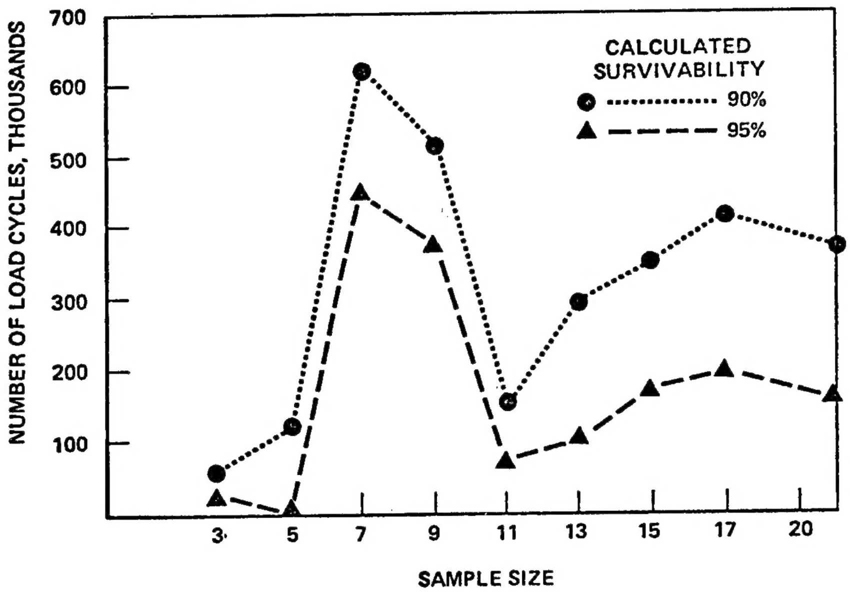

TABLE 34

SUMMARY OF OBSERVED DAMAGE GROWTH AND FAILURE MODES

	Test Type	Static Tension	Static Tension Residual Strength	Static Compression	Static Compression Residual Strength	T-T Fatigue	T-C Fatigue
Laminate 1	Damage Growth During Test	None	None	None	None	Delamination between the two -45° plies starting at free edge progressing along edge and toward center.	a. Delamination between the two -45° plies starting at free edge progressing along edge and toward center. b. More pronounced out-of plane buckling of delaminated plies than in T-T.
	Failure Mode	a. Small amounts of Delamination confined to fracture region b. 90° & 45° ply matrix fractures c. 0° fiber fracture d. Occasional Multiple fracture region	a. Similar to static tension failures b. Some coupons had extensive delamination due to prior fatigue loading	a. Extensive localized delamination b. Fracture of outer plies due to out-of-plane buckling c. Outer surface fractures along 45° line or irregular 90° line to load direction d. Occasional Multiple fracture region	a. Similar to static compression failures b. Some coupons had extensive delamination due to prior fatigue loading	a. One failure location often quite extensive b. Large amount of delamination especially between two -45° plies c. Many 0° fiber fractures, mostly matrix fractures in 45° & 90° plies.	a. One failure location often quite extensive b. Large amount of delamination especially between two -45° plies c. Many 0° fiber fractures, mostly matrix fractures in 45° and 90° plies d. Fractured outer 4 plies buckled out-of plane
Laminate 2	Damage Growth	None	None	None	None	Random localized delamination of fibers and fiber bundles from the outer surface 0° plies, not usually occurring at free edges, late in coupon life.	Similar to T-T coupons but with more extensive delamination
	Failure Mode	a. Extensive delamination usually between 0_2^s and 45° plies b. One failure location c. 0° fiber fracture and 45° ply matrix fracture d. Several coupons with 0° fibers fractured along a 45° line to load direction	a. Similar to static tension coupons	a. Localized delamination b. Fracture of coupon along a 45° line to load direction c. Fractured plies buckled symmetrically out-of-plane	a. Similar to static compression failures b. Some coupons had extensive delamination due to prior fatigue loading	a. Usually extensive delamination regions often between 0_2^s and 45° plies b. Rugged fracture regions dominated by 0° fiber fractures essentially at 90° to the load line and 45° ply matrix fracture c. Some coupons with 0° fiber fractures running at 45° to the load line	a. Usually extensive delamination regions often between 0_2^s and -45° plies b. Plies fractured out-of-plane due to buckling and fracture during compression load excursion

SUMMARY

1. STATIC COMPRESSION SCATTER LARGER THAN TENSION
2. LARGE FATIGUE DATA SCATTER
3. COMPRESSION LOWERS FATIGUE LIFE
4. STATIC AND FATIGUE FAILURE MODES DIFFER

SUMMARY

CONCLUSIONS (CONT'D)

5. EFFECTS OF σ_{max} AND $\Delta\sigma$ UNCLEAR, NEITHER CORRELATE WELL
6. LAMINATES 1 AND 2 DIFFER IN STATIC AND FATIGUE RESPONSE
7. FIRST CYCLE FATIGUE FAILURES OCCUR FOR LAMINATE 2; INDICATES LARGE STATIC STRENGTH SCATTER?
8. FOR LAMINATE 1, AT σ LEVELS WHERE FATIGUE FAILURE OCCURS, WEAROUT OCCURS

SUMMARY

CONCLUSIONS (CONT'D)

9. FOR LAMINATE 2, NO WEAROUT AT σ LEVELS WHERE FATIGUE FAILURE OCCURS

10. THREE PARAMETER FITS SHOULD BE USED FOR FATIGUE

11. SAMPLE SIZE TWENTY OR LARGER

12. CAN RESULTS BE EXTENDED TO LARGE COUPONS OR PANELS?

EFFECT OF STRAIN RATE ON STATIC TENSILE PROPERTIES

Laminate	Panel No.'s and Test Time	Strain Rate, ϵ, in./in./min.	Average Ultimate Stress σ_{ult}, ksi	Average Ultimate Strain ϵ_{ult}, in./in. in 2 in.	Initial Apparent Modulus of Elasticity E_a, psi x 10^6	Final Apparent Modulus of Elasticity E_b, psi x 10^6
1	10 Panels, #780 to 604 (April, 1975)	~ .08	69.2 + 9 % - 10%	.0096 +.0011 -.0010	7.64 +0.54 -0.69	6.45 +0.70 -0.68
	Panel 693 (March 1976)	~ .08	69.9 +13.3% - 8.2%	.0095 +.0009 -.0006	7.57 +0.44 -0.31	6.33 +0.18 -0.22
	Panel 693 (Sept. 1977)	~ .08	73.5 + 8.0% - 9.8%	.0106 +.0007 -.0013	7.24 +0.24 -0.45	6.36 +0.22 -0.57
	Panel 693 (Sept. 1977)	~ .0009	68.2 + 6.9% - 7.0%	-	-	-
2	4 Panels (March 1976)	~ .08	141.7 +14 % -14 %	.0092 +.0009 -.0027	15.4 +2.9 -1.9	-
	4 Panels (Sept. 1977)	~ .08	143.6 +11.5% -14.5%	.0102 +.0010 -.0014	14.2 +0.5 -1.1	-
	4 Panels (Sept. 1977)	~ .0009	135.0 +14.1% -13.8%	-	-	-

☆U.S.Government Printing Office: 1977 — 757-080/144